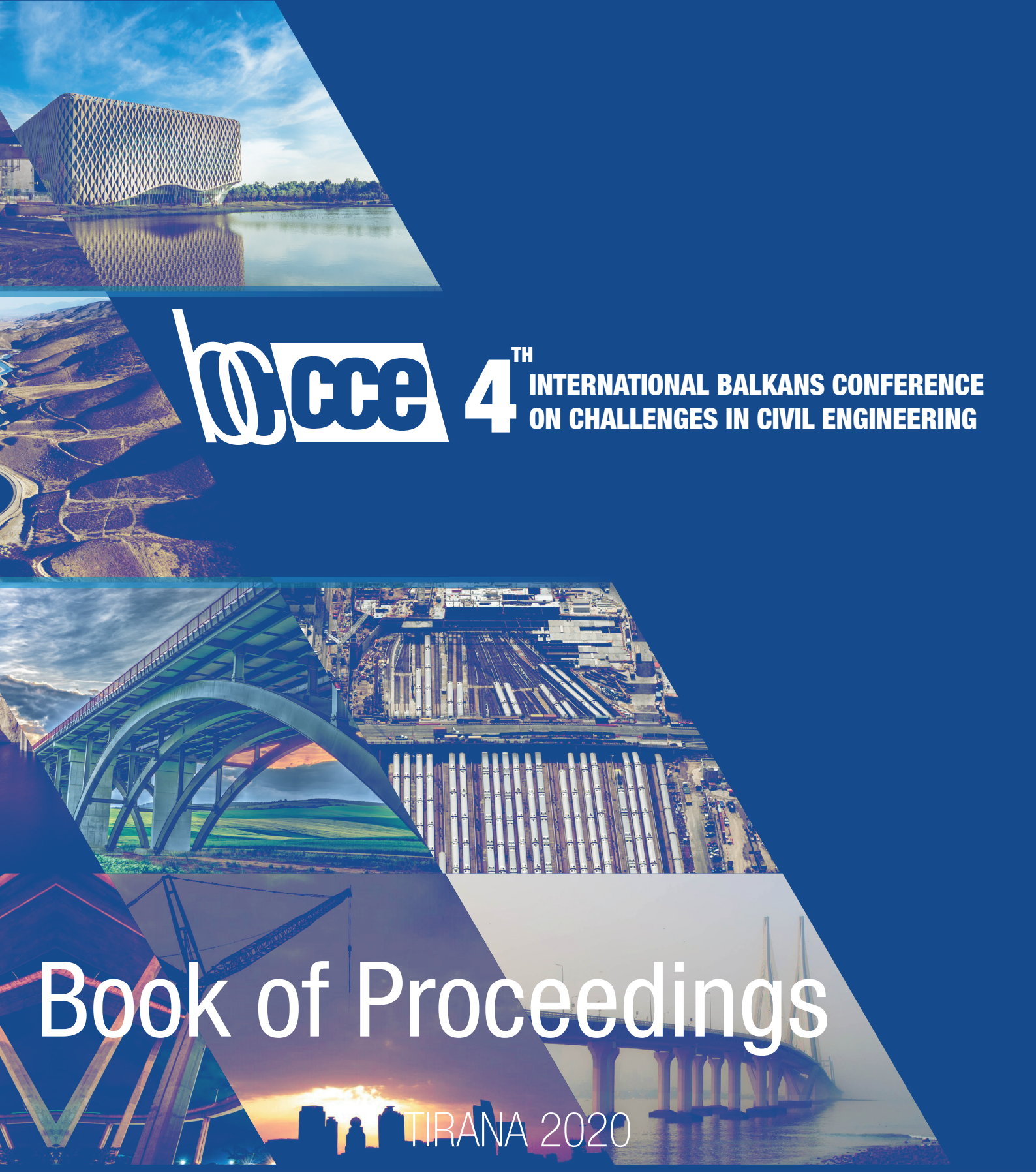


bcce

4TH INTERNATIONAL BALKANS CONFERENCE ON CHALLENGES IN CIVIL ENGINEERING

Book of Proceedings

TIRANA 2020

EPOKA UNIVERSITY
Department of Civil Engineering
Epoka University

IGJEUM
Instituti i Gjeoshkencave,
Energjise, Ujit dhe Mjedisit

DI
Department of Engineering
Universita Degli Studi di Perugia

Faculty of Tecnical Sciences
University of Novi Sad

Faculty of Civil Engineering
SS Cyril and Methodius University

Faculty of Civil Engineering and Building Services
"Gheorghe Asachi" Tecnical University

Faculty of Civil Engineering and Architecture
University of Prishtina

4th International Balkans Conference on Challenges of Civil Engineering

BOOK OF PROCEEDINGS

ISBN: 978-9928-135-37-7

International Balkans Conference on Challenges of Civil Engineering

Book of Proceedings

Editors:

Assist. Prof. Dr. Erion Luga

Dr. Enea Mustafaraj

Dr. Julinda Keçi

Publisher:



All rights reserved

Book of Proceedings of the

International Balkans Conference on Challenges of Civil Engineering

BCCCE 2020

December 18-19, 2020

Tirana, Albania

Organizers:

EPOKA University, Tirana, Albania,

Institute of Geosciences, Tirana, Albania,

University of Perugia, Italy

Polytechnic University of Bari, Italy

University of Novi Sad, Serbia

Ss Cyril and Methodius University, North Macedonia

“Gheorghe Asachi" Technical University of Iasi, Romania

University of Prishtina, Kosovo

Committees

Local Organizing Committee

Assist. Prof. Dr. Erion Luga	*Chair*
Assoc. Prof. Dr. Marco Corradi	*Co-Chair*
Dr. Julinda Keçi	*Co-Chair*
Assoc. Prof. Dr. Mirjam Ndini	
Assoc. Prof. Dr. Hüseyin Bilgin	
Dr. Enea Mustafaraj	
MSc. Armando Demaj	
MSc. Marsed Leti	*Conference Secretary*
MSc. Margarita Dajko	
MSc. Mirjeta Blloshmi	

Keynote Speakers

Construction Materials	**Prof. Dr. Jorge de Brito** *University of Lisbon, Portugal*
Structural Engineering	**Prof. Dr. Arturo Schultz** *University of Texas at San Antonio, USA*
Structural Engineering	**Assoc. Prof. Dr. Marco Corradi** *Northumbria University, UK*

International Scientific Committee

Ahmet Öztaş	*Ishik University, Iraq*
Alket Kumaraku	*Polytechnic University of Tirana, Albania*
Ancuta Rotaru	*Technical University of Iasi "Gheorghe Asachi", Romania*
Anna Bruna Menghini	*Università degli Studi "La Sapienza" di Roma, Italy*
Anna Yunitsynna	*EPOKA University, Albania*
Antonio Borri	*University of Perugia, Italy*
Artan Hysa	*EPOKA University, Albania*
Dora Foti	*Polytechnic University of Bari, Italy*
Elfrida Shehu	*Polytechnic University of Tirana, Albania*
Emanuela Speranzini	*University of Perugia, Italy*
Enea Mustafaraj	*EPOKA University, Albania*
Enkelejda Gjinali	*Polytechnic University of Tirana, Albania*
Erion Luga	*EPOKA University, Albania*
Frida Pashako	*EPOKA University, Albania*
Giorgio Rocco	*Polytechnic University of Bari, Italy*
Hüseyin Bilgin	*EPOKA University, Albania*
Jorge de Brito	*University of Lisbon, Portugal*
Julinda Keçi	*EPOKA University, Albania*
Maksim Çipi	*European University of Tirana, Albania*
Marco Corradi	*University of Perugia, Italy*
Mario Daniele Piccioni	*Polytechnic University of Bari, Italy*
Meri Cvetkovska	*Cyril and Methodius University of Skopje, North Macedonia*
Miriam Ndini	*EPOKA University, Albania*
Mirjana Laban	*University of Novi Sad, Serbia*
Mirjana Malešev	*University of Novi Sad, Serbia*
Niko Pojani	*Polytechnic University of Tirana, Albania*
Perparim Hoxha	*Polytechnic University of Tirana, Albania*
Rexhep Koçi	*IGJEUM, Polytechnic University of Tirana, Albania*
Sokol Dervishi	*EPOKA University, Albania*
Vlastimir Radonjanin	*University of Novi Sad, Serbia*
Yavuz Yardım	*University of Edinburgh, United Kingdom*
Ylber Muceku	*Polytechnic University of Tirana, Albania*

PREFACE

In this volume are included the full papers presented at the ***International Balkans Conference on Challenges of Civil Engineering*****,** by new academicians, researchers and professor invited as keynote speakers.

4th International Balkans Conference on Challenges of Civil Engineering (BCCCE) is hosted by the Department of Civil Engineering of EPOKA University in Tirana, Albania during December 18-19, 2020. This conference was jointly organized by Departments of Civil Engineering of EPOKA University, Institute of Geosciences of Albania, University of Perugia, Polytechnic University of Bari, University of Novi Sad, Ss Cyril and Methodius University, "Gheorghe Asachi" Technical University of Iasi and University of Prishtina.

The conference aimed to provide a platform for civil engineers' technology, management research and education status all over the world. The conference proposed to offer a motivating environment to encourage discussion and exchange of ideas leading to endorsement of Structural and Earthquake Engineering, Construction Management and Technology, Construction Materials, Geotechnical Engineering, Transportation Engineering, Historical and Monumental Buildings, Disaster Risk Management, Impact of Climate Change on Built Environment, Sustainable and Life Cycle Assessment and Innovative Practices in Construction Industry.

The papers were accepted for presentation in the Conference were selected after a peer reviewing process performed by the international Scientific Committee. During the conference, the papers were presented and discussed in four sessions.

We would like to acknowledge and give special appreciation to our keynote speakers, ***Prof. Dr. Jorge de Brito, Prof. Dr. Arturo Shultz, and Assoc. Prof. Dr. Marco Corradi,*** for their valuable contribution.

We would like to extend our appreciation to the International Scientific Committee and Local Organizing Committee for the devotion of their precious time, advice, and hard work to prepare for this Conference. ***Julinda Keçi*** and ***Enea Mustafaraj*** must be particularly mentioned for their hard work.

On behalf of the organizing committee of the 4th International Conference on Challenges of Civil Engineering (4th BCCCE), we thank all the authors and participants for their contribution in the realization of a successful conference even though in an extraordinary situation created by COVID-19.

Assist. Prof. Dr. Erion Luga

Conference Chair

Contents

Committees	iv
Preface	vii
Building Pathology: A Systemic Approach.	1
Earthquake-resistant cities in Albania: The Seismic Microzonation Studies (SMS) and Limit Condition in Emergency (LCE) integrated approach	4
Cementitious Grout Method Application on Tunnel Rockbolts and its Effect on Bond and Load Carrying Capacity. A Real-Scale Pull Out Test on Fan River HPP Power Tunnels	11
Evaluation of Seismic Pounding between two Adjacent Reinforced Concrete Buildings from Albanian Practice	22
The alternative stormwater system versus the traditional piped stormwater system	29
Inundation Modeling Using HEC-RAS Software Farka Stream Case Study	40
Impact of neotectonic processes of Shkumbin valley, "Xibrake-Librazhd area" on existing and future civil engineering works	48
Effect of errors on execution and design of key details in the object	55
Computational fluid dynamics modeling of submerged vegetation in open channels	64
Supplementary cementitious materials and mechanochemistry for sustainable concrete production	74
Experimental Study of FRP reinforced concrete beams according to ACI	79
Improvement of flexural strength of reinforced concrete beams using CFRP wraps	86
Structural assessment of the south-west wing timber roofs of the Loreta in Prague	93
Use of Incremental Dynamic Analysis for the seismic performance assessment of RC framed structures	104
Observations on the Domed Mosques Built During the Ottoman Empire Period in Prizren - Kosovo	113

Spatial and Morphological Potentials of Urban Informality: “Shallvaret” Block 130

Paper Folding Bio-Kinetic Façade: Application of Bat Wing Inspired Façade Design to the Building of Mediterranean University in Tirana, Albania 140

Experiencing the Research-Based Learning: Case of the graduate course “Landscape Perspectives in Disaster Risk Management and Fire Safety 149

The effect of Elbasan GGBFS addition on different properties of cement mortars 158

Towards a Disaster Risk Management Plan of Historical Centers: Case Study of The Historical Center of Gjirokastra 165

Behavior of RC frames under quasi-static diagonal loads 176

Study of Microstructure of Waste Tyre Ash (WTA) Concrete Using the Scanning Electron Microscopy (SEM) and X – ray Diffraction (XRD) Techniques 183

Polypropylene reinforced mortar coating for improvement of unreinforced masonry (URM) shear strength 191

Public-Private Partnerships in Albania: From the Legislative Provisions to Risk Management 200

Building Pathology: A Systemic Approach

Jorge de Brito[1], Clara Pereira[1]

[1]*CERIS, Instituto Superior Técnico, University of Lisbon, Portugal*

INTRODUCTION

The study of building pathology focuses on the operation and maintenance stage of a building's life cycle, during which buildings need to be followed periodically. Technical inspections allow estimating different types of degradation through observation. They also allow assessing the performance of the building elements and, thus, of the building. Well-informed decisions on maintenance planning, sudden repairs, local replacements, or overall rehabilitation should only be made considering the data collected in technical building inspections.

Building inspection systems are an important tool as they provide objective information. Inspections should be performed regularly, at predetermined intervals, collecting predefined types of data. A building inspection system should include location information about the degradation phenomena concerning: the building and its surroundings; the building element within the building; the detected defects and their causes within a building element. Furthermore, building inspection systems provide unambiguous designations for all concepts involved in technical inspections, such as defects, causes, diagnosis methods and repair techniques. Building inspection systems may also determine the use of in situ or laboratory tests to obtain qualitative or quantitative information, whether on the first inspection or a more detailed one. Information like the area of deteriorated zones, the width of cracks, the temperature of the building element and its moisture content may help to characterize the defects and confirm their causes. Finally, a building inspection system should classify levels of degradation according to a predetermined quantification system. Those levels will influence the determination of the urgency of repair. To sum up, building inspection systems aim at an independent inspection, keeping subjectivity to the minimum.

COMPONENTS OF THE INSPECTION SYSTEM

The authors' research team at Instituto Superior Técnico, University of Lisbon, has defined the structure of an inspection system, presented in Figure 1. Considering the non-structural building envelope of buildings (façades and roofs), two classification lists are highlighted [1]: defects and their causes. The classification list of defects is organized in four categories: defects of physical nature; defects of chemical nature; defects of mechanical nature; and other defects. In total, 38 types of defects are included in the list. The classification list of causes of defects is arranged in five categories: design errors; execution errors; mechanical actions; environmental actions; and use and maintenance errors. The list includes a total of 108 causes of defects. According to the structure of the inspection system (Figure 1), the relationships between the items in these lists are represented in a defects–probable causes correlation matrix [2].

BUILDING DEFECTS

To ease the identification of defects, the use of photographic examples of the listed defects is encouraged [3]. Figure 1 shows three different types of defects from the classification list of defects.

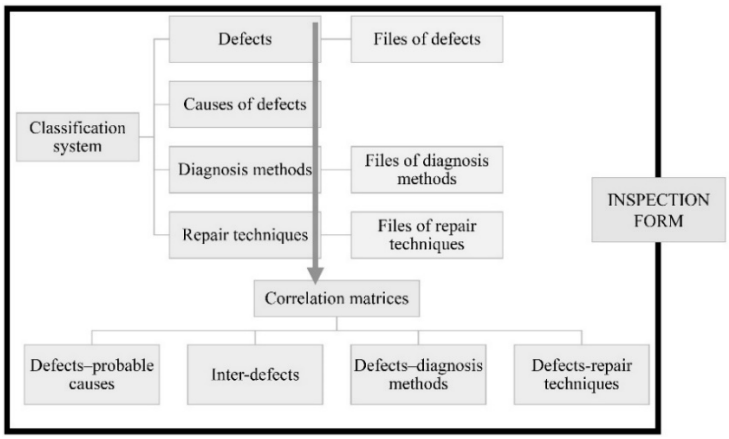


Figure 1. Organogram of the building inspection system developed at Instituto Superior Técnico, University of Lisbon



Figure 2. Examples of three types of defects [1]: a)“A-B1 Biodeterioration/biological growth”; b) “A-B2 Vegetation growth”; c) “A-B3 Efflorescence/cryptoflorescence and carbonation”

FINAL REMARKS

Nevertheless, although having a catalogue of defects may speed up the inspection process, a full diagnosis comprises more steps. After identifying the type of observed defect, its causes should also be determined. The surveyor should also analyze the need for carrying out additional diagnosis methods. Then, according to the findings, the surveyor should be able to recommend a course of action, namely: adjusting the maintenance plan with periodic maintenance works or performing curative or preventive repairs.

Finally, full data should be provided for decision-makers in view of more enlightened decisions.

REFERENCES

[1] de Brito, J., Pereira, C., Silvestre, J.D. and Flores-Colen I. (2020) Expert knowledge-based inspection systems. Inspection, diagnosis and repair of the building envelope [online]. Springer, Cham, Switzerland.

[2] Pereira, C., de Brito, J. and Silvestre, J.D. (2020) Harmonising correlation matrices within a global building expert knowledge-based inspection system. Construction and Building Materials, Elsevier, In press. doi:10.1016/j.conbuildmat.2020.121655

[3] Pereira, C., de Brito, J., Silvestre J.D. and Flores-Colen, I. (2020) Atlas of defects within a global building inspection system. Applied Sciences, MDPI, 10(17), 5879.

Earthquake-resistant cities in Albania: The Seismic Microzonation Studies (SMS) and Limit Condition in Emergency (LCE) integrated approach

Klodian Skrame[1], Iolanda Gaudiosi[2], Redi Muçi[1], Marco Mancini[2], Maurizio Simionato[2], Oltion Fociro[1], Maria Sole Benigni[2], Albora Ramollari[1], Margherita Giuffrè[2], Massimiliano Moscatelli[2]

[1]Department of Applied Geology and Geoinformatics, Polytechnic University of Tirana (PUT), Albania.
[2]Institute of Environmental Geology and Geoengineering of the Italian National Research Council (CNR-IGAG), Italy

ABSTRACT

In this work, it is intended to highlight the indispensable significance of the seismic microzonation studies (SMS) and the Limit Condition in Emergency (LCE) at the level of primary decision-making at urban planning studies and to help resolving a range of problems connected to seismic risk assessment in Albania.

Following the 1979 Montenegro seismic sequence, the Albanian government implemented a 'National Plan for Seismic Prevention', which funded the SMS of some of the biggest cities in Albania. Unfortunately, the seismic risk prevention activities were halted after the renewal of the national codes for design in 1989.

Located next to the most active fault in Albania, the main cities of the country have experienced seventeen (17) seismic events with magnitude from 5.4 to 6.6 in the last 114 years. The last earthquakes that hit Albania on September 21st, 2019 of Mw 5.4 and November 26th, 2019 of Mw 6.2 severely damaged the cities of Durrës, Thumanë, Tirana, Vora, Shijak and the villages around. The main event of the 26th November caused the deaths of 51 persons and the damaging of hundreds of buildings. The degree of damages produced by these earthquakes has been, in some cases, significantly enhanced by the characteristics of the earthquake ground motion affected by the local subsurface soil structure of the cities.

The seismic events of 2019 evidenced the crucial importance of the earthquake risk reduction and mitigation. In the process of creating earthquake-resistant cities, the SMS and the LCE could be the best tools for a better seismic hazard mitigation and prevention in Albania.

***Keywords**: seismic microzonation studies, Limit Condition in Emergency, Durrës earthquakes, seismic mitigation, seismic prevention.*

INTRODUCTION

Albania is a Balkan country with very high seismic activity. It is geologically and seismo-tectonically a rather complicated region. The country is characterized by obvious micro-seismicity (a high number of small earthquakes), sparse medium-sized earthquakes (magnitude M from 5.5 to 5.9), and rare large earthquakes with magnitude M>6.5. Most strong Albanian earthquakes have occurred along three well-defined seismic belts: i. the Ionian-Adriatic coastal belt extending northwest to southeast and coinciding with the boundary between the European plate and the Adria microplate; ii. the Peshkopia-Korça belt (the so called Drini), extending north-south in the eastern part of the country and iii. the Elbasani-Dibra-Tetova transverse belt, extending southwest to northeast across the former two belts. During the last 114 years, along these seismic belts, have been generated seventeen (17) seismic events with magnitude from 5.4 to 6.6. These earthquakes caused 407 victims and hundreds of thousands injured. One of the most destructive earthquakes in Albania has been the seismic event of 1979 in Montenegro. Following this seismic event,

the Albanian government implemented a "National Plan for the seismic prevention" funding the seismic microzonation studies (hereafter SMS) of some of the biggest cities in Albania. Unfortunately, the seismic risk prevention activities were halted after the implementation of the renewed national codes for design in 1989.

The November 26th, 2019 earthquake caused the deaths of 51 people and damaged hundreds of buildings in the cities of Durrës, Thumanë, Tirana, Vora, Shijak and their villages. Damage caused by these earthquakes has been, in some cases, significantly worsened by the characteristics of the earthquake ground motion affected by the local subsurface soil structure of the cities [9].

In the process of creating earthquake-resistant cities, the geophysical and engineering-geological methods, which take into account the geological and geomorphological characteristics of the local subsoil, for an effective SMS, could be fundamental.

The integrated studies of the SMS with the Limit Condition in Emergency (hereafter LCE) could be the best tools for a better seismic hazard mitigation and prevention in Albania.

For this purpose, a multidisciplinary research activity that integrated the existing geotechnical and geophysical data with original geophysical surveys was carried out to define the SMS of two archaeological cities in Albania: Durrës and Gjirokastër. Based on the SMS, the LCE were applied in both cities.

The integrated SMS-LCE approach studies can help decision-makers to identify the strategic buildings, structural blocks, emergency areas and the strategic paths for a successful emergency plan at a municipality level.

1ST LEVEL OF SMS OF THE DURRËS AND GJIROKASTRA MUNICIPALITIES

SMS are an important tool in correct urban planning and in the prospective of seismic hazards mitigation and prevention. The main goal of the SMS is to delineate areas, within a municipality level, with homogenous seismic response in terms of stratigraphic and topographic amplification, as well as areas of earthquake-induced phenomena such as landslides, liquefaction and sinkholes.

The main goal of the SMS is to identify, on a local scale, the areas that manifest a homogeneous seismic behavior during an earthquake event. According to the Italian guidelines (firstly proposed from the International Society for Soil Mechanics and Geotechnical Engineering ISSMGE in 1999), a municipality territory could be characterized in accordance to three types of areas: i) stable areas, ii) stable areas susceptible to local seismic amplification and iii) areas susceptible to instability (e.g. earthquake-induced landslides, soil liquefaction and surface fractures and faulting). Three levels of SMS are considered in these guidelines. The 1st level is based on the collection of the existing data and on the distribution of the new surveys, in such a way as to acquire the most in-depth information possible for the municipality territory. This level identifies the areas with the same seismic behavior, based on the three typologies described above. The results are shown on the Seismically Homogeneous Microzones Map (SHMM) (in 1:5000 or 1:10000 scales) and the databases of the investigations are then uploaded into a geographic information system. The 1st level process is totally based on the detailed engineering-geological and geophysical models of the subsoil. The target of the 2nd and 3rd levels is the evaluation of the local seismic response and seismic amplification factors of the entire territory of the municipalities. The municipalities involved in the process are those with highest values of peak ground acceleration, agR, corresponding to the reference probability of exceedance PNCR=0.10 in TL=50 years, or equivalently to a reference return period of TNCR≈ 475 years [11]. A one and two-dimensional numerical modeling analyses based on the modification of the reference seismic signal due to the specific site conditions is needed to quantify the local amplification, the dynamic analyses of slope instability and the liquefaction susceptibility [10].

Referring to these criteria, two different ancient cities in Albania were chosen for the 1st level of SMS, specifically, the cities of Durrës and Gjirokastra.

Located next to the most active fault in Albania, these cities have experienced a number of strong earthquakes in the past, sometimes exceeding a magnitude of 6. The seismic event of October 10th, 1858 destroyed many buildings in the city of Gjirokastra. Historians claim that it had a huge impact on the economic life of the archaeological city [12].

The ancient city of Dyrrachium (modern name: Durrës) is not new at seismic risk and has been severely destroyed by a series of earthquakes. The most important ones on record are: the earthquake of 177 B.C., May 1st or 2nd, then in 58 A.D., 334, 345, 506 (that almost destroyed the entire ancient city), March 1st, 1273, 1279, 1869, 1870 and December 17th, 1926 of Ms 6.2 and seismic intensity of IX (MSK-64 scale) [1].

The last earthquake sequence started in September 21st, 2019 with a ML 5.4 and a relatively deep hypocenter (around 17 km referring to cnt.rm.ingv.it). The main event occurred in November 26th, 2019 with Mw 6.2 causing 51 victims and extensive damage to hundreds of buildings in the cities of Durrës, Thumanë, Tiranë, Vorë, Shijak and many others. The earthquake sequence produced 8 high seismic events with magnitude larger than 5. The activation of the reverse faulting system produced many phenomena connected to the local soil conditions such as: seismic stratigraphic amplification, soil liquefaction, surface fractures and earthquake-induced landslides [4].

The city of Durrës is located along the Adriatic coast in the central part of Albania, in the lowland of the Periadriatic Depression.

In the process of collecting existing data, the engineering-geological map of the city of Durrës [3] was taken into account, alongside data obtained through laboratory testing regarding the geotechnical parameters of the clayey formation of Lower Pliocene at Durrës Hill, thus determining their key role in the generation of landslides [5,6]. These results were incorporated to the geological map in 1:10.000 scale, the previous microzonation map of the city [1], the bedrock map presented in [2] and the private engineering-geological reports and studies conducted on the city of Durrës. All the collected data were integrated into a detailed Gis-database for the SMS activity.

In order to make a better assessment of the local seismic hazard at the historical center of the city of Durrës and determine the distribution of Quaternary deposits, a series of different geophysical investigations were carried out. Twenty-two single-station noise measurements, processed through the HVSR technique, two MASW surveys and two 2D array measurements were performed to cover an area of around 3 km^2 of the historical center of Durrës (Figure 1) [4]. The fundamental frequencies of resonance f0, were determined for each HVSR curve from noise measurements. Afterwards, the corresponding fundamental periods T0 as 1/f0 were computed. Four different groups of T0 ranges were obtained: i) shows no peak; ii) refer to very thin surficial layers (i.e. top few meters) prone to amplification; iii) show the predominant peak period in the range of 0.7 - 1.1s and iv) show the presence of the highest fundamental periods T0 (higher than 1.1s) indicating a deep bedrock interface [4].

The fundamental frequencies of resonance f0 were used to estimate the thickness (h) of the Quaternary deposits overlaying the Messinian-Pliocene bedrock [4].

The city of Gjirokastra is located in the southern part of Albania as shown in Figure 2. The first stage of the SMS of the city of Gjirokastra consisted in the reconstruction of the engineering-geological model of the subsoil, with the aim of defining the geometrical setting of soil deposits and their geotechnical and geophysical properties. On this purpose, the available geological, geotechnical and geophysical data, together with the private engineering-geological reports and studies were collected and analyzed. All the collected data were integrated into a detailed Gis-database for the SMS activity. Based on the geological survey and on the previous data, it was possible to reproduce the Engineering-Geological Map in 1:10.000 scale of the city of Gjirokastra, the Slope Map (in 1:10.000 scale) and the DEM Map (in 1:10.000 scale) of the city of Gjirokastra.

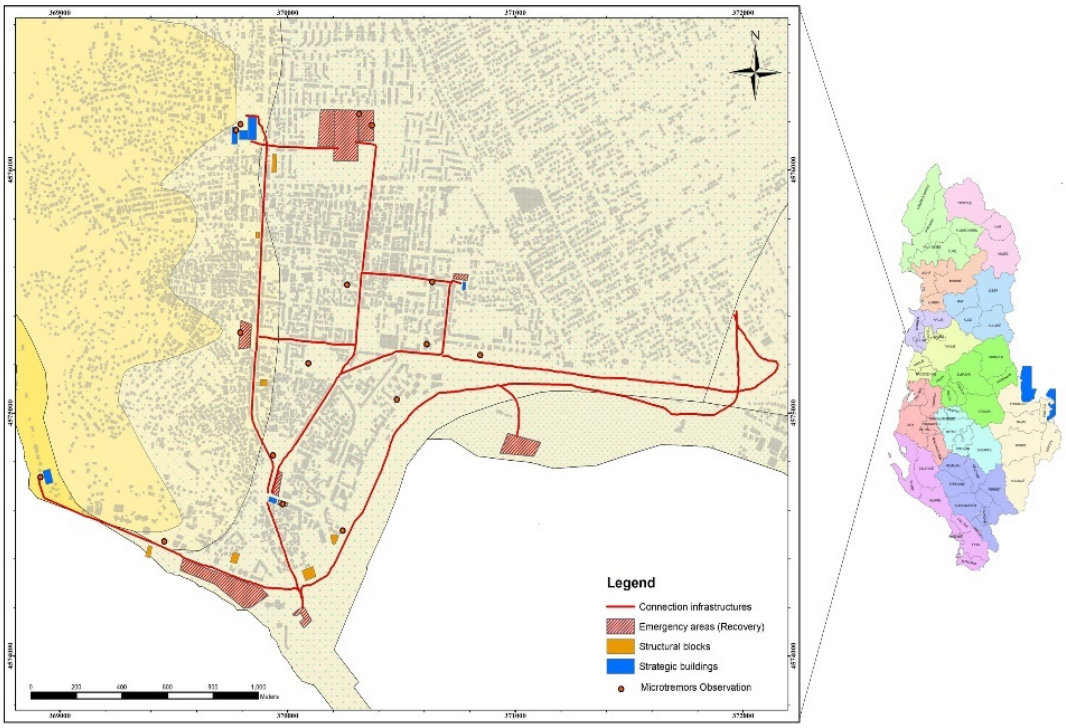


Figure 1. Shows the integrated approach of the SMS and the LCE for the center of the city of Durrës.

In order to define the stable areas, the stable areas susceptible to local seismic amplification and the areas susceptible to instability for the entire territory of the city of Gjirokastra, a research approach that integrated different geophysical methods were performed. To this purpose, 25 ambient vibrations measurements were carried out for the most important buildings and across the historical center of the city and recent settlements (Figure 2). Six 2D array and six MASW measurements were performed to provide useful elements for a geophysical subsoil characterization [9].

Based on the data obtained, the municipality of Gjirokastra was divided into six zones of susceptibility to local ground amplification and two zones of geological instability. Due to the different geological, engineering-geological, geophysical and geomorphological settings that characterize the subsoil of the city, the earthquake-induced phenomena that could be manifested during the seismic events might vary significantly. The city of Gjirokastra is subject to extensive landslides and earthquake-induced landslides on the fractured calcareous and siliciclastic rocks and on the turbidite units. Due to the presence of the buried narrow valleys and isolated narrow ridges, this area is prone to a stratigraphic and topographic amplification of the seismic motion [9].

THE LIMIT CONDITION IN EMERGENCY - LCE

The LCE - Limit Condition in Emergency, is the condition whereby, following a seismic event, the urban settlement as a whole suffers physical and functional damage resulting in the interruption of almost all urban functions, including residency. However, the urban settlement preserves the functionality of most of the strategic functions for the emergency and their accessibility and connection to the territorial context.

The analysis involves:

i) the identification of the buildings and areas that guarantee strategic functions for the emergency;

ii) the identification of the infrastructures for accessibility and connection with the territorial context;

iii) the identification of structural elements and individual structural units that may interfere with accessibility infrastructures and connection with the territorial context.

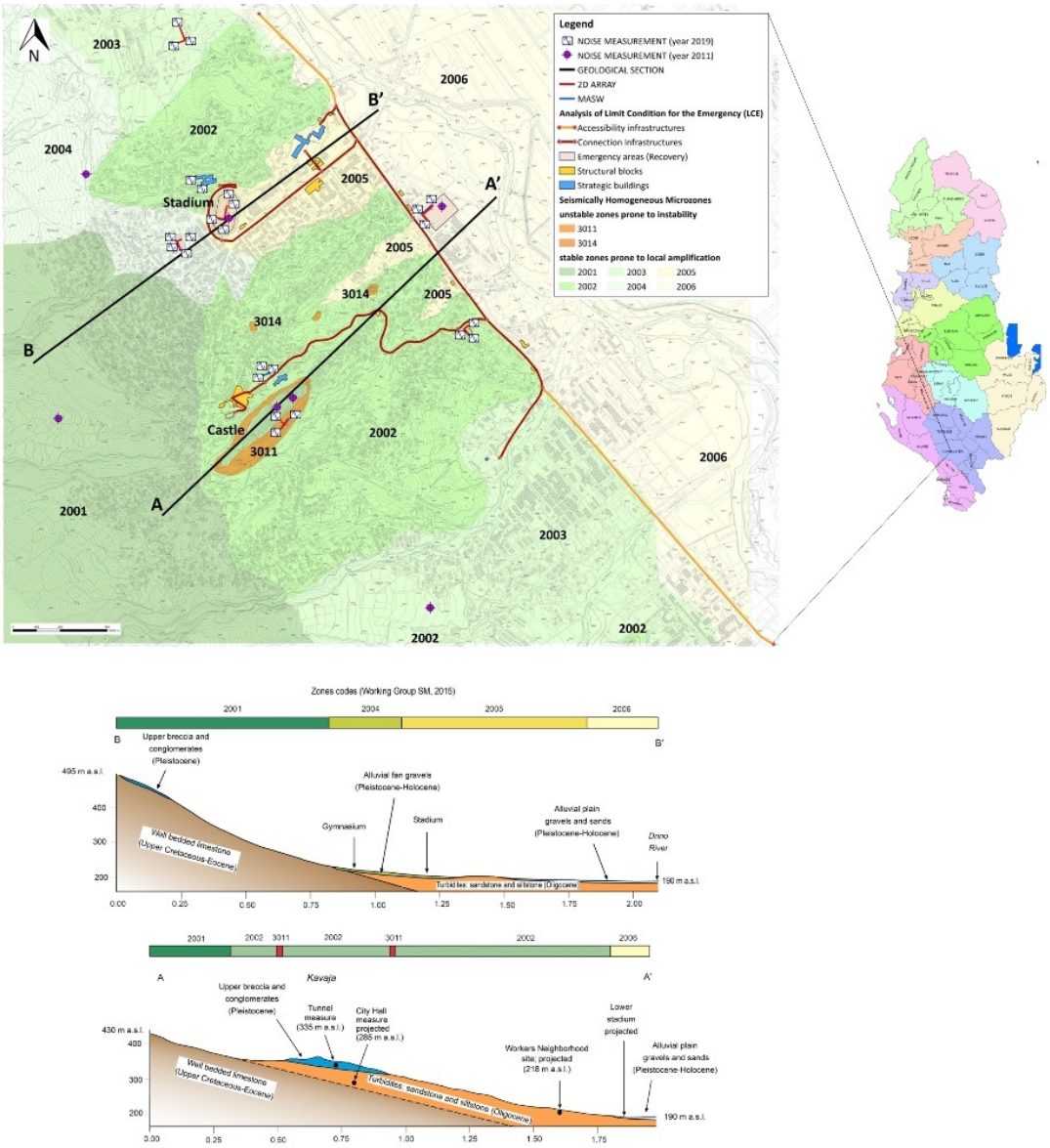


Figure 2. The conjugate approach of the SMS and the LCE of the city of Gjirokastra, allows the systematic association of strictly geological information with the strategic elements functional to emergency management. Basemap is the Seismically Homogeneous Microzones Map modified from Cavinato et al., 2014. Codes 2001:2006 and 3011-3014 are defined according to the Working Group SM, 2015 guidelines [9].

By spatially superimposing the elements of LCE on the microzones identified by the SMS, criteria and guidelines can be defined that are more targeted to the choices of ordinary planning of the territory: i) orienting the choices for the new settlements; ii) defining the eligible interventions in a given area; iii) establishing methods and priorities for intervention in urbanized areas.

An absolute ranking of seismic hazard should include the regional seismic hazard and the amplification due to the geological and geophysical setting [7]. Realizing these kinds of studies before an earthquake occur can help decision-makers to highlight priority intervention areas and to define best

practice for existing structures where higher overall seismic hazard values are expected. For both cities the LCE was conducted in conjunction with SMS (Figure 1 and 2).

CONCLUSION

In this work, it is intended to highlight the indispensable significance of the SMS and the LCE at the level of primary decision-making at urban planning studies and to help resolving a range of problems connected to seismic risk assessment.

The first level of SMS in Durrës is still in process but considering the high seismic activity of the region, the PGA value of 0.268 corresponding to the reference probability of exceedance PNCR=0.10 in TL=50 years [1] the high seismic vulnerability of the buildings and the many uncertainties about the thickness of the Quaternary deposits and the geometry of the depression, the authors strongly recommend the beginning, as soon as possible, of the third level of the SMS for the entire municipality of Durrës. Furthermore, the studies of the local seismic response for all the important and strategic buildings of the city of Durrës must be obligatory.

Preliminary results from 2D arrays fixed the maximum depth that could be investigated and fully described the site effects in the city of Durrës. Detailed engineering-geological and geophysical investigations are needed for the third level of MS. In order to determine the distribution and the thickness of the Quaternary deposits, and to provide an image of the buried morphology for a 3D bedrock modeling of the entire municipality, an accurate array of the gravity survey together with further noise measurements could be the most economic and strategic choice [8].

The authors of this paper emphasize that the studies for the first level of the seismic microzonation for all the cities in Albania are long overdue. They would provide the basis for the third level of SMS in the cities with higher values of peak ground acceleration, agR, such as Durrës, Tirana, Shkodra, Vlora, Saranda, Berat, Gjirokastra, Korça, Pogradeci etc., before the next earthquake hits.

The following step would have to be an analysis of the Emergency Limit Condition – ELC for civil protection planning.

REFERENCES

[1] Aliaj, Sh., Koçiu, S., Muço, B. and Sulstarova, E. (2010). Sizmiciteti, sizmotektonika dhe vleresimi i rrezikut sizmik në Shqipëri. Akademia e Shkencave e Shqipërisë, Tirana.

[2] Koçiu, S. (2004): Induced Seismic Impacts Observed in Coastal Area of Albania: Case Studies. Proceedings of Fifth Int. Conf. on case histories in Geotech. Eng., New York, NY, April 13-17.

[3] Konomi, N. (1980): Harta rajonizimit gjeologo-inxhinierik e zones se Durresit. Shkalla 1:10000.

[4] Mancini, M., Skrame, K., Simionato, M., Muçi, R., Gaudiosi, I., Moscatelli, M. and Daja, Sh. (accepted for 2021): Site characterization in Durrës (Albania) in a seismic microzonation perspective. Bollettino di Geofisica Teorica e Applicata.

[5] Muçi, R., Skrame K., Mancini, M., Gaudiosi, I. and Simionato M. (accepted for 2021): Effect of cement and fly-ash on the geotechnical properties of expansive clay soils. Italian Journal of Geosciences.

[6] Muçi, R., Fociro, O. and Skrame, K. (2018): The effect of lime as a stabilizing agent in plastic clayey soils in Vila hill, Durres, Albania. Muzeul Olteniei Craiova. Oltenia. Studii şi comunicări. Ştiinţele Naturii. Tom. 34, No. 2/2018.

[7] Mori, F., Gaudiosi, I., Tarquini, E., Bramerini, F., Castenetto, S., Naso, G. and Spina, D. (2019). HSM – a synthetic damage-constrained seismic hazard parameter. Bulletin of Earthquake Engineering, 1-24.

[8] Skrame, K. and Di Filippo, M. (2015). The importance of the geophysical methods for the determination of the urban subsurface structures. Rendiconti Online della Società Geolologica Italiana, 33, 92-95.

[9] Skrame, K., Muçi, R., Simionato, M., Benigni, M. S., Gaudiosi, I., Giuffrè, M., Mancini, M. and Moscatelli, M. (2020) New seismic microzonation studies in Albania: from the past to the future. First Break. Vol. 38, Issue 8, August 2020: 39-45.

[10] SM Working Group, Guidelines for Seismic Microzonation, Conference of Regions and Autonomous Provinces of Italy – Civil Protection Department, Rome, (2015).

[11] Solomos, G., Pinto, A. and Dimova, S. (2008): A review of the seismic hazard zonation in national building codes in the context of eurocode 8. Support to the implementation, harmonization and further development of the Eurocodes.

[12] UNDP Albania (2003): Disaster Risk Assessment in Albania – Executive Summary Report. United Nations Development Programme, Albania, Disaster Management and Emergency Preparedness Project, Department for International Development (DFID, UK), Tirana, 105 pp.

Cementitious Grout Method Application on Tunnel Rockbolts and its Effect on Bond and Load Carrying Capacity. A Real-Scale Pull Out Test on Fan River HPP Power Tunnels

Erion Periku[1], Erion Luga[1], Drilon Dushaj[1], Paulin Sheperi[2]

[1]*Department of Civil Engineering, EPOKA University, Albania*
[2]*A.L.T.E.A. & GEOSTUDIO 2000 Sh.p.k, Albania*

ABSTRACT

This paper presents the investigation of 144 in situ rock bolt pull-out tests conducted during the construction of Fan River hydropower plant's power tunnels. The pull-out tests are performed on 22 and 25mm diameter; 3, 4 and 6m usually full grouted rock bolts installed in different parts of the tunnel with different angles to gravitational direction. The pull-out tests were performed to analyze the bond and load carry capacity of rock bolts based on their installation angle and grouting efficiency. To optimize the rock bolt performance, two different grouting methods have been used. The results indicate that rock bolts' bond strength declines as the installation angle goes closer to the gravitational direction and majority of the failure cases are due to grouting problems.

Keywords: Cement grouted rock bolts, pull out test, bond, and load-carrying capacity.

INTRODUCTION

The stability of the excavated tunnel sections is mainly affected by the geological conditions and the dynamic load caused by the blasting process in the drilling and blasting tunnel construction method. The blasting process creates distortions and cracks in the surrounding rock mass, weakening the perimeter of the tunnel. Rock bolts limit rock deterioration to rock mass by transferring loads to solid rock. The nature of the load transfer is driven by three main elements: the type of bolt system, the properties of the cement grout material and the suitability of the rock adjacent to the bolt. [1,2]. According to anchoring systems, rock bolts can be divided into three main groups such as: mechanically fixed rock bolts, friction anchored rock bolts and fully grouted rock bolts. [3]. Flexibility, ease of installation and low cost makes fully grouted rock bolts a method of choice in tunnel engineering [4]. Fully-grouted rock bolts are divided into three standard types SN (Stor Norfors) rock bolts, PG (Post Grouted) rock bolts, IBO (injection bore bolts) rock bolts [5]. For the purpose of our research, only fully grouted SN and PG rock bolts have been tested, the bearing capacity is mainly provided by the shear resistance at the bolt–grout or grout–rock interfaces [6,7]. The length, pattern and severity of the rock bolts are determined based on rock mass quality. Standard rock mass classification for tunnel engineering is the Rock-Mass Rating (RMR) system, Rock-Mass index (RMi), and rock-quality index (Q) system [8]. In the present study, the rock-quality index (Q) system was used to determine the rock mass quality. All the direct support of tunnel-like, shotcrete thickness, wire mesh, steel or plastic fibers, steel ribs, umbrella arches, rock bolts, etc. are determined on-site based on Q value.

Typical SN and PG rock bolt elements and installation are shown in Figure 1. The elements of rock bolt, shown on the left, are hex nut, beveled washer, bearing plate, and steel anchor. A fully grouted rock bolt is shown on the right.



Figure 1. Typical SN and PG rock bolt elements and installation.

Mahrenholtz et al. studied the failure mechanism of post-installed reinforcing bars as end anchorage or as a bonded anchor. The research states that that the failure of a reinforcing bar, post-installed in a hole drilled into a base material like concrete or rock, may occur as a result of: steel failure (rupture or yielding of steel), concrete cone failure (concrete breakout), bond failure (pull-out) and splitting failure (cracking of concrete cover) [9].

Moosavi et al. studied the bond capacity of cement grouted steel bars under constant radial pressure by testing the specimen with a modified Hoek cell. They concluded that grout quality directly affects the bond capacity, emphasizing the importance of quality control of grout preparation and its application [10].

Kılıc et al. analyzed the effect of bar shape on fully grouted rock bolts' pull-out capacity. They have performed laboratory pull-out tests in 24 types of fully grouted rock bolts, out of them: in 3 types or 12.5% steel bar failure occur, in 1 type or 4.17% steel bar-grout failure occur, in 19 types or 83.33% grout failure occur [3].

Clay et al. summarized some practical problems encountered in rock bolts' site applications. They have concluded that only rock bolts that are not adequately grouted may fail in lower forces than the designed ones [5].

As shown also from the abovementioned literature, rock bolt method is a widely used technique for supporting underground excavations or stabilize damaged or cracked rock masses [11]. Their behavior and failure mechanisms are still an important topic of research. Worldwide laboratory tests show that failure of fully grouted bolts is more likely to happen at the bolt-grout interface because of a deboning process that begins when the axial force of the rod exceeds a critical value [4]. Ideally, the bolt is designed and implemented so that the bolt anchored to the solid rock will extend as the cracked rock mass moves towards the open/excavation site [12]. Thus, the bond capacity is the crucial element that makes the system work as designed which is also the main focus of this study.

TESTING MATERIALS

This paper investigates the bond capacity of rock bolts applied to different: rock mass qualities, bolt lengths and bolt inclination angles. Elements affecting bond capacity are rock bolt, grout, and surrounding rock/soil. The rock bolt support systems can be divided into three types: Continuous Mechanically Coupled (CMC) system, Continuous Frictionally Coupled (CFC) system, and Discreetly Mechanical and Frictionally Coupled (DMFC) system [13,14]. The CMC system is widely used among the three, as it is faster, simpler, needs less labor and is cheaper than the others. Also, within the CMC system there are several techniques, from which the cement grout system is the most common [15].

Rock Bolts

The rock bolts in this study were made of standard steel rebar, as shown in Figures 1 and 2 of B500C grade and only two diameters of rock bolts, such as: Φ22 and Φ25 were used. An atomized machinery was employed to arrange the length and properties of the thread. The average mechanical properties of tested rock bolt are shown in Table 1.

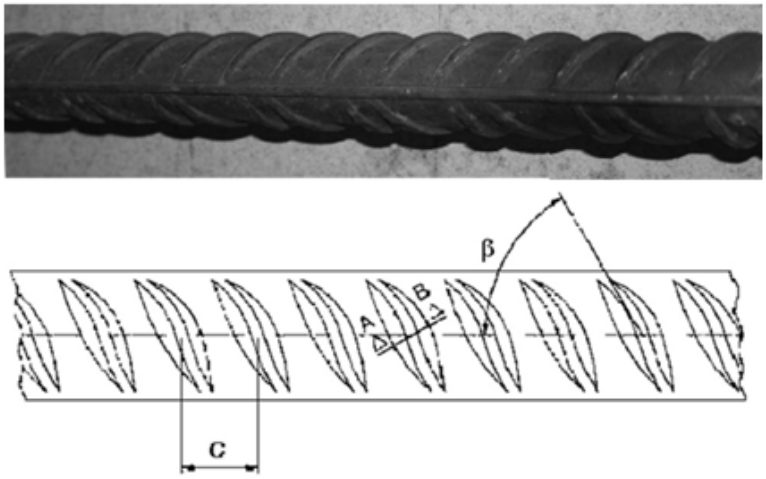


Figure 2. B500C grade steel bar material of which rock bolt is produced, adapted from [4].

Table 1. Rock bolt mechanical properties.

Rock bolt	Effective diameter (mm)	Yield capacity (N/mm²)	Tensile capacity (N/mm²)	Relative Extension (%)
Φ25	25.09	552.13	664.5	21.20
Φ22	22.15	531.96	632.5	19.55

Cementitious Grout

The grout used in this study is a cement-based mixture that protects the rock bolt from corrosion and transfers the bolt's acting forces to the surrounding rock mass [16]. The mix design of cementitious grout, Portland cement, water and necessary admixtures proportions were defined based on site and weather conditions and grouting pump capacities. The laboratory test performed on cementitious grout are: (a) Marsh funnel viscosity, (b) strength, (c) Vicat needle setting time and (d) Bleeding, as shown in Figure 3. The average values of compressive and flexural strength are reflected in Table 2.



(a) (b) (c) (d)

Figure 3. Laboratory test performed on cementitious grout.

Table 2. Properties of cementitious grout and surrounding rock/soil.

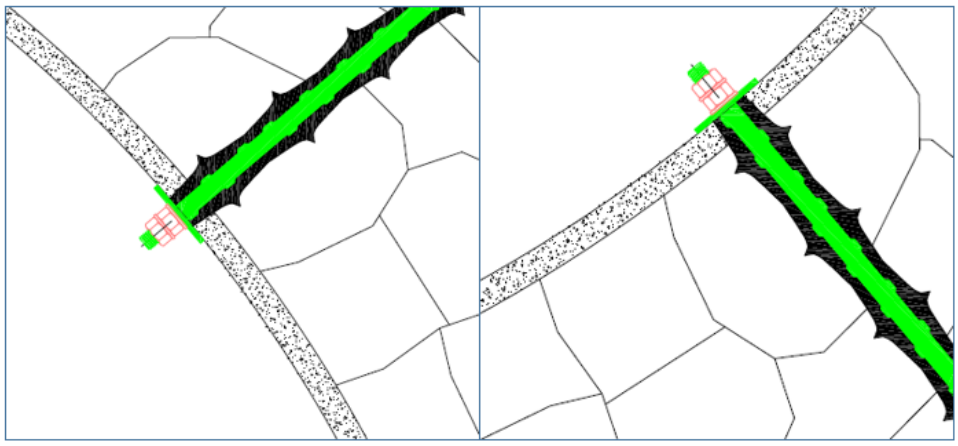
	Compressive Strength (MPa)	Flexural Strength (MPa)
Grout (7 days)	32.31	4.73
Grout (28 days)	43.56	6.67
Rock/soil	64.87	

Surrounding rock/soil

The tunnel axis passes through ultra-basic and basalt rocks. For this study purpose, 16 samples of surrounding rock are tested, and the results are presented in Table 2. Laboratory tests show that the average uniaxial compression strength of rock is 64.87 MPa with a standard deviation of 11.03 [17].

EXPERIMENTAL PROGRAM

The pull-out tests were performed on 22 and 25mm diameter; 3, 4 and 6m usually full grouted rock bolts installed in different parts of the tunnel with different specific angles to gravitational direction.



(a) Bolt inclined upwards (b) Bolt inclined downwards

Figure 4. The direction of rock bolts in a tunnel section.

The rock bolt installation in a specific tunnel section can be of two different directions, bolt inclined upwards and bolted inclined downwards, as shown in Figure 4. The bolts installed in the top head of the tunnel, from 0° to 180°, are inclined upwards, and bolts installed in the bench of the tunnel, from 180° to 360°, are inclined downwards. The tested rock bolts are installed on drilled holes in surrounding rock/soil of 50mm diameter and 3, 4 and 6m depth. The average uniaxial compressive strength in the tested rock is 64.87 MPa. The grout was mixed in a water-cement ratio varying from 0.35 to 0.40. Initially, the rock bolts were grouted as SN, and then the pull-out test was performed.



(a) (b)

Figure 5. Rock bolt pulls out test apparatus.

The pull-out test was performed with the apparatus shown in Figure 5. composed of (a) hydraulic jack and (b) hand pump. Hydraulic jack is composed of housing, cylinder, claw, spindle, bushing and nut, while the hand pump is composed of pump, gage and hose. The manual gauge shown in Figure 5 (b) is connected to a 30 tons' capacity hydraulic jack shown in Figure 5 (a).



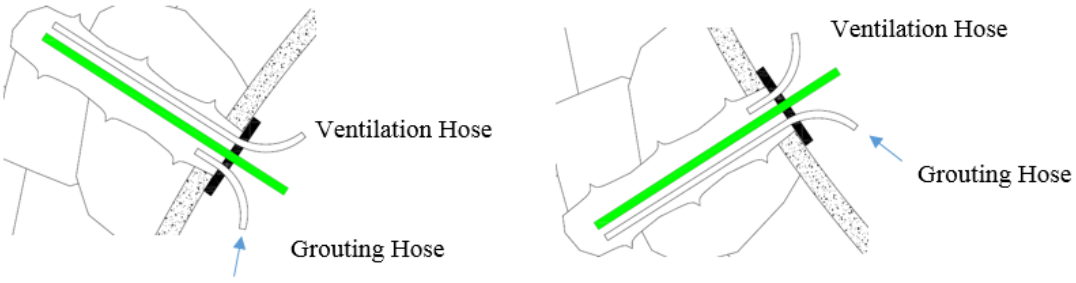
(a) (b) (c)

Figure 6. Rock bolt pull test performed on-site.

Real scale test on bond strength and force carrying capacity of rock bolts is presented in Figure 6. During this study there were performed two types of tests: one defined by technical specifications of construction works of water utilization and project implementation HPP of Fani i Madh and Fani i Vogel river

[18], and another one to determine the ultimate capacities of rock bolt anchors. Figure 6 (a) shows the central hole hydraulic jack bonded on the rock bolt and fixed in the central hole of a 20 mm thick steel plate placed on the shotcrete surface. Figure 6 (b-c) shows the performed test's recording process. The pull-out load is indicated on the loading gauge. An external dial gauge was fixed to measure the displacement of rock bolt with regard to the applied load, and a stopwatch measured the precise experimental time.

The testing procedure is done in compliance with ASTM D4435–08, Standard Test Method for Rock Bolt Anchor Pull Test [19].



(a) Bolt inclined upwards, (b) Bolt inclined downwards

Figure 7. Arrangement of grout for a PG rock bolt.

At the beginning of the investigation and the experimental program, SN rock bolts, also known as mortar embedded anchors, were applied. From the first experimental results, it was observed that all the rock bolts failed at low applied loads, due to bolt-grout bond. In the upward inclined bolts, this phenomenon was even more evident. So, it was decided to test the PG (post grouted) rock bolts as well. The grouting implementation for a PG rock bolt inclined upwards and downwards is shown in Figure 7.

The grout mechanism for upward inclined rock bolts is shown in Figure 7 (a), and for the downward inclined rock bolts are shown in Figure 7 (b). There were used two hoses for each type of rock bolts, one for grouting and the other to release the air out of the drilled hole without creating any pressure. The application process starts with drilling the 50 mm diameter holes up to the respective rock bolt depth. Attach two hoses in the rock bolt, and place them in the drilled hole. For safety reasons during the application process, there were used two different colored hoses; the one used for grouting is transparent while the one used to release the air out is black. After the rock bolt and the attached hoses are inserted, the hole entrance is closed with a plaster. As the plaster is hardened enough, the cement grouting is injected from the grouting hose till some grout came out from the ventilation hose. After that, the hoses are blocked, and the process is completed.

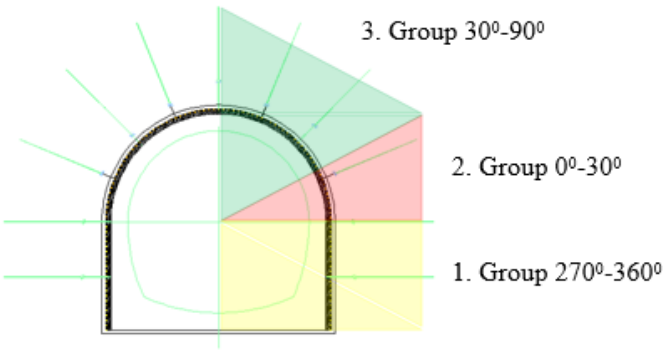


Figure 8. Typical rock bolt application pattern in a tunnel cross-section.

The typical rock bolt application pattern in a tunnel cross-section is shown in Figure 8. The rock bolts are symmetric according to the vertical axis passing from the center of the tunnel, so the details of one half apply in the same way to the other half. At the beginning of this study, we found that the inclination angle directly affects the SN type rock bolt capacity, so we grouped the tested rock bolts into three groups. Rock bolts of the first group, applied in the yellow part of Figure 8, are inclined downwards; second and third groups, applied in the red and green part of Figure 8, are inclined upwards. Upward inclined rock bolts are divided into two groups because the grouting shows different behavior as the inclination angle increases.

RESULTS AND DISCUSSIONS

Table 3. Pull out test results of SN type rock bolts.

Rock Bolt				Grout	Rock Type	Failure	Max.	Failure
Type	Φ	Lenth (m)	Group	(w/c)		Load (kN)	Displacement(mm)	Type
SN	22	3	1	0.37	Moderate	116.54	21	Grout Failure
				0.36	Weathered	112.13	20	Grout Failure
SN	25	3	1	0.38	Moderate	118,27	22	Grout Failure
				0.35	Weathered	115,12	21	Grout Failure
SN	22	3	2	0.35	Moderate	68.45	8	Grout Failure
				0.36	Weathered	67.81	10	Grout Failure
SN	25	3	2	0.39	Moderate	71.24	21	Grout Failure
				0.38	Weathered	69.52	20	Grout Failure
SN	22	3	3	0.36	Moderate	48.36	-	Grout Failure
				0.35	Weathered	46.81	-	Grout Failure
SN	25	3	3	0.39	Moderate	51.29	-	Grout Failure
				0.37	Weathered	50.24	-	Grout Failure
SN	22	4	1	0.38	Moderate	124.58	24	Grout Failure
				0.36	Weathered	120.51	21	Grout Failure
SN	25	4	1	0.38	Moderate	125.68	25	Grout Failure
				0.37	Weathered	125.01	22	Grout Failure
SN	22	4	2	0.37	Moderate	66.28	15	Grout Failure
				0.39	Weathered	65.98	14	Grout Failure
SN	25	4	2	0.36	Moderate	70.59	17	Grout Failure
				0.35	Weathered	71.53	12	Grout Failure
SN	22	4	3	0.38	Moderate	50.27	-	Grout Failure
				0.36	Weathered	52.01	-	Grout Failure
SN	25	4	3	0.37	Moderate	51.98	-	Grout Failure
				0.35	Weathered	52.87	-	Grout Failure
SN	22	6	1	0.36	Moderate	132.52	29	Grout Failure
				0.36	Weathered	133.25	32	Grout Failure
SN	25	6	1	0.35	Moderate	135.69	31	Grout Failure
				0.38	Weathered	137.84	28	Grout Failure
SN	22	6	2	0.38	Moderate	68.51	21	Grout Failure
				0.37	Weathered	67.48	20	Grout Failure
SN	25	6	2	0.36	Moderate	67.21	19	Grout Failure
				0.36	Weathered	68.09	20	Grout Failure
SN	22	6	3	0.37	Moderate	58.83	-	Grout Failure
				0.36	Weathered	56.18	-	Grout Failure
SN	25	6	3	0.36	Moderate	59.37	-	Grout Failure
				0.35	Weathered	55.14	-	Grout Failure

The pull-out test results of SN type rock bolts are shown in Table 3. There are three different rock bolt lengths; for each bolt length, there are three types of arrangement as shown in Figure 8, and for every

arrangement there are three types of the rock mass. In total there is a number of 36 cases. For SN bolt types, there was tested one bolt for each case, so 36 tested bolts.

Table 4. Pull out test results of PG type rock bolts.

Rock Bolt				Grout		Failure	Max.	Failure
Type	Φ	Length (m)	Group	(w/c)	Rock Type	Load (kN)	Displacement (mm)	Type
PG	22	3	1	0.35	Moderate	124.87	32	Grout Failure
				0.35	Weathered	122.36	30	Grout Failure
PG	25	3	1	0.36	Moderate	126.53	28	Grout Failure
				0.37	Weathered	126.04	27	Grout Failure
PG	22	3	2	0.35	Moderate	121.74	27	Grout Failure
				0.35	Weathered	120.35	28	Grout Failure
PG	25	3	2	0.38	Moderate	120.58	26	Grout Failure
				0.38	Weathered	121.98	24	Grout Failure
PG	22	3	3	0.33	Moderate	121.42	28	Grout Failure
				0.35	Weathered	121.35	26	Grout Failure
PG	25	3	3	0.36	Moderate	122.01	26	Grout Failure
				0.37	Weathered	120.94	25	Grout Failure
PG	22	4	1	0.35	Moderate	132.56	34	Grout Failure
				0.35	Weathered	131.48	32	Grout Failure
PG	25	4	1	0.36	Moderate	131.52	32	Grout Failure
				0.37	Weathered	130.78	32	Grout Failure
PG	22	4	2	0.35	Moderate	128.96	33	Grout Failure
				0.36	Weathered	129.04	29	Grout Failure
PG	25	4	2	0.36	Moderate	127.04	30	Grout Failure
				0.35	Weathered	126.89	31	Grout Failure
PG	22	4	3	0.37	Moderate	128.78	30	Grout Failure
				0.36	Weathered	128.05	32	Grout Failure
PG	25	4	3	0.35	Moderate	130.09	31	Grout Failure
				0.35	Weathered	128.56	31	Grout Failure
PG	22	6	1	0.36	Moderate	142.52	38	Grout Failure
				0.36	Weathered	143.25	36	Grout Failure
PG	25	6	1	0.38	Moderate	142.04	39	Grout Failure
				0.37	Weathered	142.52	39	Grout Failure
PG	22	6	2	0.36	Moderate	141.86	38	Grout Failure
				0.35	Weathered	141.25	36	Grout Failure
PG	25	6	2	0.35	Moderate	142.87	37	Grout Failure
				0.36	Weathered	140.65	37	Grout Failure
PG	22	6	3	0.35	Moderate	141.89	36	Grout Failure
				0.35	Weathered	141.57	35	Grout Failure
PG	25	6	3	0.36	Moderate	140.12	38	Grout Failure
				0.35	Weathered	140.36	37	Grout Failure

The pull-out test results of PG type rock bolts are shown in Table 4. Similar to SN type bolts, there are three different rock bolt lengths; for each bolt length, there are three types of arrangement as shown in Figure 8, and for every arrangement, there are three types of the rock mass, so there are 36 cases. For PG bolt types, there were tested three bolts for each case, so in total, there are tested 108 bolts. The comparison of average values of Table 3 and Table 4 are shown in Table 5.

Each value shown in Table 3 is the value of the pull-out test results carried in a single rock bolt, each value shown in Table 4 is the average value of the pull-out test results carried in three different rock bolts, each value shown in the SN columns of Table 5 is the average value of the pull-out test results carried in four different rock bolts and each value shown in the PG columns of Table 5 is the average value of the pull-out test results carried in twelve different rock bolts.

Table 5. Comparison of results.

Length (m)	Group	Failure Load (kN)		Max. Displacement (mm)		Increase in Load Cap. (%)	Increase in displacement (%)
		SN	PG	SN	PG		
3	1	114.34	124.95	21.00	29.25	9.28	39.29
	2	69.25	121.16	14.75	26.25	74.96	77.97
	3	49.17	121.43	-	26.25	146.96	-
4	1	123.95	131.58	23.00	32.50	6.16	41.30
	2	68.60	127.98	14.50	30.75	86.56	112.07
	3	51.78	128.87	-	31.00	148.88	-
6	1	134.82	142.58	30.00	38.00	5.76	26.67
	2	67.82	141.66	20.00	37.00	108.88	85.00
	3	57.38	140.98	-	36.50	145.70	-

There were tested 36 different SN type rock bolts out of which 12 were inclined downward, and 24 were inclined upward. Half of the upward inclined rock bolts were installed in Group 2. (between 0^0 and 30^0) and the other half have installed in Group 3. (between 30^0 and 90^0). The highest ultimate load capacity/ (failure load) and maximum displacement measured in downward inclined ones are respectively 137.84 kN and 32.00 mm. While there was possible to take some values for the downward inclined rock bolts, it was not the same for the upward inclined ones. The lowest ultimate load capacity/(failure load) measured on upward inclined is 46.81 kN (34% of the highest one), and there could not be taken any record in the displacement of the Group 3. upward inclined rock bolts.

The majority of rock bolts installed in tunnel construction, as shown in Figure 8, are upward inclined, so it is crucial to be sure that they are correctly installed and fully grouted. As previously mentioned, the failure of fully grouted bolts most likely occurs at the bolt-grout interface; in our study, 100% of failure occurred at the bolt-grout interface.

Rock bolt load carry capacity depends on two main elements: 1. grout mechanical properties 2. bolt diameter and length. Increasing the values of these two parameters will directly increase the bolt carry capacity; however, it must be emphasized that the bolt upper limit is the ultimate tensile strength of the bolt materials.

The results show that rock bolt load carry capacity decreases as the angle of upward inclined bolts increases. This explains that the application of SN rock bolts, especially for the upward inclined ones, causes problems in proper grouting; consequently, the bolt–grout interface is not well achieved. It can be easily seen in Table 4 that there are significant differences in load carry capacity of the same rock bolts having opposite incline direction. A downward inclined rock bolt has a load carry capacity more than two times higher than an upward inclined rock bolt in the same bolt type, grout, and rock properties. To achieve a better bolt–grout interface, the SN rock bolts were replaced with PG ones.

The results of PG bolt pull out test results are better, as shown in Table 4. By applying PG bolts, we achieved much better results in load carry capacity and bolted maximum displacement, as shown in Table 5. Replacing SN bolts with PG ones increased the load carry capacity to 148.88% and maximum displacement until the 112.07% level.

CONCLUSION

This study is critical because it was conducted in a real-scale rock bolt application and working environment. The study tested 144 rock bolts with a total length of 624m size, which is impossible to perform in the laboratory or small or medium projects.

The rock/soil on which the tunnel is built, and the rock bolts installed must be tested at representative intervals. Although basalt and ultrabasic rock formations have an ultimate compressive strength capacity (USC) above 100 MPa, in our case, the rock has an average (USC) 64,87 MPa.

In their entirety, the tested SN bolts have low values in bearing capacity and small displacement. SN bolts that are inclined upwards have an even smaller bearing capacity and almost zero displacements; this is due to an improper grouting method that fails to fill the drilled hole.

The change of the grouting method from SN to PG has dramatically improved their bearing capacity and maximum displacements. The bearing capacity of the bolts has increased to values ranging from 5.76% to 148.88%, and the maximum displacements have increased to values ranging from 26.67% to 112.07%

In our study, the bolt-grout interface's failure of grouted bolts occurred due to the deboning process and/or grout failure. This clearly expresses the importance of grouting as a material, its mechanical properties, and its application in the field.

It is suggested that PG should be set as a conditional grouting method for tunnel rock bolts. Our study proved that it filled the drilled hole fully, leading to a better bolt-cement-rock bond.

REFERENCES

[1] Das, R., & Singh, T. N. (2020). Effect of rock bolt support mechanism on tunnel deformation in jointed rockmass: A numerical approach. Underground Space.

[2] Li, C.C. (2017) Principles of rockbolting design, Journal of Rock Mechanics and Geotechnical Engineering 9(3), 396-414

[3] Kılıc, A., Yasar, E., & Atis, C. D. (2003). Effect of bar shape on the pull-out capacity of fully grouted rockbolts. Tunnelling and Underground Space Technology, 18(1), 1-6.

[4] Thenevin, I., Blanco-Martín, L., Hadj-Hassen, F., Schleifer, J., Lubosik, Z., & Wrana, A. (2017). Laboratory pull-out tests on fully grouted rock bolts and cable bolts: Results and lessons learned. Journal of Rock Mechanics and Geotechnical Engineering, 9(5), 843-855.

[5] Clay, R.B. Takacs, A.P. (1996) Contractual aspects of testing shotcrete and rockbolts, International SCA/ACI Conference Proceedings, E&FN Spon, London.

[6] Kılıc, A., Yasar, E., & Celik, A. G. (2002). Effect of grout properties on the pull-out load capacity of fully grouted rock bolt. Tunnelling and underground space technology, 17(4), 355-362.

[7] Zhan, Y., Zheng, P., Wang, H. & Wang, Q., (2020) The Influence of Radial Stress on Mechanical Properties of Anchorage Structure, Applied Sciences, 10(20), 7029

[8] Kim, H., Rehman, H., Ali, W., Naji, A. M., Kim, J. J., Kim, J., & Yoo, H. (2019). Classification of Factors Affecting the Performance of Fully Grouted Rock Bolts with Empirical Classification Systems. Applied Sciences, 9(22), 4781.

[9] Mahrenholtz, C., Eligehausen, R., & Reinhardt, H. W. (2015). Design of post-installed reinforcing bars as end anchorage or as bonded anchor. Engineering Structures, 100, 645-655.

[10] Moosavi, M., Jafari, A., & Khosravi, A. (2005). Bond of cement grouted reinforcing bars under constant radial pressure. Cement and Concrete Composites, 27(1), 103-109.

[11] Cao, C., Jan, N., Ren, T., & Naj, A. (2013). A study of rock bolting failure modes. International Journal of Mining Science and Technology, 23(1), 79-88.

[12] He, L., An, X. M., & Zhao, Z. Y. (2015). Fully grouted rock bolts: an analytical investigation. Rock Mechanics and Rock Engineering, 48(3), 1181-1196.

[13] Chang, Q., Zhou, H., Xie, Z., & Shen, S. (2013). Anchoring mechanism and application of hydraulic expansion bolts used in soft rock roadway floor heave control. International Journal of Mining Science and Technology, 23(3), 323-328.

[14] Cai, Y., Esaki, T., Jiang, Y. (2004) Arock bolt and rock mass interaction model, International Journal of Rock Mechanics & Mining Sciences, 41, 1055–1067

[15] Zhu, C., Chang, X., Men, Y., & Luo, X. (2015). Modeling of grout crack of rockbolt grouted system. International Journal of Mining Science and Technology, 25(1), 73-77.

[16] Ozhan, H. O., & Guler, E. (2018). Critical tendon bond length for prestressed ground anchors in pull-out performance tests conducted in sand. International Journal of Civil Engineering, 16(10), 1329-1340.

[17] Bukaçi E. Korini T. Periku E. Allkja S. Sheperi P. (2016) Reliability Analysis for Tunnel Supports System by Using Finite Element Method. American Journal of Engineering Research, 5(1), 1-08.

[18] Technical specifications of construction works (2014) Water utilization and project implementation HPP of Fani i Madh and Fani i Vogel river.

[19] ASTM D4435 – 08, Standard Test Method for Rock Bolt Anchor Pull Test.

Evaluation of Seismic Pounding between two Adjacent Reinforced Concrete Buildings from Albanian Practice

Margarita Dajko[1], Hüseyin Bilgin[1]

[1]*Department of Civil Engineering, EPOKA University, Albania*

ABSTRACT

Seismic pounding is the colliding action between two adjacent structures that occurs during earthquake vibrations. Due to insufficient separation gap between buildings that own different dynamic characteristics, structural damages to both structural and non-structural elements are magnified during the impact of buildings. Since a country like Albania is considered to have moderate-size seismicity, it is important to provide and check the necessary separation distance to avoid the impact between structures. A parametrical approach is followed up in this study to evaluate the sufficient seismic gap in the middle of two existent Reinforced Concrete (RC) structures. Ten pairs of structural models are analyzed in Sap2000 by using the Equivalent Static Force Method (ESFM). The change of structural parameters such as concrete grade, seismic zone factor and story height are inspected to study the influence they have in the separation gap between the structures. At the end, a comparison with a similar study is done and conclusions, as well as recommendations for further studies are generalized.

Keywords*: Seismic Pounding, Separation Gap, Sap2000, Adjacent Buildings, Eurocode, Static Analysis*

INTRODUCTION

Pounding phenomenon occurs during the vibration and the existence of small gaps between the existing structures. Buildings are very often constructed close to one another, as the example of residential structure complexes or in highly populated cities, due to the high price for land usage. So, for this reason, buildings have often been found to collide with each other during the response to earthquake ground motions. The insufficient gap is not only a result of the high cost of the land, but also because the past seismic code provisions did not provide specific guides to calculate the most probable minimum building separation needed to prevent impact [1].

Albania is a developing country, and more buildings are being constructed and land usage limitation has started to be a present issue. Due to this, structures are built very close to each other and sometimes without providing the safe separation distance in-between. Moreover, it is categorized as a moderate seismic country, being one of the most active seismic zones in Europe. Since buildings are prone to frequent earthquake ground motions seismic, pounding is a phenomenon that occurs whenever the safety separation distance between adjacent buildings is not provided.

Pounding has been observed in global earthquakes including here the Alaskan seismic motion of 1964, the San Fernando earthquake of 1971, the Mexico City earthquake of 1985, the Chi-Chi earthquake of 1999, the Bhuj earthquake of 2001, Chuetsu-Oki Japan earthquake of 2007. [2] In Europe, pounding has been observed during the L'Aquila earthquake of 2009, during the earthquake in Athens, in 1999, etc. [3] In Albania, the latest severe earthquake was the one that happened in November 2019, in Durres. [4]

Pounding or hammering effect has been observed between adjacent structures during the site investigations after the Durres earthquake and the main reason is the inadequate seismic gap [5].

Several works, experiments and research have been carried out to understand the occurrence this phenomenon analytically and numerically. Namboothiri has made a generalising summary on the concept of seismic pounding by quoting that the main cause for the pounding effect is the lack of enough gap distance in between the adjacent structures [6]. Raheem, states in his study that pounding can be an issue to the closely built buildings if a seismic excitation occurs because floor accelerations and inter-story deflections are significantly amplified, threatening the functionality of the structure [7]. Different mitigation methods are introduced, but the simplest one is the provision of enough separation gap between buildings through codes and standards.

CODE RECOMMENDATIONS FOR SEISMIC SEPARATION GAP

The square root of the sum of squares (SRSS) and the absolute sum method are the most elementary formulae and they are implemented in seismic codes such as **IBC**, *International Building Code*. In some other codes the heights of adjacent buildings are taken into consideration while calculating the separation gap. According to Federal Emergency Management Agency (FEMA 356), minimum seismic gap for adjacent buildings is calculated with the SRSS formula. The value of the separation gap should be less than 4% of the height of the level under consideration above grade at the position where the potential pounding might occur. The Egyptian code of practice and the Eurocode 8 employ formula of the square root of the sum of squares (SRSS). [8] The Indian Standard IS 1893:2016 states that the seismic gap between two adjacent structures is equal to the response reduction factor (which in Eurocode 8 is denoted by letter "q") times the sum of floor displacements u_i and u_j of the buildings. The default value of the reduction factor in Eurocode 8 for R/C ductile buildings is equal to 6, while in the Albanian Earthquake Resistant Design Regulations 1989, the reduction factor is 5 [9]. During the past 50 years, most of structures in Albania have been designed according to Albanian national code. The code was lastly updated in 1989 and it is still in force (KTP-89), as due to Albanian legislation in the construction field, the construction of buildings still must have to follow the KTPs (Albanian Technical Codes) [10].

STRUCTURAL MODELING

In order to observe seismic pounding between adjacent reinforced concrete buildings, G+11 and G+7 bare framed building models are selected and designed. Buildings which are modeled are two symmetric eleven story and seven story RC residential buildings with equal story height. Both buildings are designed as 2D frame models with fixed supports at the ground level (Figure 1). Sap2000 v.16.0.0 is utilized to run the linear static analyses.

For this study, a parametric approach is followed, where the systems of structures are analyzed in three general cases. The variables considered to evaluate the separation gap (SG) are the concrete class, seismic zone factor and story height. In the first case, three distinct concrete classes (C) are considered as follows, C20/25, C25/30 and C30/37. For two other cases C is taken as C25/30. While, for the second case, the influence of the seismic zone factor (Z) on separation gap is taken into consideration. The selected factors are 0.30, 0.25, 0.20 and 0.15. The seismic zone for the first and the third case is taken as 0.25, as Korca is rated as an active seismic zone in Albania. Lastly, for the third case, the change of SG with the story height is observed, where three different story levels 2.8m, 3.0m and 3.5m are chosen. The height (H) of every column is the vertical floor to floor distance. The heights of each story are the same in both structures. For the first and the second case, the heights are 3.0 m.

Two representative R/C frames of structures are modelled in Sap2000 by using the technical plans

of the buildings. Frames consist of columns with (40 cm x 40 cm) dimensions and beams with (35 cm x 30 cm) dimensions. The number of bays in y direction for the 11-th story frame is 3, with 5 m spacing each. Meanwhile, for the 7-th story building the number of bays is 4, where the width of each bay is 5 m. The frame is assumed to be resting on soil of class C, according to Eurocode classifications. Steel bar class is S500. The thickness of the slabs is 15 cm. The concrete unit weight is taken as 25 kN/m^3. The frames are loaded under the dead loads (DL), live load (LL), wall load (WL) and earthquake loads (EQ). According to Eurocode, the loads are combined as in the following equations: DL+EQ, DL+EQ+0.33LL, 1.35DL+1.5LL, DL+1.5LL.

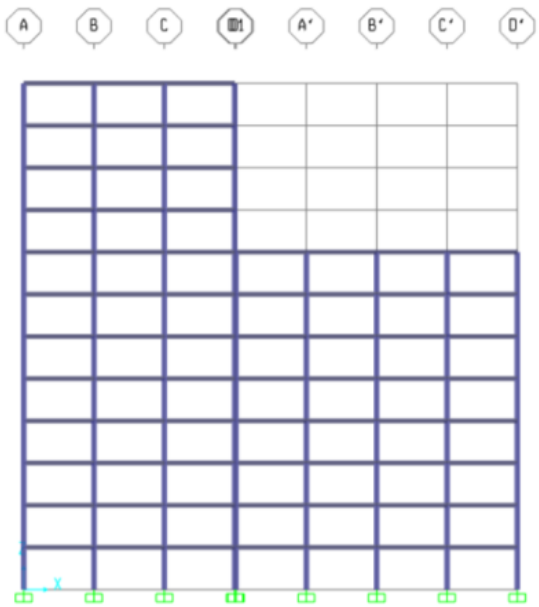


Figure 1. Elevation view of G+7 & G+11 building

ANALYSIS AND RESULTS

In this paper, all two-dimensional representative models and analysis are performed in Sap2000. Structures are loaded under DL, LL and EQ combinations, as it is indicated in Eurocode 2 [11]. Different evaluations for SG through square root of the sum of squares method (SSRSS), absolute sum method (S_{ABS}), IS1893, 2016 provision $Sq^*(u_i+u_j)$ and FEMA 356 maximum SG S_{max}, are done. The calculations for each evaluation methods for SG are tabulated in the table. N1 and N2 are the numbers of stories of the first structure and second building, respectively. From the results in the table, the SRSS method estimates the minimum values of SG, but it is not an adequate approach to follow in case out of phase vibrations occur simultaneously. So, for a safer evaluation, the S_{ABS} method is used to calculate the optimal SG. The $S_{q^*(ui+uj)}$ and S_{max} give overestimated amount of SG, which is not convenient due to limitations of land usage. So, for the graphs and results, the S_{ABS} numerical values are used. The SG provision calculation according to KTP-89 is also evaluated, to check and compare the results with Eurocode and other provisions. According to KTP-89, the minimum seismic joint is calculated using Eq. (1): [12].

$$\mathbf{SG= u_i+u_j+2cm} \quad (1)$$

Table 1: Calculation for Separation Gap

Building Combination	C	Z	H	N1	N2	S_{ABS} (cm)	S_{SRSS} (cm)	$S_{q*(ui+uj)}$ (cm)	S_{max} (cm)
1	20	0.25	3.0	12	8	11.3907	8.967373	68.3442	96
2	25	0.25	3.0	12	8	11.2834	8.896947	67.7004	96
3	30	0.25	3.0	12	8	11.2322	8.840752	67.3932	96
4	25	0.30	3.0	12	8	13.6723	10.76199	82.0338	96
5	25	0.25	3.0	12	8	11.2834	8.896947	67.7004	96
6	25	0.20	3.0	12	8	8.987	7.072979	53.922	96
7	25	0.15	3.0	12	8	6.8367	5.3795	41.0202	96
8	25	0.25	2.8	12	8	9.2692	7.292811	55.6152	89.6
9	25	0.25	3.0	12	8	11.2834	8.896947	67.7004	96
10	25	0.25	3.5	12	8	13.3747	10.68654	80.2482	112

where C is concrete class, Z is seismic zone factor, H is story height, N1 is the number of stories for building 1 and N2 is the number of stories for building 2

Table 2: Calculation for Separation Gap according to KTP-89

Building Combination	C	Z	H	N1	N2	KTP-89 (cm)
1	20	0.25	3.0	12	8	13.3907
2	25	0.25	3.0	12	8	13.2834
3	30	0.25	3.0	12	8	13.2322
4	25	0.30	3.0	12	8	15.6723
5	25	0.25	3.0	12	8	13.2834
6	25	0.20	3.0	12	8	10.987
7	25	0.15	3.0	12	8	8.8367
8	25	0.25	2.8	12	8	11.2692
9	25	0.25	3.0	12	8	13.2834
10	25	0.25	3.5	12	8	15.3747

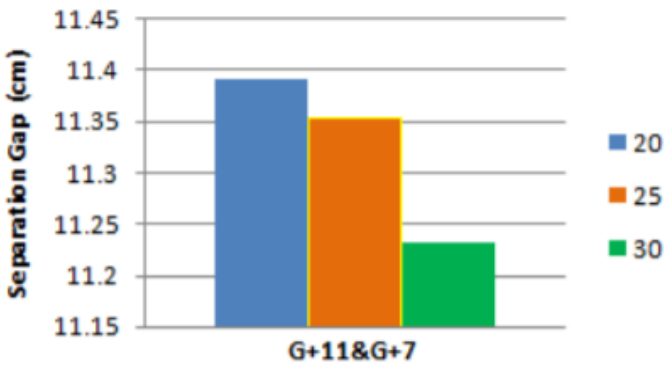


Figure 2. Variation of Separation Gap with Grade of Concrete

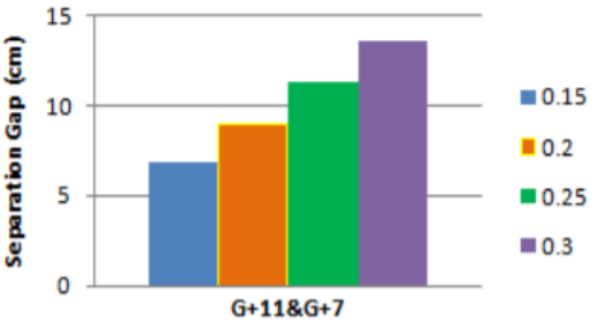


Figure 3. Variation of Separation Gap with Seismic Zone Factor



Figure 4. Variation of Separation Gap with Story Height

By comparing all the results coming from the cases, the most critical case is considered the one with the highest seismic zone factor. Due to the large impact, both buildings suffer greater damages during the earthquake. So, in order to prevent serious damages, the provision of sufficient SG is very crucial while designing adjacent structures. By analyzing the first case, it can be noticed that by increasing the concrete class (C), the SG between adjacent structures decreases. The percentage of decrease for SG is calculated to decrease with the increase of the concrete class.

Meanwhile, in the case number two it is observed that with the increase of the zone factor, the SG gets larger. For the increase of zone factor from 0.15 to 0.20, the percentage increase is 31.5%, for the increase from 0.20 to 0.25, the percentage increase is 25.5 % and for the increase from 0.25 to 0.30, the percentage increase is 21.2%. For the case number three, where the variable is the change of story level, it is observed that with the increase of story height, the lateral displacements of the structures increase. With the increase of story height from 2.8m to 3.0m, the SG increases by 21.7% and with the increase of story height from 3.0m to 3.5m, the SG increases by 18.5%.

CONCLUSIONS

Since the urbanization rate is increasing day by day, the available land is very limited, and this results in higher costs of land and closely built structures. In order to avoid the seismic pounding, which is a serious issue during an earthquake, a solution for such problem is the provision of a safe separation gap between adjacent structures. For that reason, the focus of the work has been to evaluate the minimum separation gap which provides enough security and safety during seismic vibrations of adjacent structures.

- It has been noticed that in most of the studies and code provisions, SG is evaluated based on the

overall elevation of buildings, meanwhile this study gives an emphasis in the influence of other parameters such as concrete class, seismic zone factor and story height. By analyzing these parameters in the buildings, it is concluded that with their variation, the SG changes as well.

- All results presented in this study are derived from linear static analysis performed on regular two-dimensional RC framed structures.
- It can be noticed that by increasing the concrete class (C), the SG between adjacent structures decreases. The percentage of decrease for SG is calculated to decrease with the increase of the concrete class (0.94% and 0.45%). Even though providing a higher concrete class will reduce the spacing of separation gap, for construction companies this approach might increase the total cost of the project, which is not convenient, especially for Albanian practices. Beside this, considering the amount of percentage change, the difference of the SG is not very significant.
- For the change of zone factor from 0.15 to 0.20, the percentage increase is 31.5%, for the increase from 0.20 to 0.25, the percentage 35 increase is 25.5 % and for the increase from 0.25 to 0.30, the percentage increase is 21.2%. With the increase of story height from 2.8m to 3.0m, the SG increases by 21.7% and with the increase of story height from 3.0m to 3.5m, the SG increases by 18.5%.
- Based on the limited number of the analyses and the constraints considered in this study, the required SG calculated by using IS1893, 2016 provision $Sq^*(u_i+u_j)$ and FEMA 356 maximum SG S_{max} values are remarkably higher than the values calculated in this study, which is not convenient for land usage and cost.
- The closest building combination for the current existing set of buildings is the combination 2. Since the existent buildings are designed and constructed based on Eurocodes, the SG of the adjacent buildings is calculated using SRSS method. For building combination 2, according to SRSS method, the SG is 8.896947cm. The current separation joint between the structures is 10 cm. This means that the model results are in consonance with the real provided gap.
- The KTP-89 provision from Albanian Seismic Design Code requires a minimum separation gap that is larger than Eurocode minimum separation gap required. From the safety perspective we can say that the Albanian practice provides a safer seismic joint, but from the economic perspective we would say that it is more costly to implement it due to high price of land usage.

RECOMMENDATIONS FOR FUTURE RESEARCH

This study was focused only on reinforced concrete, mid-rise buildings designed by Eurocodes, meanwhile in Albania most of the buildings are constructed using old Albanian code practice or without any code. For an accurate estimation of SG between adjacent buildings in Albanian practice, further studies should include in investigation different types of structure. 36 Buildings are assumed as symmetrical in plan and structural irregularities are not included. Further investigations can be done taking into consideration asymmetrical structures with irregularities and non-linear analysis can be performed for more realistic results.

NOMENCLATURE

ABS	Absolute Sum Method
C	Concrete Class
DL	Dead Load in kN/m^2
EQ	Earthquake Loading

ESFM	Equivalent Static Force Method
FEMA	Federal Emergency Management Agency
H	Storey height in meters
LL	Live Load in kN/m^2
N1	Number of Floors of Structure 1
N2	Number of Floors of Structure 2
q	Response Reduction Factor
RC	Reinforced Concrete
S_{ABS}	Separation Gap as per ABS method in cm
SG	Separation Gap in cm
S_{max}	Separation Gap as per code FEMA 356 maximum SG provisions in cm
$S_{q*(ui+uj)}$	Separation Gap as per IS1893-2016 provision in cm
SRSS	Square Root of Sum of Squares Method
u_i	Maximum Displacement of Structure 1 at pounding location in cm
u_j	Maximum Displacement of Structure 2 at pounding location in cm
WL	Wall Load
Z	Seismic Zone Factor

REFERENCES

[1] M. J. Favvata, "Key issues regarding interaction of adjacent RC structures," WIT Transactions of the Built Environment, 2015.

[2] C. Rajaram and R. P. Kumar, "Study on Impact Between Adjacent Buildings: Comparison of Codal Provisions," in 15th World Conference on Earthquake Engineering, Lisbon , 2012.

[3] R. Jankowski and S. Mahmoud, "Earthquake-Induced Structural Pounding," Switzerland: Springer International Publishing, 2015.

[4] E. Lekkas, S. Mavroulis, C. Filis and P. Carydis, "The September 21, 2019 Mw 5.6 Albania," Newsletter of Environmental, Disaster, 2019.

[5] H. Bilgin, M. Leti, M. Hysenlliu and A. Bidaj, "The Adriatic, Albania Earthquake of November 26, 2019 Technical Report, September 2020," DOI: 10.13140/RG.2.2.27842.40649, 2020.

[6] V. P. Namboothiri, "Seismic Pounding of Adjacent Buildings," International Research Journal of Engineering and Technology (IRJET) , pp. 1443-1448, 2017.

[7] S. E. Raheem, "Mitigation measures for earthquake induced pounding," Bulletin of Earthquake Engineering, pp. 1706-1724, 2014.

[8] M. Abdel-Mooty, M. Raafat and N. Zaki, "Evaluation of Seismic Pounding between Adjacent Buildings," Fifth International Conference On Advances in Civil, Structural and Mechanical Engineering, 2016.

[9] L. Sanchez-Ricart, "Reduction factors in seismic codes: On the components to be taken into account for design purposes," Georisk Assessment and Management of Risk for Engineered Systems and Geohazards, pp. 208-229, 2010.

[10] Q. Sizmiologjike and D. e. Projektimeve, "Kusht Teknik Projektimi per Ndertimet Antisizmike KTP-N.2-89," 1989.

[11] The European Union Per Regulation, "Eurocode 2: Design of concrete structures," 2004.

[12] "KTP-N2-89 Albanian seismic design code," 1989.

The alternative stormwater system versus the traditional piped stormwater system

Alket Kumaraku[1], Eduart Bllloshmi[2], Lavdim Osmanaj[3]

[1] Department of Hydraulic and Hydrotechnics, Polytechnic University of Tirana, Albania,
[2] Department of Geodesy, Polytechnic University of Tirana, Albania
[3] Prishtina University, Kosovo

ABSTRACT

The urbanization process is an issue concerning many branches of urban planners and civil engineering, not only to ensure proper spaces and environment or living places, but moreover to offer a comfortable manner of life, serving to the people by all the types of services needed. Stormwater drainage system is a type of service not directly connected to people daily living activities, such as drinking water, electricity, etc., but directly to their properties and indirectly to their outside activities, such as work, leisure time, etc. Despite of the urbanization process, which is going to be increased in many big cities, the intensity of the rainfall is also going to be increased more and more due to climatic changes. Nowadays, we are facing more rare rainfalls, but with more and more severity and higher intensity (the less frequent intensities forecasted before are happening more frequently). Then, which of this phenomenon is the most likely to impact on highest levels/volumes of surface runoff, in order to take the proper measures?

In this article, to express better the up-mentioned impact, it is developed a hydraulic model of a city wastewater combined system. The model has been developed based on the city urban plan and in the registered rainfall intensities for this city. During the model construction, there are performed preparatory work in to fronts. The first work has been based on the division of the urban area into storm water catchments, to be also in conformity with the pipelines trace and connection, from the upper and farthest point of each part of the system inside the catchment, to the discharge point into the river. Another issue is the exact value of the runoff coefficient in the respective areas. The runoff coefficient is function of the surface type, the impervious vs. pervious surfaces inside a catchment, the slope of the surface where runoff is created, etc. The next goal of the preparatory work for the model is to define the IDF curves, for different rainfall intensities' return periods and durations. Upon hydraulic model development, different scenarios are created. The scenarios have taken into the consideration the change of the urban area and its development, vs the same rainfall intensities and the change of rainfall intensities vs the stable and not dynamic urban process.

***Keywords**: SUDS, attenuation measures, stormwater system, hydraulic modelling*

GENERAL

The stormwater system has been changed over times and its elements have been developed during these periods. So, from the simple open channel as gutters, channels, grated channels etc., it has been later developed as piped system, in order to avoid the contact of the human being with these waters, as per aesthetically or hygienic motives.

The elements of the piped or even grated or other types of stormwater systems have been developed during the years, from concrete pipes and manholes, brick-wall manholes, and to the latest ones, plastic pipes and plastic manholes (with also composite material covers).

The purpose of all of these elements and the whole system is to drain and deliver away from the urban area (or the runoff "creation" flows), the whole runoff waters. The waters are delivered and discharged to the natural main watercourses, such as streams, rivers, lakes or even seas. The runoff flow depends as much as from the physical characteristics of the urban areas surfaces, and also from the rainfall intensity parameters (duration, frequency, etc.). The surfaces characteristics are changing over the years, turning from the natural permeable areas to the paved impermeable ones. The rapid urbanization of the cities, accompanied by the increase of the impervious area, is not followed by real-time response in the re-dimensioning of the piped system part affected by the increase of the impervious area. These issues are actually a real challenge in stormwater system concept.

This problem is going to be not only an economical issue (due to high costs of piped system construction) but it is going to be an environmental issue. The economic issue is overcome in many areas (the availability of the money in rich countries and the frequent floods in poor countries), but the environmental issue cannot be solved if not proper measures or change in the stormwater drainage system concept change.

The environmental issue and the negative impacts generated during the storms by the rapid urbanization process are mainly:

- The runoff water management on the ground surface;
- The underground water table preservation;

There are given 2 examples how the urbanization is impacting the increase of the runoff[1]

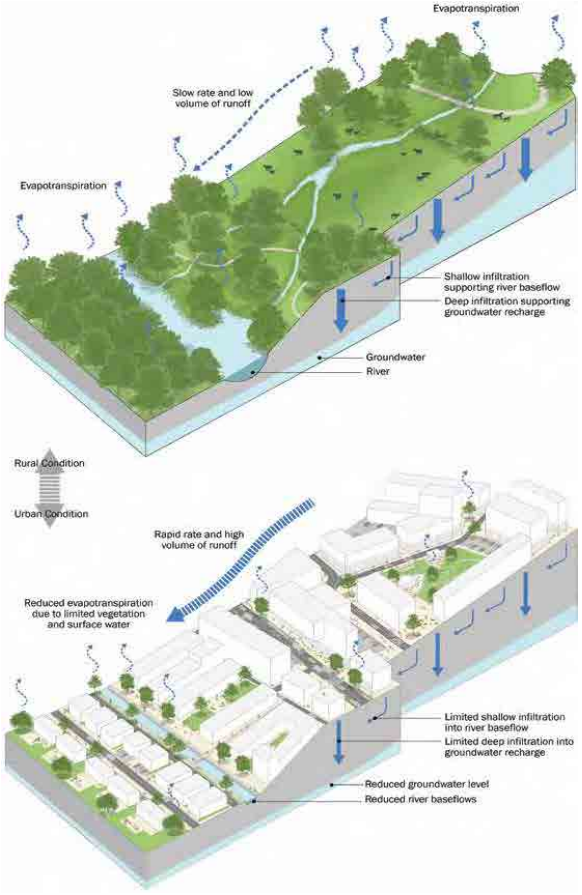


Figure 1. The change of runoff flow due to urbanization process

The alternative solution, which are spreading and finding more and more use in the urban area design, is the use of sustainable drainage systems, or the so-called SUDS.

[1] The SUDS Manual C753 by CIRIA

THE SUSTAINABLE DRAINAGE SYSTEMS – SUDS

The sustainable drainage system (hereinafter SUDS) concept has derived mostly by the 2 (two) up-mentioned problems (or negative impacts) generated by the stormwaters in the impervious areas.

The main purpose is that the surface water should be managed for maximum benefit, now and in the future. The sustainable drainage systems are designed to maximize the opportunities and benefits we can secure from surface water management. There are four main categories of benefits that can be achieved by SUDS: water quantity, water quality,amenity and biodiversity. These are referred to as the four pillars of SUDS design [1]:

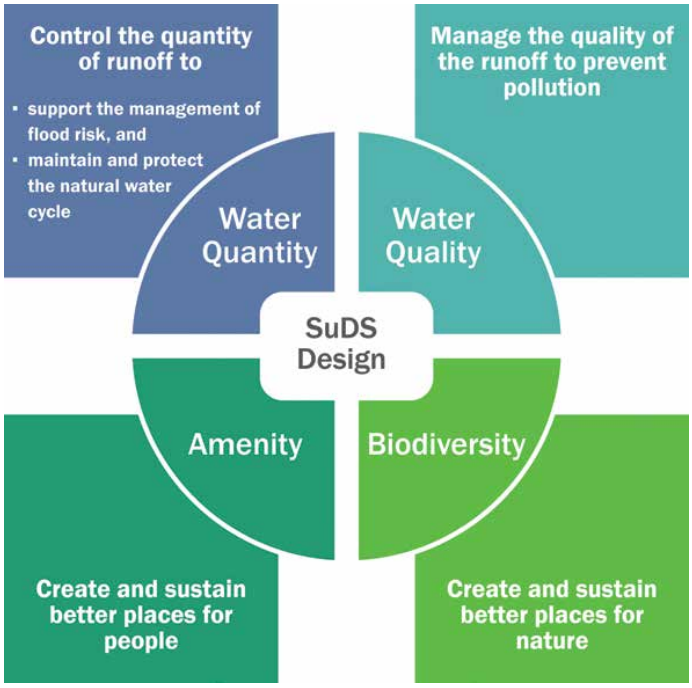


Figure 2. The four pillars of SUDS solution impact

The SUDS can be used to harvest rainwaters from the impervious areas (such as roofs, asphalted or concrete paved roads, paved squares or parking lots, etc.); to reduce the stormwater peak by maintaining the water and discharging it a lower flow rate (such as underground inline or not inline reinforced concrete tanks, soakaways or infiltration systems, bio – retention systems, swales and ponds, etc.

In the urbanized developed areas, the runoff after urbanization of the natural ground area is much higher and it can be discharged quicker than in the pre-urbanized or natural ground area. This is because of the high infiltration rate of the natural area versus the impervious urbanized areas. So, the runoff hydrograph of the impervious area is much higher and shorter than the runoff hydrograph of the natural areas. The difference between them can be diminished, if not totally removed, by using SUDS for water or peak flow attenuation, as it can be seen in the following figure.

As mentioned in the above for pillars, the SUDS can be used to increase the quality of life in the urban areas by reducing the flooding probability, increasing the drainage capacity of the system (even through maintaining it), increasing amenities and to help using better the landscaping area. Most of SUDS should be design in a close collaboration with landscaping specialist, in order to make more useful their use or if possible, to have even double functions ones.

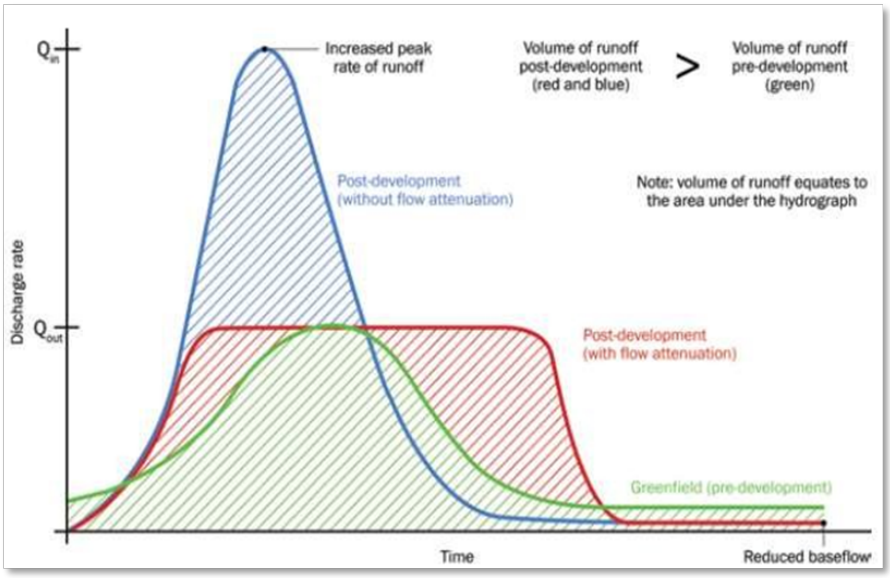


Figure 3. Runoff hydrographs of the different land developments [1]

Such SUDS as mentioned above should be design in parallel with the landscape design process, to find better location, from the hydraulically point of view and the urban design point of view, because these systems could also be used (if possible) even as playgrounds or recreational areas (permanent ponds, etc.). But the main priority is the peak flow maintaining, which is being presented in a hydraulic model at the following paragraphs.



a) Bioretention

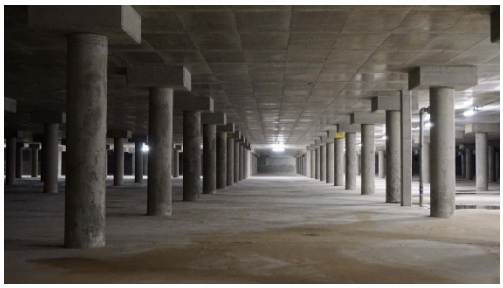


b) Swale





c) Temporary detention ponds



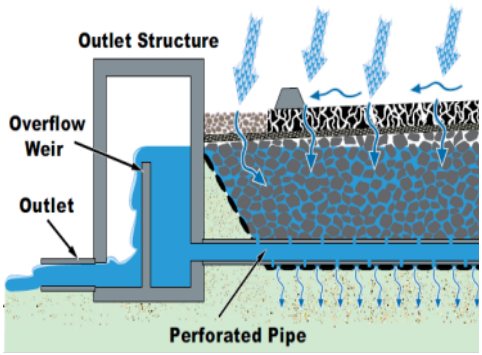

d) Attenuation stormwater tank




e) Rain harvesting and maintaining plastic systems



f) Stormwater maintaining pond (double function, even as a playground)

g) Parking lot with porous asphalted layers and its sketch of the draining

Figure 4. Different types of SUDS solutions

HYDRAULIC MODEL

The hydraulic model needs

The hydraulic model to compare the traditional stormwater drainage piped system and the alternative stormwater drainage system (SUDS) has been built for an urban area.

The urban area has the been developed during the years and the impervious area has been drastically decreased. There are analyzed the urban area data in a time interval of 25 years, which is the nearly the service period of a water system in an urban area, and between them the stormwater drainage system. These systems are designed based on the urban area development plan, so in the end of this plan period, it is needed to increase or to interfere in the existing system, in order to cope with the new development plan, but also to keep in mind both environmental problems due to urbanization.

So, hydraulic models are needed to compare both solutions and to analyze, which of them is better, by the financial point of view, and by the amenities increasing.

The hydraulic model data and built-up

The hydraulic model has been developed for a part of the city area, splitting this area into catchments, each of them discharging in the proper main combined collectors (through many catch pits on the tertiary and secondary pipes, not visualized in this model, since it has been skeletonized). The main collectors are installed with concrete or reinforced concrete pipes, connected and controlled from the reinforced concrete pits, manholes and chambers. The pipes are considered in an average condition, better that they can be in reality, since there are not enough data about their situation, the diameter blockage percentage, etc.

Another assumption is the runoff coefficient, which has been calculated, analyzing the type of the surface, the coefficient for each of them and a composite one has been resulted, using it as one value for all the catchments. That is because some of there are areas, actually are almost more than 95 % paved, but some other areas are not so urbanized, with much less impervious surface. Therefore, the former paved areas have higher runoff coefficient than the latter areas, generating higher runoff flows in their discharging pipes, during the shortest and most intense rainfalls.

The hydraulic model has been created, based on the following data:

- Land development maps of the city in the last 25 years.
- The rainfall intensities of the measured and evaluated hydrological data series of the rainfalls.
- The runoff coefficients are given by literature but also analyzed and evaluated because of the

surfaces with different permeability inside each of the catchment areas.

The maps of this model are given in following figure, presenting the part of the city water system being modelled.

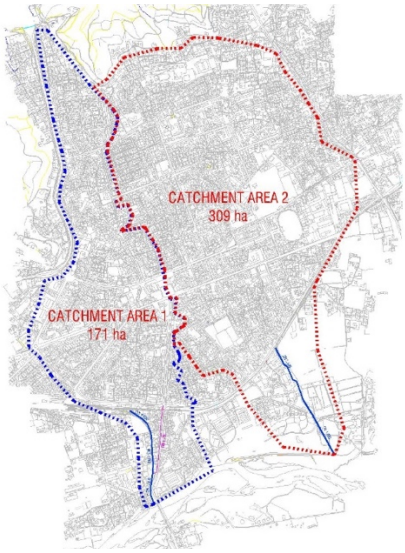


Figure 5. The catchment areas plan

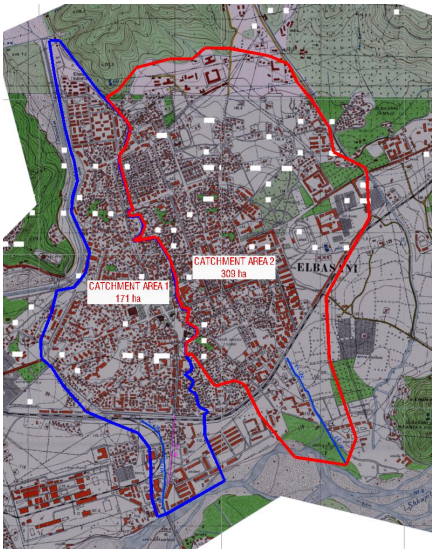


Figure 6. The catchments areas map 1990 [2]

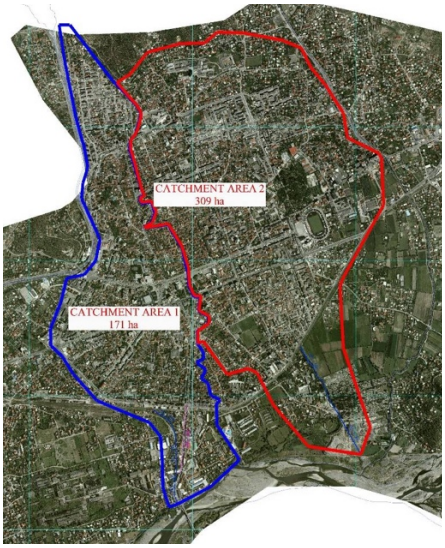


Figure 7. The catchment areas map 2015 [2]

The rainfall data and intensities, used to build up the hydraulic model, are given in the table, as follows:

Table 1. IDF curves data of the rainfalls in the city area [3]

PLACE	Rainfall Duration [hours]	Return Period T (years)			
		100	50	20	10
CITY	24	7.21	6.50	5.58	4.83
	12	10.17	9.25	8.00	7.00
	6	18.67	16.67	14.00	12.00
	2	40.00	35.50	29.50	25.00
	1	62.00	55.00	46.00	39.00
	0.50 (30 min)	110.00	96.00	80.00	68.00
	0.33 (20 min)	111.01	99.01	84.01	72.01
	0.1667 (10 min)	167.97	149.97	125.97	107.98

The catchment areas data for this hydraulic model are given in the table below.

Table 2. The catchment data

Catchment	Surface [ha]									
	Total	Year 1990				Year 2015				
		Apartm.	M-F attac	Suburb.	Unimpr.	Total	Apartm.	M-F. attac.	Suburb.	Unimpr.
1	171	0	69	67	35	171	5	89	62	15
2	309	20	95	108	86	309	35	137	110	27

The runoff coefficient of the different types of ground surfaces are given in the table below (acc. Viessman and Lewis at 2003).

Table 3. The runoff coefficients proposed by Viessman and Lewis [4]

Residential	
Single-family	0.30–0.50
Multi-family detached	0.40–0.60
Multi-family attached	0.60–0.75
Residential suburban	0.25–0.40
Apartments	0.50–0.70
Parks, cemeteries	0.10–0.25
Playgrounds	0.20–0.35
Railroad yards	0.20–0.40
Unimproved areas	0.10–0.30
Drives and walks	0.75–0.85
Roofs	0.75–0.95

The runoff of the catchment areas is calculated according to the following formula:

$$C = \frac{C_1 \times S_1 + C_2 \times S_2 + C_3 \times S_3 + C_4 \times S_4}{S_1 + S_2 + S_3 + S_4}$$

And these coefficients are given in the following table for each catchment in the respective years, taken into the consideration during this hydraulic modelling study.

Table 4. The runoff coefficient for the catchments of the city in different years

Catchment	Surface [ha]	C (Runoff coefficient)	
		Year 1990	Year 2015
1	171	0.52	0.58
2	309	0.50	0.60

The time of concentration has been calculated using the Kirpich method for the sheet flow (the shallow concentrated flow is not considered, due to the surface type) and the Manning formula for the

channelized flow. The resulted time of concentration is nearly t = 30 - 35 min ≈ 0.5 hours, from the furthest point to the outfall of each catchment areas.

The hydraulic model consists of some scenarios, but we've chosen to analyse 2 scenarios for each type of catchment (one type of catchment without SUDS and the next one with SUDS integrated in the drainage system).

The different scenarios are presented in the figure below:

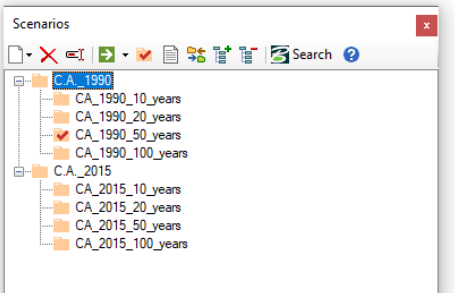


Figure 8. The scenarios of the hydraulic model

The scenarios that are analysed and which data are compared are the scenarios CA_1990_20 years and CA_2015_20_years. The catchment models used in both scenarios are given in the figures below.

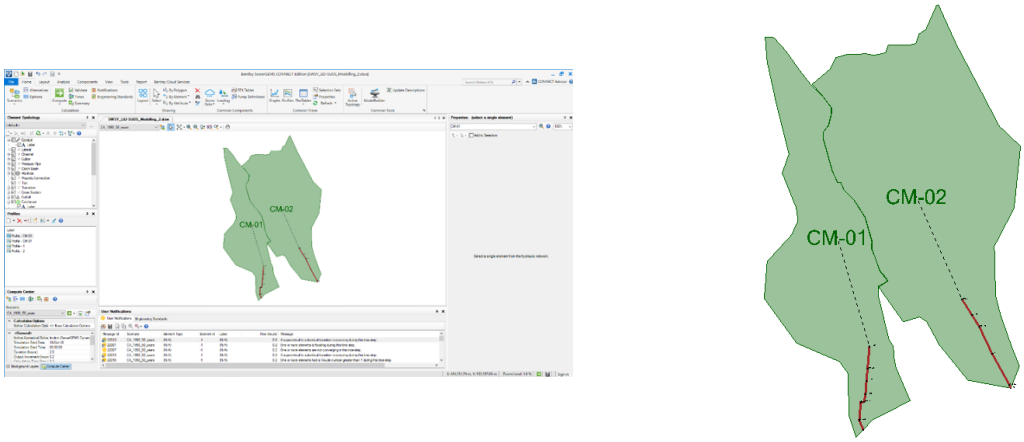


Figure 9. The catchment layout without attenuation system.

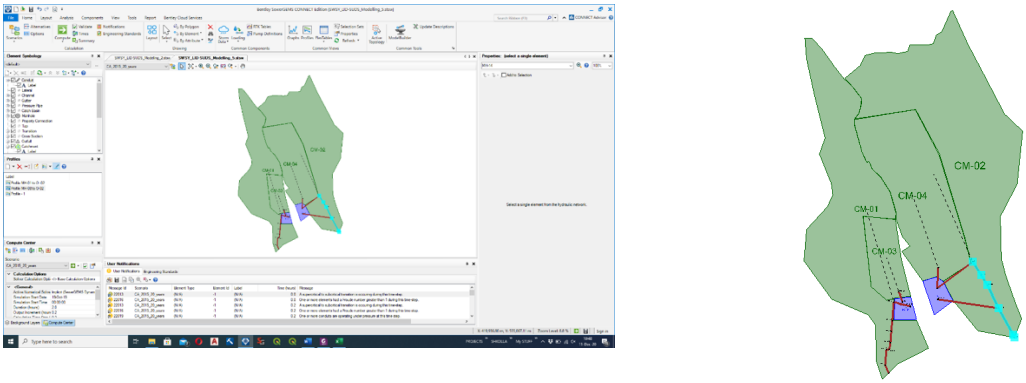


Figure 10. The catchment layout with attenuation system (SUDS – Swale type)

The results of the hydraulic simulation

As it is mentioned above, the storm with a return period T =20 years has been taken into the consideration to analyse the hydraulic model simulation. In the graphs and tables below are given the hydraulic line or water level at the peak flow, for both types of catchments, with or without attenuation system.

After the simulation, it has been clear the distinction between the runoff flows in the pipes in both types. There are higher levels or bigger depths of the water flows inside the pipes in the system without attenuation measures than in the system with attenuation measures.

In the figures and tables below are given the results from these hydraulic model simulations, which shows the important role of SUDS in peak flow attenuation during the storms.

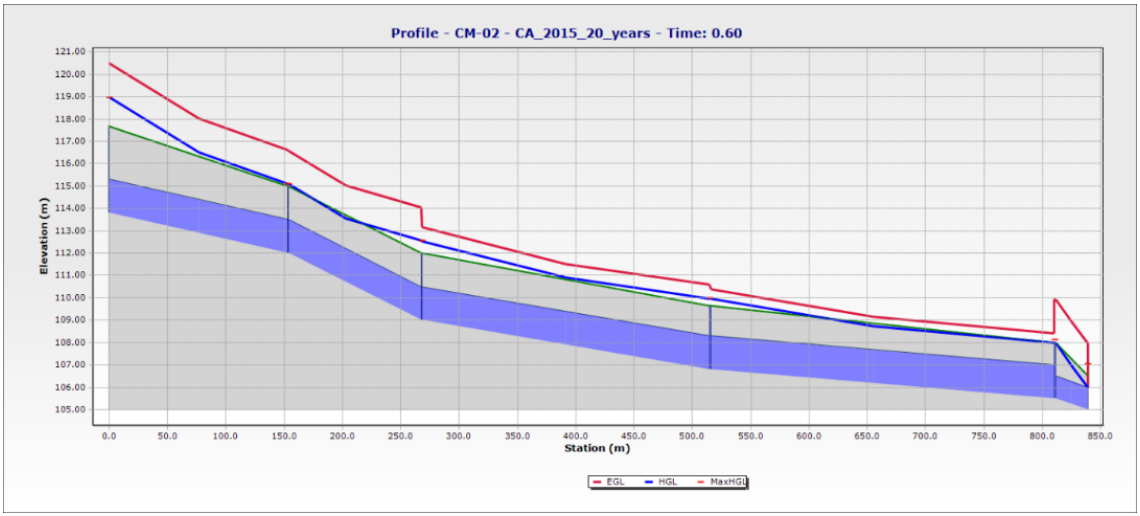


Figure 11. The profile of hydraulic and energy line in the pipeline of the catchment 2(without attenuation) year 2015, return period T = 20 years

Table 5. The hydraulic data of the pipeline of the catchment 2 (without attenuation) year 2015, return period T = 20 years

Label	Elevation (Ground) (m)	Elevation (Invert) (m)	Flow (Total In) (L/s)	Flow (Total Out) (L/s)	Hydraulic Grade Line (In) (m)	Hydraulic Grade Line (Out) (m)	Is Overflowing?
MH-08	117.66	113.8	32,956.83	9,680.73	118.95	118.95	TRUE
MH-09	115	112	9,680.72	9,572.04	115.1	115.09	TRUE
MH-10	112	109	9,571.77	6,202.55	112.55	112.54	TRUE
MH-11	109.64	106.8	6,199.28	5,046.38	109.97	109.96	TRUE
MH-12	108	105.5	4,896.74	4,850.08	108	108	FALSE

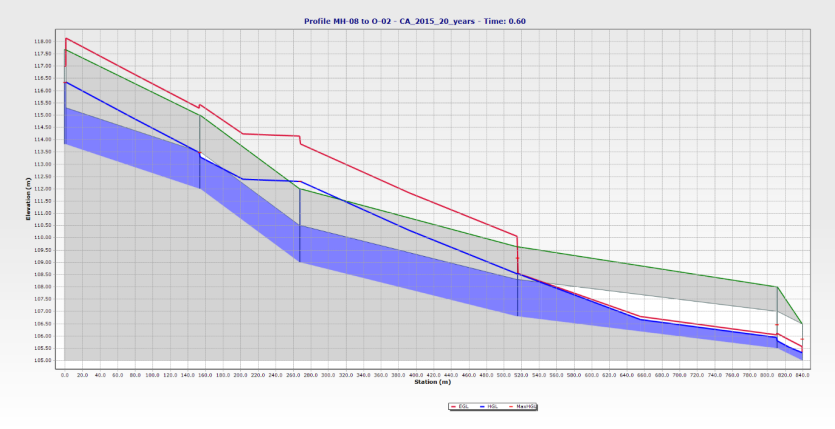


Figure 12. The profile of hydraulic and energy line in the pipeline of the catchment 2 (with attenuation) year 2015, return period T = 20 years

Table 6. The hydraulic data of the pipeline of the catchment 2 (with attenuation) year 2015, return period T = 20 years

Label	Elevation (Ground) (m)	Elevation (Invert) (m)	Flow (Total In) (L/s)	Flow (Total Out) (L/s)	Hydraulic Grade Line (In) (m)	Hydraulic Grade Line (Out) (m)	Is Ever Overflowing?
MH-08	117.66	113.8	16,766.04	16,849.84	116.32	116.32	FALSE
MH-09	115	112	10,511.26	10,514.12	113.47	113.3	FALSE
MH-10	112	109	10,655.24	9,660.11	112.3	112.3	TRUE
MH-11	109.64	106.8	9,366.39	957.11	108.54	108.54	FALSE
MH-12	108	105.5	633.46	616.1	105.93	105.81	FALSE

CONCLUSION

As it can be seen the attenuation measures integrated in the stormwater system affect the whole system and it can avoid the flooding of the system by the peak flows of a storm. The biggest depth in the first case (without attenuation) is approximately H = 1.30 m in the area of manhole no. 08, while in the second scenario presented above, there is no flooding in the area of the manhole no. 08, as it has be seen in the system without attenuation measures.

REFERENCES

[1] The SUDS Manual C753 by CIRIA;

[2] ASIG Website, Albania;

[3] Buletini i shirave maksimale IHM, Tiranë, 1985;

[4] ASCE 1975, Viessman, et al. 1996, and Malcom 1999.

Inundation Modeling Using HEC-RAS Software Farka Stream Case Study

Mirjeta Blloshmi[1], Mirjam Ndini[1]

[1]*Deparment of Civil Engineering, EPOKA University, Albania*

ABSTRACT

This study analysis how water flow corresponding to maximum discharge of Q=240m^3/s is distributed along Farka stream. To visualize flow dispersion, two modeling approaches 1-dimensional and 2-dimensional HEC-RAS models are implemented, and unsteady flow analysis is simulated. HEC-RAS models and hydraulic analysis are used to analyze water depth planimetry and flow hydrograph of each stream segment. The objective is to develop 1-dimensional and 2-dimensional models, representing possible stream rehabilitation scenario and performing unsteady flow analysis in order to make a comparison of results. In this study, it is concluded that flow distribution along stream was not the same for 1 and 2-dimensional models. These two modeling approaches, under the same conditions, produces different results and only engineering experience together with project aim can decide which one of them to use while performing flood modeling.

Keywords*: rehabilitation, unsteady flow, hydraulic analysis, flow hydrograph, simulation*

INTRODUCTION

Throughout history flooding has proved to be one of the most devastating natural hazards all over the world due to intense distribution of water streams. Based on available data Albania is considered to be as high-risk region related to flooding [1] [2] [3].

The high probability of flooding events has developed the necessity for flood protection. There has been a great, consistent effort to comprehend, rate and anticipate flooding events and their effect.

Several studies have been conducted related to flood modeling, their priorities and their deficiencies also. It is crucial to have a clear understanding of flood modeling approaches and to precisely distinguish them from one another. Only in this way the selection of the appropriate model will be easier [4] [5] [6] [7] [8].

Flood history of the study area

In year 2011 a government investment was made with the intention to rehabilitate the stream bed, by constructing a concrete covered trapezoidal cross section into the stream covered with concrete at a length of 140m, and by implementing a culvert with dimensions base b=5m, height h=3m and length l=90m to pass near the State Reserve Depots. Trapezoidal cross section has suffered numerous damages and water has found its path outside banks of stream.

The most critical discharge was registered in 30 November 2014, which based on the maximum water level measurements turns out to have been Q=240m^3/s. This unusual discharge caused considerable damage to the left concrete covered stream bank and to the bad of the stream.

The temporary interventions in Farka stream could neither provide an effective protection for the stream itself nor for the abovementioned structures located there

In order to, provide an effective and efficient evaluation of the Farka stream rehabilitation this project is based on 1-dimensional and 2-dimensional flood modeling.

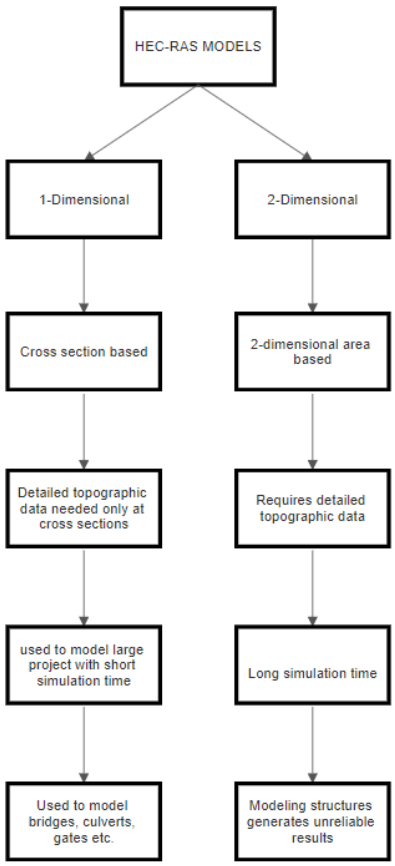


Figure 1. Flowchart of 1D and 2D HEC-RAS Models Potentials and Limitations.

RESEARCH DOMAIN

Figure 2 presents the location of Farka stream. In this study Farka stream is divided into three segments that are used as checking points to compare the results of unsteady flow simulation of each corresponding model. Topographic data required for modeling were obtained from topographic measurement of the area done by MANETCI Company and reference system used was WGS 1984/UTM zone 34. Besides HEC RAS software, ARC-GIS was used to generate 3-dimensional terrain model.

Furthermore, the same boundary conditions were used to perform 1D and 2D unsteady flow analysis. Flow Hydrograph and Normal Depth were used respectively as upstream and downstream boundary conditions. Also, the data from 1 in 100-year repetition flow hydrograph generated from hydrological analysis of the study area, performed by other researchers, was used as an input in HEC RAS hydraulic modeling, to perform unsteady flow analysis.

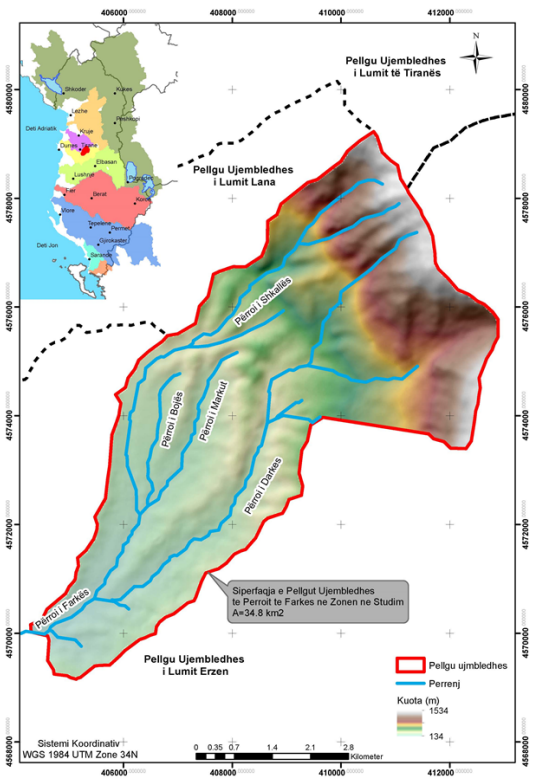
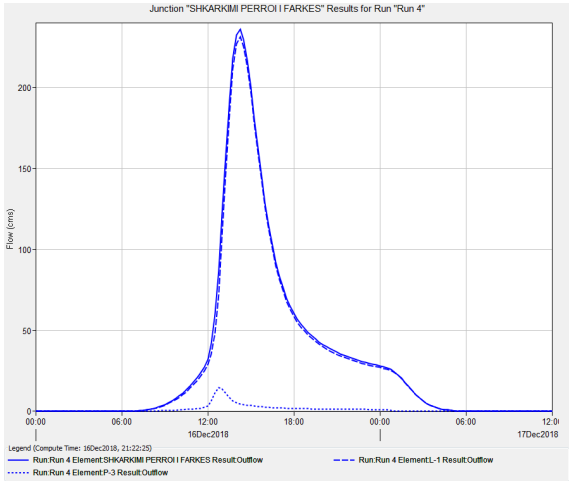
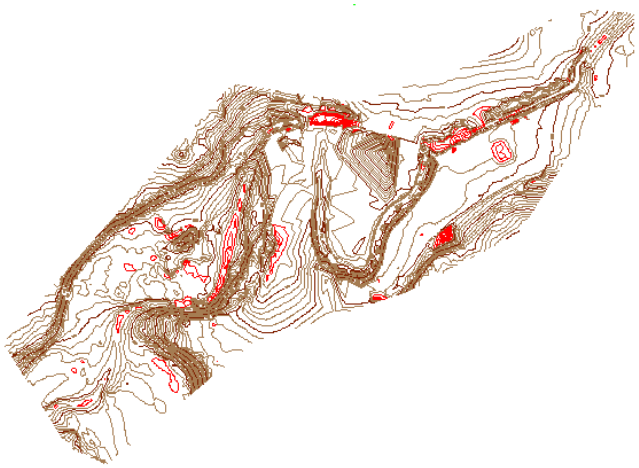


Figure 2. Location of the Case Study, Farka Stream



(a)



(b)

Figure 3. (a) Hydrograph of Farka Stream, 1 time in 100-year repetition, Q=236m^3/s, (b) Topographical Data of Area Under Study, Farka Stream

METHODOLOGY

Different procedures were followed do develop 1-dimensional and 2-dimensional models. As 1-dimensional model is more cross section-oriented modeling approach, attention was paid to cross section implementation also, junctions along the stream were carefully defined. Meanwhile, to set up 2-dimensional

model, 2D flow are was developed. After specifying upstream, downstream boundary conditions the simulation of unsteady flow was performed and results related to water depth planimetry, flow hydrographs were obtained for both models. In this way the accuracy of each models and their capability could be rated.

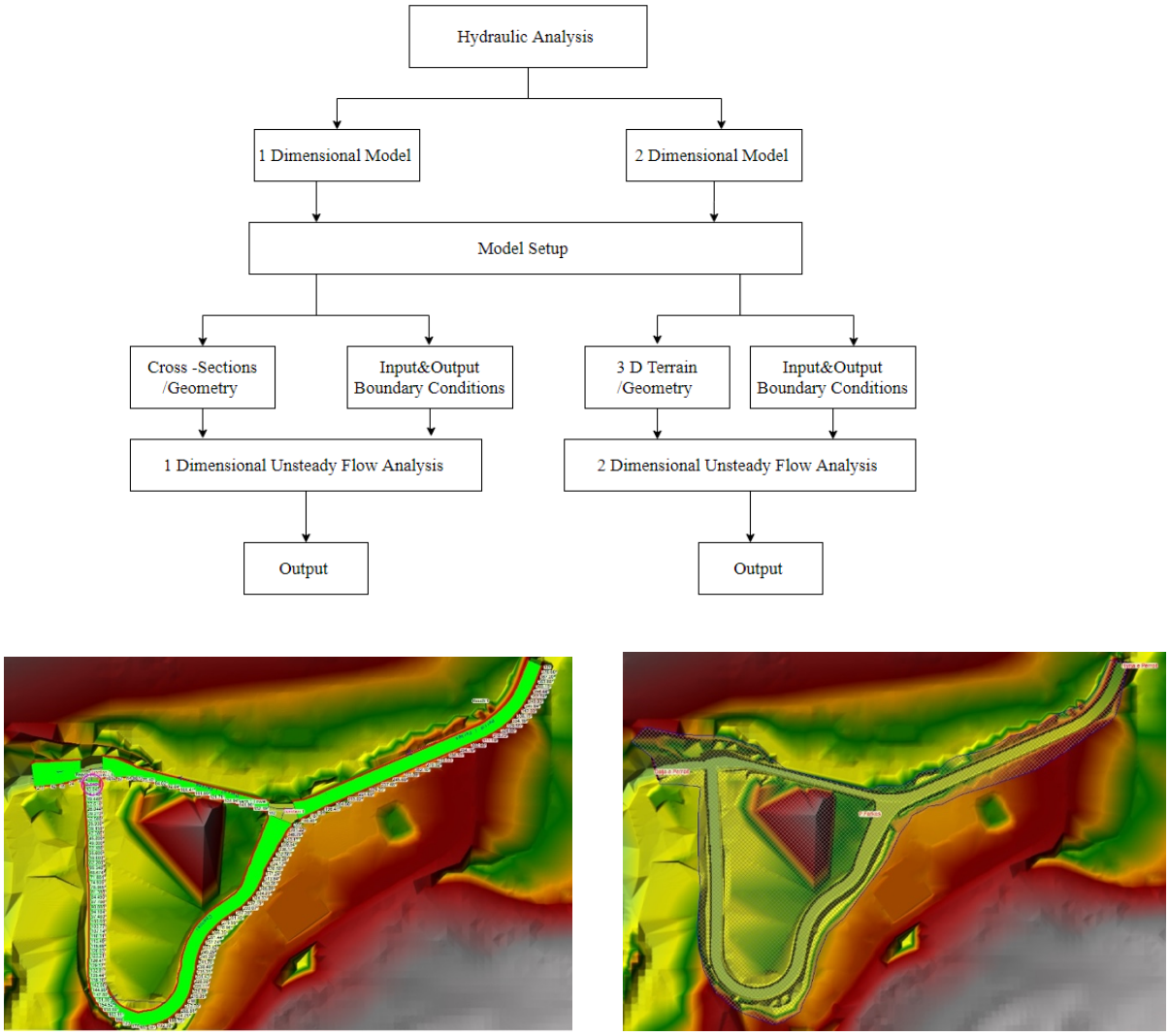


Figure 4. (a) Flowchart of Hydraulic Analysis of Modeling Approach Using HEC-RAS 5.0.7, (b) 1D Model Setup, Cross Sections, Junctions, (c) 2D Model

RESULTS AND ANALYSIS

In order to study whether the flow inundated the rehabilitated channel for both models and also to interpret flow distribution on junctions for 1-dimensional model and flow distribution along stream for 2-dimensional model, it was important to carefully interpret the results obtained from the simulations. Water depth planimetry represented the distribution of water into the channel and the areas nearby it and visualizes if the water inundated the area or not.

Moreover, three segments were defined on each corresponding part of the stream and for each segment there were obtained results corresponding to flow capacity.

The simulation is developed based on maximum water flow 240m^3/s which occurs 1 in 100 years, generated from the hydrological study.

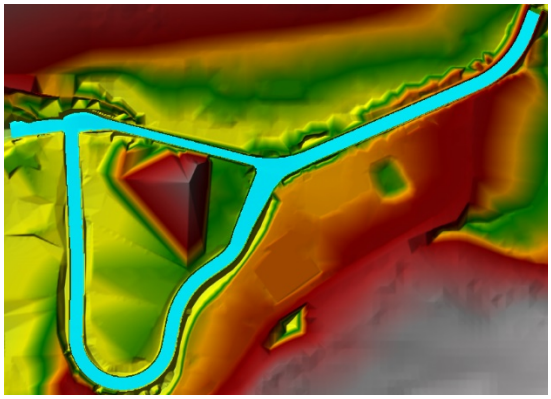


Figure 5. Water Depth Planimetry, 1-Dimensional Model

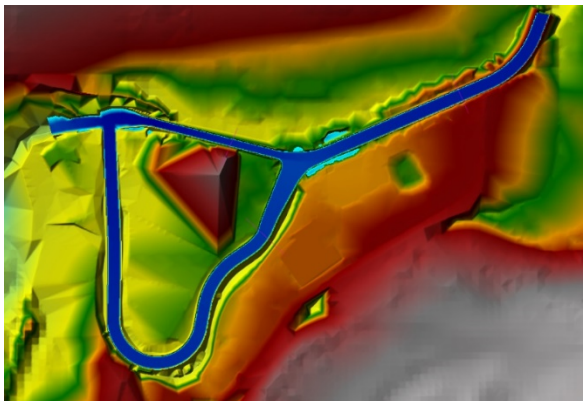


Figure 6. Water Depth Planimetry, 2-Dimensional Model

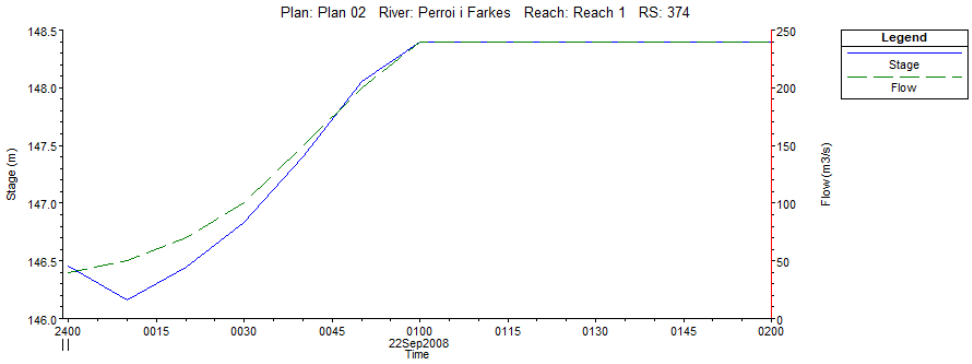


Figure 7. Stage & Flow Hydrograph, Q=240m³/s, Section 1, 1-Dimensional Model

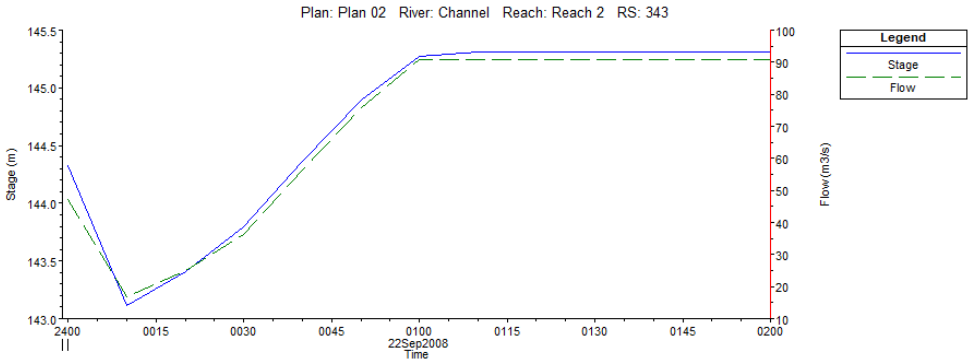


Figure 8. Stage & Flow Hydrograph, Q=90.91m³/s, Section 2, 1-Dimensional Model

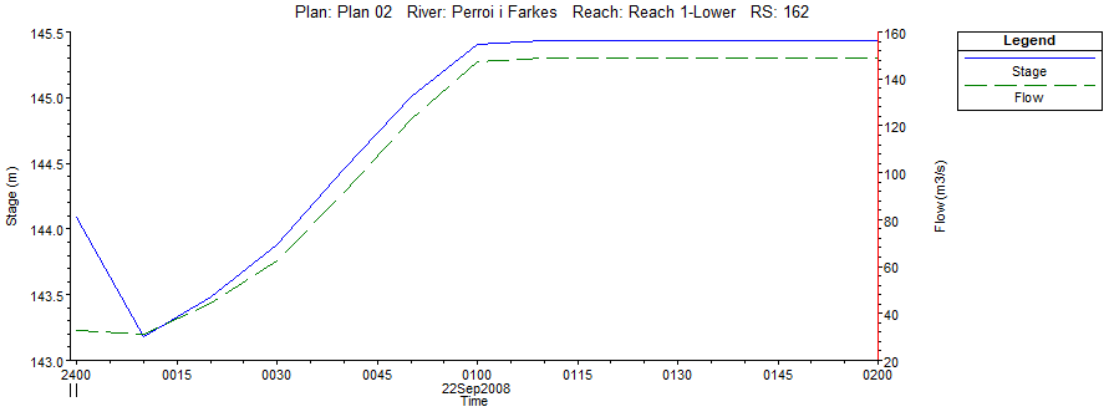


Figure 9. Stage & Flow Hydrograph, Q=149.09m³/s, Section 3, 1-Dimensional Model

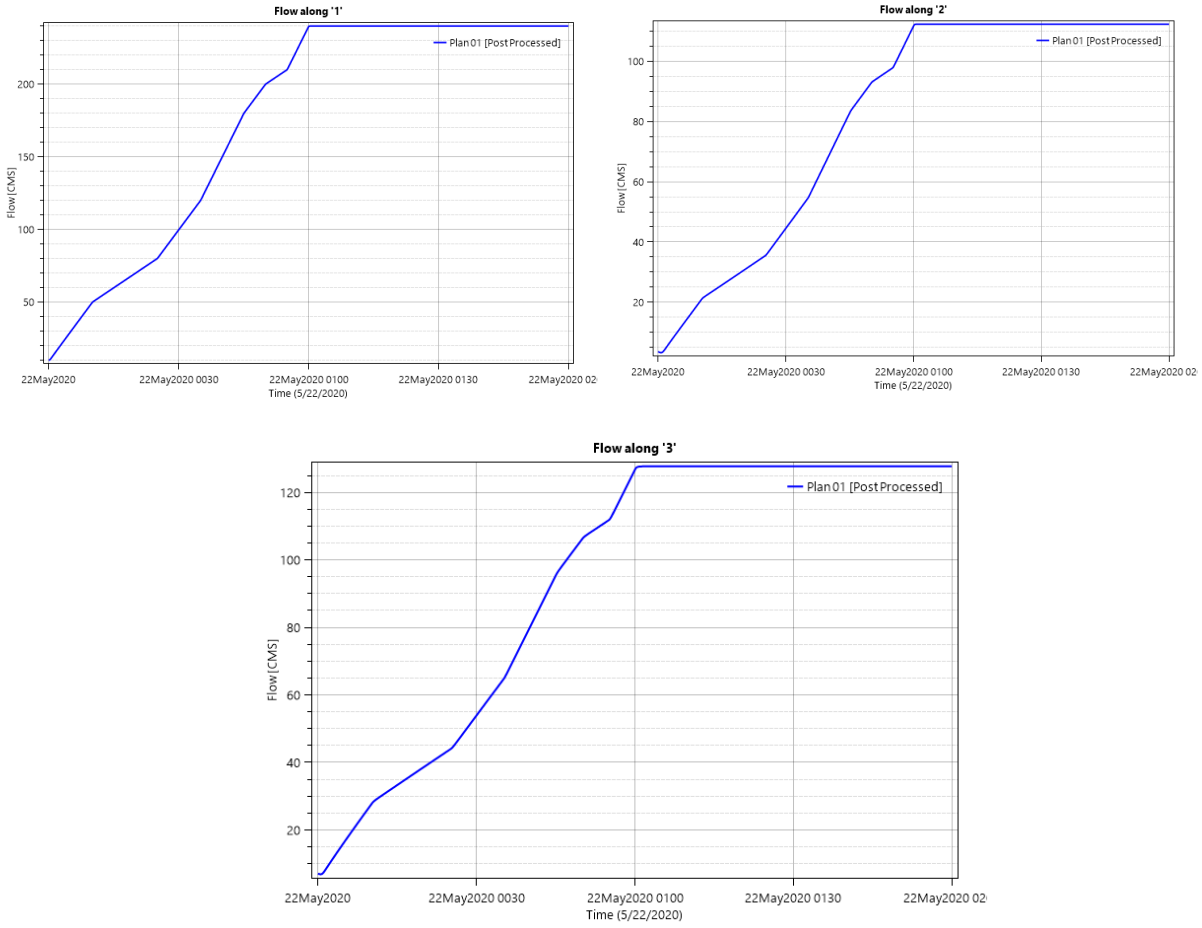


Figure 10. Flow Along Section 1 Q=240 m³/s, Section 2 Q=112.3 m³/s, Section 3 Q=127.7 m³/s, Variant 1

The result generated from 1-dimensional model, (Figure 5), is similar to water depth planimetry received from 2-dimensional model, (Figure 6). In both cases, the area, under the specified conditions is not inundated.

Continuing with, Flow Hydrograph, (Figure 7), (Figure 8), and Figure 9 (Figure 9), the primary water stream known as 'Reach1', (Figure 7), corresponding to segment 1 has a discharge of Q=240 m³/s, maximum discharge. This segment is reconstructed with a rectangular cross section BXH=8x3m. This segment ends into a split junction that reorganizes water flow into, 'Reach 2' corresponding to segment 2,

(Figure 8), and 'Reach 1-Lower'corresponding to segment 3, (Figure 9), where the flow distribution is Q=90.91m^3/s and Q=149.09m^3/s respectively. Even thought, segment 2 has the same cross section as segment 1 the flow will not be the same in both of them. Segment 3, where a culvert of dimensions BxH=5x3m, will provide a stream with optimal conditions for the water to flow there.

Considering flow hydrograph of 2D model, (Figure 10), the primary water stream corresponding to segment 1 has a discharge of Q=240 m^3/s, maximum discharge, segment 2 and segment 3 the flow distribution is Q=127.7m^3/s and Q=112.3m^3/s respectively. Even thought, segment 2 has the same cross section as segment 1 the flow will not be the same in both of them. Segment 3, where a culvert of dimensions BxH=5x3m, will provide a stream with optimal conditions for the water to flow there. In all three segments water flow does not overcome the limits of each segment.

Water flow distribution, in both models (Figure 7-10) is not as consistent. Comparing both models, segment 2 and 3 differs with ± 21.39 m^3/s flow capacity.

CONCLUSION

In the presented thesis, hydraulic analysis was provided to perform a comparison of 1-dimensional and 2-dimensional flood models. Unsteady flow analysis was simulated under the same boundary conditions for both 1-dimensional and 2-dimensional models. These two models were compared to each other, in terms of water distribution along stream in order to define their capability and accuracy.

Moreover, results obtained from 1-dimensional model, did not align with results obtained from 2-dimensional model. Two modeling approaches showed that, under the same boundary conditions, the proposed rehabilitation case offered valid conditions to prevent flooding of the area around, Farka stream. But, on the other hand, the flow distribution along streams changed for both models.

1-Dimensoional and 2-dimensional HEC-RAS models, can both be efficiently used for flood mitigation. However, selection of appropriate model strongly depends on project aim. Further studies are required to be conducted in order to clearly define project characteristic linking it to the most realistic modeling approach.

REFERENCES

[1] I. F. o. R. C. a. R. C. Societies, "Albania Floods," DREF operation, 2010.

[2] E. &. D. M. ,. &. M. M. Toto, "Mbledhja e të Dhënave Historike të Humbjeve në Shqipëri".

[3] D. Vogli, "Gazeta Dita," 2 December 2017. [Online]. Available: http://www.gazetadita.al/veshtrim-mbi-permbytjet-me-syrin-e-nje-eksperti-shqiptar/.

[4] A. K. A. &. A. M. Selenica, "Risk assessment from floodings in rivers of Albania," in International Ballkans Conference on challenges of Civil Engineering, BCCE,, Tirana, 2011.

[5] L. &. D. B. G. Brandimarte, "Uncertainty in design flood profiles derived by hydraulic modelling," Hydrology Research Journal , pp. 753-761, 2012.

[6] J. J. A. J. C. B. Teng, "Flood inundation modeling: A review of methods, recent advances and uncertainity analysis," Environmental Modeling and Software, p. 16, 2017.

[7] C. F. E. K. &. A. M. Y. Fosu, "RIVER INUNDATION AND HAZARD MAPPING," Journal of Global Geospatial Conference, 2012.

[8] C. B. &. N. V. Okoye, "MAPPING OF FLOOD PRONE AREAS IN SURULERE, LAGOS, NIGERIA: A GIS APPROACH," Journal of Geographic Information System , vol. 7, pp. 158-176, 2015.

[9] F. A. &. B. J. P. Maniyar, "Literature study on hydraulic modeling of floodplain mapping," International Journal of Research in Engineering Technology , vol. 4, no. 11, p. 5, 2015.

[10] U. K. N. M. &. R. H. Khalil, "Flood Mapping for Indus River: Chashma-Taunsa Reach," pp. 30-48, 2017.

[11] S. K.-A. C. M. B. A. &. B. U. Gülbaz, "zFlood Modeling of Ayamama River Watershed in Instambul, Turkey," Journal of Hydrologic Engineering, pp. 1-10, 2019.

[12] G. W. Brunner, HEC-RAS River Analysis System Users Manual, 2016.

[13] G. W. Brunner, HEC-RAS, River Analysis System Hydraulic Reference Manual, 2016.

[14] C. Goodell, "The RAS Solution," 23 May 2011. [Online]. Available: https://www.kleinschmidtgroup.com/ras-post/modeling-junctions-for-unsteady-flow-analysis/.

[15] S. S. S. L. I. D. R. &. T. S. Kane, "Modeling unsteady flow through junction in rectangular channels: impact of model juction in downstream channel hudrograph.," Scientific Research Publishing, pp. 304-319, 28 July 2017.

[16] C. Goodell, "The RAS Solution," 19 February 2009. [Online]. Available: https://www.kleinschmidtgroup.com/ras-post/severe-energy-jump-at-junctions-for-unsteady-flow/.

[17] "Surface Water Solution," 2020. [Online]. Available: https://www.surfacewater.biz/ratingtheory/.

[18] W. R. Perry, "WithersRavenel," [Online]. Available: https://withersravenel.com/.

[19] F. Rubiu, "Flood Risk Assessment in the Vicinity of Kartena Town Using HEC-RAS 1D-2D Models," pp. 1-56, 2018.

[20] D. Y. K. &. H. A. Lea, "Case Study of HEC-RAS 1D–2D Coupling Simulation: 2002 Baeksan Flood Event in Korea," Water, p. 14, 2019.

[21] N. S. Y. Z. &. I. A. Z. Romali, "Application of HEC-RAS and Arc GIS for floodplain mapping in Segamat town,," International Journal of GEOMATE ·, p. 8, 2018.

[22] A. I. &. A. P. G. Pathan, "River Flood Modeling Using GIS, HEC-GeoRAS And HEC-RAS For Purna River,," p. 8, 2019.

[23] A. E. B. R. H. I. &. e. M. J. S. Azouagh, "Integration of GIS and HEC-RAS in Floods Modeling," p. 13, 2018.

[24] I. &. N. U. K. Bose, "Flood Mapping for Dharla River in Bangladesh using HEC-RAS 1D/2D Coupled Model," International Journal of Science and Research (IJSR), p. 5.

Impact of neotectonic processes of Shkumbin valley, "Xibrake-Librazhd area" on existing and future civil engineering works

Dashamir Gega[1]

[1]*Albanian Geological Survey*

ABSTRACT

The rock type contacts on both sides of Shkumbin river valley indicate that the neotectonic movements from west to east are not uniform. This has been verified through continuous field investigations in both sides of the Shkumbin valley (Xibrake-Librazhd area). This paper aims to show the results of these field investigations followed by geological and geotechnical assessments on the impact of these neotectonic processes on the civil engineering works.

Based on this verified neotectonic movement as well as the results of the analysis of this study, recommendations will be given that should be taken into account in the maintenance of existing works as well as the construction of future works of national interest (roads, tunnels, residential centers, etc.).

Keywords: geological investigations, petrographic contact, tectonic movement

INTRODUCTION

Field surveys on both sides of the Shkumbin River "Xibrake-Librazhd area" point fields shown in Figure 1, in the framework of previous research [1-2] on complex relations between the western part of the Shebenik ophiolitic massif and the eastern part of the ophiolitic massif of Kuturmanit have identified:

a) Tectonic zone of shale type extending in the valley Shkumbin south-west (Labinot- Xibrakë area) to the northeast (Murrash-Librazhd area.) [3-4]
b) Movement in general of the massif ophiolitic Shpat- Kuturmavit from west to east, creating morphologically from the Shkumbin valley and geologically from the Shkumbin syncline. (Mokerr-Gurakuq)
c) The intensity of this neotectonic movement (west-east) was not uniform, as in a distance - 800 ml from Cesmja e Myftarit- parallel to the highway that leads to the village of Babje, we have an overflow of the older formations over the newer ones.
d) The main amplitude of neotectonic movements from west to east in the area "Xibrake-Librazhd" is different on both sides of the river Shkumbin.[5]
e) Given that this area passes the railway line Elbasan-Librazhd with several tunnels and bridges, the existing national road Elbasan-Librazhd and what is planned to be built, the evidence of these neotectonic movements, their amplitude is important in the maintenance of existing facilities and construction of works in the most stable areas.

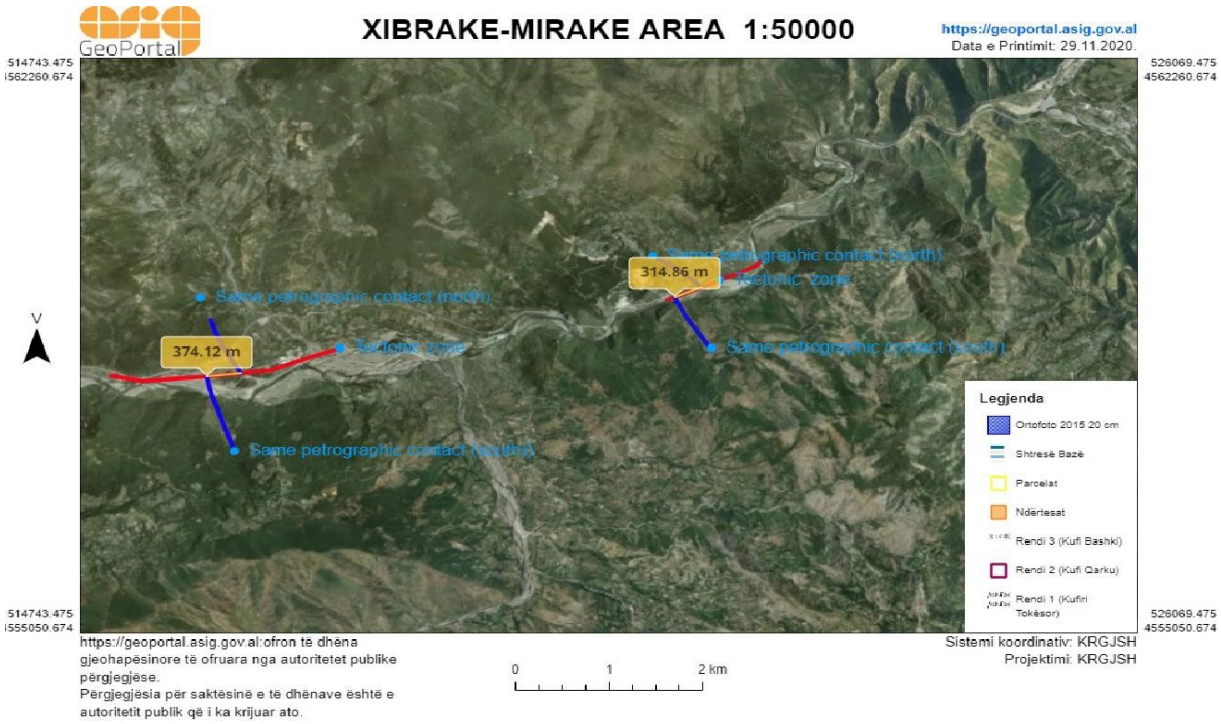


Figure 1. The point fields in Xibrake-Librazhd Area.

During field observations it was noticed that these two masses move towards each other, the one of Shpat-K towards the east and that of Shebenik towards the west. As a result of this movement, the Librazhd intermountain pit was created with molasses deposits. The city of Librazhd was built on these deposits created by these neotectonic movements, as well as many inhabited centers from Librazhd to Qukes shown in Figures 2 and 3. During the field studies of the Shkumbini river [6] it was noticed that it represents a strong tectonic zone which emerges in the village of Babje and continues towards the SW being covered with alluvial deposits of the Shkumbin River.

This powerful tectonic zone at a length of 10 kml clearly shows: that the movement of rock blocks on both sides of it, in time and space was not uniform.

The north arm is moving and is moving 300-400ml more advanced towards the east compared to the west.

Given that in this length of 10 km (according to the Shkumbin River) is built the national road, railway line and the construction of Corridor-8 (Durres-Skopje-Sofia-Istanbul) is necessary that the constructions carried out in the northern part of the river of Shkumbin to be reviewed in the framework of this phenomenon to be improved and new constructions to be concentrated on the western side of the river Shkumbit in this area of 10 kml (XlbrakeLibrazhd).

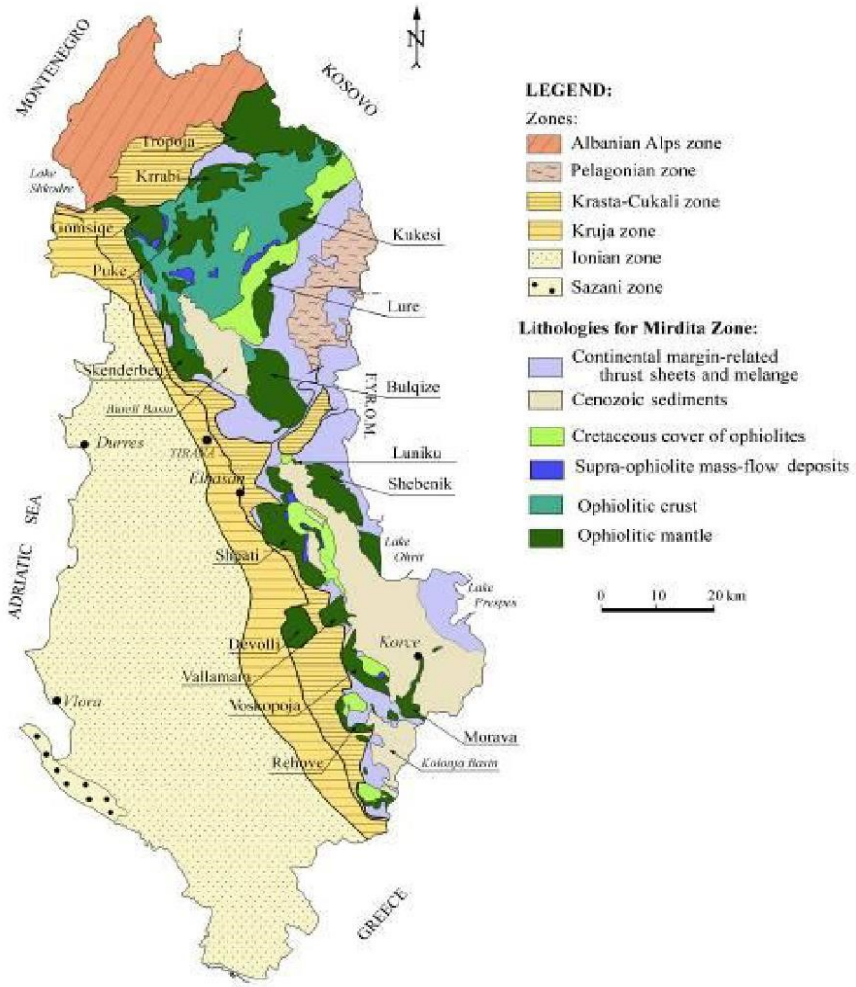


Figure 2. Geological map of Albania

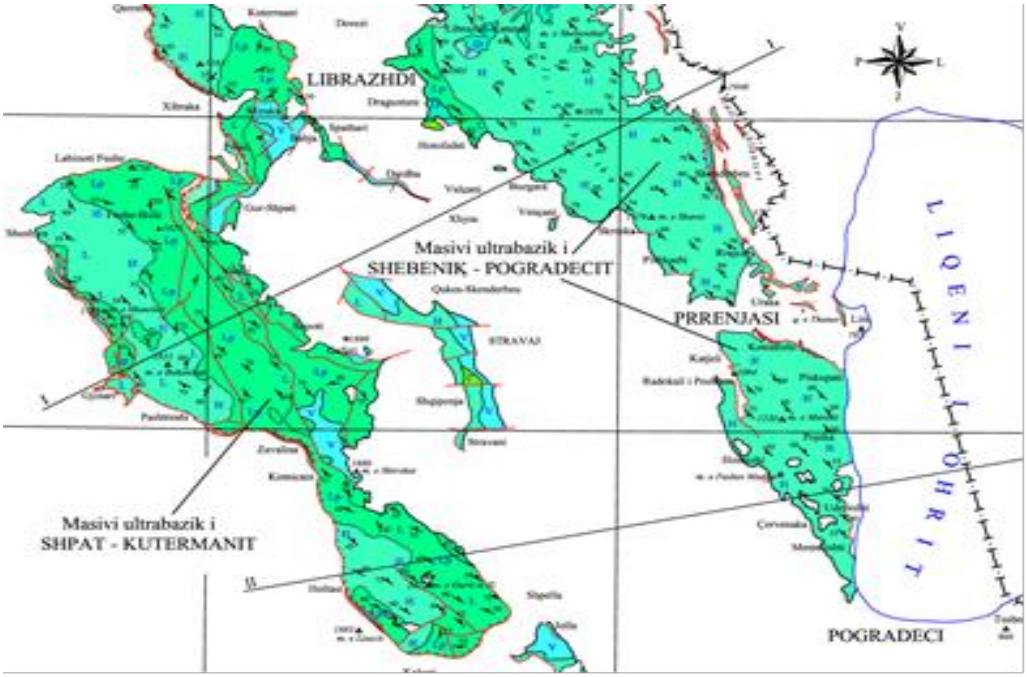


Figure 3. Ophiolitic complexes of Shpat-Kuterman and Shebenik-Pogradec

METHODOLOGY

This tectonic and neotectonic phenomenon was studied by petrographic [7-11] rock contacts in the section "Xibrake-Mirake-Librazhd". In Xibrake at the very end of the national road Elbasan Librazhd, we have the petrographic contact between the carbonate deposits of the Cretaceous and the crushed flysch of (Pg-2Eocene) with coordinates: N-41º09'43 "; E-20º11'40" are shown in Figures 4 and 5.

This petrographic contact in the southern part of the Shkumbin River with coordinates: N-41º09'33 "; E-20º11'30" is shifted towards the west with a horizontal amplitude = 370ml. (Fig-). Continuing eastwards in the village of Mirake, the petrographic contact between the massive limestones of the Upper Triassic and the thick flysch (melange) is found on the other side of the Shkumbin River.

This petrographic contact in the eastern part emerges on the right side of the highway at the point with coordinates: 41º10'10 "; E-20º15'05, while in the southern part it emerges at the point with coordinates N-41º10'03"; E-20º15'06 "with a displacement of 315 meters. Evidence of the tectonic zone in the village of Babje and its pursuit towards the SW for

10 kml (photo-) along the Shkumbin river shows that the Shkumbin river in its studied length Librazhd-Kraste Elbasan represents a tectonic zone with two wings, the northern and ate South.

Both blocks move eastwards, towards the city of Librazhd, where in its vicinity they overlap with an angle of up to 60º shown in Figures 6 and 7. But what is special and distinct is that the northern side of the Shkumbin River moves faster than the western one. From today's measurements according to the petrographic contacts on both sides of it we have a movement difference of 320-350ml.

The west side is less stable as it moves less. A part of the railway tunnels of the Elbasan Librazhd line have been built on this side.

A part of the national road Elbasan Librazhd passes on the northern side of the Shkumbin river and has had engineering problems at certain times.

Evidence of non-uniform movements of the rocky wings (north and south) of the Shkumbin River requires that in the future in the constructions to be carried out be taken into account the tectonic laws, which occurred at different geological times, and neotectonic that continue and days today giving the appropriate recommendations in the protection of works built and those to be built.

Since human activity is much later than the creation of the Shkumbin syncline, we need to recognize today's neotectonic movements that continue and affect the constructions that have been carried out and those that will be carried out. Evidence of benchmarks (identical rock contacts) on both sides of the Shkumbin River from the Xibrake-Librazhd area, allows us to assess the heterogeneity of movement and the solution of areas that move less or take additional engineering measures in areas that move more.



Figure 4. The direction of movement (Shebenik Massiv)



Figure 5. The direction of movement (Kuturmani-Shpat Massiv)

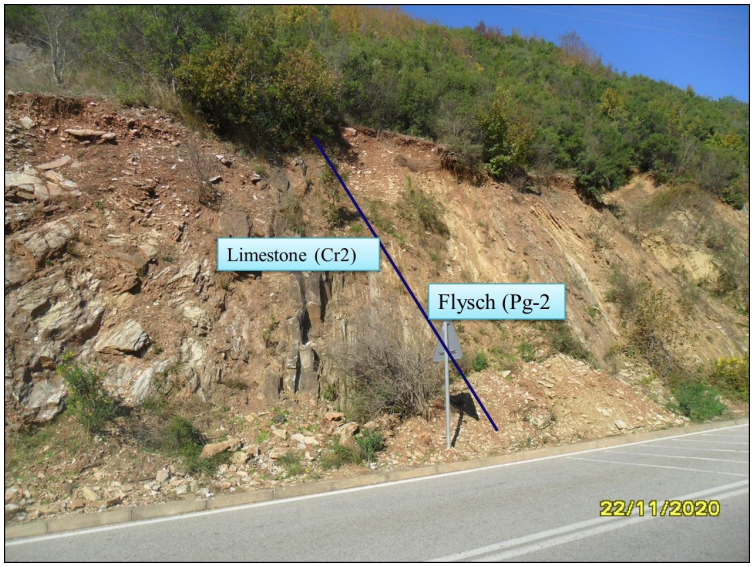


Figure 6. The petrographic contact (limestone-flysch) in the north of Shkumbin river.

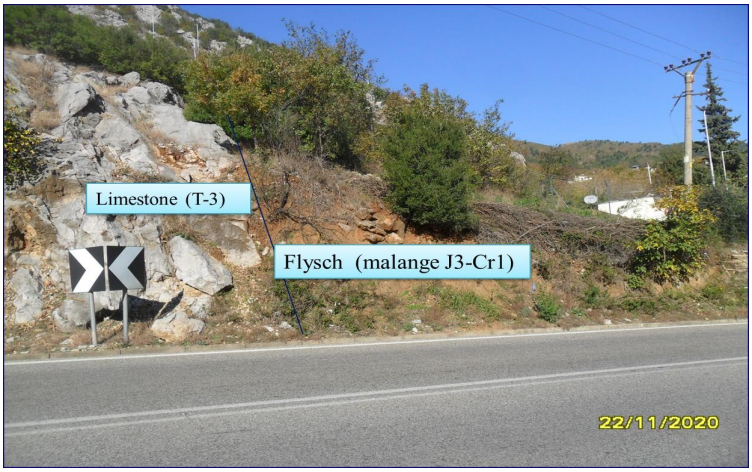


Figure 7. The petrographic contact [massive limestone (T-3) -flysch (J3-Cr1)] in the north of Shkumbin river.

CONCLUSIONS

The study of two ophiolitic massifs, Shebenik in the east of Shkumbin valley and Shpat-Kuturman in the west identified:

- The movements of the Shebenik massif along its entire length from east to west and that of Shpat-Kuturman from the west to the east, creating the mountain pits where then formed the molasses that we meet today from the south (Pishkash) to Funares in the north.
- The continuation of this movement created the Shkumbin syncline with its two wings, the eastern one that meets the east and the western meeting in the west.
- According to the Elbasan-Librazhd axis, a tectonic zone developed according to which the Shkumbi River flows today. This tectonic zone met in Babje and covered to the south east by alluvial deposits has a considerable length over 10kml.
- Movements to the east on both sides of this tectonic zone that runs along the course of the Shkumbin River are not uniform in time and space. The north wing moves faster in time than the south.
- Movements to the east on both sides of this tectonic zone that runs along the course of the Shkumbin River are not uniform in time and space. The north wing moves faster in time than the south.
- During the observations, the same petrographic benchmarks were fixed on both sides of the river. Future monitoring of the amplitude of movement of these petrographic benchmarks would be a data on the intensity of movement in time.
- Making measurements every 10 years, in the reference points reflected above we would design accurate projects on the works that are expected to be built in
  this area. On this basis the construction of major infrastructure works in the future on the axis Elbasan - Librazhd would be well we build in the southern part of the Shkumbin river.
- Their construction in the northern part would require additional engineering measures, significantly increasing their cost.
- The engineering works built in the northern part (especially the railway bridges) must be repaired in time, given that the movements are not homogeneous.
- Monitoring of horizontal movements in the time unit (most suitable 10-year unit) would provide data on the lifespan of the constructed objects and the engineering measures to be taken.

REFERENCES

[1] Blaceri, F. (1986). The geological and tectonic development of the Hotolisht-Shebenik region and the feature of the tectonics of the axial part of the anticlinorium of the Shebenik Ultrabasic massif. Bul. Shk. Gjeol. 3 , 27-42.

[2] Manika, K. Gega, D (1999) Petrogenesis of podiform chromitites of the Shebenik Massif Albania Bul. Shk. Gjeol. 1 51–57.

[3] Manika, K. and Fabries, J. (1997) Preliminary results on the oxidation stage of two mass ophiolitic agents from Shebenik (Albania). Ofioliti, 22,207-212.

[4] Manika, K. Shalla, M. and Gega, D. (1997) The plutonic sequence of the Shebenik ophiolite complex, Albania: evidence for dual magmatism. Ofioliti, 22; 93-99.

[5] Bebien, J. Shallo, M. Manika, K. and Gega, D. (1998) The Shebenik massiv (Albania): A link between MOR– and SSZ- type ophiolites? Ofioliti, 23 (1), 7-15.

[6] Blaceri, F. (1986). The geological and tectonic development of the Hotolisht-Shebenik region and the feature of the tectonics of the axial part of the anticlinorium of the Shebenik Ultrabasic massif. Bul. Shk. Gjeol. 3 , 27-42.

[7] Cili, P. Brace, A. Alliu, I. and Kotani, V. (1985) Petrologjia dhe kromitet e masivit te Shebenikut. ISPGJ, 300-377 .

[8] Gawwlick, H. Frisch, W. and Hoxha, L. (2008) Mirdita Zone ophiolites and associated sediments in Albania reveal neotethys Ocean origin. International Journal of Earth Sciences 97; 865-881.

[9] Hoeck, V. Koller, F. Meisel, Y. Onuzi, K. and Kneringer, E. (2002) The Jurassic South albanian ophiolites: MOR-vs.SSZ-type ophiolites.Lithos 65: 143-164.

[10] Onuzi, K. Koller, F. Hoeck, V. Gega, D. and Marku, S. (2012): Some data of mineral resources in Southeastern Albania, the regions Korce-Librazhd. Acta: MineralogicaPetrographica, 7, 98-106.

[11] Robertson, A.H.F. Ionescu, C. Hoeck, V. Koller, F. Onuzi, K. Bucur, II. and Gega, D. (2012) Emplacement of the Jurassic Mirdita ophiolites (southern Albania): evidence from associated classic and carbonate sediments, International Journal of Earth Sciences, 101, 1535-1558.

Effect of errors on execution and design of key details in the object

Alush Shala[1], Jelena Bleziffer[2]

[1] *ALB-Architect, Pristina, Kosovo*
[2] *Faculty of Civil Engineering, University of Zagreb, Croatia*

ABSTRACT

Key details must be given major attention in design and execution of a building. Errors which may lead to increase of damage in case of an earthquake and additional loads, can be of different nature, especially those related to beam-column joints. There should be strict attention to details execution by the supervision engineer and contractor. The contractor and the supervisor should correct the design errors, if such exist. The execution in an improper way can have major consequences. The local ductility on the cross-section of vertical elements and their importance is vital for the building. The severity and extent of such damage shall be illustrated with some examples from a recent earthquake in Albania, as the lead author was invited by the state institutions of Albania to assess the degree of damage to school buildings. The paper shall discuss observed damage, possible causes in relation to design errors, as well as some solutions that may be employed for the renovation of damaged buildings.

Keywords*: Concrete, earthquake, building, design, errors, responsibility*

INTRODUCTION

During the visits in Albania in the assessment of the damage of the objects, we encountered some errors during the execution of the details. Working out the details of the structural elements correctly has a great value for the building. Conform implementation of the project and strict supervision will not only increase the sustainability to seismic impacts but also the age of the building. During the inspection we encountered destruction not only of old buildings but also of new ones. Therefore, the details of the joints between the columns and the beam, reinforced concrete walls and slabs, foundations, placement of seismic walls have a major role in the building and great care must be taken in execution. Care should be added especially for seismic areas starting from the first stages of design, preparation of the main project and execution, in the phase of construction and supervision of works. Errors encountered are of various natures. The damages are also of various kinds. In most cases the damages show the degree of the earthquake. However, the biggest damages are due to age, errors in the realization of details, lack of strict supervision and in certain cases even the design drafted not conform standards for areas with high seismicity. Improper execution of the details of the structural elements has a high cost for the building and the investor. The building will be damaged in duration even if we will not have additional impacts from the earthquake. In this paperwork I have presented some details which were not realized correctly and the alternative way of realization. In seismic areas particular importance has the analysis of local ductility of vertical elements. Checking the local ductility of vertical elements and meeting the condition according to EC8 will provide a security for the building in the resistance to additional seismic impacts. This increases the quality of construction, increases the bearing capacity and duration of the building. In this paperwork are presented the most serious damage that occurred by illustrating them with examples and photos from the field, the quality of damage and the possibility of repairing them or not. The value of the investment and the possibility

of the building's duration to such earthquake or even higher. All this in compliance with European technical norms of construction such as Eurocodes (EC0-EC9) and local technical regulation. In this paperwork there are proposed ways of rectification of buildings to be vital and sustainable. Finally, we have the conclusion of this paperwork, which summarizes the opinion and the way of future research and opportunities to address field problems and construction of capital projects.

BUILDING AND DAMAGES DESCRIPTION

During the visit to Albania after the earthquake that occurred in November 2020, we encountered various damages to various objects. The facilities were built from the 1930s until recent years. The damage is mainly cracking of the plaster, which is mainly in accordance with the description in the European norms for this type of earthquake as in photo 1. The damages were also structural, especially in cases when the execution of the basic elements was not done adequately. We encountered non-compliance with the protective layer according to photo 2, failure to realize the detail of the reinforcement according to technical conditions, minimum dimensions of supporting columns photo – 6&8, improper positioning of seismic walls in accordance with the technical conditions in seismic areas or even without seismic walls. In the old buildings there were cracks in the plaster due to thick layers of plastering, displacement of bricks and damage to the bounding between them see photo 3. In the superstructures of the buildings there were cracks in the part which was superstructure or added. Now we will illustrate with pictures these defects according to the description above.



Photo 1



Photo 2



Photo 3



Photo 4

There were also cases of buildings built in 1990-2000 where the beam was supported on the wall and had no connecting strip, which moved it towards the longitudinal axis of the beam as in photo 5.



Photo 5



Photo 6

The damages were evident from the age and the absorption of moisture and as consequence there was the corrosion of the reinforcement as in picture 7. From the corrosion of the reinforcement, we have an increase in diameter which with the action of additional earthquake forces has led to the appearance of damages and cracks.



Photo 7



Photo 8

FAILURE ALONG CONSTRUCTION AND HOW MUST CONSTRUCT RIGHT

During the design, execution, supervision and maintenance of the project, errors are made. Errors are of different natures such as: instant errors, unnoticed errors or during design elaboration, errors from non-compliance with technical norms in the respective areas, errors from investor pressure, errors in execution due to negligence, errors due to ignorance, errors in the supervision phase, and errors also during the maintenance of the building.

During the inspections of objects damaged by the 6.4 magnitude earthquake in Albania we have encountered all these types of errors. We will now analyze some of the errors and the way they work properly.

Errors in the design phase

If we look carefully at the stagnation of the object in the design, we notice that we have negligence in respecting the regulations for areas with high seismicity repeated in the return period of 465 years. In most cases we have soft catheters which bring problems and errors in the reaction object to additional seismic impacts as in photos 2 & 6 & 8. We do not have a good setting of the object's inclination to its mass. The solutions encountered in fig.1 are unfavorable for seismic areas because they represent the soft floor. While in other floors we have filling the spaces between the columns and beams. Satisfactory solution is the presentation in figure 2, where the response to seismic loads is given by reinforced concrete walls. With this way of placing the walls we will meet an important seismic requirement by eliminating the soft floors that have posed a problem everywhere where we had earthquakes. of larger dimensions.

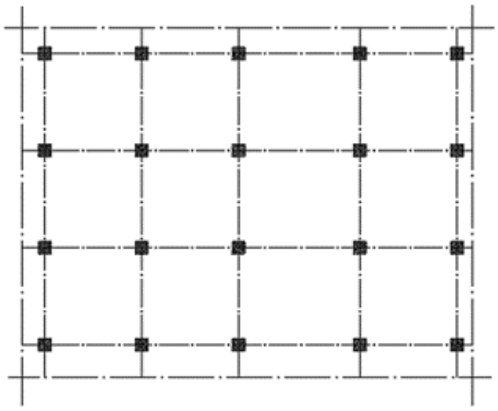


Figure .1 Not good solution, Soft floor

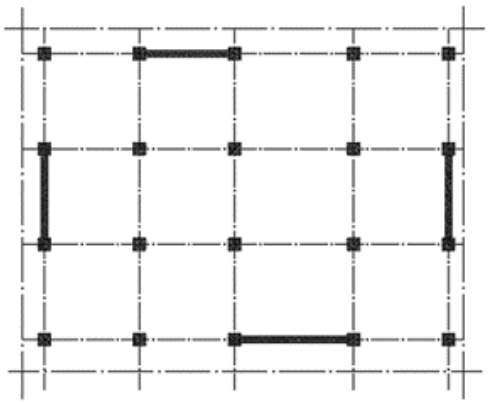


Figure. 2 Solutions that meets seismic requirements

Another error encountered in the design phase is presented in photo 5, where we have the support of the beam in the wall and it is not connected to a beam in the walls of the building. Here is its displacement from the support in the direction of the longitudinal axis of the beam. In seismic areas it is advisable to provide staggering beams to have a better connection of them. In figure 4 we will present one of the appropriate ways of execution, while figure 3 shows the way executed as in photo 5. The object is built in 1995 and it is not of a high floor to present such damages that it has gone into total collapse.

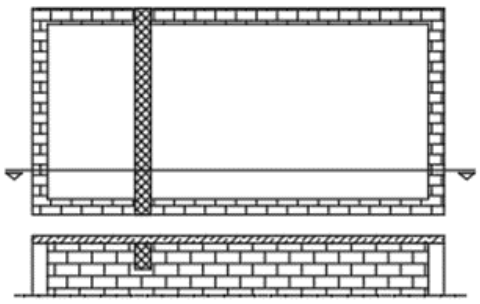


Figure 3. Executed way in photo 5

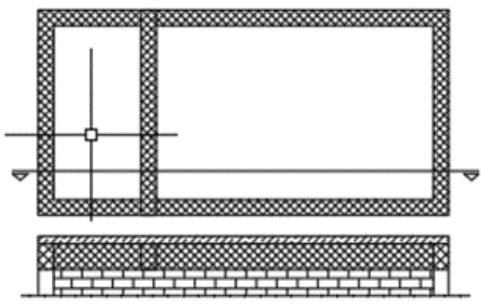


Figure 4. The way it should be executed

Errors in the Construction and Supervision Phase

Execution error not good according to the site view, we now have the connection between the column and the beam. In picture 9 below we present the error in realization, while in figure 5 will present the regular way of execution according to EC8. Resistance for bending forces and cross section forces according to rule 3a of EC8 we have: for primary seismic beams framing into exterior columns, the effective flange width

is taken, in the absence of a transverse beam, as being equal to the width bc of the column (fig.5.b) or if, there is a transverse beam of similar depth equal to the width increased by 2hf on each side of the beam (figu.5.a) [1]

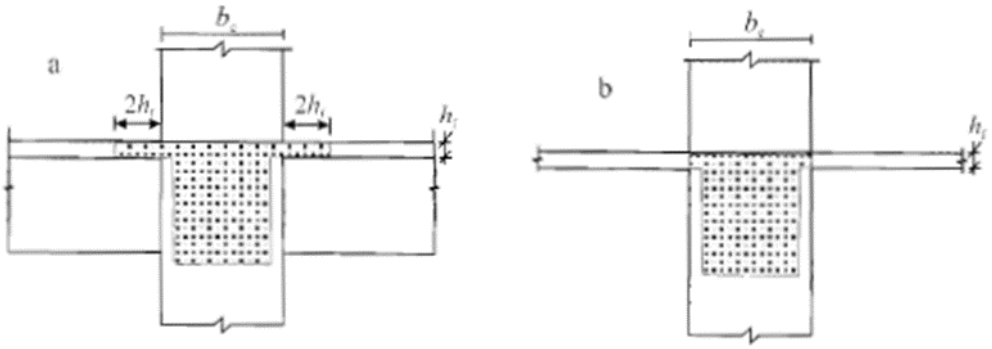


Figure.5 Effective flange width b_{eff} for beams framing into columns [1]

In figure 7 we present figuratively how the regular way of reinforcement for objects in seismic areas is. This detail satisfies the seismic requirements of reinforcement. In detail (fig.7.b) it is presented how reinforcement should be placed in the beam junction to meet the seismic requirements for buildings in areas with seismicity that should not be neglected by the designer and the contractor. In our inspections it was noticed the omission in reinforcement of beams and columns near the joint has not been respected the recommendation of EC8 that near the node to have a density of staff as in fig.7a. Therefore, designers must always take into account that in their deign must respect the technical conditions and norms for areas seismic and have a more rigorous supervision of the implementation of works on site.

The control of local ductility also plays an important role in the pillars, always taking into account the observance of the normalization coefficient of the axial force νd. The main condition is not to exceed the value of 0.65 by EC8 [1] which is expressed by the formula: ($\nu_d = N_{Ed} / A_c f_{cd}$).

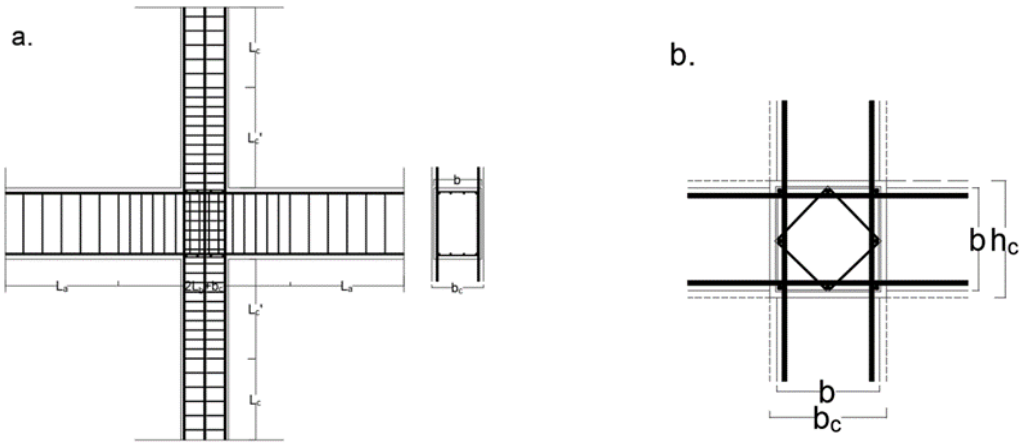


Figure 6 a. Outline of beam column connection armature, b. the detail of the connection of the column beam joint

Another error during the design, supervision or execution that we have encountered will be presented in photo 9. In this photo we have the error of connecting the stairs with the floor slab or beam. Such an error is often encountered in our projects but also in execution not according to the detail design which is a serious omission of the supervisor of works.



Photo 7. Wrong ladder support



Photo 8. Short element ladder support

In picture 10 we have the creation of the short element in the column which is a mistake when designing the stair support. Always in seismic areas we must eliminate such elements by creating stairwells for and walls to support the stairs in the area between floors.

In the figures below we will present a solution that satisfies the technical construction and seismic requirements. Figure 8 a schematically shows how the connection of the stairs to the area between floors is executed, which is totally wrong.

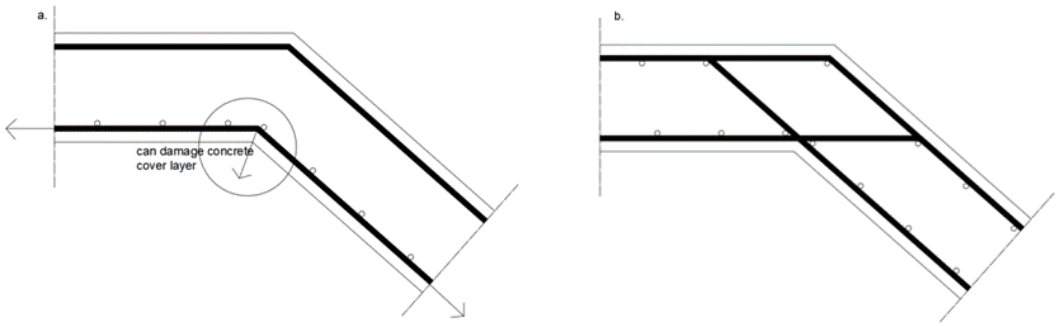


Figure 9. a. Wrong reinforced support, b. Right reinforcement support.

Figure 9 shows the possibilities of eliminating the short column element. The possibility to meet the best seismic requirements is the construction of the stair cage, which eliminates the possibility of collapse of the support. We have now presented the support of the stairs in the wall cage with reinforced concrete fig.9a, then we have, the support on the side walls again in reinforced concrete or retaining wall fig. 9b, which represents a satisfactory solution. Whereas in fig.9c is shown the support only in the front wall which is a better solution than the support in the columns that creates the short element.

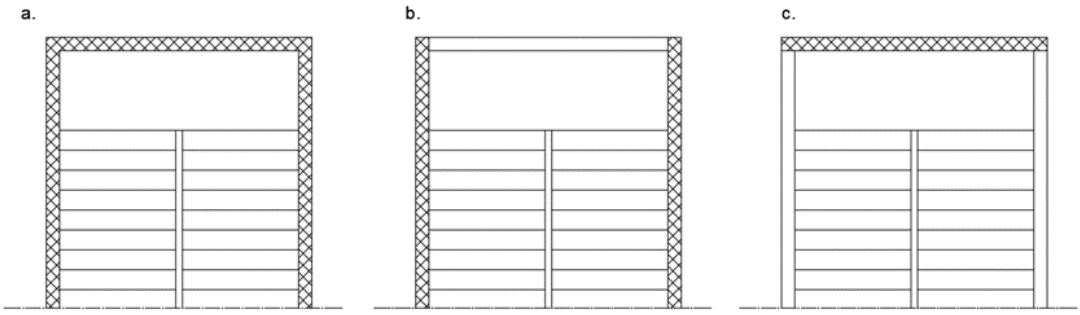


Figure 10. Ways of supporting the stairs by eliminating the support on the column

Following we will present the defects presented by the thick layer of plaster which is a problem in itself during the action of dynamic seismic impact. In photos 1 & 3 we have cracks which are due to adequate sampling of the plastering layer, exceeding the optimal layers without the use of reinforcement additives, such as reinforcement meshes, FRP or other connecting additives. Whereas in photo 4 we have cracks instead of continuing the superstructure. In this sequence the connection is not treated properly using materials which accept the eventual stretching forces from dynamic impacts.

REHABILITATION OF BUILDINGS

Before deciding on rehabilitation or renovation of damaged elements a commitment is first required to identify the damage and address the reasonableness of the rehabilitation or renovation. In every phase of the rehabilitation process acceptability criteria plays the decisional role, from the initial evaluation, to design process and quality assurance of the erection process. [2]. It follows that we have several stages of evaluation to come to the decision for rehabilitation of objects damaged by seismic or earthquake actions. The stages that must be followed in this process are: Strategy document, concept document and detail document. Each stage contains the activities that must be followed. Very important is the purpose of the performance of facilities in rehabilitation. A rehabilitation Objective consists of one or more rehabilitation goals, each goal consisting of the selection of a target Building Performance Level and Earthquake Hazard Level [3], see fig10.

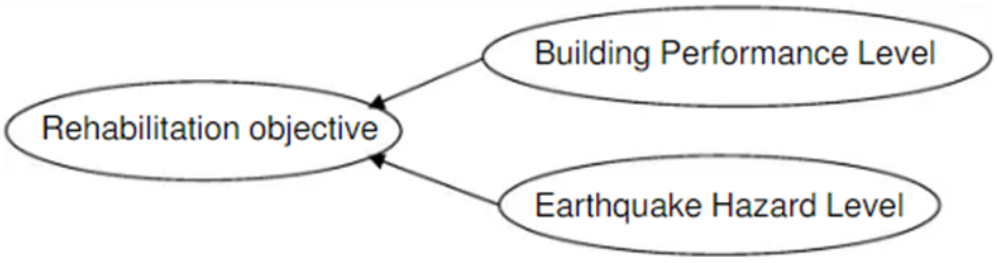


Figure 11. Establish Rehabilitation Objective Principles [3]

Ones that the performance level for structural and non-structural elements have been establish the designer could decide the target building performance level [2]. So, we must first determine the goals of the action and the level of rehabilitation and earthquake risk. Ones that the performance level for structural and non-structural elements have been establish the designer could decide the target building performance level [2].

Throughout our facility evaluation engagement, we need to have general analysis and facility modeling requirements. Due to the dynamic nature of seismic action, the structural model should adequately represent not only the distribution of stiffness, but also the distribution of mass with the structure [2]. During the course of evaluation, we need to take into account the stiffness, deformations and the level of current inelasticity, where their stiffness is based on the elastic module to the real values of force. Special attention should be addressed to joints between structural elements, which do not explicitly model when their stiffness differs significantly from the fully rigid or pinned assumptions, or when their strength is lower than one of the connected elements [4]. Therefore, during the evaluation phase impact of secondary effects has high impact and their stability after the action of the earthquake. When a structure is very flexible under lateral loads, a first-order analysis may underestimate substantially forces and deformation. [2] The stability check will be done using the formula for the stability coefficient θi.

If it passes the necessary verifications of the evaluation, then it goes to designing in stages to complete the detailed design, for the realization of rehabilitation.

Some of the ways of rehabilitation is using concrete, injection of cracks, use of rabic metal meshes, use of different polymers for wall reinforcement. In the case of the most severe damage to the columns, different hydraulics should be used to raise the facility to the previous level before deformation and start with repairs, always if it passes the evaluation test by the relevant engineer.

We will now give some examples of rectifications in following figures.

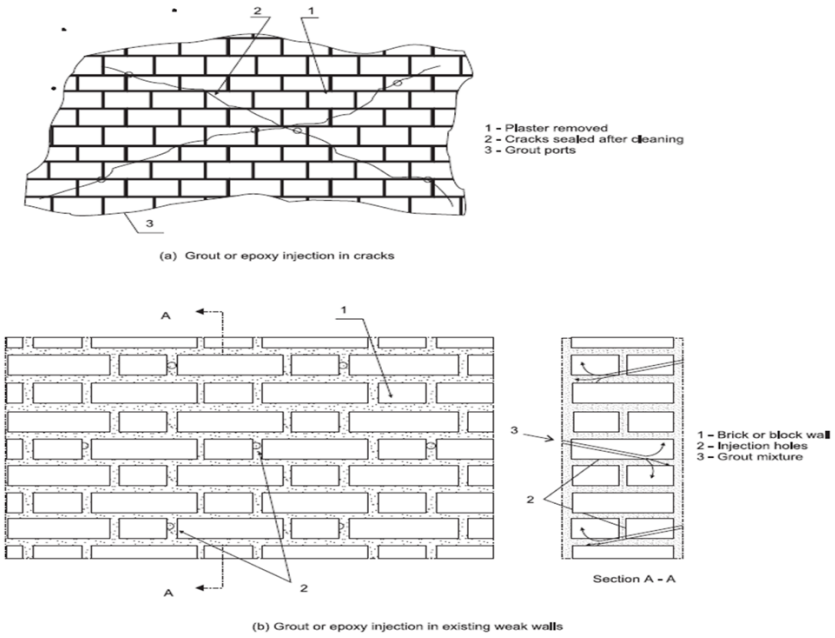


Figure 12. strengthening of existing masonry [5]

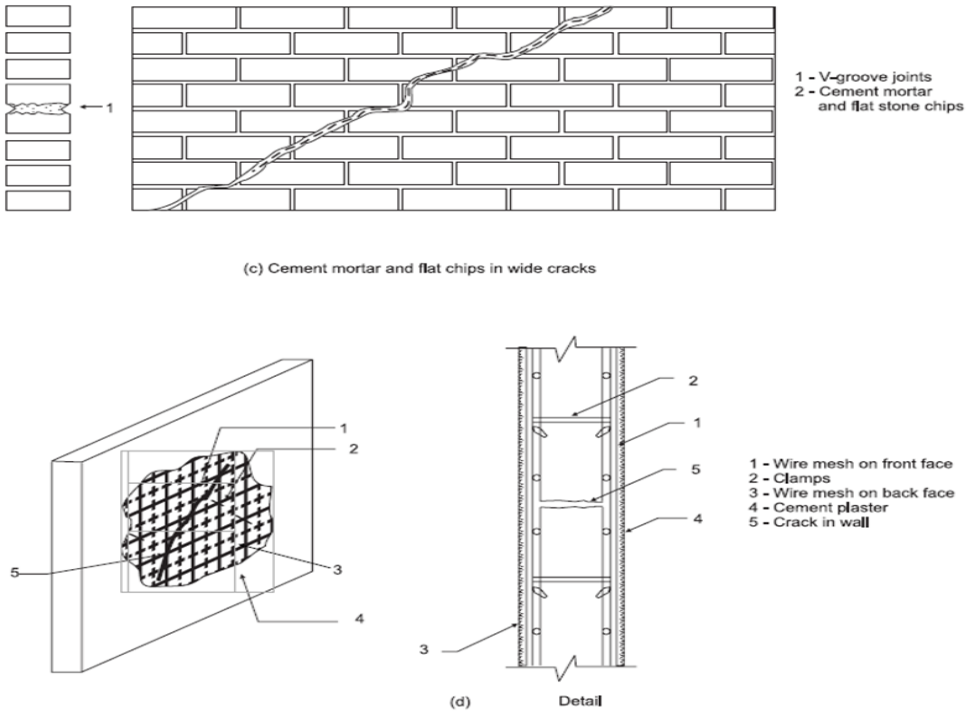


Figure 13. Strengthening of existing width crack masonry [5]

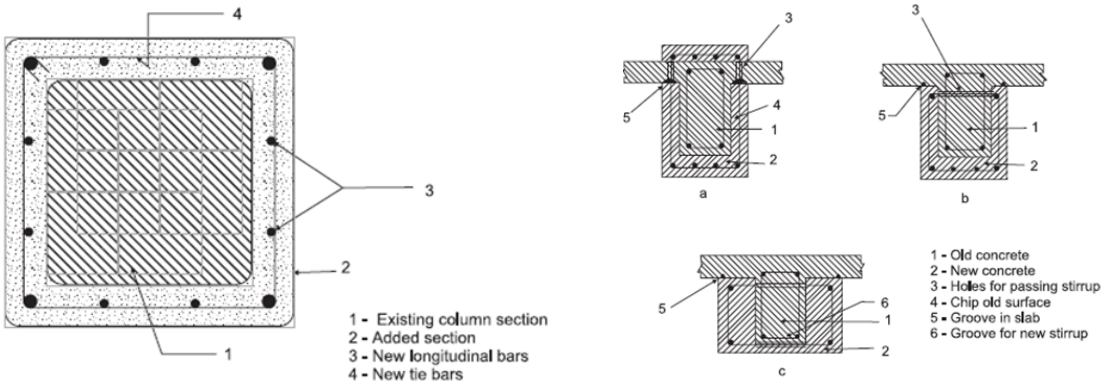


Figure 14. a) Jacketing a concrete column, b) Increasing the section and reinforcement of existing beams

CONCLUSION

Based on the findings from the field and the analysis of defects encountered in the field and the documentation presented, we conclude that the implementation and complying with technical norms for seismic areas would reduce the damage. Before starting renovations or demolition a proper analysis to determine a realistic assessment of the condition of buildings is needed. Damages caused are due to poor maintenance of concrete, inadequate realization of details of structural and non-structural elements. The use of seismic walls will reduce the risk of destruction in mass and the causes of the victims. A more rigorous control of the state institutions is required in the issuance of permits and on-site control for the realization of the objects.

REFERENCES

[1] Eurocode 8: Design of structures for earthquake resistance – Part 1: General rules, seismic actions and rules for buildings [Authority: The European Union Per Regulation 305/2011, Directive 98/34/EC, Directive 2004/18/EC]

[2] DAN DUBINA.,Adrian Dogariu., Aurel Stratan.,Sorin Bordea.,Performance based seismic assessment of buildings for evaluation of retrofitting systems efficiency.,Politehnica Univetsity Timisoara.,Timisoara, February,2008

[3] FEMA 356, Guidelines for seismic rehabilitation of Buildings,Vol 1:Guidelines ,FEMA 356 ,Washington DC,2002

[4] Stratan A., Dubina D.-Models and Analysisprocedure for global analysis-FP6 PROHITTECH,WP9 Calculation Models

[5] INTERNATIONAL ASSOCIATION FOR EARTHQUAKE ENGINEERING KENCHIKU KAIKAN, Guidelines for Earthquake Resistant Non-Engineered Construction, Japan ,2004

Computational Fluid Dynamics Modeling of Submerged Vegetation in Open-Channels

Izet Mehmetaj[1], Mirjam Ndini[1]

[1]*Department of Civil Engineering, EPOKA University, Albania*

ABSTRACT

This study examines how the submerged vegetation affects the hydraulic properties of the open-channel flow.

To predict the impacts of vegetation presence, a Computational Fluid-Dynamic (CFD) model has been developed. ANSYS CFX 18.2 is used to analyze vertical velocity distribution and other flow characteristics as resistance to varying densities, length and positioning of solid cylindrical rods representing vegetation.

The main objective is to create a CFD approach to identify, determine and measure the parameters that contribute to additional resistance due to vegetation. The aim is to better understand hydraulics in stream flow with vegetation systems and to suggest a design tool for evaluating the potential effect of vegetation on stream water management and ecology in Albania. In this study, it is found that the model for the three considered cases gave different results for each of the evaluated parameters, so a correlation exists between the development of the flow hydraulic properties and the vegetation configurations. Also, the obtained results showed that vegetation has a great influence on the characteristics of the flow.

***Keywords**: CFD, flow resistance, open-channel, submerged vegetation, simulation*

INTRODUCTION

Anticipating the pattern of flow through the presence of vegetation is becoming important to hydraulic engineers. That is because vegetation is responsible for additional resistance to the flow in rivers, slows down the water flow, it alters the channel flow and results in patterns that are unlike those in non-vegetated systems.

Moreover, vegetation in open channels induces higher bed roughness, lower flow velocity and has an impact on flood capacity. Thus, a better understanding of hydraulic characteristics in vegetated flow is significant for the management of rivers and their ecosystems.

Albania is a country that experiences flooding very often. The need to have a solution for overcoming the risk of flooding is sometimes very costly and has a huge impact on the environment, so relying on natural processes is more sustainable. Vegetation in riverbanks, emergent or submerged, improves the riverbank stability, reduces erosion, and impacts the floodwater storage. The engineering approach to this issue requires determination of the hydraulic resistance resulting from the existence of vegetation.

This study discusses the presence of submerged vegetation by means of a CFD (Computational Fluid Dynamics) model to predict the additional resistance based on vegetation geometric properties like spacing and height.

The main idea is to establish a CFD modeling approach to identify and quantify the parameters that contribute to the induced resistance due to vegetation presence. A CFD 3D model will be considered such

as RANS (Reynolds-averaged-Navier-Stokes) employing a standard k-ε turbulence model for the vegetation simulation on ANSYS CFX software 18.2.

Research shows that the presence of vegetation in the flow increases the hydraulic resistance by causing dragging and turbulence. The mixing induced by the turbulence will have significant effect on ecology, sediment transport in water, pollutants in water, etc. [1].

Different research has been recently carried out on this topic. Authors mainly reviewed aquatic vegetation effect on flow velocity vertical profiles.

For example, Klopstra et al. [2] and Meijer and Van Velzen [3] worked on a method to analytically define the velocity profile into two layers flow domain, one within the vegetation and another above the vegetation. The model is a two-layer model type and consisted on solving the momentum equation in the vegetation layer while considering a logarithmic profile of velocity in the upper layer. Model simulations were consistent with the results of flume experiments reported in these studies.

Lopez and Garcia [4] proposed a model to calculate the mean velocity profiles and turbulence characteristics in open-channel vegetated flows under a 1D framework. This model is a two-equation turbulence approach and was built since the drag due to vegetation is appearing not only in the momentum equation, but also in the equations of a modified k-ε turbulence model. Numerical results including mean velocities, Reynolds stresses, turbulence intensities and different terms in the turbulent kinetic energy, were compared with the experimental observations.

Wilson et al. [5] conducted a study using 3D Finite Volume (FV) numerical model to describe the hydraulic effect of vegetation on the velocity distribution concentrated on the drag-force approach; the model provides solution for the continuity and momentum equations for each cell and for the modelling of turbulence uses the k-ε model.

In recent years, the impact of vegetation in flow resistance and turbulence as well as its influence on sediment transport were inspected.

Yan et al. [6] studied the effects of vegetation rigidity on the hydraulic roughness. The experimental results showed that a rigidity coefficient of vegetation can be used to describe the vegetation rigidity relating to the flowing water.

Nepf [7] discussed the impact of vegetation distribution on sediment movement, by working on methods for estimating bed stress within regions of vegetation.

Izni et al. [8] studied the development of vegetative roughness estimation for hydraulic modelling through laboratory experiments and remote sensing. The study concluded that there is a possibility to utilize the data of remote sensing to accurately estimate the main vegetation properties such as height and density. These would allow to define the parameters to be used as input for the calculations of surface roughness in any practical application.

Timothy et al. [9] employed a three-dimensional model to predict the flow and turbulence dynamics in open-channels. Two different CFD-biomechanical models are suggested on this study. The model's suggestions are based on whether the vegetation is dominated by bending or tensile forces. For bending plants (vegetation is dominated by bending forces), a model structured on the Euler–Bernoulli beam equation has been suggested, while for tensile plants (vegetation is dominated by tensile forces), a N-pendula model has been suggested. The results showed that both models predict the spatial characteristics of the mean flow, turbulence as well as plant-flow interactions.

Panigrahia et al. [9] conducted an experiment in a straight open channel flow using unbending cylindrical rods to investigate the effect of vegetation. In this study, has been investigated the effect of emergent rigid vegetation on the prediction of the effective vegetal drag coefficient for various flow depth combinations.

Richard et al. [10] provided a new method that integrates the complexity of the plant morphologies into a computational fluid dynamics (CFD) model. The complexity of plant morphology, including the vertical and horizontal distribution of their branches and leaves is gathered through earthly laser scanning (TLS) and

is kept up in the numerical prediction of flow fields. This approach provides a full flow numerical description of the pressure field. It also allows the vegetative drag force to be measured. The methodology used in this study shows the significance of accurately representing complex plant morphology in hydraulic models.

Evaluating these studies, many physical and numerical models had been proposed and approved. Most of them use numerical modelling within Computation Fluid Dynamics (CFD) framework that enables the representation of realistic vegetation patterns. Also, they validate the application capability of CFD for solving the problem of flow resistance in vegetated systems. But, the majority of these investigations depend on a 2D model development.

NUMERICAL MODELLING

Vegetation is commonly modeled as arrays of rigid, circular cylinders that simplify and generalize plant forms of vegetation in riverine systems. This approach is commonly applied to several laboratory flow conditions, including both, submerged and emergent case [25].

Generally, the model is based on the analysis of forces acting on the volumetric element surrounding a given number of elements of vegetation. Specifically, as water flows through vegetation, drag is produced. The drag creates eddies and velocity gradients that causes the loss of momentum. There exist several numerical approaches that describe the effect of vegetation on flow resistance. Most of recent models are concentrated on a drag-force approach [7].

Wilson et al. [7], introduced a drag-related force term to be implemented on Navier – Stokes equation to describe the flow resistance induced by vegetation. The approach consists of a 3D Finite Volume method. The finite volume method is a numerical method to solve partial differential equations. The finite volume method calculates the values of the conserved averaged variables across the volume. This drag force F_D usually has the form:

$$F_D = \rho \frac{u^2}{2} C_D \lambda \tag{1}$$

Where C_D is the drag coefficient and λ represents the projected area of a single plant in stream wise direction. This force can be included as a sub grid force per fluid mass unit in a finite volume (FV) cell.

In this study, the 3D Navier-Stokes equations for steady, incompressible flow in combination with the standard k-ε turbulence model will be solved by the ANSYS CFX code (ANSYS 18.2, 2017).

In this code as in the most typical Computational Fluid Dynamics models, to define the flow field, are solved the Navier-Stokes equations. The Navier-Stokes equations describe the forces acting on a body of water.

In CFD, turbulence models are empirical mathematical models that describe the turbulence in the flow. In these numerical stimulations, there are three approaches for the prediction of the turbulent flow summarized below [28]:

- Reynolds Averaged Navier- Stokes (RANS) simulation
- Large Eddy simulation (LES)
- Direct numerical simulation (DNS)

RANS has been widely used in designs and research since the 70's. K-epsilon (k-ε) turbulence model is the most common RANS model used in Computational Fluid Dynamics (CFD) to simulate turbulent flow conditions.

The standard k-ε model is firstly proposed by Launder and Spalding in 1974 [29]. This turbulence model gives a general description of turbulence by means of two model equations. The first equation considers the kinetic turbulent energy k and the second one for the rate of dissipation of turbulent kinetic energy per unit mass, ε.

The parameters k and ε are determined by solving transport equations:

- For turbulent kinetic energy k:

$$\frac{\partial(\rho k)}{\partial t} + \frac{\partial(\rho k u_i)}{\partial x_i} = \frac{\partial}{\partial x_j}\left[\frac{\mu_t}{\sigma_k}\frac{\partial k}{\partial x_j}\right] + 2\mu_t E_{ij}E_{ij} - \rho\varepsilon \quad (2)$$

- For dissipation ε:

$$\frac{\partial(\rho\varepsilon)}{\partial t} + \frac{\partial(\rho\varepsilon u_i)}{\partial x_i} = \frac{\partial}{\partial x_j}\left[\frac{\mu_t}{\sigma_k}\frac{\partial \varepsilon}{\partial x_j}\right] + C_{1\varepsilon}\frac{\varepsilon}{K}2\mu_t E_{ij}E_{ij} - C_{2\varepsilon}\rho\frac{\varepsilon^2}{k} \quad (3)$$

Where u_i represents velocity component, E_{ij} represents component of rate of deformation, μ_t represents eddy viscosity.

$$\mu_t = \rho C_\mu \frac{k^2}{\varepsilon} \quad (4)$$

The equations also incorporate some constants σ_k, σ_ε, $C_{1\varepsilon}$, $C_{2\varepsilon}$. The values of these constants have been defined empirically for a variety of turbulent flows by numerous iterations of data [29]. These constants are as follows: $C_\mu = 0.09$; $\sigma_k = 1.00$; $\sigma_\varepsilon = 1.30$; $C_{1\varepsilon} = 1.44$; $C_{2\varepsilon} = 1.92$.

CFD MAIN APPROACH AND METHODOLOGY

In general, most applications of CFD take the same basic approach. The basic procedure is described as follows:

Pre-processing: To define the geometry and physical bounds of the problem computer aided design (CAD) tools can be used. Like that, data can be processed, and the fluid volume (or fluid computational domain) is added. The volume limited by the fluid domain (filled with water, air etc.) is divided and broken up into discrete cells (the mesh generation process). The mesh may be uniform or non-uniform, structured or unstructured. It is made of a combination of hexahedral, tetrahedral, prismatic, pyramidal or polyhedral elements. The modeling is defined physically –the equations describing the fluid motion are set. Boundary conditions are determined either by specifying them on each edge of the computational domain (2-D flow models) or on each face of the domain (3-D flow models). They describe and specify the fluid behavior and properties at all bounding surfaces of the fluid domain. In case of transient problems (time dependent problems), the initial conditions are also defined.

Solving: The simulation is started, and the equations are solved iteratively as a steady-state or transient type of analysis.

Post-processing: As a final step, a postprocessor is used to obtain useful information for the analysis and visualization of the resulting solution.

DEVELOPMENT OF THE MODELS FOR SIMULATION WITH ANSYS CFX (18.2)

In this work, ANSYS CFX (Release 18.2) is used to simulate water flow within the vegetation. The numerical reference is associated with finite volume solution of the three-dimensional Navier-Stokes equations in a Cartesian co-ordinate system, and under a standard k-ε turbulence model.

A rectangular fluid domain with 2.052 m length, 0.232 m width and 0.420 m height with bottom slope 1:5000 is used.

Vegetation is considered as an idealized plant with reference to the approach proposed by Wilson et al. [7]. For that reason, the vegetation is modelled as arrays of rigid, circular cylinders. A rigid vegetation is not changing its position within time.

Following this theoretical viewpoint suggested by Wilson at al. [7], three main cases are modelled:

- Case 1: Submerged vegetation scenario with a parallel simulated pattern
- Case 2: Submerged vegetation scenario with a staggered simulated pattern
- Case 3: Double-layered submerged vegetation with a parallel simulated pattern alternately arranged with tall and short rigid circular cylinders.

These configurations and their sizes are shown in Figure 1. Respectively, there are 838 rods/m^2 for case 2 and 3, and 850 rods/m^2 for case 1.

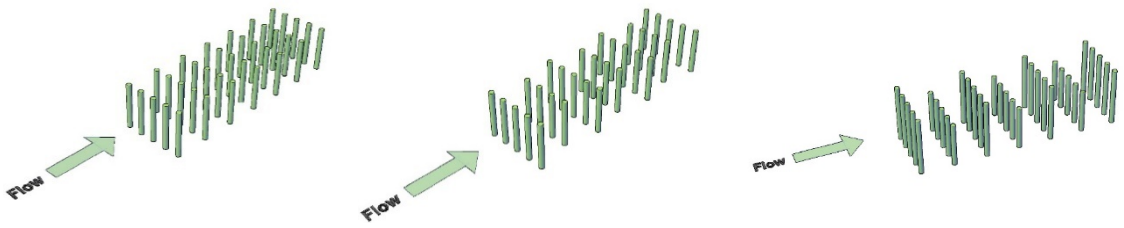


Figure 1. Sketch of vegetation patterns used for modelling (case 1 at the left, case 2 in the middle and case 3 at the right).

Vegetation is simulated with 12 mm diameter rigid circular cylinders of two lengths, k_1= 120 mm and k_2 = 160 mm. In all the three cases the spacing between cylinders is 40 mm in the direction of the stream and 30 mm in the transverse direction of the stream.

In all the scenarios the water is assigned to be used for the fluid domain, at a temperature of 25°C and reference pressure of 1 atm. A normal speed equal to 4 m/s will be imposed as boundary detail for the inlet boundary condition. Also, the no-slip boundary condition is assigned on the both wall type boundaries. Furthermore, the initial conditions are specified globally for the analysis and set equal to 0 m/s for x component, 4 m/s for y component and 0 m/s for the z component. The effect of slope of the channel in the fluid domain will be reflected on resolved gravity components.

Symmetry as a boundary condition is set in the models to specify the zero-shear slip walls in the fluid domain free surface [3]. The flow field will be simulated as transient and over a specified time of 25 s. The time step is set to be 2 s providing 12.5-time steps to be solved.

The time step controls the spacing in time between the variable of interest. The correct choice of the time step will influence the convergence of the simulation.

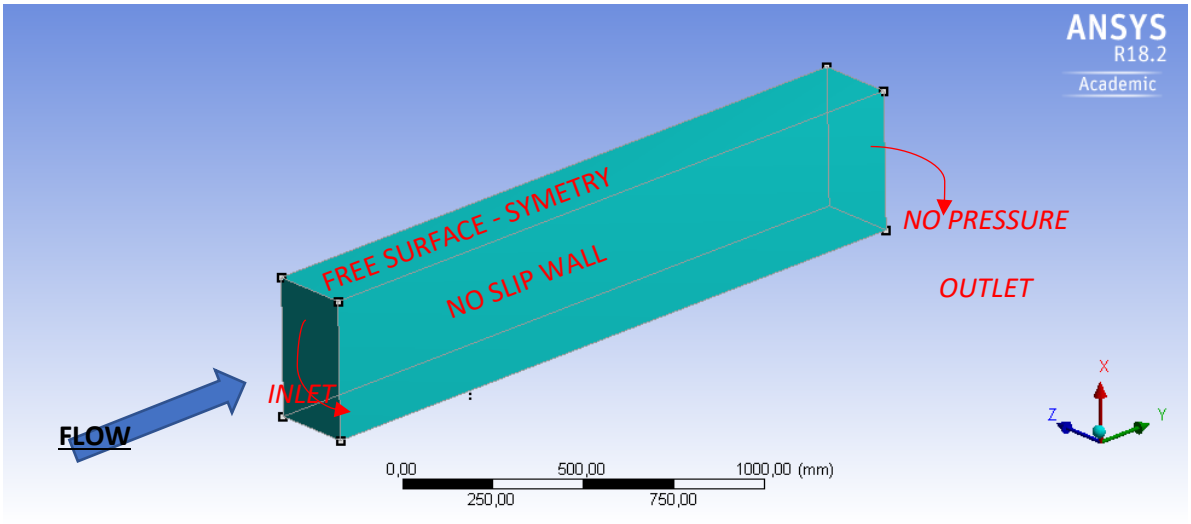


Figure 2. Computational fluid domain schematic

The standard k–ε turbulent model will be used in CFX code, with the model constants $C_\mu = 0.09$, $\sigma_k = 1.00$, $\sigma_\varepsilon = 1.30$, $C_{1\varepsilon} = 1.44$ and $C_{2\varepsilon} = 1.92$. This model is the simplest turbulence model because only initial and boundary conditions needs to be defined.

The three considered cases are employed separately in CFX-Pre. The case 1 refers to time dependent turbulent fluid model with submerged vegetation in a parallel simulated pattern; case 2 refers to time dependent turbulent fluid model with submerged vegetation in a staggered simulated pattern and case 3 refers to time dependent turbulent fluid model with double-layered submerged vegetation in a parallel simulated pattern alternately arranged with tall and short rigid circular cylinders.

In all the cases, water is assigned to be used for the fluid domain, at a temperature of 25°C and reference pressure of 1 atm. For all the three cases, 5 boundary conditions types were inserted for the computational domain: inlet, outlet, wall at the computational domain side faces, the structure wall defined from the vegetation surface region, and the symmetry for the open channel flow free surface.

A normal speed equal to 4 m/s is imposed as boundary detail for the inlet boundary condition. Furthermore, the initial conditions are specified globally for the analysis and domain for Cartesian velocity components and set equal to 0 m/s for x component, 4 m/s for y component and 0 m/s for the z component. Also, the no-slip boundary condition is assigned on both wall type boundaries, that is, the fluid particles on the body move with body velocity. The boundary conditions at the free surface of an open-channel flow suggests that both the pressure and the shear stress are equal to zero everywhere. Here is why a symmetry boundary condition is defined in order to determine a zero value of all the quantities into the symmetry plane. Such definition reassembles the free surface of an open channel flow. The velocity pattern is modelled to be almost uniform along x-axes by adding the free-surface boundary condition. This means that initially, the water will be in movement with a velocity 4 m/s very near to the free-surface and with the depth going increased the velocity will have some curvature providing a 0 value to the fluid domain bottom wall.

RESULTS AND DISCUSSIONS

To study the variations of the velocity distribution at the global scale around rigid vegetation, several analyses of the velocity component data into the open channel fluid domain have been carried out, at XY section's planes along the stream wise direction (Z = 78 mm).

To assign a quantitative value that represent the flow patterns and variations due to vegetation, Manning's roughness coefficient is estimated using The Manning's formula. For all the three considered cases, the estimation is made in the middle of vegetation zone as well as directly after the vegetation.

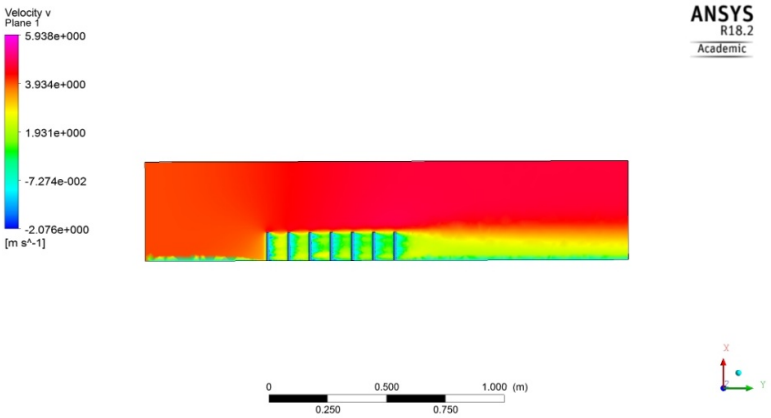


Figure 3. Case 1: Vertical velocity variations at the centrally located XY plane

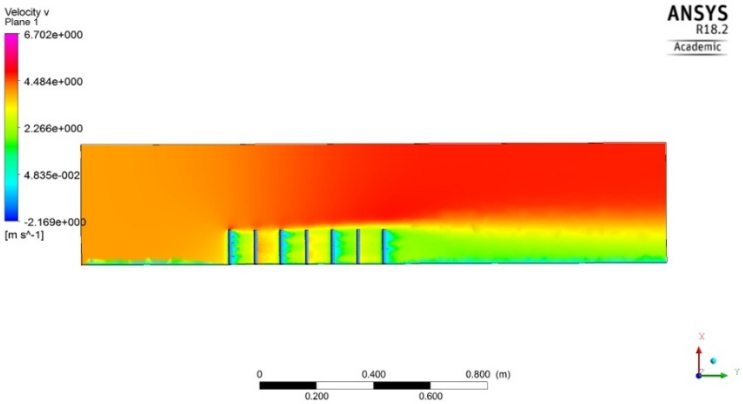


Figure 4. Case 2: Vertical velocity variations at the centrally located XY plane

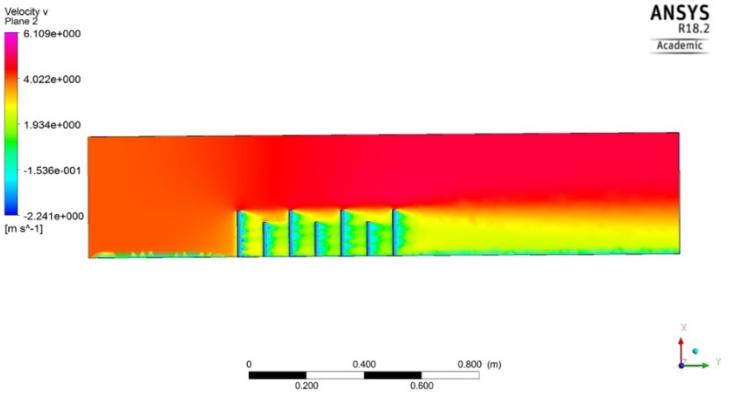


Figure 5. Case 3: Vertical velocity variations at the centrally located XY plane

It is noted that the vertical velocity profile stays almost unchanging in the upper part of the vegetation region. Whereas in the vegetation region the velocity fluctuations are significantly noticeable. A transition occurs at the top of the vegetation height. The fluctuations of the vertical velocity on two distinguished patterns (invariably on the upper part and variable within vegetation) result due to the vegetation existence. At the top of vegetation height is where the transition between these two patterns happens. The presence of vegetation makes the velocity to slow down in comparison with the initial flow velocity. Also, there is a correlation between the velocity development profiles and the vegetation spacing distribution.

In general, it is observed that the flow resistance characterized in terms of n (Manning's coefficient) decreases as the flow depth X is increased. This finding is count by taking as 0 level the bottom of the fluid domain. A similar result is taken at both locations of interest where estimations are made (in the middle of vegetation and directly after the vegetation).

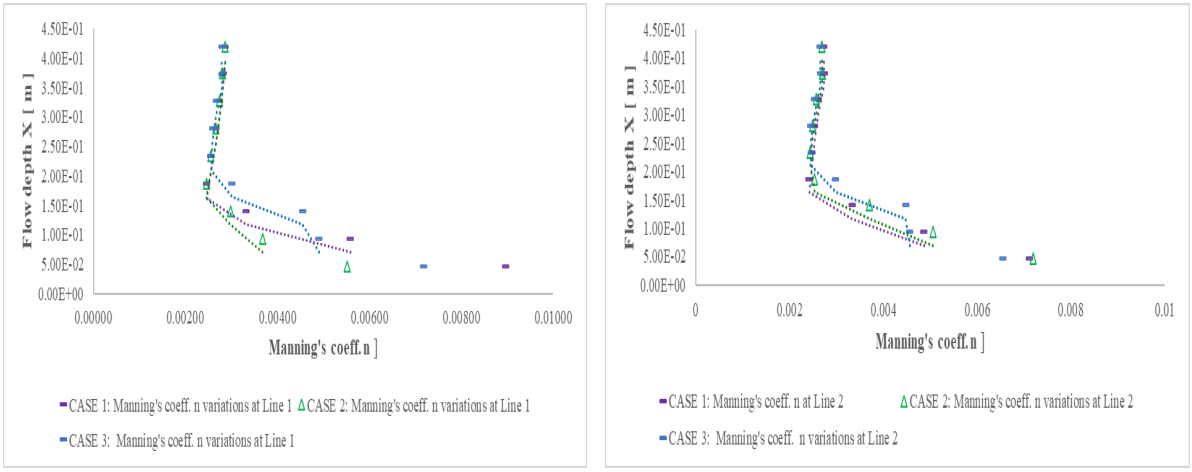


Figure 6. Manning's coefficientn variations within the depth of the open channel domain X, for vegetated zone (left) and non-vegetated zone (right)

A reason is that with increasing flow depth (starting from the bottom of the fluid domain) the absorbing area of vegetation is reduced, that is no vegetation is present as an obstacle. Besides, for the line location directly after the vegetation the effect of flow-rods interaction is different due to rods space arrangement following different flow project areas.

Exceptionally, large values of n are obtained for double-layered vegetation case in the middle of vegetation for the flow depth X range between 0.14-0.187 m. A reason may be the alternation between the tallest and shortest vegetation on this flow depth range that makes the interaction between the rods higher than that in case 1 or 2 as well.

For the case 1, in the middle of vegetation, the values of n are 9 % greater than values of case 2 and 2% less than values of case 3. This observation is notable in the range values of n between 0.003-0.006. However, for the range of n values between 0.002-0.003, the Manning's coefficient leans towards values close to each other.

These variations may occur due to the vegetation properties like height or density. The interaction zone is different between the cases and due to these different vegetation properties, the flow retarding takes different profile to each case. Notable differences are noticed on the vegetation zone. For the given densities, the flow-vegetation produces different values of n.

For the case 2, at location directly after the vegetation, the values of n are 2% greater than values of case 1 and 2% less than values of case 3. Such observation is evident in the range values of n between 0.003-0.007. For the other n range values, they are not varying significantly same as in the zone at the middle of vegetation. For all these readings at the non-vegetated zone, the n values vary and have also

different profiles. This proves that vegetation is an important factor while evaluating the flow resistance and modifies it.

To sum up, the obtained results showed that vegetation has a great influence on the characteristics of flow and can be an important feature affecting the flow frictional resistance in channel.

CONCLUSION

In this study, a computational model is provided to predict the impact of submerged vegetation in a constant rectangular cross-section open channel. A 3D-CFD modeling approach is established to quantify resistance and flow patterns in a vegetated open-channel system based on vegetation geometric properties like spacing and height.

For flows through submerged vegetation, model results indicate that vegetation slows down the flow and causes turbulence within the vegetation layer, resulting in reduced velocity gradients. It is found that the model for the three considered cases gave different results for each of the evaluated parameters, so a correlation exists between the development of hydraulic properties and the vegetation spacing distribution. The computational model allows also to predict Manning's coefficient values.

The obtained results demonstrate the application capability of CFD for solving the problem of flow resistance in vegetated systems. It also provides a framework for future study of flow interactions with vegetation to improve the river stability or flood storage capacity. However, further detailed investigations need to be done in river modeling when such solutions must be provided.

To validate the present approach a field study would be of interest. Having the vegetation present in watercourses has advantages and disadvantages. Planting or taking away the vegetation may increase or decrease the flood risk of watercourses in riverine systems. Resistance is a key parameter to define water levels especially in floods considering that the most important effect that vegetation has, is on the flow velocity. To investigate on this, is important to understand and estimate the resistance due to vegetation. By combining the filed data with the proposed CFD approach as a design tool, new insights would come up and at the same time would test the application capability of this tool.

REFERENCES

[1] J. J. Jochen Aberle, "Chapter 21 Hydrodynamics of Vegetated Channels," in Rivers - Physical, Fluvial, Environmental Processes, Springer, 2015, pp. 519-541.

[2] Y. O. R. H.-P. a. O. N. Wilson C.A.M.E., "3D numerical modeling of a willow vegetated river/floodplain system," Journal of Hydrology, pp. 13-21, 2006.

[3] W. W. Y. H. Y. Z. Z. Y. Wenxin Huai, "Analytical model of the mean velocity distribution in an open channel," Advances in Water Resources, Science Direct, pp. 106 - 113, 2014.

[4] B. H. V. N. J. a. V. V. E. Klopstra D., "Analytical model for hydraulic roughness of submerged vegetation, Managing Water: Coping With Scarcity, and," 27th IAHR Congress, San Francisco, USA, 1997.

[5] D. M. E.H. Van Velzen, "Prototype-scale flume experiments on hydraulic roughness of submerged vegetation," 28th IAHR Congress, Graz, Austria, 1996.

[6] F. L. a. M. Garcia, "Mean flow and turbulence structure of open-channel flow through non-emergent vegetation," Journal of Hydraulic Engineering, p. 392–402, 2001.

[7] W. X. Yan Z., "The Effect of Vegetation Rigidity on Flow Resistance," Advances in Water Resources and Hydraulic Engineering. Springer, Berlin, Heidelberg, 2009.

[8] H. M. Nepf, "Hydrodynamics of vegetated channels," Journal of Hydraulic Research, 50:3, pp. 262-279, 2012.

[9] B. Y. M. C. Izni Zahidi, "Vegetative Roughness Estimation for Hydraulic Modelling: A Review," Research in Civil and Environmental Engineering, pp. 1-10, 2014.

[10] R. J. H. S. N. L. &. D. R. P. Timothy I. Marjoribanks, "High-resolution numerical modelling of flow—vegetation interactions," Journal of Hydraulic Research, pp. 775-793, 2014.

[11] K. K.Panigrahia, "Prediction of Velocity Distribution in Straight Channel with Rigid Vegetation," Aquatic Procedia , pp. 819-825, 2015.

[12] R. J. H. J. W. a. T. I. M. Richard J. Boothroyd, "The importance of accurately representing submerged vegetation morphology in the numerical prediction of complex river flow," Earth Surface Processes and Landforms, pp. 567-576, 2016.

[13] T. S. a. P. B. C.A.M.E. Wilson, "Modelling of open channel flow," in Computational Fluid Dynamics: Applications in Environmental Hydraulics, Chichester, England, John Wiley & Sons, Ltd, 2005, pp. 395-428.

Supplementary cementitious materials and mechanochemistry for sustainable concrete production

Ilda Tole[1], Andrzej Cwirzen[1]

[1]*Department of Civil, Environmental and Natural Resources Engineering, Luleå University of Technology, Sweden*

ABSTRACT

Excavation and removal of instable clayey soils before construction works, e.g., in infrastructure, residential or commercial buildings etc., can generate vast amounts of waste clay deposits. Treatment of those clays to achieve suitable supplementary cementitious materials (SCMs) for use in concrete production can extensively contribute to a circular economy. Mechanical activation (MC) by ball milling has shown suitability to be an alternative and sustainable method to process clays and to obtain dehydroxylation at reduced temperatures and without the addition of chemicals. Furthermore, BM can induce amorphization, increased chemical reactivity and improved pozzolanic properties. Amorphization of crystalline phases can be achieved also for poorly reactive materials as air-cooled blast furnace slags (ACBFS), which can be further utilized as a precursor in sodium silicate alkali activated systems. This study shows how mechanical activation is promoting the reactivity of clay and ACBFS, and their potential to be used as replacement of cement in concrete production. Evaluation of the pozzolanic activity before and after treatment was performed for the treated clay, suggesting increased pozzolanic properties. While alkali activated systems based in mechanically treated ACBFS reached, after 28 days, comparable compressive strength values with the commonly used ground granulated blast furnace slag (GGBFS)

***Keywords**: sustainability, SCM, mechanical activation, clay, air-cooled slag*

INTRODUCTION

The 17 sustainable developmental goals of the 2030 UN´s agenda [1] address awareness in fields as innovation, circularity, climate change, inclusivity and sustainable living. According to this agenda and to the Paris Agreement [2], by 2030 the European Cement Association (CEMBUREAU) aims to reduce with 30% the CO_2 emissions for cement and by 2050 to achieve zero net emissions. Several stages of the value chain of concrete production and constructions can be improved in order to achieve carbon neutrality. The "5C approach", elaborated in the latest Roadmap by the CEMBUREAU, encourages actions in this 5 areas: Clinker, Cement, Concrete, Construction and Carbonation [3]. Cement manufacturing includes primarily the clinker production, which is based in the extraction of the materials (e.g. limestone, clay and sand) and the following kiln-processing step. Production of Portland cement is contributing for approximately 8% of the overall anthropogenic CO_2 emissions and the calcination process delivers alone approximately 60-65%. The remaining part comes from the fuels used in the kiln-process, so approximately 35-40% [3]. This is the reason why clinker production gives various opportunities for CO_2 reduction.

A rapid and proven countermeasure to this issue is partial replacement of cement with supplementary cementitious materials (SCMs). SCMs are siliceous, aluminosiliceous or calcium aluminosiliceous materials in form of powders. These can be natural, e.g. clay, or by-products of other industries, e.g. slag, fly ash or tailings [4]. Ground granulated blast furnace slags (GGBFS) and fly ash are the two main SCMs utilized, but their forthcoming usage is unreliable due to the environmental concerns associated with the industries they

are generated from. On the other hand, clay is a commonly occurring material but a pretreatment is required. Amorphized structures are fundamental for increased reactivity of these sources and preliminary heat treatment is often performed for this purpose. Kaolinitic clay is thermally treated at around 600-1000 °C to produce metakaolin, which is a well-established and highly reactive SCM. Not only kaolinitic clays but also mixed layer clays, after treatment, can have a great potential as SCM [5,6]. Thermal treatment of clays or natural pozzolans can contribute at some degree to the CO_2 emissions and requires high temperatures. However, studies have shown that clay can be activated by a cleaner technology without the need to use high temperatures [7]. Mechanical activation in a ball mill can induce amorphization of the structure increasing the pozzolanic reactivity of clays.

Another efficient solution to increase the sustainability of building materials is by replacing Portland Cement (PC) with alkali-activated materials (AAM). This solution implicate a full replacement of PC and the requirement to use strong alkalis, as e.g. sodium hydroxide or sodium silicate, for inducing the chemical reaction and hydration process [8–11]. For AAM production, the main precursor is GGBFS, which is obtained by the water-cooling process of the slag removed from the blast furnace. However, this quenching method requires large amounts of water and produces pollution. Another quenching method that can be utilized is the air-cooling, which on the other hand leads to a poorly reactive material characterized by reduced amorphized phases. Nonetheless, poorly reactive sources as ACBFS can be treated with mechanochemistry to increase their reactivity and utilize them as valid precursors in AAM [12].

This article summarizes opportunities and utilization potential of SCMs, including clay and ACBFS can have for the future. Utilization of mechanochemistry to increase reactivity of these materials is crucial for efficient utilization of these resources, which in their natural form have not a great performance.

MATERIALS

According to their behaviour during the hydration and hardening process, SCMs are divided in two categories: *hydraulic* and *pozzolanic*. Hydraulic SCMs have a similar behaviour to cement and harden due to an irreversible hydraulic reaction when combined with water. On the other hand, pozzolanic SCMs do not react when in contact with water. Blended cements, both with hydraulic and pozzolanic SCM, are characterized by metastable phases developed during hydration.

In this study, two different types of SCMs are used: clay (pozzolanic) and ACBFS (hydraulic). Both of the materials were mechanically treated before their solidification. The chemical composition is shown in Table 1.

Table 1. Chemical composition of ACBFS and clay

	SiO_2	Al_2O_3	CaO	Fe_2O_3	K_2O	MgO	Na_2O	LOI
ACBFS	31,3	11,9	31,1	1,67	0,639	13,7	0,515	-1,6
Clay	52,6	15,1	6,41	6,9	3,78	2,51	1,68	7,5

METHODS

Both materials were processed in a ball mill, using the same process parameters. The time of grinding (20 minutes), filling ratio (25 ball to powder ratio) and rotation speed (500 rpm). The ball mill was a Retsch equipment, type PM100.

Phase composition and amorphization rate were determined through the XRD analysis, using an X-ray diffractometer type Empyrean. The XRD samples were not pre-treated and back-loading sample holders

was used to avoid preferred orientation of the particles. The main identified phases by Panalytical´s Highscore Plus equipped with a COD database, include kaolinite (Kln), muscovite (Ms), illite (Ilt), montmorillonite (Mnt), quartz (Qz), and calcite (Cal). In the untreated ACBFS crystalline phases as akermanite (A), melilite (Ml), and merwinite (Me), were identified. Decreased intensities and broaden peak areas were produced upon the application of mechanical activation process suggesting a partial destruction of A and Ml phases.

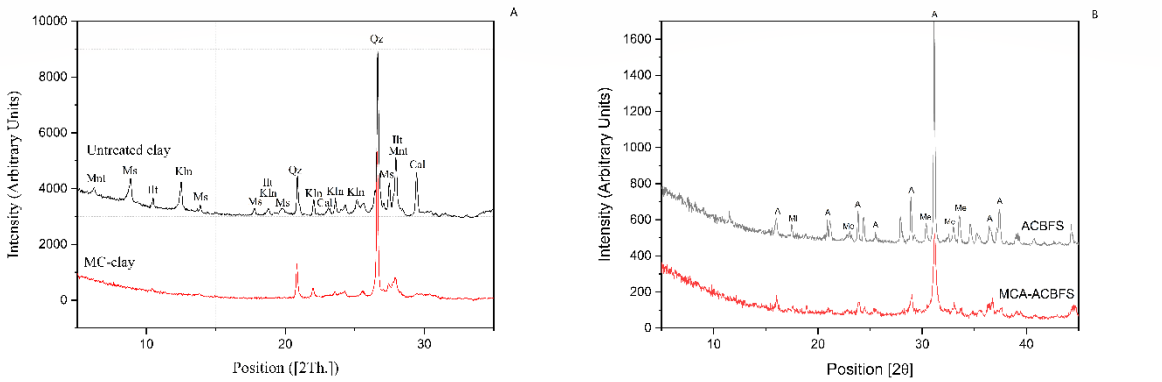


Figure 1. XRD pattern of a) clay and b) ACBFS, before and after mechanical treatment.

Pozzolanic activity was evaluated with the indirect method of Strength Activity index (SAI) through comparison of compressive strength tests, according to standard ASTM C 618 [13]. Compressive strength tests were done on mortar beams with dimensions 40*40*160 mm^3, prepared with the water to binder ratio (w/b) of 0.5 and the binder to sand ratio of 1:3. A Hobart mixer was used to prepare the mortar mixes and the mixing time was 5 minutes. Mortar beams were produced using cement as a binder and a mixture of 80 wt. % of cement and 20 wt. % of the processed clay and mine tailings. SAI was calculated as a percentage of the ratio between the compressive strength value of the control beam (containing only the PC) and the compressive strength value of the mortar beam prepared with 20 wt.% of cement replacement.

For AAM samples, activation was done with liquid sodium silicate (SS) provided by the PQ Corporation. The water to binder (W/B) ratio was 0.45 and the mass ratio of sand to slag was kept constant at 1:1. The SS had an alkali modulus AM (mass ratio SiO2/Na2O) of 2.2, with 34.37 wt. % of SiO2, 15.6 wt. % of Na2O and a solid content of 49.97 wt.%. The AM of the SS was adjusted to reach three different values of 1, 1.5 and 2.0, by addition of sodium hydroxide pellets (98% purity). The alkali activator was added as 10 wt. % of the binder content calculated as a solid material. The compressive strength was determined using a CTM test machine combined with the QuantumX MX440B, universal measuring amplifier. The test specimens had dimensions of 12x12x60 mm3 and 76 were cast into Teflon moulds without application of demolding oil.

RESULTS

After 7 days, compressive strength of mortar prepared with 20% replacement of untreated clay decreased slightly, suggesting the poor reactivity of the natural clay (Figure 2a). On the other hand, replacement by the mechanical treated (MC) clay has achieved higher values for the compressive strength. Similar trend was evidenced for the results of the compressive strength after 28 days. Further information and results about parameters of the MC process were reported earlier, assessing that mechanical activation can enhance the reactivity of natural clays [7]. According to the results from the compressive strength tests, strength activity index (SAI) after 7 and 28 days was calculated (Figure 2b). All samples have reached the

minimum required index. However, mechanically treated samples had exceeded these values by 100%, suggesting an increased pozzolanic activity and improved mechanical properties.

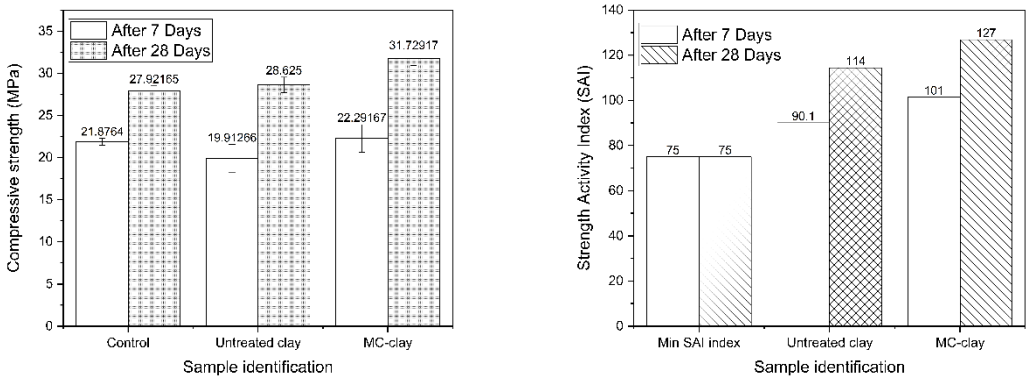


Figure 2.a) Compressive strength and b) SAI after 7 and 28 days of clay samples, before and after mechanical treatment.

All mortar samples made from ACBFS with alkali modulus 1.0 and solid solution of 10%, were characterized by an acceptable workability. MC-ACBFS based mortars activated with the SS having the alkali modulus of 1 showed 28-day compressive strength values comparable with the commonly used GGBFS [11,12]. Higher alkali modulus of the used SS activator decreased the compressive strength values after both 7 and 28 days.

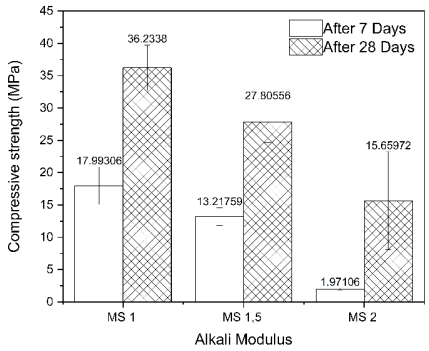


Figure 3. Compressive strength after 7 and 28 days of alkali activated ACBFS samples after mechanical activation, with different alkali modulus.

CONCLUSION

Mechanical activation in a ball mill is an environmentally friendly process enabling to increase the chemical reactivity and pozzolanic activity of clay.

An optimized mechanical activation process can enhance the reactivity of poorly reactive and crystalline air-cooled slag.

Mechanically treated clay showed enhanced mechanical properties when utilized as a cement replacement, while mechanically treated slag can be utilized as a precursor for production of alkali activated materials.

Compressive strength values measured after 7 and 28 days increased for the mortar samples prepared containing 20%wt% of MC-clay. SAI after 7 and 28 days overpassed the minimum required value

of 75% for both MC-clays. MC-ACBFS reached after 28 days compressive strength values comparable to similar AAM systems prepared with GGBFS as a precursor.

REFERENCES

[1] The Sustainable Development Agenda – United Nations Sustainable Development, (n.d.). https://www.un.org/sustainabledevelopment/development-agenda/ (accessed November 18, 2020).
[2] The Paris Agreement | UNFCCC, (n.d.). https://unfccc.int/process-and-meetings/the-paris-agreement/the-paris-agreement (accessed November 18, 2020).
[3] REACHING CLIMATE NEUTRALITY ALONG THE CEMENT AND CONCRETE VALUE CHAIN BY 2050 Cementing the European Green Deal, n.d.
[4] M.C.G. Juenger, R. Siddique, Recent advances in understanding the role of supplementary cementitious materials in concrete, Cem. Concr. Res. 78 (2015) 71–80. doi:10.1016/j.cemconres.2015.03.018.
[5] A. Alujas, R. Fernández, R. Quintana, K.L. Scrivener, F. Martirena, Pozzolanic reactivity of low grade kaolinitic clays: Influence of calcination temperature and impact of calcination products on OPC hydration, Appl. Clay Sci. 108 (2015) 94–101. doi:10.1016/J.CLAY.2015.01.028.
[6] R. Lemma, E.F. Irassar, V. Rahhal, Calcined Illitic Clays as Portland Cement Replacements, in: Springer, Dordrecht, 2015: pp. 269–276. doi:10.1007/978-94-017-9939-3_33.
[7] I. Tole, K. Habermehl-Cwirzen, M. Rajczakowska, A. Cwirzen, Activation of a raw clay by mechanochemical process-effects of various parameters on the process efficiency and cementitious properties, Materials (Basel). 11 (2018). doi:10.3390/ma11101860.
[8] A. Cwirzen, R. Engblom, J. Punkki, K. Habermehl-Cwirzen, Effects of curing: comparison of optimised alkali-activated PC-FA-BFS and PC concretes, Mag. Concr. Res. 66 (2014) 315–323. doi:10.1680/macr.13.00231.
[9] J.L. Provis, Geopolymers and other alkali activated materials: why, how, and what?, Mater. Struct. 47 (2014) 11–25.
[10] A.A. Adam, Strength and durability properties of alkali activated slag and fly ash-based geopolymer concrete, Chem. Eng. (2009) 219.
[11] A.M. Humad, J.L. Provis, A. Cwirzen, Alkali activation of a high MgO GGBS – fresh and hardened properties, Mag. Concr. Res. 70 (2017) 1256–1264. doi:10.1680/jmacr.17.00436.
[12] I. Tole, M. Rajczakowska, A. Humad, A. Kothari, A. Cwirzen, Geopolymer Based on Mechanically Activated Air-cooled Blast Furnace Slag, Materials (Basel). 13 (2020) 1134. doi:10.3390/ma13051134.
[13] C. ASTM, ASTM C 618, Standard specification for coal fly ash and raw or calcined natural pozzolan for use in concrete, C618-12a. (2012) 1–5. doi:10.1520/C0618.

Experimental study of FRP reinforced concrete beams according to ACI

Besart Avdyli [1], Arbër Këpuska [2]

[1]*Department of Civil Engineering, University of Zagreb, Croatia*
[2]*Department of Civil Engineering, University of Rijeka, Croatia*

ABSTRACT

The paper presents the experimental analysis of static behavior of twelve simply supported beams reinforced with FRP (Fiber Reinforced Polymers) bars. The design procedures, cracks and deflection parameters were calculated according to American (ACI 440.1R-06) guidelines. All beams were reinforced with CFRP and GFRP bars with different diameters. The bars came from different manufactures. A total of twelve beams dimensions was 2200 mm x 130 mm x 220 mm and were tested up to failure under four-point bending. The main parameters, deflections and cracks were recorded. The results were used to evaluate SLS stage of RC with FRP bars.

***Keywords**: GFRP, CFRP, Cracks, Deflections, Beams*

INTRODUCTION

Steel bars have been used for many years in concrete structures. In addition to positive attribute, they also have some issues related to their lifespan such as corrosion. Looking at these problems during several years' researchers have started to explore new materials that could replace steel bars and their issues. So, it came to discovering the FRP bars that come as a result of a technological process. FRP bars by nature are isotropic and non-homogeneous because they consist of fibers and resin. Their non-corrosive properties and high tensile strength have made their use in different constructions not to be seen as "impossible". This work is based on the twelve experimental examination beams, the purpose of this examination is to evaluate the usefulness of these materials, namely their behavior at the SLS stage. Evaluation of this stage is made through the main parameters such as deflections and cracks which have been the main focus of this examination. Beams are reinforced with two types of CFRP and GFRP bars, both of which have different diameters because the change of bar diameters leads to different reinforcement ratio and so on different behavior during the apply loads. The surface of the bars has been two types, sand coated, and helically grooved. Special considerations should be made in the design of FRP reinforcing concrete members resulting from the low modulus of elasticity especially to GFRP bars. As a result, GFRP reinforced concrete members after cracking have relatively les stiffness. Examination was done with the four-point load method, with load increase up to failure in order to evaluate the type of failure.

MATERIAL PROPERTIES

Concrete mixes design was prepared with requested class of concrete C 30/37. The different types of reinforced bars were used in our research, first step was determinations of mechanical properties of FRP bars. The results are presented in Table 1, based on the testing process according the Standard ASTM D 7205. In the edges of the bars were set metallic shells in order to avoid constriction of the FRP bars shown in Figure 1. The properties of conventional steel bars were used from known parameters based on the

previous research works. FRP bars used in our research were two types: GFRP (helically grooved) and CFRP (sand-coated), shown in figure 1. The mechanical properties of testing GFRP and CFRP are presented in table 1.

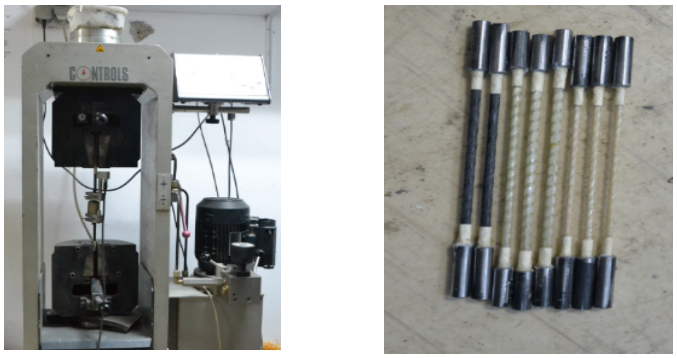


Figure 1. Testing the mechanical properties of Reinforced bars (GFRP CFRP)

Table 1. Mechanical properties of used GFRP and CFRP bars

	GFRP			CFRP	
	Ø6	Ø8	Ø10	Ø8	Ø10
Strain (‰)	0.0204	0.0234	0.0256	0.0095	0.015
Tensile (MPa)	1022.10	1108.2	1194.3	1265.4	1420
Elas. Mod. (GPa)	55			155	



Figure 2: Testing the mechanical properties of concrete.

DESIGN GUIDELINES

The flexural capacity of an FRP reinforced flexural member is dependent on whether the failure is governed by concrete crushing or FRP rupture. The failure mode can be determined by comparing the FRP reinforcement ratio to the balanced reinforcement ratio (that is, a ratio where concrete crushing and FRP rupture occur simultaneously). Because FRP does not yield, the balanced ratio of FRP reinforcement is computed using its design tensile strength. However, once the beam cracked, the stiffness of the GFRP reinforced concrete beam decreased at a faster rate compared with the control beam. This resulted in a larger deflection of the GFRP reinforced concrete beam.

Due to the brittle nature of concrete and because of changing loading conditions and other factors which are not considered in the design (such as internal stresses resulting from casting), cracks in concrete infrastructures, can't completely be avoided in practice. Design-codes give guidelines for checking the amount of reinforcement that is required in a structure to keep the crack-width limited to a certain value at specified load-levels. Checks in design codes are mainly based on the forces and bending moments in the cross-section of the structure and are unreliable for relatively thin plate-shaped structures but are conservative for non-standard structures with more complex loading and support conditions. Analyzing the cracks is based on the basic parameters using in ACI 318, for cracking and deflections in concrete beams. The beams divided to four groups due to difference in the type of the reinforcement as mention in table (2). The expression and calculations procedure according to ACI codes is presented in table 2.

Table 2. Analyzing methods and theories of behavior the concrete beams

Expression	Procedure
Cracking	
$w = 2.2k_b \cdot \beta \cdot \frac{f_f}{E_{frp}} \sqrt[3]{d_c \cdot A} \quad (MPa)$	ACI 440.1R-06 & CSA.
Deflection	
$\Delta = \frac{P \cdot a}{24EI_e}(3L^2 - 4a^2)$	ACI 318

EXAMINATION

The beams were reinforcement with one layer of FRP reinforcement comprising two bars. The entire beams were reinforcement in compression with two 6mm steel bars, and shear failure was avoided by providing closely spaced steel stirrups (6mm spacing in the shear span. In addition, stirrups spaced at 12mm were placed in the constant moment zone to ensure the positions of longitudinal bars and minimize the confinement provided by the stirrups.

Figure 3 shows the geometry of the specimens. A linear variable differential transformer (LVDT) was used to measure the width of the first flexural crack right under the concentrated force. The beam was observed during the test until the first flexural crack appeared. As soon it appeared, the load was paused until the initial crack width was measured on the beam's side surface (at the reinforcement level).

During the test, crack formation on the side of each beam was marked and the corresponding loads were recorded Also compression concrete zone were instrumented with LVDT to measure the strain of concrete, and another LVDT was in mid-span of the beam to measure the deflection. All beam specimens were tested under four-point bending over a clean span of 200cm (Figure 4). The load was monotonically applied using 400 kN hydraulic actuator with a stroke-controlled rate of 300 N/s. The actuator, strain gauges, and LVDTs were connected to a data-acquisition unit to continuously record their readings.

Table 3. Characteristics and reinforced of different sets of concrete beams

	Beam	Reinforcement in upper zone	Reinforcement in down zone	Bending Moment $\mathbf{M_{max}}$ $\mathbf{[kNm]}$	Percent of reinforcement $\boldsymbol{\rho_b}[\%]$
Set 1	B1	Ø6 Steel	Ø6 GFRP	8.60	0.00501
	B2	Ø6 Steel	Ø8 GFRP	8.60	0.00415
	B3	Ø6 Steel	Ø10 GFRP	16.34	0.00353
Set 2	B1	Ø6 Steel	Ø6 GFRP	16.34	0.00501
	B2	Ø6 Steel	Ø8 GFRP	27.00	0.00415
	B3	Ø6 Steel	Ø10 GFRP	27.00	0.00353
Set 3	B1	Ø6 Steel	Ø8 CFRP	17.90	0.00737
	B2	Ø6 Steel	Ø8 CFRP	17.90	0.00737
	B3	Ø6 Steel	Ø8 CFRP	17.90	0.00737
Set 4	B1	Ø6 Steel	Ø10 CFRP	42.88	0.00329
	B2	Ø6 Steel	Ø10 CFRP	42.88	0.00329
	B3	Ø6 Steel	Ø10 CFRP	42.88	0.00329

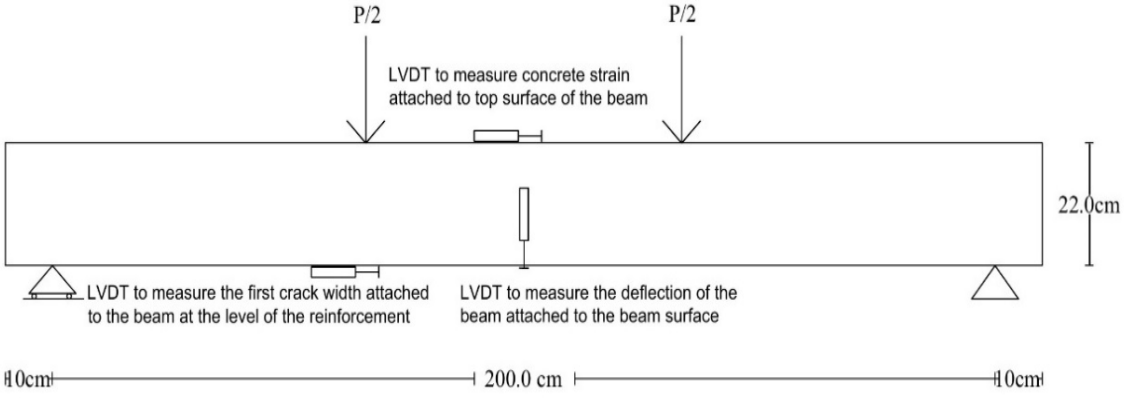


Figure 3: Beam measuring instruments position

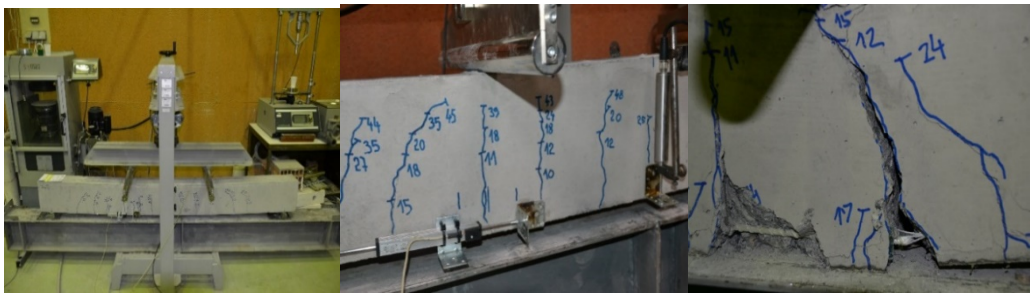


Figure 4: Beams during examination

ANALYSIS OF RESULTS

As can be seen from the results in the table 4, the maximum strength of GFRP and CFRP reinforced bars is very high, but their serviceability limit state stage ends very quickly. GFRP reinforced bars are characterized by deep cracks that occur rapidly in the direction of the forces line, a phenomenon that is not emphasized at this level in reinforced concrete slabs with conventional steel bars. This condition is due to the low modulus of elasticity of the GFRP bars while the CFRP bars are seen to be a greater percentage of the use since the CFRP bars have a module of elasticity about three times greater than the GFRP bars but the CFRP bars are limited due to of their poor bond with the concrete resulting from their smooth surface.

Table 4. Behavior the testing beams for different type of reinforcement

Type of bars	Bar diameter (mm)	Limit of strength between SLS & ULS [kN]	Maximum strength [kN]	Serviceability limit state [%]
GFRP	6	8.21	29.24	28.0
GFRP	6	9.59	35.00	27.4
GFRP	8	9.54	37.00	25.7
GFRP	8	10.57	43.00	24.5
GFRP	10	15.43	70.00	22.0
GFRP	10	15.69	72.11	21.7
CFRP	8	23.74	59.00	40.2
CFRP	8	20.98	72.00	29.1
CFRP	8	23.39	72.90	32.0
CFRP	10	29.18	80.00	36.4
CFRP	10	27.81	85.00	32.7
CFRP	10	28.30	84.00	33.7

Cracks and Deflection parameters in testing beams

The balanced reinforcement ratio and the nominal flexural strength defined in the presented sections can be obtained by using a sectional analysis in different stages of SLS theory, including the percent of ratio "Moment-M/M_u"

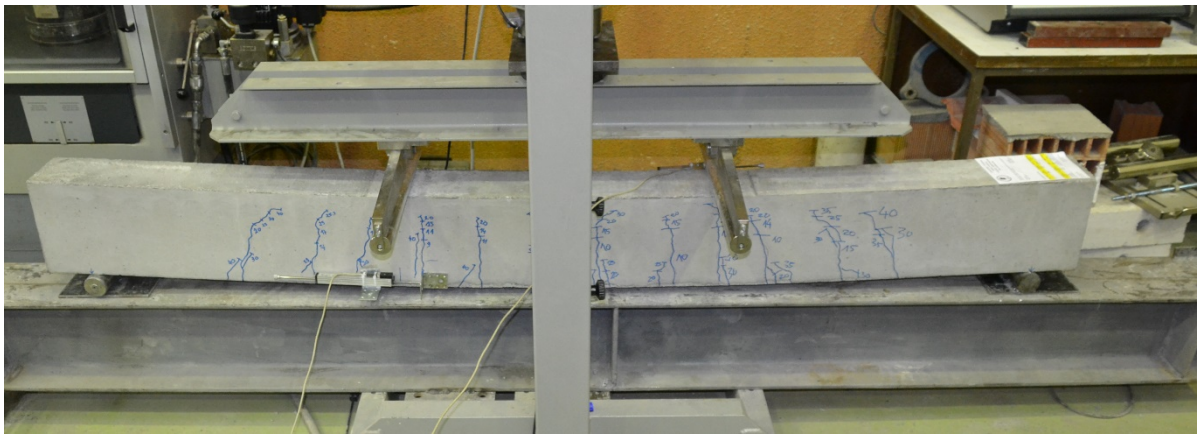


Figure 5: Four-point load.

Table 5. The load deflection behavior for all the beams

Beams		Codes	SLS %	"SLS"		75%-Ratio		100%-Ratio	
				Cracks	Deflection	Cracks	Deflection	Crack	Deflection
S1	Ø6 GFRP	ACI	27.4	0.89	8.68	2.44	38.13	3.25	51.76
		CSA		0.89	11.16	2.44	38.17	3.25	51.58
		EC2		1.33	6.12	4.06	35.86	5.45	49.82
		Exp.		0.73	7.57	2.91	44.8	3.81	44.90
		Exp2		0.69	1.7	2.25	36.29	2.98	49.61
S2	Ø8 GFRP	ACI	24.5	0.89	5.28	2.44	27.25	3.25	36.87
		CSA		0.89	7.4	2.44	27.38	3.25	36.84
		EC2		0.69	4.5	2.33	26.22	3.12	35.96
		Exp.		0.71	8.29	2.91	43.25	3.81	48.31
		Exp2		0.68	4.10	2.80	23.11	3.90	31.53
S3	Ø10 GFRP	ACI	21.7	0.58	6.89	1.99	31.21	2.66	41.81
		CSA		0.58	8.31	1.99	31.22	2.66	41.77
		EC2		0.61	6.75	2.2	30.73	2.94	41.4
		Exp.		0.31	8.30	1.54	39.87	2.04	46.61
		Exp2		0.34	6.69	1.69	30.33	2.49	40.64
S4	Ø8 CFRP	ACI	31.3	0.38	6.64	0.92	15.78	1.23	21.04
		CSA		0.38	6.23	0.92	15.63	1.23	20.92
		EC2		0.49	5.52	1.20	15.31	1.61	20.68
		Exp.		0.70	8.06	1.86	22.50	2.59	32.22
		Exp.		0.38	8.30	0.60	18.50	0.79	28.43
		Exp.		0.34	8.29	0.87	22.80	1.27	33.42
S5	Ø10 CFRP	ACI	33.7	0.35	3.98	0.78	8.92	1.05	11.89
		CSA		0.35	3.90	0.78	8.87	1.05	11.86
		EC2		0.37	3.69	0.85	3.76	1.14	11.77
		Exp1		0.29	8.29	0.76	21.06	1.07	30.19
		Exp2		0.46	4.11	1.20	8.49	1.62	11.33
		Exp3		0.30	3.91	0.70	9.02	0.93	12.03

CONCLUSION

- At RC beams with GFRP bars is noticed that with increasing bar diameter, increases their bearing capacity and decreases their SLS, vice-versa at RC beams with CFRP bars is noticed that, with increasing bar diameter increases their bearing capacity and value of SLS
- The use of GFRP bars in the construction nowadays is difficult to achieve as a replacement of steel bars, due to the low modulus of elasticity and characterized by great deformations.
- The use of CFRP bars as a direct replacement of steel bars is difficult to achieve because of poor bonding with concrete. with the improvement of adhesive properties of concrete bars, from different manufacturers, the use of these bars can be increased because they have a relatively elastic modulus of steel
- The use of these bars at this stage is limited due to some properties that may be improved in the future by different manufacturers. These types of bars in general at this stage can be used for constructions that do not have rigorous SLS condition criteria. especially their full use instead of steel bars in skimmers subject to aggressive ambient conditions, such as salt water and so on.

REFERENCES

[1] ACI 440.1R-06; Guide for the Design and Construction of Concrete Reinforced with FRP Bars", ACI Committee, 2006

[2] L.C.Bank; Composites for Constructions: Structural Design with FRP Materials", John Willey &Sons, New York, 2006

[3] N.Kabashi, at.al; Flexural Behavior and Cracks in Concrete beams reinforced with GFRP bars, ICPIC 2018, Washington DC, 2018

[4] Alsayed, SH.; Flexural Behavior of Concrete Beams Reinforced with FRP Bars, Journal: Cement and Concrete Composites, nr.20. pp.1-11, 1998

[5] CNR-DT 2032006; Guide for Design and Construction of Concrete Structures Reinforced with Fiber-Reinforced Polymer Bars" National Research Council, Rome; Italy,2006

[6] CSA-S806-02; Design and Construction of Building Components with Fiber Reinforced Polymers" Canadian Standards Association, Ontario, 2002.

[8] Arduini, M., & Nanni, A. (1997). Parametric study of beams with externally bonded PRP reinforcement. AC'I Structural Journal, 94(5), 493—501. 79 Flexural Behaviour and Cracks in Concrete Beams Reinforced with GFRP

[9] CEB-FIB, Bulletin 40

Improvement of flexural strength of reinforced concrete beams using CFRP wraps

Enea Mustafaraj[1], Erion Luga[1], Gegë Cena[1], Aleksander Nikolli[1]

[1] *Department of Civil Engineering, EPOKA University, Albania*

ABSTRACT

In this paper are presented the results of an experimental study on flexural behavior of reinforced concrete beams strengthened with Carbon Fiber Reinforced Polymer (CFRP) wraps. Three identical reinforced concrete beams of a section dimensions of 210 mm x 270 mm and span of 2.5 m were built and tested in the laboratory under four-point flexural test. The CFRP technique was applied on a pre-cracked beam, and on an un-cracked beam.

The results were compared with the control specimen parameters. The CFRP system provided a considerable increase in those parameters; 133 - 156 % in terms of load bearing capacity and 128 - 131 % in deformation capacity.

***Keywords**: CFRP, strengthening, reinforced concrete beam, four-point flexural test*

INTRODUCTION

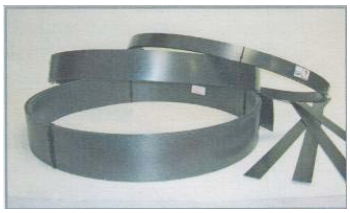
Since its discovery in the 19th century, reinforced concrete was proven to be a highly versatile material for construction of various types of civil engineering structures. It is one of the most widely used construction materials and the first choice of selection for many architects and engineers.

Despite all the advantages such as versatility, durability, economy, energy efficiency, resistance to fire and ability to be cast on-site, over time and due to many external factors, old reinforced concrete buildings have degraded and have lost their initial design characteristics. Moreover, old reinforced concrete structures and bridges located in highly active seismic regions are found to have insufficient capacities to comply with modern seismic design standards or with today's vehicular traffic flow. For this reason, there is a need for an upgrade of their structural elements in order to resist higher forces.

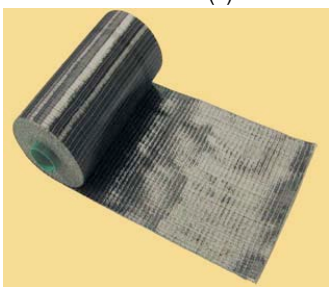
Strengthening of reinforced concrete elements such as beams or columns by was done by inserting additional reinforcing steel bars, jacketing of elements with new reinforced concrete of higher resistance, increasing the elements' cross-sectional area, thus increasing the overall weight of the structure.

To overcome this drawback, fiber reinforced polymeric (FRP) materials in the form of wraps, strips, laminates, rods or ropes are used to strengthen the structural elements are widely applied for repairing and strengthening of RC beams, columns, frames, column joints, deep beams, etc. A FRP system is a composite material made of a continuous polymer resin called matrix and reinforcing fibers. For the resins, putty fillers, saturants and adhesives are used. The fibers, made of very thin filaments of glass (GFRP), carbon (CFRP) or aramid (AFRP) are the most important element which provides the system strength and stiffness. The FRP fibers' density varies from 1.2 to 2.1 g/cm^3. The FRP systems' characteristics are defined by type of fiber volume, orientation and thickness and type of resin. One of the most important characteristics of FRP composites is that when a structural member is reinforced with FRP, stresses are transferred from substrate

to the FRP through shear and epoxy interface. In general, FRPs are used to increase out-of-plane flexural strength, in-plane shear strength and stiffness at service loads.



(a)



(b)



(c)

Figure 1. FRP laminate (a), sheet (b), bars (c) [1]

Some of the advantages why these materials are used are: lower cost, corrosion resistance, flexibility in usage, minimum disturbance to structure, minimum of loss of free space, impermeability to water, resistance against chemicals, good material properties and could be easily removable. They are available in two types: single layered and multi layered [4].

Application of CFRP wraps to increase the flexural resistance of RC beams was firstly used by Meier by the end of 1980s [2].

In later studies conducted by other researchers [3-15] were documented the successful applications of FRP materials for improvement of structural performance.

MATERIALS AND METHODS

In this study, three beams of a span of 2.5 meters with nominal cross-sections of 210 mm x 270 mm were tested in bending. One of the beams was strengthened with CFRP prior to testing whereas another one was repaired with CFRP after testing and re-tested. The main aim was to assess the effect of CFRP system on the flexural capacity of the beams.

Construction of beams

The beams were built of concrete class C25/30 and were reinforced with 3H12 for tension reinforcement and 2H8 compression reinforcement. The shear links were H8 @ 100 mm centers. Before mixing of concrete, coarse aggregate granulometry was measured to be well-graded (Figure 2). The cement used was 42.5 R and water/cement ratio was 0.6.

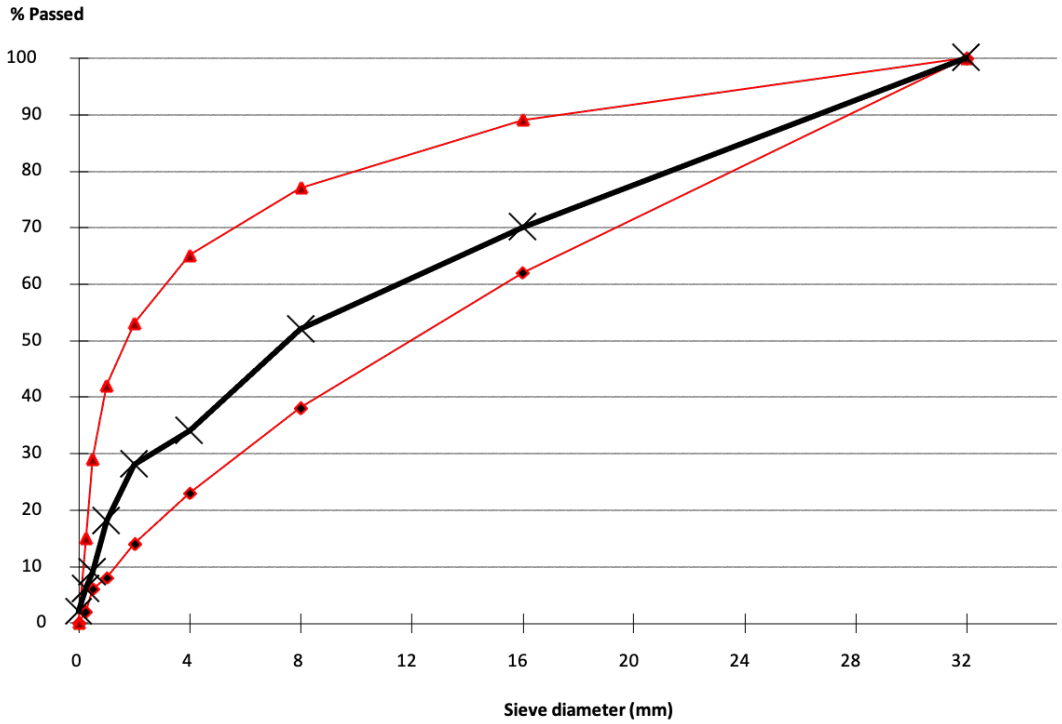


Figure 2. Aggregate grading test results.



Figure 3. Step-by-step construction of the beams.

Strengthening of Beams using Carbon Fiber Reinforced Polymer (CFRP) Wraps

The application of CFRP wraps is a three-step procedure. Firstly, surface preparation is required. The beam faces are cleaned from any grease, oil, dust residual or other contaminants that might impair adhesion. Secondly, epoxy primer is applied. It is a two-component solvent-free epoxy system which when mixed yields a penetrating medium viscosity primer [16-18]. Then, a layer of epoxy adhesive is applied, followed by the application of CFRP wrap and finished with the second layer of the adhesive.



Figure 4. (a) Epoxy Primer, (b) Epoxy Adhesive.

In Figure 5 and 6, is presented a sketch view of the reinforcement scheme and the application of all the steps.

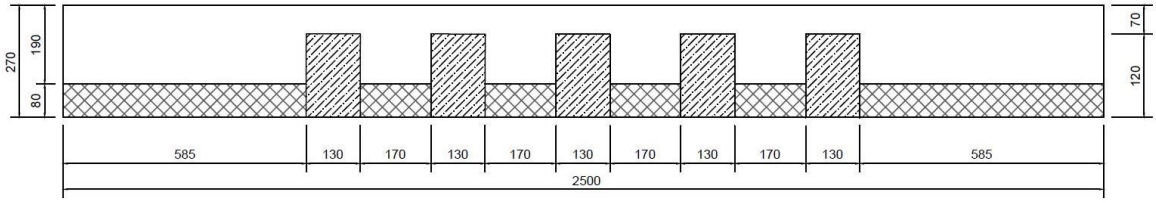


Figure 5. Reinforcing scheme.



Figure 6. Application of CFRP on beam B2.

Test set-up

All three RC beams were tested under flexural loading simply supported with a clear span 2200 mm and internal span 900 mm. Three Digital Vernier Calipers were fixed on the bottom part of the beams to measure the vertical displacements. The four-point bending (flexural) static loading was performed using a

hydraulic jack as described in Figures 7 and 8. Testing continued until the load reading of the hydraulic jack showed a few to zero kN.

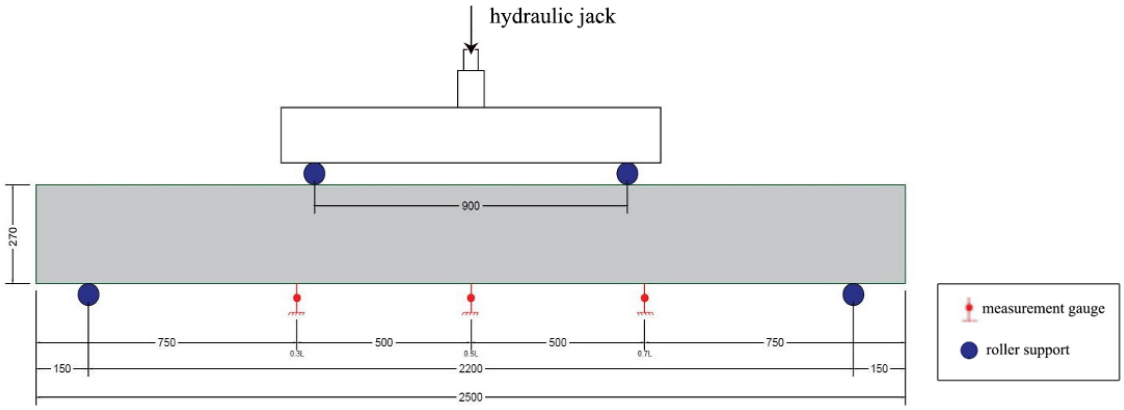


Figure 7. Four-point bending test set-up scheme.



Figure 8. Four-point bending test.

RESULTS AND DISCUSSIONS

The analysis results are expressed in terms of load-deflection curve as well as crack patterns. The Beam (B1) failed at an ultimate load of 137.34 kN and the maximum deflection was 47.93 mm. The Beam (B2) failed at an ultimate load of 127.53 kN and deflected 38.7 mm. It was then, repaired with CFRP and tested again. After the second test, the ultimate load was 176.58 kN and the maximum deflection was 50.42 mm. The Beam (B3) strengthened with CFRP wraps failed at a load of 215.80 kN with a maximum deflection of 45.65 mm. In Table 1 is presented a summary of these results.

Table 1. Ultimate load and maximum deflection of the tested beams.

Specimen name	Ultimate Load (kN)	Maximum deflection (mm)
B1	137.34	47.93
B2	127.53	38.70
B2(CFRP)	176.58	50.42
B3(CFRP)	215.80	45.65

In Figure 9, are presented the beams after testing. It can be seen the development of tension cracks at the bottom of the unreinforced beams (B1 and B2) and compressive cracks at the top of the beam. In the repaired and strengthened beams, it was observed that the CFRP wraps failed from rupture.



Figure 9. All the beams after failure.

In Figure 10 it is presented the load-deflection curves of all the tested beams. As it is seen from the graph, Beam B3(CFRP) has the highest ultimate load but is not the most ductile beam of all.

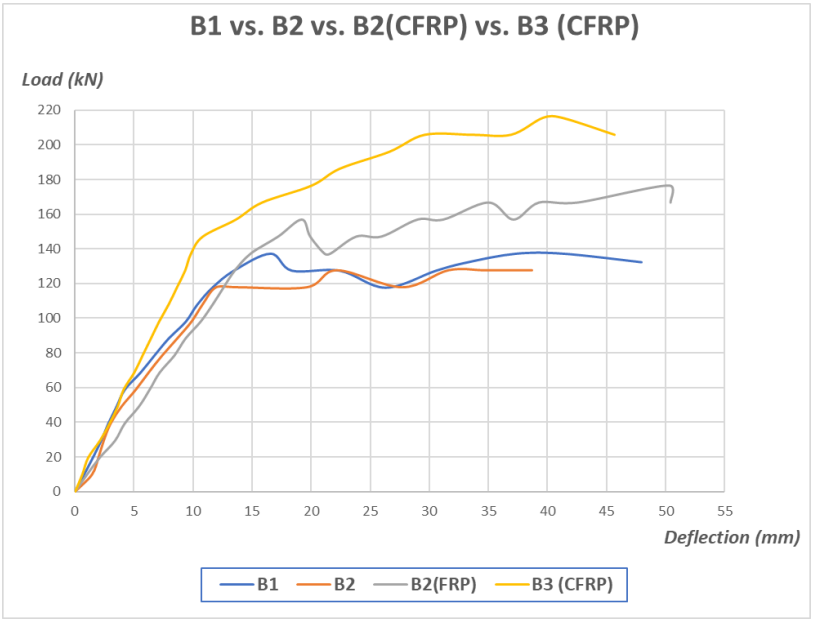


Figure 10. Load-deflection curve of all the tested beams.

CONCLUSION

From the test results it was observed that CFRP wrap strengthening system performed satisfactorily and could be a useful method to increase the flexural resistance of the reinforced concrete beams. It was observed that the repaired beam had a 138% increase in ultimate load and 131% in the maximum deflection. The CFRP strengthened beams achieved a 159% higher ultimate load but a similar maximum deflection.

REFERENCES

[1] Rankovic S., Folic R., Mijalkovic M. Effects of RC beams reinforcement using near surface mounted reinforced FRP composites. Architecture and Civil Engineering, 8 (2), 2010.

[2] Meier, U. Strengthening of structures using carbon fiber/epoxy composites. Contr. and Build. Mat., 9(6), 341-351. 1995.

[3] Triantafillou, T. C. and Pleveris, N. Strengthening of RC beams with epoxy-bonded fiber-composite materials, Mat. and Struct., 1992.

[4] Standard for Structural Calculation of Reinforced Concrete Structures, Architectural Institute of Japan, Tokyo, 1988.

[5] Norris, T., and Saadatmanesh, H. Improving the serviceability of concrete beams using carbon fiber reinforced polymer (CFRP) sheets. Federal Highway Administration, Washington, D.C, 1994.

[6] Olivova, K., Bilick, J. Strengthening of concrete columns with CFRP, 2009/1, 2008.

[7] Esfahani, M., Kianoush, M., Tajari. Flexural behavior of reinforced concrete beams strengthened by CFRP sheets. Engineering Structures, 2007.

[8] D'Ayala D., Speranza E., An integrated procedure for the assessment of seismic vulnerability of historic buildings, 12th European Conference on Earthquake Engineering, 2005.

[9] Spyrakos C.C., Kirakopoulos P.D., Smyrou E., Seismic strengthening of the historic church of Sts. Helen and Constantine in Piraeus, 3rd Thematic Conference on Computational Methods in Structural Dynamics and Earthquake Engineering, 2011

[10] Keypour H., Fahjan M.Y., Bayraktar A., Analysis and strengthening methods for historical masonry structure, 5th International Conference on Seismology and Earthquake Engineering, Iran, 2007.

[11] Portioli F., Mammana O., Landolfo R., Mazzolani F.M., Seismic assessment of historical mosques under exceptional earthquakes: A case study in Skopje, Urban Habitat Constructions Under Catastrophic Events, 2010.

[12] Casadei P., Angeloni E., Fifteen Years of applications in Italy: Case studies, 2011.

[13] Mustafaraj, E.; Yardim, Y.; Corradi, M.; Borri, A. Polypropylene as a Retrofitting Material for Shear Walls. Materials, 13, 2503, 2020.

[14] Mustafaraj, E., Yardim, Y. In-plane shear strengthening of unreinforced masonry walls using GFRP jacketing, Periodica Polytechnica Civil Engineering 62 (2), 330-336, 2018.

[15] Mustafaraj, E., Yardim, Y. Retrofitting damaged unreinforced masonry using external shear strengthening techniques, Journal of Building Engineering, 26, 100913, 2019.

[16] BASF – MasterBrace P 3500, Epoxy Primer for MasterBrace Laminate System, Master Builders Solutions.

[17] BASF – MasterBrace SAT 4500, Epoxy Based Adhesive for MasterBrace FIB system, Master Builders Solutions.

[18] BASF – MasterBrace FIB, Unidirectional High Strength Fiber Fabrics for the MasterBrace Composite Strengthening System, Master Builders Solution.

Structural assessment of the south-west wing timber roofs of the Loreta in Prague

Bledian Nela[1], Jiří Bláha[2]

[1]*Department of Civil Engineering, Czech Technical University in Prague, Czech Republic*
[2]*Institute of Theoretical and Applied Mechanics, ASCR, Czech Republic*

ABSTRACT

The Loreto of Prague is a remarkable Baroque historic monument, a place of pilgrimage with a captivating history. Behind the main façade, which is the marvelous work of the famous Dientzenhofers, there is a courtyard with a copy of the St. Mary´s Holy House of Nazareth. Since the placement of the first construction stone in 1626, the Loreto has faced many construction phases with many alterations. The majority of the works progressed between 1698 and 1748 under the supervision of Christoph and Kilian Ignaz Dientzenhofer. These alterations also generated some changes in the configuration of the roof structure and in some parts caused even damages. Some of interventions observed on timber frames are not documented and their purpose is not always obvious.

For a better understanding, a historical analysis of the Loreto complex was used recently refined by dendrochronological dating of timber roofs elements from different time periods, so the historical chronology of the building could be accomplished. Afterwards, diagnostic tests were conducted on site for the health evaluation of the members to assess their condition. The mechanical parameters are obtained with the new diagnostic tool which is the loading jack and correlates well to the compressive strength parallel to fibers. Due to the historic interventions excessive deformation is observed in one of the timber frames. Utilizing the obtained health and mechanical parameters a numerical model of the south-west wing timber roof is modeled. From this global approach then is built a numerical model of the truss of concern and three scenarios are verified to achieve a possible hypothesis of the deformation. The structural numerical model provides valuable information of the existing deformation. Additionally, the current stability of the timber frame is assessed which proves to be safe under the actual conditions. In order to eliminate future problems for the truss two possible strengthening solutions are provided with the minimal intrusiveness on the historic timber roof.

Keywords*: health assessment, historic timber structure, non-destructive tests, dendrochronology, structural analysis*

INTRODUCTION

In the Hradčany district of Prague is located the Loreta, a remarkable Baroque historic monument. The Prague Loreta is a place of pilgrimage with a captivating history. The expan-sive decorative frontal façade is a work of the prominent architects of the Czech Republic, the Dientzehofers. The clock tower in front carries on top the authentic Loreta carillon. The building on the inside hides the famous Loreta treasure, the Prague Sun, a 6222 diamonds monstrance. Beside the St.Vitus Cathedral treasure, it is the most

valuable treasure in the Czech Republic. The surrounding cloisters conceal on the inside a copy of the St. Mary's Holy House of Nazareth, which also represents the first building in the Loreta complex.

The building of the monument, since the placement of the first stone in 1626, has faced many phases of construction. The majority of the works have progressed between 1698 and 1748, where the majority of them were supervised by Cristoph and Kilian Dientzenhofer. The changes in the cloisters levels and the extension in the buildings affected the timber roofs. In many areas of the roofs, the internal configuration of the structure is altered and lead to many damages. The southern part of the west wing roof contains many of these alterations in terms of historical changes, interventions and damages. Some of the interventions are not documented and their purpose is not quite understood. One of the timber frames is significantly deformed and a strengthening column is used as reinforcement. The cause of deformation is not straightforward, and the strengthening efficiency purpose is not documented.

The scope of this paper involves the historical analysis of the chronological construction of the monument. A historical background is developed with the available literature resources enriched by the dendrochronological dating of the timber roofs. The historical background is used to make the assumptions on the historical changes in the roof with the significant deformation. After the distinction of the interventions on that area, with the help of non-destructive tests a comparison between the original and new elements is accomplished. Mechanical parameters of the timber elements are obtained from the tests and are used in the structural analysis. Structural analysis of one frame suffering deformation is executed to demonstrate the historical assumptions. The stability of the current state of the frame is controlled to evaluate its safety. A strengthening proposal is given with the results obtained from the structural mod-el.

ARCHITECTURAL FEATURES

The Loreta of Prague as an iconic place of pilgrimage in Prague is a monument which con-sists many buildings in the form of an integrated complex. The integration of this complex was achieved by the famous architects, son and father, the Dientzenhofers. The main features of this complex are namely the Santa Casa, the church, the cloisters together with the chapels, the front façade and the bell tower which consists of the famous carillon (Figure 1).

The Santa Casa or "The Holy House" is a copy of the Nazareth Santa Casa which is currently located in the Italian Loreto, whereas its copy is located in the center of the Loreta complex in Prague. Its significance comes from the legend that describes it as the building where Virgin Mary was announced to conceive the Son of God. The Church of Nativity of Our Lord is located in the eastern wing in the mid-cloister with an extension to the east. On the lateral sides of the church are located two polyhedral towers with truncated polyhedron roofs with spire finishes on top of an onion dome. The front entrance is featured with a marvelous façade with the bell-tower located in the center. The front façade is the work of the Dientzenhofers which features a Baroque style, symmetrical and divided by pilasters. The tower starts with a square base at the bottom to be followed by an octagonal one up to the roof. The truncated polyhedron roof finishes with a spire on top of an onion dome. In the tower inside lays the famous and one of the few authentic carillons that survived time. On the four corners and on the northern and southern mid-wings of the complex, are located six chapels. They are connected with two-story cloisters which enclose the entire complex and are open in the form of arcades in the ground level and are closed on the second level.

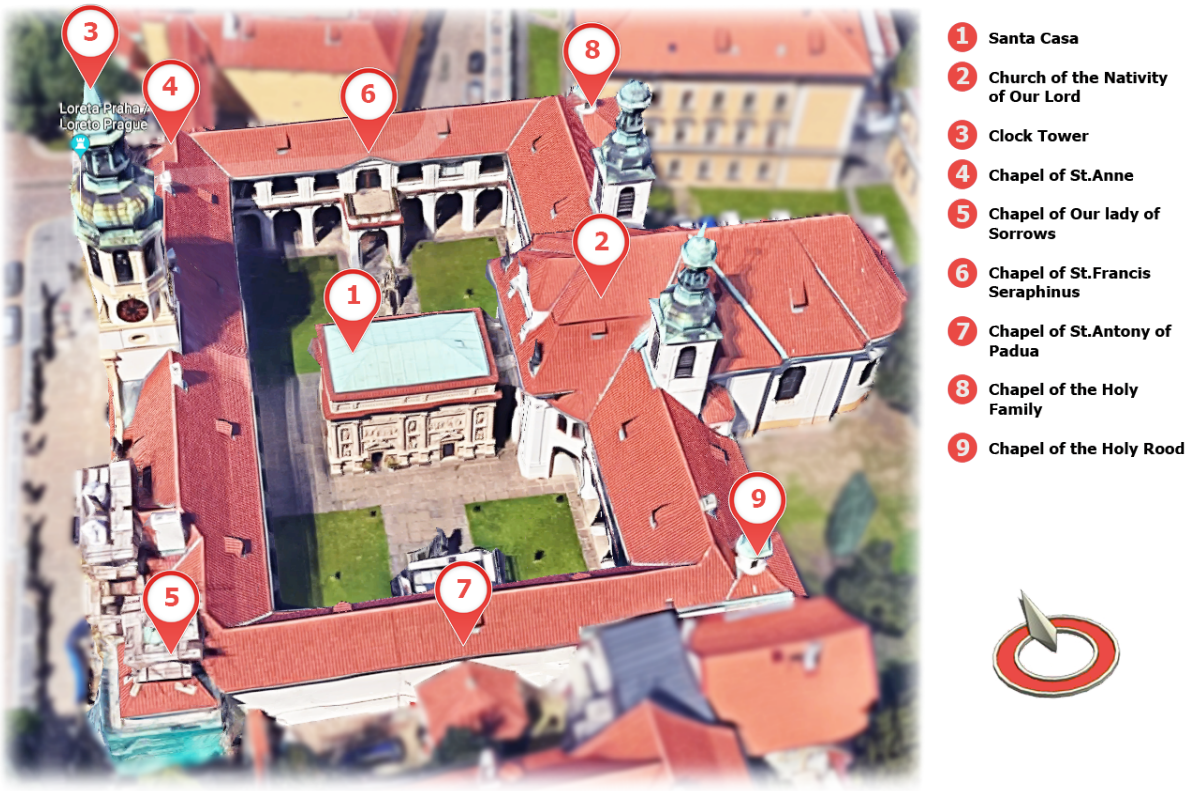


Figure 1. Compound parts of the Loreta in Prague

The construction of Loreta in Prague started in 1626 and experienced many construction phases which were influenced by political issues and diverse architectural styles. The appearance of the Loreta as of today is achieved through many changes in its structure which inflict-ed damage and stress changes in its members. The historical timeline of Loreta is explained chronologically by [1] and is presented in the form of a table in the Table 1 below with respective hypothetical models shown in Figure 2.

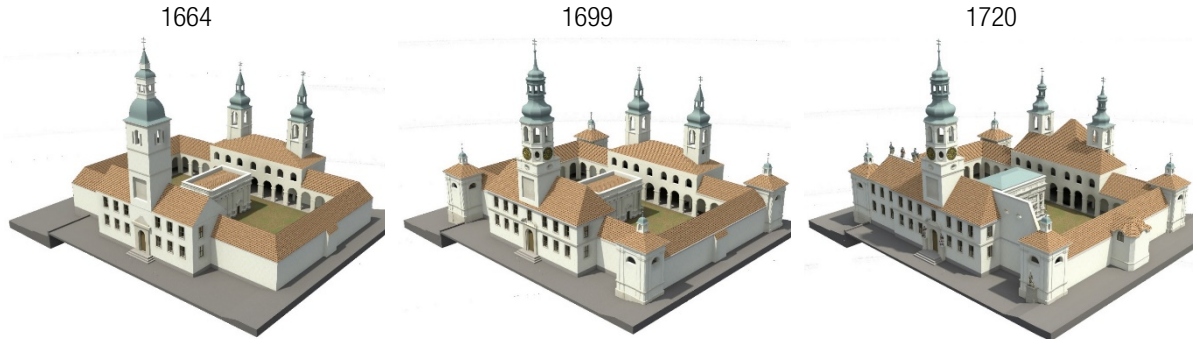


Figure 2. The hypothetical models of the year 1664 (left), 1699 (middle), 1720 (right); [1]

Table 1. Historical timeline of the Loreta construction.

Year	Event
1626	- The foundation stone for Santa Casa was laid with the financing of the Lobkowicz family
1634	- The cloisters construction in the form of a fortification, very typical for the Thirty Years' War. Works started with Giovanni Battista Orsi followed by Andrea Allio after his death
1646	- Tower was finished and the works were continued with Silvestro Carlone after Allio's death
1664	- A hypothetical model of Loreta for the year 1664 was built from these data and the archival reports presented in Error! Reference source not found. (left). It features the Santa Casa, one story cloister, no chapels, no church, the bell-tower and two towers on the eastern wing
1685	- Two chapels were added on the south-west and north-west corners
1691	- Two more chapels added on the north-east and south-east corners
1699	- The upper part of the bell-tower was shifted from a rectangular base to an octagonal base to fit the famous carillon and can be seen in the hypothetical model of 1699 in Error! Reference source not found. (middle)
1712	- The addition of the mid-cloister chapel in the southern wing and mark the beginning of Dientzenhofers works
1716	- The addition of the mid-cloister chapel in the northern wing
1717	- The church of Nativity is extended to the east and the elevation of the cloister to fit the treasury in the northern side of the front façade. The southern side cloister of the front façade is covered with an attic wall
1720	- The hypothetical model of the year 1720 presents the updated changes and can be seen in Error! Reference source not found. (right)
1722	- Cristoph Dientzenhofer is contracted for the enlargement of the Church of Nativity to the west but following his death, the works are continued by his son Kilian. He unified the front façade and divided it with pilasters
1747	- The cloisters were elevated, and Kilian finally diminished the fortification character of the Loreta complex

ROOFS OF LORETA

Timber roofs during their lifecycle develop annual rings which provide valuable information about the history of the structure. Up until the felling date, the tree develops the annual growth rings which form the cross-section of each tree. This cross-section is divided into the heartwood and the sapwood part and each growth ring layer consists of the earlywood and the latewood. From these layers a tree can be assessed its growth conditions and can be further dated through the dendrochronological dating. A dendrochronological survey was per-formed in Loreta by [3] and the results are presented in Figure 3 (left). Comparing it to a stratigraphy model in Figure 3(right) a correlation of the dates can be made with some differences. The date

differences in the church are clearly seen to match in the two models where the dendrochronological model compared to the stratigraphy one provides the felling dates of the timber elements used. The central part of the church has an earlier construction date, nevertheless the dating shows a later date. This can be a result of the adjustment of the central part to the extensions on the western part followed later with the eastern extension. The cloisters, as previously mentioned, were elevated from one to two levels. The dates of construction match the felling dates of the cloisters with exceptions to the northern and western wing. The northern wing timber elements match the construction date of the chapel and this can justify it. On the other hand, the front façade as it was mentioned, faced many diverse changes. The dendrochronological dating of these changes matches the construction phases of the western part of the complex. The room made for the treasury can be clearly distinguished in the dating together with the clear differentiation of the cloisters on the southern part of the front façade.

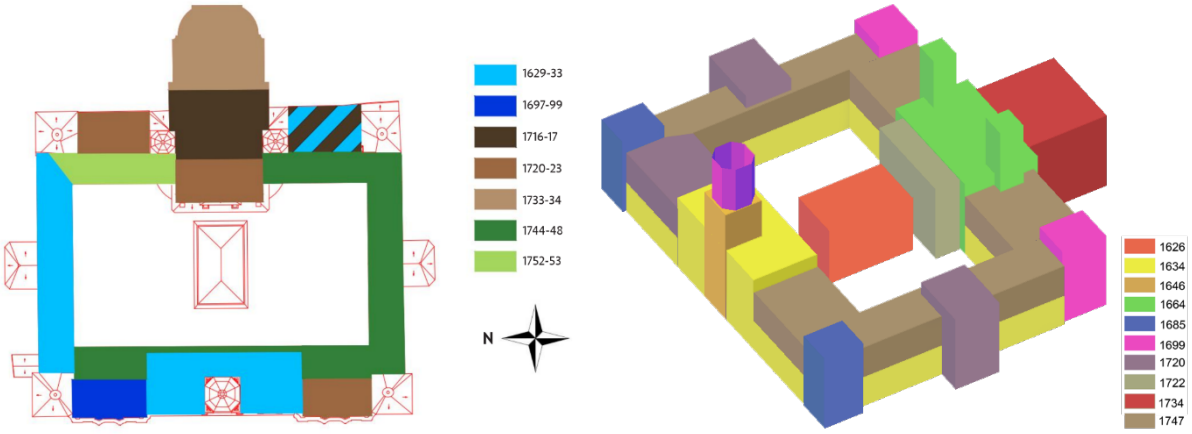


Figure 3– Dendrochronological dating of the timber roofs (left) [2] and the stratigraphy model of Loreta (right);

DIAGNOSTIC TESTS

The area of interest and the focus of this paper are mainly the roof of the church and the roof on the south part of the western wing. This was chosen since there were some damages seen in these two areas, where the roof of the church was already under restoration at the time of inspection. Nevertheless, a huge deformation was found on a frame of the southern part of the west wing. The cause of deformation and its stability where unknown and are assessed and presented in this paper. Initially a visual inspection was carried out in the roof for assessment and for the choice of diagnostic tests. It was seen suitable and not invasive to use the resistance microdrilling, loading jack and the moisture content.

Diagnostic tests

Following UNI-LEGNO [4], a visual inspection was carried out in the southern part of the west wing. The structural timber elements were classified into classes, namely S1, S2 and S3 and according to [4] are obtained the mechanical parameters. The authentic joint connections of the structural timber elements are carpentry joints with some minor late modifications. There are not many archival reports on the past interventions carried out in the roof therefore many statements are made from observation only. Strengthening short columns are seen to reinforce the lower ends of the roof rafters, which are connected to an embedded timber beam on the concrete floor (Figure). Additionally, small diameter holes are seen in the majority of the timber elements which can be due to the injections as a manner of protection against insects (Figure). Furthermore, fireproofing is identified in some elements and metal connectors are detected

in some other as measures of joint reinforcement (Figure 4). Afterwards, in order to perform the timber grading as per [4] the features examined were the wane, growth rate, knots, slope of grains, fissures and other geometric features. The final class found for the timber elements as per these norms was found to be S1 leaning towards S2. This classification gives a range of values to be further assessed and verified with other tests.



Figure 4. Characteristic features on the elements from the visual inspection;

Resistance microdrilling

Utilizing the Resistograph a small diameter hole is driven into the timber elements. The output provides the timber profile of the section in terms of energy required to keep the needle at constant speed. Therefore, the difference in the energy output shows a variation in material resistance and thus interprets decays and damage inside the timber. The microdrilling was per-formed in the frame which showed the extensive deformation and especially on the lower end support where it is resting on the wall. Furthermore, on that lower end a strengthening with a prosthesis can be seen and from the results the effectiveness is assessed. The microdrilling was carried out in 18 locations. Following the correlation between the resistance measure (RM) and the compressive strength of wood (Sc) provided by [6] with a correlation factor of R^2=0.807 from the equation (1), the results are given in Table 2. Additionally, equation (2) with a correlation factor of R^2=0.746 provides the correlation between RM and density (ρ). The average compressive strength is around 22.3 [MPa] and the average density is around 176 [kg/m³].

$$RM = (-343.83) + (22.296) * S_C \quad (1)$$

$$RM = (-137.67) + (1.665) * \rho \quad (2)$$

Table 2. Correlation of RM to compressive strength and density of timber;

Test no.	RM	Sc [MPa]	ρ [kg/m³]
R1	161.8	22.68	179.85
R2	146.1	21.97	170.41
R3	145.1	21.93	169.81
R4	150.7	22.18	173.21
R5	146.2	21.98	170.52
R6	133.9	21.43	163.12
R7	131.4	21.31	161.60
R8	161.9	22.68	179.94
R9	155.8	22.41	176.27
R10	190.2	23.95	196.92
R11	139.9	21.70	166.74
R12	180.3	23.51	190.96
R13	174.3	23.24	187.36

R14	152.4	22.26	174.24
R15	168.8	22.99	184.07
R16	173.2	23.19	186.72
R17	143.4	21.85	168.83
R18	142.1	21.79	168.01

From the output profile of the timber cross-section the damage and decays were able to be observed. Furthermore, following the peaks of the resistances in the results from the Resistograph the rings of the tree are constructed hypothetically and utilized for the qualitative categorization of the element. An example can be seen in Figure 5.

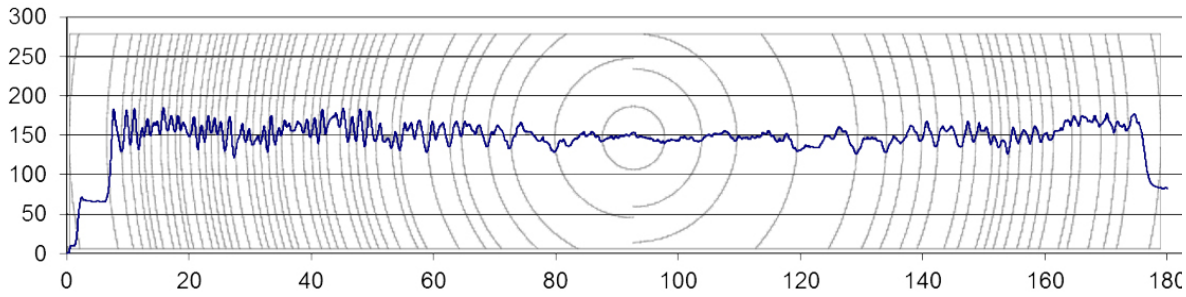


Figure 513. Ring trees and possible damage obtained from resistance microdrilling;

Loading Jack

One innovative diagnostic test with minimalistic invasion on the timber elements is the loading jack device. It is used to evaluate directly the compressive strength of the timber elements parallel to fibers. The jack is inserted into a predrilled hole of 12 mm wide and the jaws of the device are opened apart by pushing laterally up to 1.5 mm. A force-displacement curve is plotted following this procedure and from the maximum force achieved is obtained the maximum compressive strength. For further information on this intuitive and innovative de-vice the reader can be directed to [5,8,10]. The loading jack test is carried out in the south part of the west wing (6 locations) and in the roof of the church in the east (5 locations). The results for the conventional strength and (CSc) and the modulus of deformability (MOD) are shown in the following charts in Figure 6.

Kloiber et al. [9] provides correlation between the loading jack results and the compressive strength, modulus of elasticity and the density. The correlation follows the results from specimens with 12, 18 and 24% moisture content. However, only the correlation for 12% is used since the moisture measured and shown in the subsequent section, in the frames does not exceed 12%. The correlation between conventional strength measured from loading jack (CSc) and the compressive strength (Sc) with a correlation factor of R^2=0.887 is shown in equation (3). The correlation between the modulus of deformability (MOD) from the loading jack and the modulus of elasticity (MOE) with a correlation factor of R^2=0.679 is shown in equation (4). Lastly, the correlation between the conventional strength (CSc) and the density (ρ) with a correlation factor of R^2=0.840 is shown in equation (5). The results are shown in Table 3. From the Czech annex of Eurocode [7] the elements are classified as C20 structural timber class.

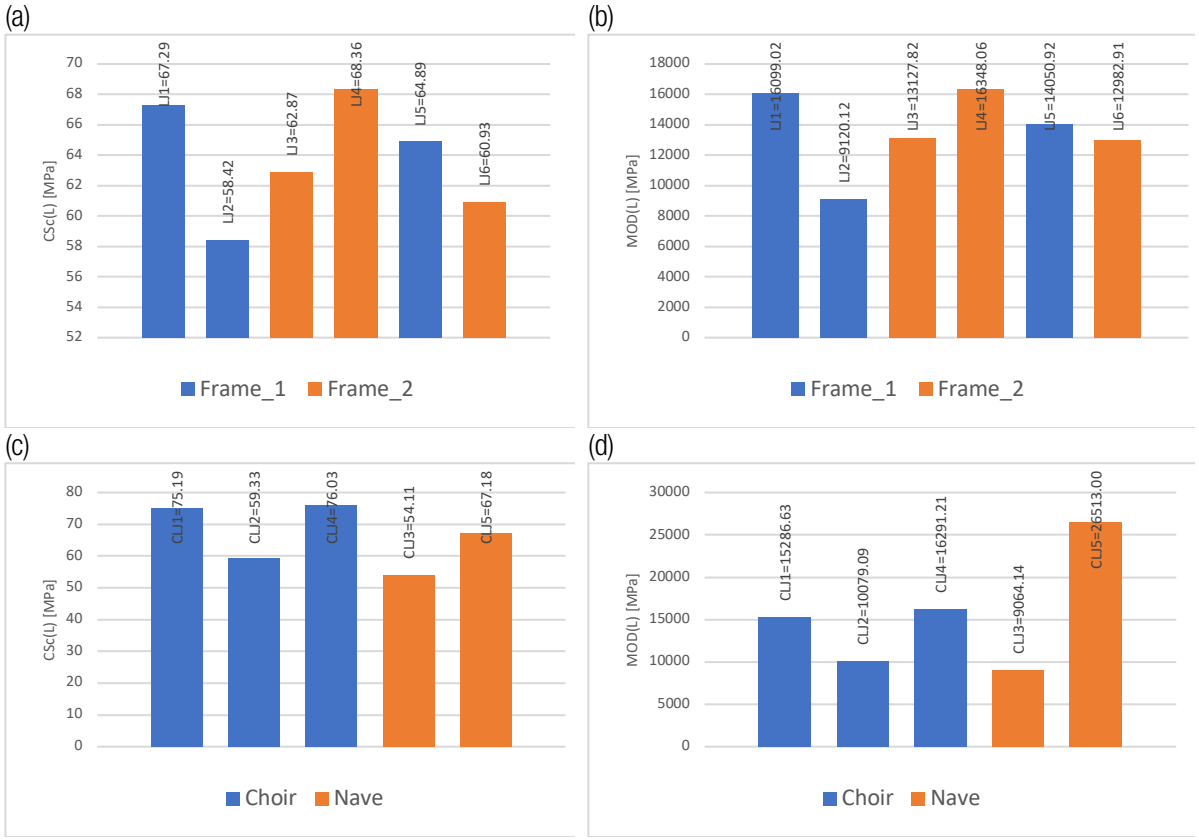


Figure 6. Loading jack results for south part of the west wing CSc (a) and MOD (b) and the Church CSc (c) and MOD (d);

$$S_{C\,(L)} = 0.5661 * CS_{C\,(L)} - 3.3584 \quad (3)$$

$$MOE_{(L)} = 0.4934 * MOD_{(L)} - 1901.7 \quad (4)$$

$$\rho = 5.1214 * CS_{C\,(L)} + 27.265 \quad (5)$$

Table 3. Correlation between loading jack and mechanical parameters;

		CSc [MPa]	MOD [MPa]	Sc [MPa]	MOE [MPa]	ρ [kg/m³]
South part of the west wing	FR-LJ1	67.29	16099.02	34.73	6041.56	371.86
	FR-LJ2	58.42	9120.12	29.71	2598.17	326.44
	FR-LJ3	62.87	13127.82	32.23	4575.56	349.26
	FR-LJ4	68.36	16348.06	35.34	6164.43	377.38
	FR-LJ5	64.89	14050.92	33.37	5031.02	359.58
	FR-LJ6	60.93	12982.91	31.13	4504.07	339.29
Church roof	CH-LJ1	75.19	15286.63	39.21	5640.72	412.34
	CH-LJ2	59.33	10079.09	30.23	3071.32	331.12
	CH-LJ3	76.03	16291.21	39.68	6136.38	416.65
	CH-LJ4	54.11	9064.14	27.27	2570.55	304.38
	CH-LJ5	67.18	26513.00	34.67	11179.81	371.32

Moisture content

The moisture content provides a significant qualitative measurement of the level of decay and strength of the timber elements. The durability of timber decreases with the increase of moisture above fiber saturation point. This due to the vulnerability of timber towards insects and fungi. Furthermore, the strength and elasticity are reduced, and the elements swell. The moisture content is measured on some elements of interest and is shown in Figure 7. The moisture levels on the timber elements do not present any threat to the health of wood.

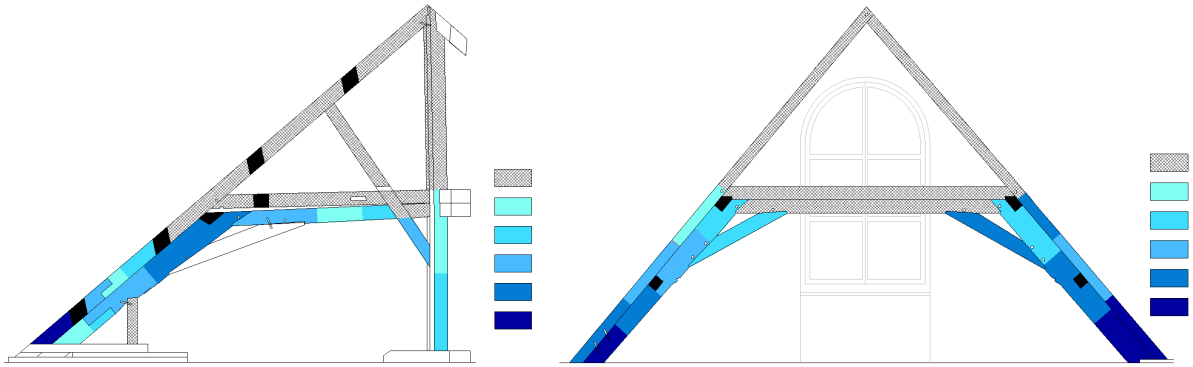


Figure 7. Moisture content for the Frame no.1 (left) and Frame no.3 (right);

STRUCTURAL ANALYSIS

The different construction phases of Loreta present many challenges for the health assessment and structural stability of the structure. The cause of damage and decay may be from different reasons and the evaluation is not always accurate and many hypotheses are to be constructed to achieve the most probable cause. The main focus of this paper is the cause of deformation of the frame in the south part of the west wing and the evaluation of its safety, stability and a possible strengthening measure. The structural analysis is carried out only for this portion of the roof by simplifying its geometry to a simpler one. This enables a detailed computation of wind and snow forces acting on the roof, according to the present codes [11,12]. From the global analysis of this portion of the roof, are calculated the internal forces acting on each element. Afterwards, a two-dimensional model is built to assess the different phases of construction. The deformation is assumed to have been caused during the restoration works which were present on the roof. Three scenarios are proposed for the analysis and the determination of the deformation on the frame. The first scenario consists of the phase before the strengthening and it is used to justify the need for a reinforcement of that frame. The first scenario consists of the frame without the short column and the concrete slab which are existing on the roof. Typically, a tie beam is usually placed at the bottom of the frame and it is modelled as a support with a specific stiffness according to the assumed axial stiffness of the tie beam. The second scenario is assumed that during the process of strengthening the effect of the tie beam on the truss is removed. Finally, a third scenario is built to represent the current state of the frame containing the actual deformation and to evaluate its stability. Rigid links are created to transmit the deformation of the principal rafter to the secondary one. The rigid links work only under compression to depict the transmission of the deflection by contact. To reproduce the superficial friction between the elements a tangential axial force is computed and input in the model. The results of interest are shown in Figure 8.

The loading conditions at the time of Scenario 1 are unknown and therefore the results are only relative. A large deflection is seen in Figure 8(a) in the middle of the principal rafter which can justify the need for a strengthening. In Scenario 2 after the removal of the tie beam the diagonal truss starts acting on

tension and loses its function and the horizontal beam on the left side can be seen to suffer a large deflection Figure 8(b), which is still present on the frame. Scenario 3 shows a strengthened frame and reduced deflections seen in Figure 8(c) and the same scenario is evaluated to be stable for the actual level of forces acting on it presented in Figure 8(d). This hypothesis presents a high level of reliability for the cause of deformation. Nevertheless, if more hypothesis can be formed a comparative analysis can be done to assess the most reliable one. After this assessment the frame does not require excessive strengthening measures. A possible strengthening proposal can be the placement of a tie beam at the bottom to take the horizontal thrust.

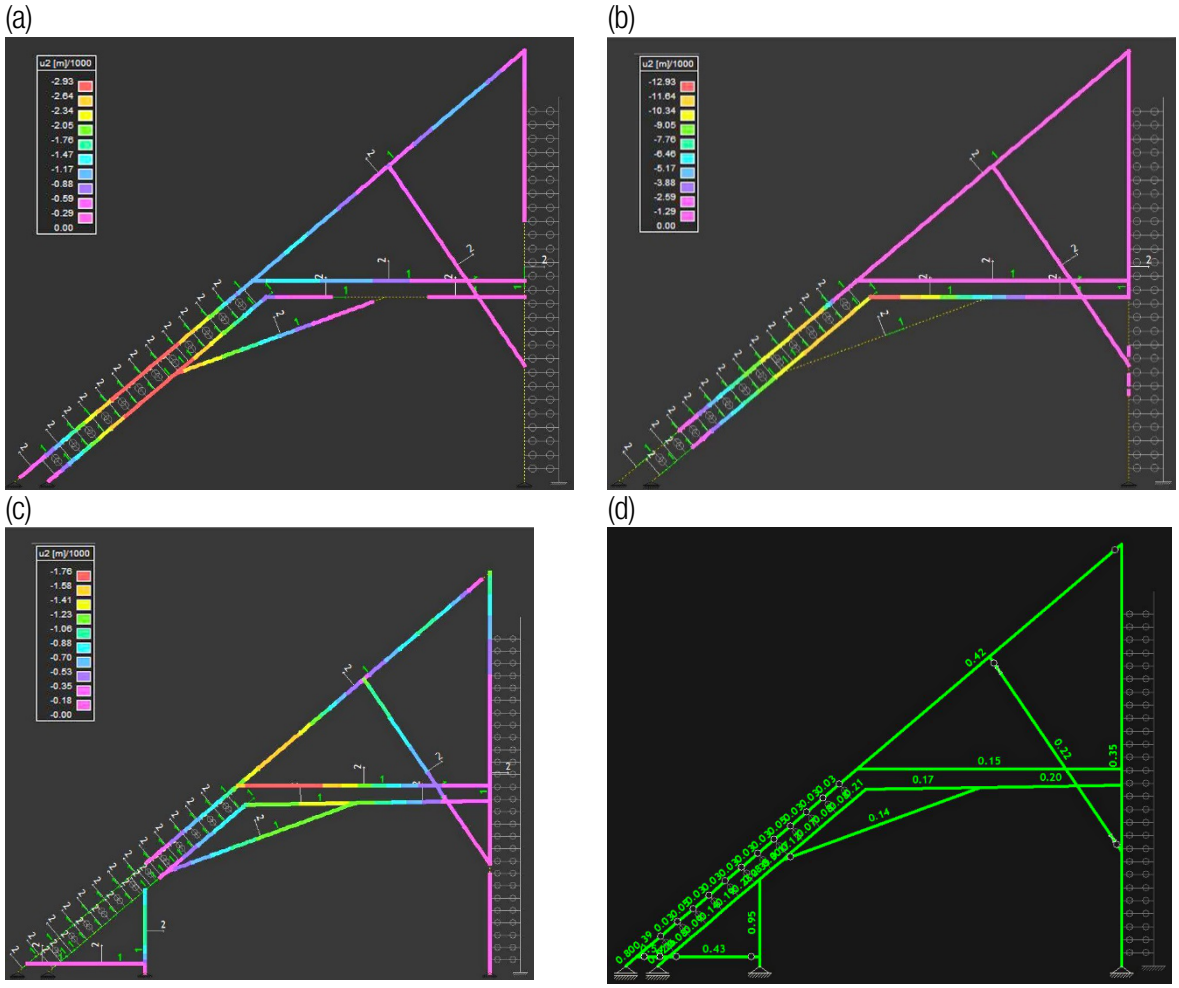


Figure 8. Results for: Scenario 1 deflections (a), Scenario 2 deflections (b), Scenario 3 deflections (c) and structural stability evaluation (d);

CONCLUSION

A chronological timeline and the understanding of construction phases can aid the assessment of any structure. From the historical construction phases, it was able to make an assessment of the roof.

Diagnostic tests performed on the roof help on the health assessment of the timber ele-ments. The roof does not show any potential threat of extensive decay or damage. Further-more, the mechanical parameters are obtained with satisfactory correlation factors from the tests. Utilizing these parameters, a more reliable assessment of the cause of deformation is car-ried out. The hypothetical scenario for the cause of deformation shows a high reliability and unless a more accurate one is presented, this can be the actual cause.

REFERENCES

[1] M. Líčeníková, "Outline of Construction Development of the Prague Loreto," in Dientzenhofers and Loreto: The Story of Loreto Façade, Prague, Czech Capuchin Province, 2017, pp. 13-25.Chow, V. T. (1959) Open Channel Hydraulics. McGraw-Hill Book Co., New York, NY, USA.

[2] J. Bláha, "The Roofs of the Loreto in Prague," in Dientzenhofers and Loreto: The story of Loreto Façade, Prague, Czech Capuchin Province, 2017, pp. 27-35.

[3] T. Kyncl, "The Loreto in Prague, Report of dendrochronological dating," DendroLab, Brno, 2016.

[4] UNI - LEGNO, UNI 11035-1:2003: Legno strutturale - Classificazione a vista di legnami italiani secondo la resistenza meccanica: terminologia e misurazione delle caratteristiche, Milano: Ente Nazionale Italiano di Unificazione, 2003.

[5] M. Kloiber, J. Kunecký, J. Tippner and V. Sebera, "A new diagnostic device for in-situ determination of strength and modulus of deformability in compression of wood parallel to fiber," in SAHC - 9th International Conference on Structural Analysis of Historical Constructions, Mexico City, 2014.

[6] M. Kloiber, M. Drdácký, J. Tippner and J. Hrivnák, "Conventional compressive strength parallel to the grain and mechanical resistance of wood against pin penetration and microdrilling established by in-situ semidestructive devices," Materials and Structures, pp. 3217-3229, 2014.

[7] ČNI, ČSN EN 1991-1-3: Eurokód 1: Zatížení konstrukcí - Část 1-3: Obecná zatížení - Zatížení sněhem, Český normalizačni institut, 2005.

[8] K. Kloiber, J. Tippner, V. Heřmánková and J. Štainbruch, "Comparison of results of measuring by current NDT methods with results obtained through a new device for wood mechanical resistance measuring," in SAHC - 8th International Conference on Structural Analysis of Historical Constructions, Wroclaw, 2012.

[9] M. Kloiber, J. Tippner, L. Praus and J. Hrivnák, "Experimental verification of a new tool for wood mechanical resitance measurement," Wood Research, pp. 383-398, 2012.

[10] M. Kloiber, M. Drdácký, J. Tippner and V. Sebera, "New construction NDT device for in situ evaluation of wood using compression stress-deformation measurement parallel to grain," 2013.

[11] CEN, EN 1991-1-4:2005: Eurocode 1: Actions on structures - Part 1-4: General actions - Wind actions, European Comittee for Standardization, 2005.

[12] CEN, EN 1991-1-3:2003: Eurocode 1: Actions on structures - Part 1-3: General actions - Snow loads, European Comittee for Standardization, 2003.

Use of Incremental Dynamic Analysis for the seismic performance assessment of RC framed structures

Marsed Leti[1], Hüseyin Bilgin[1]

[1]*Department of Civil Engineering, EPOKA University, Albania*

ABSTRACT

In this study seismic performance assessment of existing low and mid-rise reinforced concrete buildings is presented by using Incremental Dynamic Analysis. Incremental dynamic analysis (IDA) is known as an accurate method and it can provide the whole range of structural responses from elastic range to collapse. The method performs a series of nonlinear dynamic analyses in which the intensity is incrementally increased for the ground motion selected to investigate the behavior until the global collapse capacity of the structure is reached. The mathematical models are prepared in the environment of Zeus-NL software, a finite element program developed especially for earthquake engineering applications. IDA curves are developed considering spectral acceleration (Sa (T1,5%)) as intensity measure (IM) parameter. The nonlinear dynamic analyses were conducted using a set of twenty natural ground motion records selected with a range from 0.042g-3.5g peak ground acceleration and without directivity influence. In addition, the immediate occupancy (IO), collapse prevention (CP) and global instability (GI) limit states are defined based on FEMA guidelines. Moreover, the IDA curves are summarized based on 16%, 50% and 84% fractiles. Finally, conclusions are summarized based on the findings done from the analysis results, while recommendations for the future research are presented.

Keywords*: Low and Mid-Rise Buildings; Nonlinear Analysis; Seismic Performance; Incremental Dynamic Analysis; Zeus-NL*

INTRODUCTION

The proper design of the structures to resist the severe ground motions, causing as few as possible losses, whether they are human or material, has been the main attention of both researchers and professional engineers. Consequently, the Performance-Based Earthquake Engineering (PBEE) was born as a new but innovative and fast-growing idea. Recently a new method has been developed in association with PBEE principles, known as Incremental Dynamic Analysis to help the engineers in assessing the performance of structures [1]. This procedure is able to replicate time history analyses, while scaling the ground motion records in order to evaluate the structural performance from elasticity until the total collapse of the building occurs. Considering multiple records, this tool aims to plot the capacity curve for the structure modelled. By appropriately summarizing the IDA curves, defining limit states and combining the results with Probabilistic Seismic Hazard Analyses (PSHA), will easily reach the goals for a better structural design [2]. In this paper the seismic performance of a low and mid-rise reinforced concrete building is conducted under nonlinear analysis procedures. For the estimation of the structures vulnerability due to the earthquake motion, the Incremental Dynamic Analysis (IDA) was applied under a set of records. The numerical model of the buildings selected is prepared in the environments of Zeus-NL software, a finite element program developed specifically for earthquake engineering applications [3] [4]. For the development of IDA curves, a

set of twenty ground motion records have been selected with peak ground acceleration from 0.042 to 3.50g. The maximum response parameters, intensity measure (IM) and damage measure (DM), are plotted on a two-dimensional graph for every scaling factor. According to previous studies [1] [2], it is selected 5% damped first mode spectral acceleration Sa(T1,5%) for the intensity measure and maximum global drift Θ_{max} for the damage measure while plotting the IDA curves. Additionally, the immediate occupancy (IO) and the life safety (LS) limit states are defined for every IDA curve. The structural performance under seismic loadings is done by interpretation of the IDA fractiles categorized as 16%, 50% and 84%.

METHODOLOGY FOR SEISMIC VULNERABILITY ASSESSMENT

In this study two RC buildings are selected without any geometrical irregularities and modelled as framed structures in the environments of Zeus-NL software for both x and y directions. A new nonlinear dynamic analysis proposed in literature, known as Incremental Dynamic Analysis, is utilized to achieve the objectives of this paper. Incremental Dynamic Analysis (IDA) was initially proposed by Bertero in 1977 and was adopted by the Federal Emergency Management Agency [5]. The first computer algorithms for the implementation of this method were introduced and presented by Vamvatsikos and Cornell [6]. Unlike from static pushover analyses, this method incorporates the use of time history analyses as an increasing intensity measure. Also called as dynamic pushover analyses (DPO) [7], this method uses the ground motion records to perform the analyses. Hence, IDA can be expressed as a repetition of the time history analyses, while the intensity of the record increases step by step to plot the two-dimensional graph same as static pushover procedure. Figure 1 illustrates the dynamic pushover curve as an increasing scale of time history analyses.

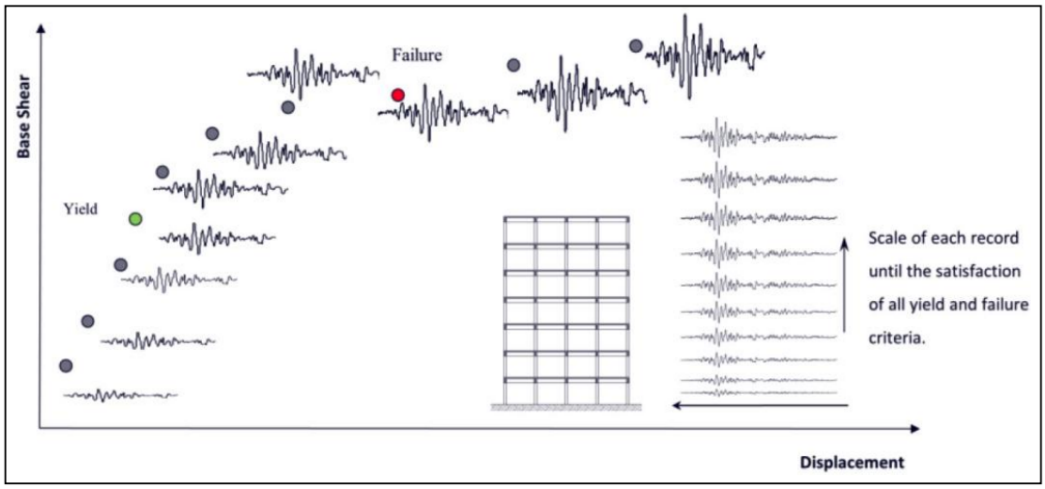


Figure 1. Incremental dynamic capacity curve [8]

IDA curves are developed under a set of ground motion records showing no directivity, so they do not influence the intensity measure parameter. In literature, researchers have suggested to use ten to twenty records for midrise buildings [9]. For this study a suite of twenty earthquake records with peak ground acceleration from 0.042g up to 3.50g are selected as shown in table 1. Ground motion records are taken from the Pacific Earthquake Engineering Research Centre (PEER) [10] and from the U.S Geological Survey (USGS) [11].

The IDA calculation parameters involve the scale factor, measure intensity of the earthquake and the measure of structural response. The scale factor produces a scaled accelerogram applied to the natural acceleration time history. The earthquake intensity measure has been selected as 5% damped of first mode spectral acceleration Sa(T_1,5%). The damage measure is considered the maximum global drift $\Theta_{max.}$ In

addition, the interpolation of the results to generate the IDA curves without needing to generate massive analysis, is done using super spline function as presented by [12].

Table 1: The suite of twenty ground motion records used for this study

No	Event	Year	Station	Ø°	Soil	M	R (km)	PGA (g)
1	Erzincan	1992	Turkey, Erzincan	90	C	6.7	8.9	0.488
2	Imperial Valley	1979	Westmoreland Fire Station	90	C,D	6.5	15.1	0.074
3	Loma Prieta	1989	Agnews State Hospital	90	C,D	6.9	28.2	0.159
4	Loma Prieta	1989	Coyote Lake Dam Downstr.	285	B,D	6.9	22.3	0.179
5	Loma Prieta	1989	Hollister South & Pine	0	D	6.9	28.8	0.371
6	Loma Prieta	1989	Sunnyvale Colton Ave	270	C,D	6.9	28.8	0.207
7	Imperial Valley	1979	Chihuahua	282	C,D	6.5	28.7	0.254
8	Imperial Valley	1979	Plaster City	45	C,D	6.5	31.7	0.042
9	San Fernando	1971	LA, Hollywood Stor. Lot	180	C,D	6.6	21.2	0.174
10	Northridge	1994	LA, Hollywood Storage FF	360	C,D	6.7	25.5	0.358
11	San Fernando	1971	LA, Hollywood Stor. Lot	90	C,D	6.6	21.2	0.210
12	Spitak	1988	Armenia, Gukasian	90	C	6.8	36.1	0.207
13	Sup.erstition Hill	1987	Wildlife Liquefaction Array	360	C,D	6.7	24.4	0.200
14	Tabas	1978	Iran, Dayhook	280	B	7.4	20.6	3.500
15	Loma Prieta	1989	WAHO	0	D	6.9	16.9	0.370
16	Loma Prieta	1989	WAHO	90	D	6.9	16.9	0.638
17	Northridge	1994	LA, Baldwin Hills	90	B	6.7	31.3	0.239
18	Friuli	1976	Italy, Tolmezo	270	B	6.5	20.2	0.345
19	Corinth	1981	Greece, Corinth	0	C	6.6	19.9	0.264
20	Kocaeli	1999	Turkey, Duzce	180	C	7.1	1.6	0.427

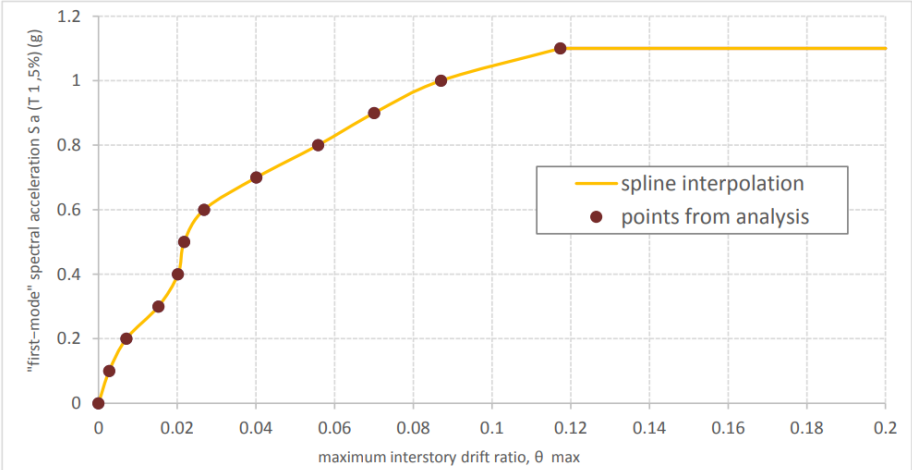


Figure 2. The interpolation of dynamic analyses points for Loma Prieta Sunn. Colton.

For each of the IDA curves the Immediate Occupancy (IO), Collapse Prevention (CP) both defined in [FEMA-350, 2000; FEMA (2000a), 2000], and Global Instability are determined. Defining especially the collapse prevention limit state is not an easy task and required an accurate procedure to get the most appropriate 20% of elastic slope in the IDA tangent. To achieve this step, the study involves the usage of a parametric curve used in computer graphics known as “Bezier curve” function. Finally, IDA curves are summarized as 16%, 50% and 84% fractiles as suggested by authors [1].

DESCRIPTION OF THE BUILDING AND MATHEMATICAL MODELLING

For this study two reinforced concrete buildings are selected, a three story and a seven story as shown in the figure 3. Both buildings have the same plan dimensions, 23 m long and 14 m wide. The plan is composed of 5 bays and 4 frames and is symmetrical in x and y directions therefore there will develop no torsional effect due to structural irregularities. The story height is 3 meters in each story elevation. Both buildings are modeled in the environment of Zeus-NL software as reinforced concrete structures with a concrete strength of fck = 30 MPa and steel class fy = 355 MPa. From the available library of the selected software, a cubic elasto-plastic type 3D element was used to model beams and columns. The bilinear elasto-plastic material model with kinematic strain hardening (stl1) was used for the steel reinforcement and rigid links modeling, while the uniaxial constant confinement concrete material model (conc2) was used for the concrete [4].

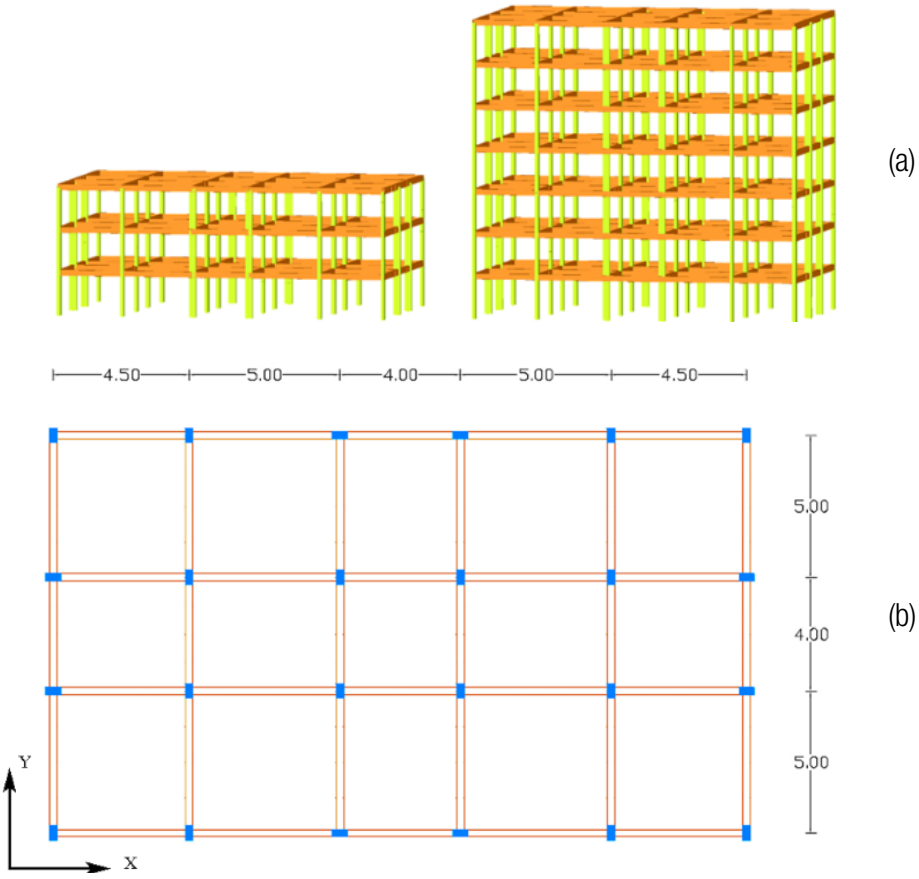


Figure 3. a) Structural plan (units in m); b) Elevation view of the frames

Each of the buildings has different element details. The low-rise model is composed of two types of columns and two types of beams, while the mid-rise building is composed of four types of columns and two types of beams as presented also in the Table 2. The element types change from each other according to their cross-sectional size and reinforcement. The infill walls have a thickness of 20 cm and slab thickness of 15 cm according to plan details.

Table 2. Column and Beam details

Column Type	Column size	Longitudinal reinforcement (No. of bars / bar size)	Beam Type	Beam size	Longitudinal reinforcement (No. of bars / bar size)	Structure
Type 1	40 * 70 cm	12 Ø18	Type 1	30 * 50 cm	8 Ø14	7-Story
Type 2	40 * 70 cm	8 Ø18	Type 2	30 * 50 cm	8 Ø12	7-Story
Type 3	30 * 70 cm	12 Ø16	---	---	---	7-Story
Type 4	30 * 70 cm	8 Ø16	---	---	---	7-Story
Type 5	25 * 50 cm	8 Ø16	Type 3	25 * 40 cm	8 Ø12	3-Story
Type 6	25 * 50 cm	6 Ø16	Type 4	25 * 40 cm	6 Ø12	3-Story

Both buildings are modeled in Zeus-NL program, a platform which uses finite element analyses facility developed especially for earthquake engineering applications [3] as moment resisting frames. Zeus-NL uses a fiber approach for the nonlinear analyses, monitoring the cross section into several fibers such as reinforcement fiber, confined concrete fibers and unconfined concrete cover. The structural elements (Beams and Columns) are modeled according to project details to increase the accuracy of the results. The self-weight of the structural members is calculated and assigned as distributed load in beams and as concentrated loads in columns. Since there is no slab or infill wall member type in the Zeus-NL library, the self-weight, dead loads and live loads are calculated and assigned over the beams as distributed load. At the base nodes all the degrees of freedom are restrained.

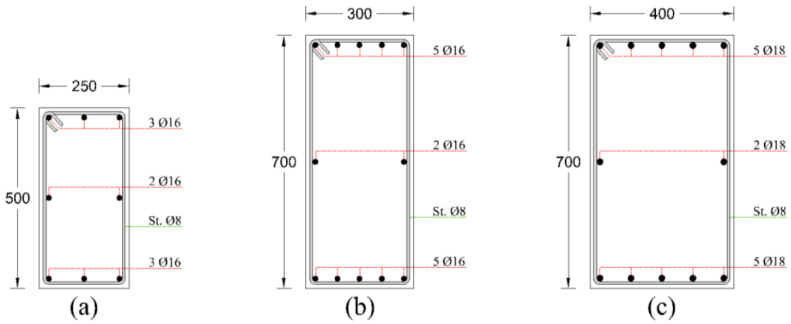


Figure 4. Lower story columns: a) 3-story column, b) 7-story column, c) 7-story column (units in mm)

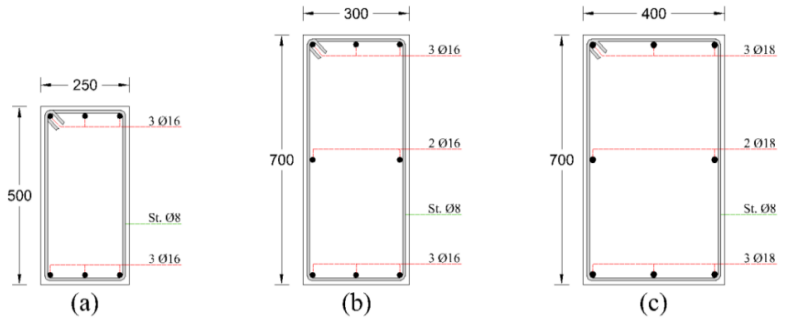


Figure 5. Upper story columns: a) 3-story column, b) 7-story column, c) 7-story column (units in mm)

Zeus-NL does not provide a very user-friendly method to model structural elements, especially for the reinforcement. To accelerate the modeling stage for this study a new methodology is followed while modeling the structural elements. Since the software allows easily to modify the element library, a new

library has been prepared using Microsoft excel 2013 and the allocation of the steel bars in each member is calculated in common with reinforcement area aiming to minimize the calculation mistakes.

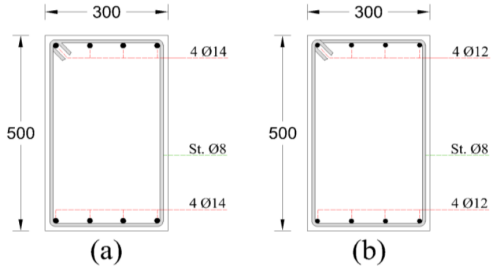


Figure 6. Mid-rise model beams: a) lower story beams, b) upper story beams (units in mm)

RESULTS

Four moment frames, representing the low-rise and mid-rise building cases, are subjected to more than thousand nonlinear dynamic analyses. These values are used to plot the IDA curves. The fragility curves developed from incremental dynamic analysis will be considered as a suitable tool to conduct an earthquake assessment as well as structural damage under a suite of twenty ground motion records. 80 IDA curves are ploted and illustrated as simple IDA curves, with dots to represent each increment scale, together with limit states. In addition, these curves are summarized as 16%, 50% and 84% fractiles as presented below.

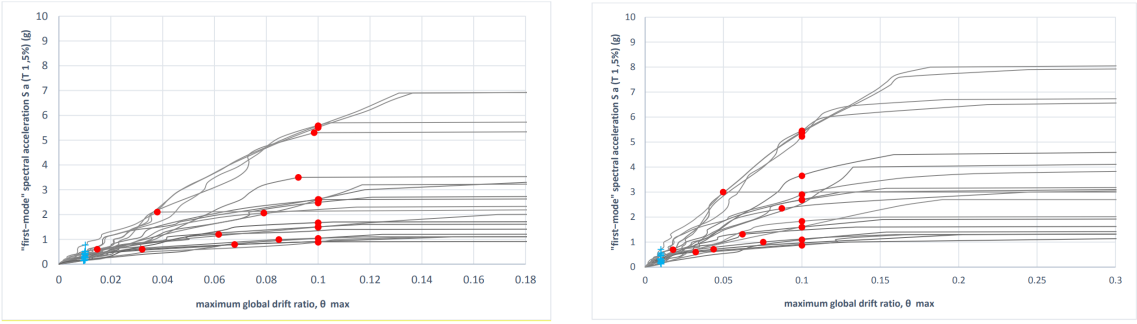


Figure 7. Twenty IDA curves and associated limit-state capacities for 3-Story Building in x-direction (left) and y-direction (right). The IO limit is represented by plus sign, collapse prevention limit is represented by dots and global instability with flatlines.

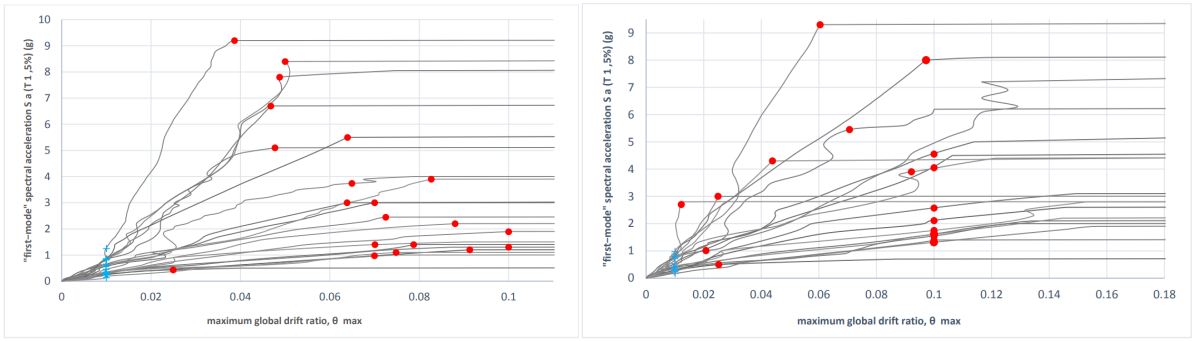
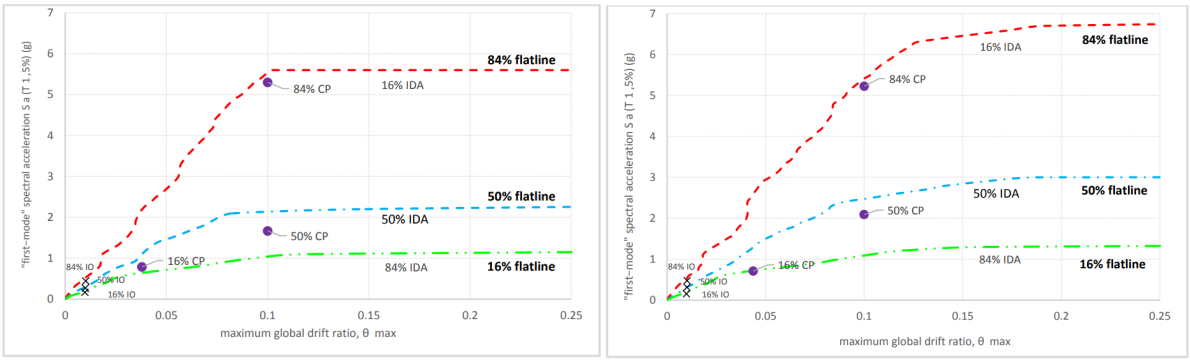


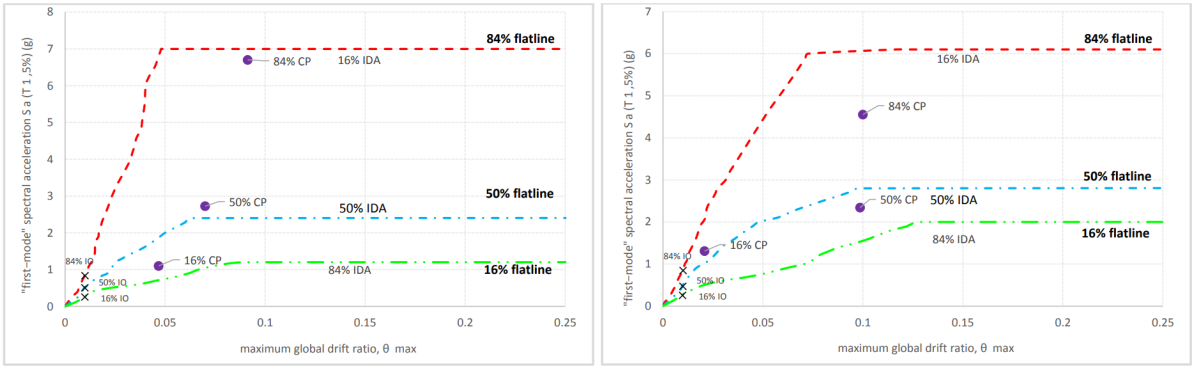
Figure 8. Twenty IDA curves and associated limit-state capacities for 7-Story Building in x-direction (left) and y-direction (right). The IO limit is represented by plus sign, collapse prevention limit is represented by dots and global instability with flatlines.

As can be seen from the presented IDA curves, it is very practical to observe the hardening and softening on each of the curve until the global instability (GI) is reached. This limit state is represented by the flatline segment on the curves. The constant line of the IDA curve shown in the graph indicated that the building reached the maximum load bearing capacity and total collapse with take place. The immediate occupancy limit state is shown with a "+" sign in the IDA curves which corresponds to 1% of the damage measure parameter. Similarly, the collapse prevention is demonstrated by dots on each of the curves plotted in the graph.



(a) (b)

Figure 9. 16%, 50%, 84% IDA fractile for the 3-Story, X-direction Frame on the left and Y-direction Frame on the right



(a) (b)

Figure 10. 16%, 50%, 84% IDA fractile for the 7-Story, X-direction Frame on the left and Y-direction Frame on the right

IDA curves can represent very detailed information by plotting the fractiles into 16%, 50% and 84% according to the methodology provided in previous studies. From the generated IDA fractiles, it is possible to observe the structural response for any increase of intensity measure until the global collapse limit state is reached. Reading from the IDA graphs, it can be summarized that for an IM equal to 1.0g, 16% of the samples produce approximately $\theta_{max} \leq 1.77\%$, 50% of the samples produce $\theta_{max} \leq 3.62\%$ and 84% produce $\theta_{max} \leq 9.31\%$ for the 3-Story X-direction frame. For the same IM value (1.0 g), the 3- Story, Y-direction frame at the 16% of samples produce $\theta_{max} \leq 1.84\%$, for the 50% $\theta_{max} \leq 3.51\%$ and for the 84% produces $\theta_{max} \leq 8.72\%$. 7-Story, X-direction frame produces at the 16% IDA curves, $\theta_{max} \leq 1.13\%$, at 50%, $\theta_{max} \leq 2.28\%$, and at the 84% IDA curves produces $\theta_{max} \leq 6.67\%$. Lastly, 7-Story, Y-direction frame produces $\theta_{max} \leq 1.10\%$ for 16% of fractiles, $\theta_{max} \leq 1.98\%$ for 50% of the curves and $\theta_{max} \leq 7.07\%$ for the 84% of the IDA curves. In an alternate way, the summarized fractiles can be used inversely to gather more information. For a specific damage measure, the respective value of the intensity measure depending on the 16%, 50% or 84% fractiles can be observed. Simultaneously, as graphically illustrated in Figure 9 it is

observed that for Sa(T_1,5%) = 1.667g and 2.090g or equivalently at θ_{max} = 0.10, 50% of the ground motion records have forces the three-story structure to violate the Collapse Prevention performance level in x- and y-direction respectively. In the same way it can be interpreted that for the seven-story building for the Sa(T_1,5%) = 2.723g and 2.340g or equivalent at θ_{max} = 0.070 and 0.099, 50% of the records are violating the CP limit state in x- and y-direction respectively as shown in the Figure 10. Finally, it is observed that due to inherent characteristics of the accelerograms some records (I.Valley - Westmoreland Fire Station; S.Fernando - LA, Hollywood Stor. Lot; Friuli –Italy, Tolmezo; Tabas - Iran, Dayhook; L.P – WAHO 090; Northridge - LA, Baldwin Hills; Corinth – Greece and Kocaeli - Turkey, Duzce) forced the low-rise building to fail before the mid-rise one.

CONCLUSION

In this study, Incremental Dynamic Analysis is used for the seismic performance assessment of reinforced concrete buildings. A three story and seven story buildings have been used as representative of low and midrise constructions. Mathematical model is prepared using Zeus-NL software. For the nonlinear analysis, a set of twenty ground motion records is selected showing no directivity. In addition, a methodology is presented for the development of IDA curves as well as Immediate Occupancy, Collapse Prevention and Global Instability limit states based on FEMA guidelines. From the results, it is observed that due to inherent characteristics of the accelerograms some records forced the low-rise building to fail before the mid-rise one. The limit states can be very useful to interpret the structural performance for each earthquake. Finally, IDA curves and IDA fractiles provide detailed information for the demand calculation due to any intensity measure increase. More information can be gathered from IDA fractiles for the structural performance due to ground motion forces, nevertheless this requires a deep research which can be a beneficial recommendation for the further studies.

REFERENCES

[1] Dimitros Vamvatiskos, Cornell C.A, "Incremental dynamic analysis. Earthquake Engineering," doi:10.1002/eqe.141, pp. 491-514, 2002.

[2] D. Vamvatsikos, "Seismic Performance Capacity and Reliability of Structures as seen," Stanford: Stanford University, 2002.

[3] A. Elnashai, "Zeus NL - A system for Inelastic Analysis of Structures," Urbana–Champaign: Creating a Multi-hazard Approach to Engineering, 2002.

[4] A.S Elnashai, V. Papanikolaou, D.H Lee, "ZEUS-NL User Manual," Mid-Amerika Earthquake Center, University of Illinois at Urbana-Champaign, 2002.

[5] F. (2000a), "Recommended seismic design criteria for new steel moment-frame buildings," Washington, DC.: Federal Emergency Management Agency, 2000.

[6] P. Spears, "Parameters Influencing Seismic Structural Collapse with Emphasis on Vertical Accelerations and the Possible Related Risks for New and Existing Structures in the Central and Eastern United States," Blacksburg, VA: Virginia Polytechnic Institude and State University, 2004.

[7] A.M Mwafy, A.S Elnashai, "Static pushover versus dynamic collapse analysis of RC buildings," Eng. Struct., vol. 23, pp. 407-424, 2001.

[8] C. Constantinos, "Seismic Performance Evaluation of Existing RC Buildings Without Seismic Details. Comparison of Nonlinear Static Methods and IDA," The Open Construction and Building Technology Journal, pp. 158-179, 2016.

[9] N. Shome, C.A.Cornell, "Probabilistic seismic demand analysis of nonlinear structures," Stanford: Stanford University, 2002.

[10] PEER, "Pacific Earthquake Engineering Research Center, University of California," 12 December 2020. [Online]. Available: http://peer.berkeley.edu/.

[11] U. USGS, "Geological Survey, U.S. Department of the Interior," 12 December 2020. [Online]. Available: https://www.usgs.gov.

[12] D. Vamvatsikos, C.A Cornell, "Applied Incremental Dynamic Analysis," EarthquakeSpectra, pp. 523-553, 2003.

Observations on the Domed Mosques Built During the Ottoman Empire Period in Prizren - Kosovo

Edmond Manahasa[1], Hadis Toçilla[2]

[1]*Department of Architecture, EPOKA University, Albania*
[2]*Freelance Architect, Prizren, Kosovo*

ABSTRACT

This study focuses on the domed mosques built during the Ottoman Empire period in Prizren, a southern Kosovo city. It aims to reveal these buildings' architectural and ornamental features, emphasizing the transitional elements from cubical mass to domes.
Based on on-site observation, there are examined six domed historical mosques in Prizren. The explanation of the mosques is explained under three primary sections. Firstly, an introduction part includes the historical background of the mosques and information about the builder/commissioner. The study uses both local (Kosovo-based) and central (Istanbul-based) literature to provide this information. Their architectural features are explained in the second section based on four elements: plan schemes, roofing structures, materials, and façades. The third section is explained the ornamental features of the buildings, including the stone decoration, the wooden decoration, the calligraphic art, and paintings, and the last one stained glass. The methodology used in the study includes archival research, visual documentation through photos, drawings, and analytical interpretation of architectural and ornamental features of the buildings. In conclusion, the buildings are compared to each other, aiming to reveal the proper period's architectural values peculiarities.

Keywords*: Domed Mosques, Ottoman Period, Prizren, Kosovo*

HISTORICAL BACKGROUND OF PRIZREN

Prizren is a city which is located in the southern part of Kosovo. Historically, the region around Prizren was inhabited by the Illyrian tribe of Dardani [1]. Based on Procopius of Caesarea [2], by the 5TH century, the city was known as Petrizen. By the 11th century, the Byzantine Emperor Basil II Charter gives the city name of Prisdriana [as mentioned in 3]. Before being invaded by the Ottomans, the city was a subject of invasion by the Bulgarian tsar and later in 1216 ruled by Slavic Serbs under Stefan II Nemanjic [4].

The Ottomans invaded Prizren in 1455, approximately 60 years after the “Battle of Kosovo.” The Ottomans used various forms for city names like Pirzerin, Pürzerin, or even Zerrin. These toponyms are evident in the inscriptions of gravestones of local poets like Suzi Çelebi or Nehariu [5]. The city under the Ottoman rule remained the most important one of Kosova Vilayet (governorate). There was even established a short living Prizren Vilayet also (1871-1877), which included Sanjaks of Prizren, Dibra, Skopje, and Nish. However, in 1877 was re-incorporated into a greater Sanjak of Kosova, whose center was Prishtina and later became Skopje [12]. Within Kosovo's disputed history, between Albanians and Serbs, Prizren maintains a crucial role for the Albanian national movement. This is due to the organization Albanian League of Prizren in 1878. Although, after the Treaty of London in 1912, until the independence of Kosovo in 2008, it was part of the Serbian Kingdom and later Yugoslavia.

Being under different rules, especially during the Ottoman period, Prizren was dwelled by different ethnicities, who also belong to different religions. It is featured by a rich variety of building typologies like mosques, churches, madrasas, hammams, and even synagogues (Figure 1).

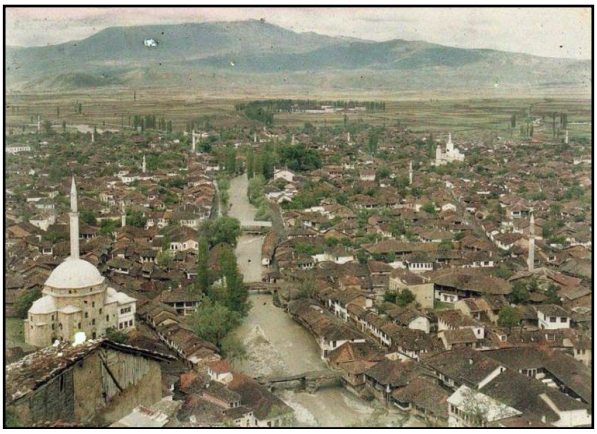


Figure 1. An image of Prizren urban texture in which mosques and church are visible in 1913 [©Albert Kahn] retrieved from https://gazetainfokus.com/20-foto-te-rralla-me-ngjyra-te-prizrenit-dhe-prishtines/ in 01/12/2020

The study, beyond the depiction of the construction process, also gives information about the Prizren socio-political context and the person who commissioned the mosques, who at the same time appear to be influential figures of the period. There are reported 28 mosques built during the Ottoman period in Prizren [6]. The first religious building is Namazxhahu (or Kırık Mosque in Turkish), which was constructed by Isa Bey in 1455 (the Ottoman military commander who invaded the city) for the spiritual needs of his soldiers (Figure 2).



Figure 2. “Namazxhahu” the first Islamic worship place in Prizren [©Shkelzen Rexha]

THE OTTOMAN PERIOD DOMED MOSQUES IN PRIZREN

Due to this conference's engineering nature, the scope of this study is related to the historical domed mosques built during the Ottoman period in Prizren. Based on that, there are examined six mosques which are covered by domes. The domed mosques included in this study are Kukli Beg Mosque (1531), Gazi Mehmet Pasha Mosque (1563-1574), Sinan Pasha Mosque (1614), Maksud Pasha Mosque (1644), Emin Pasha Mosque (1831), and Katip Sinan Beg Mosque (1893-1894). The mosques are in explained chronological within three main divisions: historical background, architectural features, and ornamental features. The transitional elements from the cubical base to the dome is also explained within architectural features. In the conclusion part, the architectural and ornamental features are analysed through being

grouped within similar and different aspects, providing at the same time important information on the typical characteristics of the construction period.

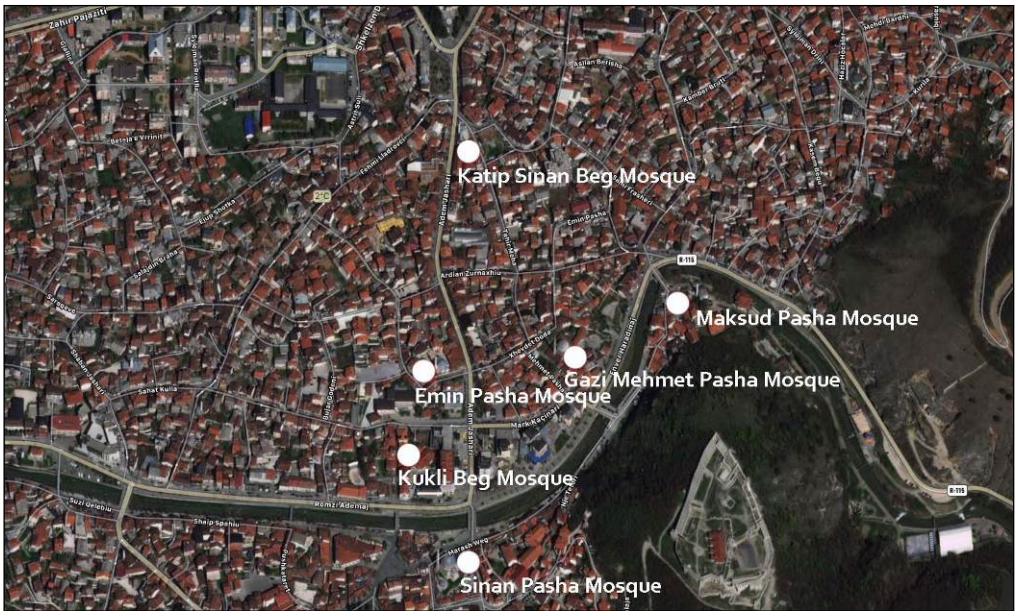


Figure 3. Location of the domed mosques within Prizren map included in the research [©Edmond Manahasa]

Kukli Beg Mosque

The Kukli Beg Mosque is one of the oldest mosques. It is located in the city centre close to the Post and Telecommunications of Kosovo building, Mehmet Pasha Hamam and Halveti Tekke. This mosque is also known as "Saraçhane" mosque, due to the neighbourhood with the same name. It is built in 1531 by Kukli Beg. According to Suroy-Recepoglu [7], Kukli Beg is the grandson of Ilyas Kuka. He built a mosque, a masjid, and a tekke in Prizren. Kaleshi (2015; as mentioned in [6]) gives the origin of İlyas Kuka from Van (Anatolia), although his name sounds like a typical northern Albanian surname. Furthermore, Kukli Beg is depicted as a wealthy person who holds a kervansaray. He donated the mosque as a "waqh" in 1538.

Architectural Features of Kukli Beg Mosque

This mosque is composed of the main prayer hall (harim) and the last prayer hall (Figure 3). The harim part has a square shape, with inner dimensions 8.3 m x 8.3 m and outer 9.2 m x 9.2 m. It also includes a women's mahfil in it. The entrance to the last prayer hall and the one to harim are found on the right side. The minaret is placed in the west corner and is entered from outside. Due to a later urban adjustments, the mosque ground level is a bit sunken compared to the street. The last prayer hall reflects better the urban context as its shape is quasi polygonal. There is also found a mihrab in the last prayer hall. The materials used for its construction is rubble stone masonry, which is unplastered in the façade, while the minaret is plastered.

The harim is covered by a dome in interior, whereas in exterior, it looks like an octagonal roof cladded by stone slates. The transition from the cubical mass to the dome is realized through pendentives, as the dome in the exterior is based on an octagonal drum. The last prayer hall is achieved in the form of a wooden porch and is covered by a tiled roof.

Although the facades refer to a classical Ottoman one, the windows are organized into two rows. There are found only two windows in the lower row, and in the upper row, there is one window, except the entrance façade. The windows are rectangular framed without pointed arches.

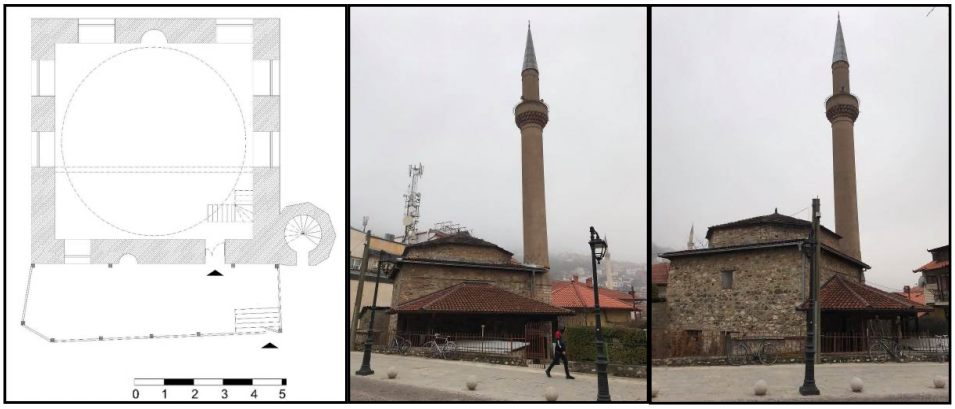


Figure 4. Plan Scheme of Kukli Beg Mosque (redrawn by Hadis Toçilla, referred to Vırmiça, 1996), (middle) north-east and (right) north-west façade [© Hadis Toçilla]

Ornamental Features of Kukli Beg Mosque

Although the mosque interior used to be rich in mural paintings, several renovations were made in 1977 and 1994. These interventions included plastering of the interior covering of murals paintings.



Figure 5. Pendentives and women mahfel in Kukli Beg mosque interior [© Hadis Toçilla]

The interventions are reported to have been realized by local masters without the needed expertise. The only remaining ornamental value that can be counted are the pointed arch frames that define the interior's pendentives. Due to these evasive interventions, there is no stone, wooden, painting, or calligraphic decoration, stained glass decoration.

Gazi Mehmet Pasha Mosque

Gazi Mehmet Pasha Mosque is located in Prizren city centre. It was built during the period 1563-1574 by Mehmet Pasha as a part of a significant ensemble [külliye], including a madrasa, a library teaching rooms [8]. It is within this ensemble that the Albanian League of Prizren was held in 1878. According to Ayverdi [9], Gazi Mehmet Pasha was the Sanjak Beg of Kyustendil in today's Bulgaria. In the inscription of the mosque is written: "Gazi Mehmet pasha built another mosque. He did not do it for himself, but for Allah. A silver mosque in the city of Prizren. He made the heaven of a city" [10]. According to Süreyya [13], he died in Kazanluk (Bulgaria), and although he also constructed a tomb, he is not buried there. Since the Albanian League was organized within the külliye of Gazi Mehmet Pasha locally, the mosque is also called "Bayrakli" (Flagbearer).



Figure 6. The külliye of Gazi Mehmet Pasha in Prizren (left) [© Granit Ismaili] and (right) view from outer street [© Hadis Toçilla]

Architectural Features of Gazi Mehmet Pasha Mosque

From an architectural perspective, Gazi Mehmet Pasha Mosque is one of the most important Ottoman buildings in Prizren. Not only due to its own architectural quality, but also related to the fact that it is part of an ensemble [külliye]. The mosque consists of the main prayer hall (harim) and the last prayer hall. The harim possesses a square plan scheme. The last prayer hall is in a "u" shape, adjoining the three façades of harim, except the qibla wall façade.

The main prayer hall is covered by a dome, which is based on squinches. Over the squinches, an octagonal drum prepares the dome's base, which is covered by leaden plates. The triangular shoulders over the squinches are kept lower than the base of the drum. The drums lower base, its upper part, and triangular shoulders are emphasized by a white cornice, defining the buildings' volumes a purist approach.



Figure 7. Plan scheme of Gazi Mehmet Pasha mosque in Prizren (left- redrawn from Hadis Toçilla referred to Vırmiça, 1996) and (right) Entrance façade [© Hadis Toçilla]

The silhouette of the mosque is featured by a noble vertical emphasized height character. The façades of the main volume are designed in classical Ottoman style in three rows. All three rows possess two windows, which are in pointed arch frames. The qibla façade is different as between the 2nd and 3rd row is added a circular window. The material used is neatly cut stone.

The last prayer hall, achieved in the form of a porch, is constructed with wooden posts and it two steps upraised from the entrance corridor. It possesses two mihrab niches in the flanking sides of the entrance façade and two others, one in each of the last prayer hall's lateral wings qibla walls. The last prayer hall contains arches whose profile appears to be similar to Bursa arch. It is covered by a roof in leaden plates. The minaret is very slender and reminding the Mosque of Abdurrahman Pasha of Peqin, although it is constructed about 1 century later.

Ornamental Features of Gazi Mehmet Pasha Mosque

The interior of this building is painted in white. In contrast, the window frames, arches, and the squinches that prepare the drum base are decorated with floral motives. The lower row windows arches are decorated with blue colour dominated floral motives. The upper row façade arched windows are decorated with floral motives in bluish and golden gilt colour.

Eight circular medallions in the same colour are found between the dome base and squinches arches. In contrast, sixteen others are found around the centre of the dome. The dome's central part is also decorated with a bigger circular ornament, which includes floral and geometric patterns. Four elliptical medallions crenelated with palm/tree like bluish floral motives are painted at the squinches surfaces. Eight similar elliptical motives, but smaller in size are painted at the dome's base in between the arched windows. The crenelation in the elliptical motives implies a crown-like visual effect.

The stone decoration in this building is used in the prayer hall and the last prayer hall. The mihrabs, both in harim and last prayer halls, have muqarnas decorations. Muqarnas is also found at the muezzin's balcony in the minaret. The main Mihrab is taken in a rectangular frame. The transition to the wall is made by muqarnas, which is enclosed by colonnettes at flanking sides. The muqarnas and colonnettes are painted in golden gilt. The stone decoration is also applied in the minbar, which is embellished by two colonnettes in its entrance. The of the minbar is constructed of massive marble. Four pointed arches colored in yellowish taken in the rectangular frame are found under the minbar's stairs. Under landing, there is an Ottoman pointed arched opening.



Figure 8. Interior of the dome (left) and (right) squinch on the corner [© Hadis Toçilla]

The wooden decoration is applied in the last prayer hall ceiling, which also stands on the wooden column. The capitals of columns are decorated with flower motifs, suggesting features from wooden mosques in central Anatolia. There is no stained glass decorations, except the second-row windows are designed in geometrical motives using gypsum frames.

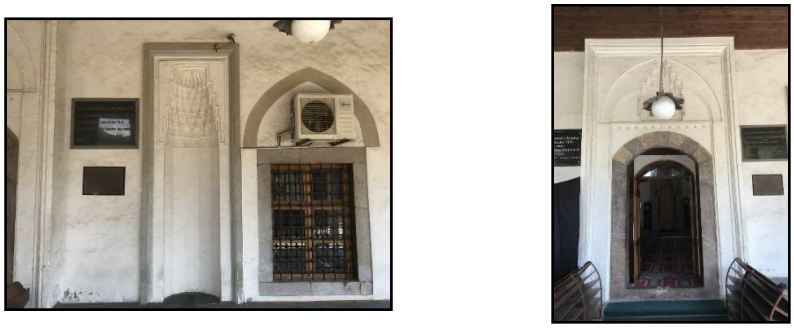


Figure 9. Entrance Door (right) and (left) mihrab niche at flanking side [© Hadis Toçilla]



Figure 10. Minbar lateral side (left), profile view (center) and (right) detail of post capitals at last prayer hall [© Hadis Toçilla]

Sinan Pasha Mosque

The Sinan Pasha Mosque is located in the historical center of Prizren. Also, it is one of the strongest landmark buildings in the city. The mosque was built in 1614 by Sinan Pasha. In fact, the commissioner of this building has been a subject of dispute. There are two important figures with the same name (both originated from the Luma region of Albania and living around the same time simultaneously): Sofi Sinan Pasha and Koca Sinan Pasha. However, Kaleshi clarified the authorship by identifying it as Sofi Sinan Pasha, the Beglerbeg of Budin in Hungary (Kaleshi, 1972; as cited in 11).

It is believed that the last prayer hall, together with the inscription of the mosque, was destroyed due to the bomb explosion in 1915 [7]. In 1968 became the property of the Islamic Union of Kosovo. It has been restored several times, and the last time was from the Turkish Agency for Cooperation (TIKA).

Architectural Features of Sinan Pasha Mosque

The plan scheme of this mosque is composed of a harim and the last prayer hall. The harim part is featured by the square plan, except the qibla wall edge, which has a protruded niche in its south-eastern side. The dimensions of square part are 17.8 m x 17.80 m, whereas the protruded niche is 6.2 m. The wall thickness is 2.00 m. The main entrance is from its north-western façade. The women's mahfil is placed on the right side of the entrance.

The last prayer hall is designed in the form of a porch supported by four columns. The mosque is placed in an upraised position approximately 3.5 m above the street level.



Figure 11. Sinan Pasha Mosque (left-retrieved in 01.12.2020 from https://www.kultplus.com/tag/xhamia-sinan-pashes) and (right) south-west façade [© Hadis Toçilla]

The harim part is covered by a dome whose diameter is 14 m. In contrast, a barrel vault and a semi-dome cover the protruded part. The transition from the square plan of the praying hall to the circular plan

of the dome is realized by squinches. The last prayer hall also is covered by three minor domes. The dome exterior is covered by leaden plates. The mosque is built with neatly cut river stones.

The lateral façades of the building are organized by four rows of windows. The lower two rows include each three windows, whereas the 3rd row has two, and the uppermost one possesses only one window. The qibla façade, due to the mihrab niche protrusion, is more three dimensional and contains three rows of windows. Just above the mihrab niche portal is found a circular window, which is more emphasized. The triangular shoulders above the niches are covered in lead plates, just like the domes. All the eaves of the lead-covered volumes are treated with a cornice. Similarly, the drum is treated with cornices in its base bringing into appearance a purist volumetric approach in the overall architectural composition.

The minaret of the mosque is built on the south-west façade and is 43 m high. It is founded on a rectangular base and transforming into a polygonal profile and ends with one balcony.

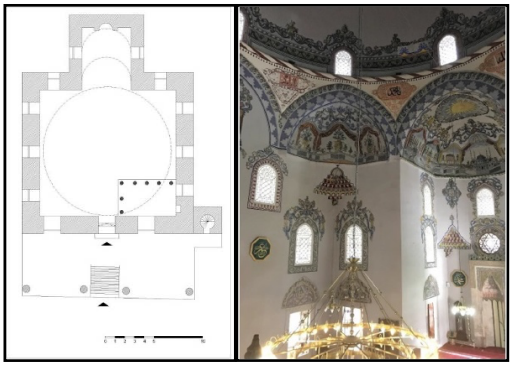


Figure 12. Plan scheme of Sinan Pasha Mosque (left-redrawn from Hadis Tocilla referred to Vırmiça, 1996) and (right) interior of harim [© Hadis Toçilla]

Ornamental Features of Sinan Pasha Mosque

The stone decoration can be seen in entrance gate of the building, in which are used polychromatic stonework to define its arched frame. Also, the stone decoration can be seen in columns of mahfil (women's balcony). The capitals of the columns are decorated in a quasi-Corinthian style. Older parts of mihrab are taken in a rectangular frame dominated with green and yellowish colors; it possesses two columns like other mosques in Prizren. The minbar is mainly made of precisely cut stone. There are six minor pointed arches under the stair part. Under the landing area, there is a pointed Ottoman arched opening. It is decorated with floral motives and dominated by yellowish color.

The wooden decoration besides the balustrade on the inner balcony is also found in its ground floor ceiling. Especially the ceiling is curated with very interesting chess-like green-reddish patterns. The wooden decoration is also found in the balustrade of the minbar.

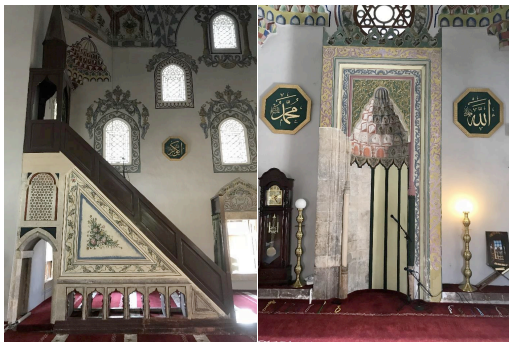


Figure 13. Decorations on the mihrab (left) and minbar (right) of Sinan Pasha Mosque

The painting decorations appear to carry Baroque features conducted in the later period during the 19th century, considering Western influence started only in the 18th century in the Ottoman empire. The mosque's interior is plastered and decorated with mural paintings that depict landscapes, floral motives, and ideal imaginary Ottoman mosques. The mural paintings are dominated by bluish colors associated with the presence of minor bright yellowish colors, giving the sense of golden gilt. The Baroque features are reflected not only on the usage of exuberant floral motives but also on undulated arches that incorporate "c" forms and are veiled partly with heavenly curtains. The large number of windows provide abundant light in the interior. All the windows are decorated by exuberant colorful floral motives.

Interestingly beyond the mihrab crowned with tulip-like motives, the circular window over it carries a six-pointed star motive. Also, the mihrab niche barrel-vaulted ceiling is decorated by a shining yellowish sun. Colorful paintings are also used in the muqarnas transitional elements in the mihrab niche and the harim part's squinches. The stained-glass decorations are used on the second, third, and fourth-row windows. The frame patterns of the windows are characterized by curvilinear and geometrical features.

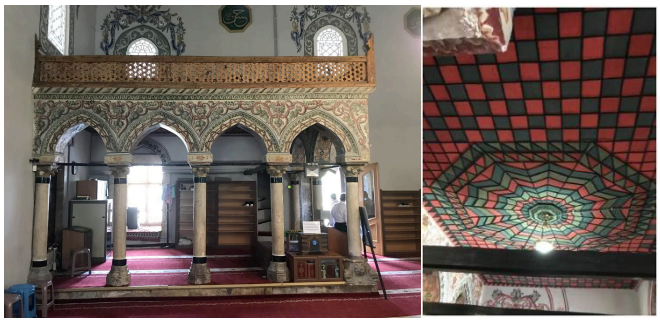


Figure 14. Women's mahfel (left) and its ceiling (right) [© Hadis Toçilla]

Maksud Pasha Mosque

The Maksud Pasha Mosque is located near the Lumbardh River close to the city center. Locally is also known as Marash Mosque meaning "a fresh place" Ottoman, although we can suggest a relation to a pre-Ottoman catholic Albanian name. It was built by Maksud Pasha who was the Ottoman governor of Egypt. There is no inscription in the mosque, but it is known that it was built before the death of Maksud Pasha in 1644 [7].

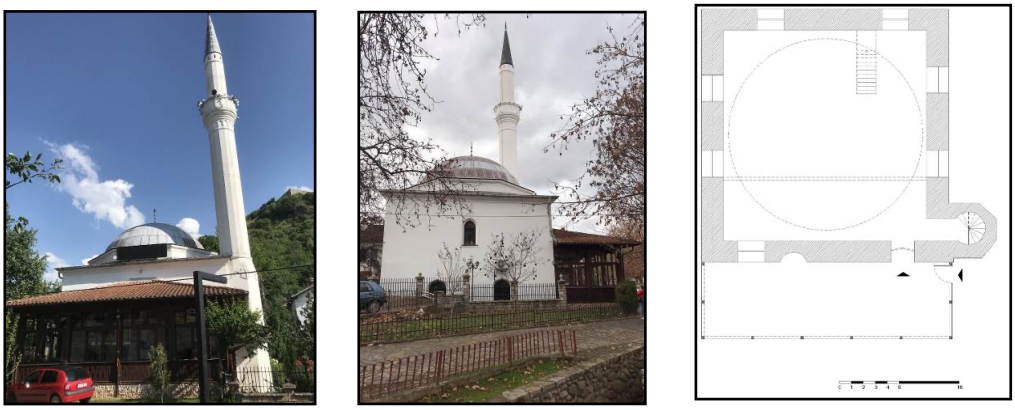


Figure 15. Maksut Pasha Mosque entrance façade (left), (center) lateral façade [© Hadis Toçilla] and (left) plan scheme (redrawn by Hadis Toçilla referred to Vırmiça, 1996)

Architectural Features of Maksud Pasha Mosque

The original mosque possessed a square shape with 10.5 m x 10.5 m consisting of a harim. There was added and wooden porch at a later period, which serves as the last prayer hall. The harim contains a mahfil and a mihrab on the qibla wall. The harim part is covered by a dome supported on pendentives. The wooden last prayer hall is covered with a tiled roof. The building is constructed with cut stones, and its exterior is plastered. The wall thickness is about 1.10 m. The main entrance is realized through the last prayer hall, whereas the minaret is placed in the western corner. The lateral façades contain three pointed arched windows organized into two rows.

Ornamental Features

The interior of the mosque is plastered in white colour. The stone decoration is found in the mihrab, realized within a carved rectangular frame and decorated with two columns and muqarnas relieves in blue and yellow colours.



Figure 16. and right interior view of the mosque (center) the mihrab and minbar and (right) last prayer hall [© Hadis Toçilla]

The minbar is in a wooden structure but appears to be not the original one. The last prayer hall is constructed in the form of a wooden porch and is also newly renovated. There is no painting or calligraphic decoration in this building.

The stained-glass decorations are found at the upper part of the windows divided into minor pointed arches and a central triangular part. This central triangular part, which is down headed, is in yellow-coloured stained glass.

Emin Pasha Mosque

Emin Pasha Mosque is also located in the city centre close to the Gazi Mehmet Pasha Hammam. It was built by Emin Pasha, the Sanjak Beg of Prizren, until 1843, according to Suroy-Recepoğlu [7]. The year of construction is mentioned in the inscription above the gate. The text is as follows: “The benefactor and constructor of the Mosque is Prizren’s Emin Pasha, son of Tahir Pasha, Mutesarif of Kiustendil. Year of construction 1831/1832”. The mosque was recently in 2016 restored by the Turkish Agency TIKA.

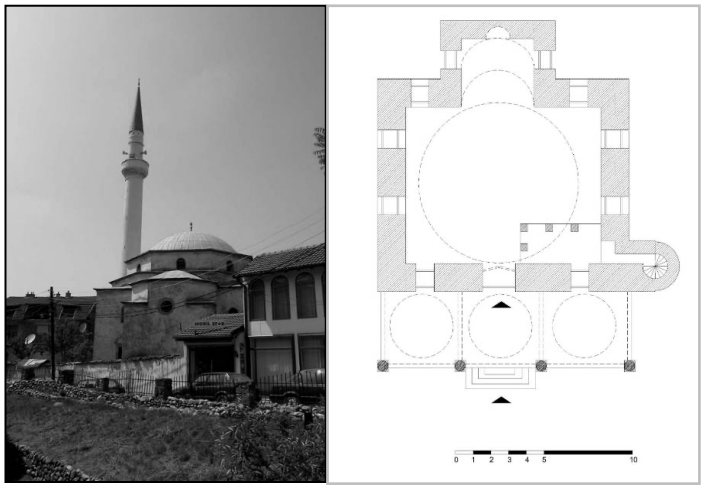


Figure 17. Image of Emin Pasha Mosque and plan scheme (redrawn from Hadis Toçilla referred to Vırmiça, 1996)

Architectural Features of Emin Pasha Mosque

The mosque has a rectangular plan scheme with a protrusion added in for the mihrab niche in the qibla wall. It is essential to mention that its plan is similar to the Sinan Pasha Mosque. It is divided into two parts: harim and last prayer hall. The mosque dimensions are 9.25 m x 9.25 m, and the niche part 3.45 m x 3.65 m. The main entrance is flanked by two windows. The last prayer hall is built on four stone columns. The entrance to the minaret is from its base outside the mosque.

Emin Pasha Mosque harim is covered with a dome and semi cupola in the mihrab area, both of which are coated with leaden sheet plates. The last prayer hall also is covered with three minor domes. The minaret is built with neatly cut stone and plastered. It has a polygonal base, and its upper structure is circular. The thickness of the mosque walls is 1.35 m. The mosque's lateral façades can also consist of five windows, which are organized into three rows. The first and the second rows possess two windows, whereas the third row has only one window. Similar logic is also continued in the qibla façade except for the protrusion part, which possesses a circular window over the mihrab portal.

Ornamental Features of Emin Pasha Mosque

The interior ornamentation of this mosque is very rich, and it was restored recently in 2016. The stone decoration in this building is used at the frame of the entrance door mihrab, minbar, and on the women's mahfil stone columns' capitals. The entrance door is decorated with a rectangular marble frame. The inscription above the gate is written on a green plate contoured with golden colour. The mihrab is decorated with two colonnettes and the muqarnas it its portal is embellished with carvings generating a triangular frame. Although prior to the restoration the mihrab was painted in golden gilt colour, after that is treated with white background and reddish-bluish nuances in the muqarnas. The wooden decoration is seen only in the inner balcony, and it appears to be a new restoration work.

The painting ornamentations in the mosque's interior are in Baroque style and probably some influence of Empire style. The interior paintings are the most important and significant elements of this mosque. Beyond the frames of the windows decorated with bluish exuberant floral motives, the painting decorations are focused between the cubical mass and the dome's base, including the squinches. The main design composition of this part is framed in the form of a series of arcades associated with curtains. In part above the circular window, the decorative arch is more articulated in a typical Baroque form, as there is painted a model of an Ottoman mosque which appears like Suleymaniye mosque.

The colours used in the painting in the interior also suggest an influence of "Empire" style, which is also seen in the 19th-century Ottoman architecture in Istanbul. There are depicted coup of fruits, cypress trees, or other figures in the other arched frames, which can be interpreted with Islamic Sufi metaphors. Floral motives are found everywhere in the interior and are stylized in the form of wreath, blossom, or bouquets. Prior to recent restoration, there appears to have been a light yellowish atmosphere in the interior; however, the walls are treated in white. The dome is decorated by eight (8) stylized elliptical motives. The windows found in the drum part at the base of the dome are heavily decorated with floral motives. The floral motives in sky bluish tones also embellish the arches of last prayer hall entrance façade. Floral bouquets are put along the arch frame and in the triangular surfaces in between arches are decorated with a bunch of flowers within emblem like other wreaths.

The glass decorations are applied in the second row and on drum windows repeatedly.

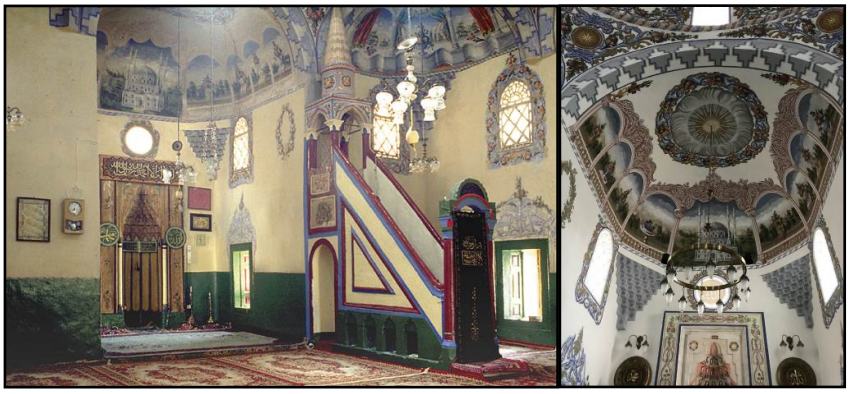


Figure 18. Interior of the Emin Pasha Mosque before restoration (left) retrieved from https://www.coe.int/t/dg4/expos/expoprizren/en/epic1029.htm and (right) mihrab [© Hadis Toçilla]

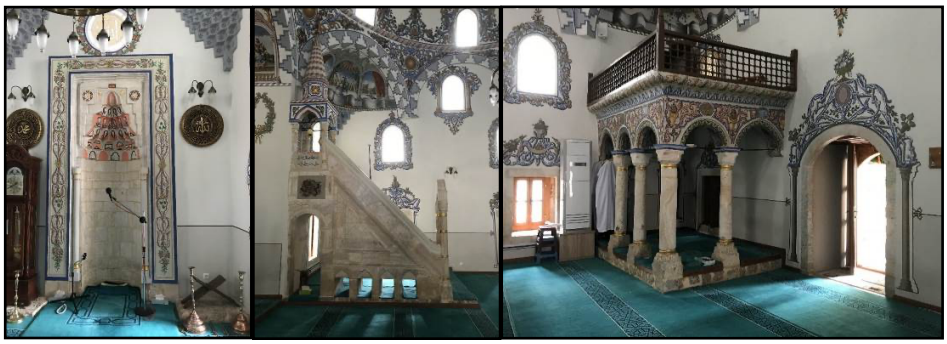


Figure 19. Interior view of the mosque after the restoration in 2016 [© Hadis Toçilla]



Figure 20. Painting decorations in the dome and squinches at its base (retrieved from https://sharriregion.com/culture/ in 01.12.2020) and (right) last prayer hall after the TIKA restoration [© Hadis Toçilla]

Katip Sinan Beg Mosque

The Katip Sinan Mosque (locally named also Levishah) is located in Adem Jashari Street. The name Levishah is believed to come from a wise elder who had lived in this street [7]. The mosque does not have any inscription about when it was built. The inscription above the entrance gate describes the restoration, which is made in 1893-1894. According to Vermica [10], this mosque was built before 1591.

Architectural Features of Katip Sinan Beg Mosque

The mosque has a rectangular shape, with 10.80 m x10.85 m dimensions. It consists of the prayer hall and the last prayer hall, which was added later. The praying hall has a square plan covered by a dome supported by squinches. Built in rubble stone, it is plastered in the exterior. The lateral façades of the mosque consist of three rows of pointed arched windows. The mosque entrance is from the last prayer hall, which possesses a slight tilt edge due to the street limitation. The entrance façade is different from the other façades. The minaret is found at the right of the last prayer hall, and its entrance is provided from outside the mosque.

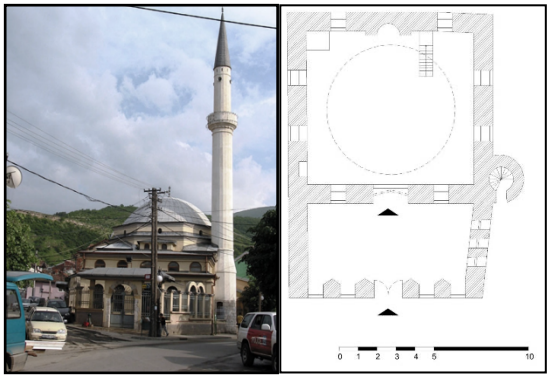


Figure 21. Image of Katip Sinan Beg Mosque (Left-©Hadis Toçilla) and its plan scheme (right-redrawn from Hadis Toçilla referred to Vırmiça, 1996)

Ornamental Features of Katip Sinan Beg Mosque

The stone decorations are found in the mihrap. The mihrab is completely painted with yellow colour, and it appears to be renovated recently. It is framed in a rectangle with muqarnas decoration in it. To the right of mihrab it stands the minbar painted in yellowish colour.
The interior of the mosque is plastered and overwhelmed by coloured painting decorations. Stylized flowers are all over the dome, arches and framing the windows that they look like they are painted after the restoration and completely new. In the centre of the dome, there is calligraphic art painted. Rather than belonging to the local tradition, the features of this painting decorations appear to be new and reflect apparently features that are recently in Istanbul's mosques. As such, they do not reflect authentic artistical values.

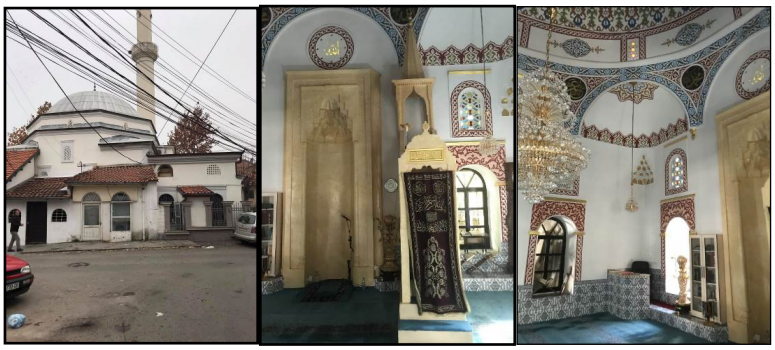


Figure 22. Lateral façade, Mihrab, minbar and squinch within the mosque [© Hadis Toçilla]

There are two-row windows with iron lattice and decorated with stained glass in the lower part of the walls. The inside windows are taken in a rectangle with two columns painted in red and golden gild colour. Blue, green, red, and yellow are the dominant colours used in the windows' stained glass.



Figure 23. Interior and women's mahfel in Katip Sinan Beg's mosque [©Hadis Toçilla]

CONCLUSION

This research analysed the architectural, ornamental, and structural transitional features used in mosques with domes built during the Ottoman Empire period in Prizren. All the domed mosques were built by eminent Ottoman administrators. Some of the administrators who commissioned the mosques were of local origin (like Sinan Pasha). In contrast, the others (like Kukli Beg, Gazi Mehmet Pasha, etc.) were appointed to Prizren and were originated from Anatolia. The domed mosques built during the Ottoman period in Prizren represent a similar building scale and quality like the mosques built in other Kosovo "vilayet" centres like Pristina or Skopje. However, compared to those in other vilayets which Albanian used to live during the Ottoman Empire (Shkodra, Manastir (Bitola) and Ioannina) due to the different political context, they appear to be in much better conditions [14, 15].

Generally, the mosque buildings consist of prayer and the last prayer hall and minaret. The plan schemes of the prayer halls dominantly are square. The plan of Emin Pasha and Sinan Pasha Mosques have a rectangular mihrab niche part which other mosques do not have. The plan schemes of the prayer halls of these two mosques consist of the longitudinal extended rectangular protrusion.

The woman's gallery is founded in all the mosques. Emin Pasha mosque's woman's gallery is accessed by separate stair as the minaret stairs are used. All the woman's galleries are decorated with wooden balustrades.

The last prayer halls of the mosques are different from each other. Due to their bad conditions or destruction, most of them have been recently renovated in reconstruction, except Gazi Mehmet Pasha's last prayer hall, which is still today without any significant intervention.

The research shows that the mosques selected as case studies are one chambered covered by a single dome. Overall, the transition from the cubical mass to the dome is realised via squinches, except the mosques of Kukli Beg and Maksut Pasha, in which interestingly there are used pendentives. Since the usage

of pendentives in Ottoman buildings in general is observed in big scale mosques, the encounter of this phenomenon in these two mosques needs to be subject of further study.

The mosques' lateral facades dominantly are featured by pointed arched windows organized in two and three rows and arcade in the last prayer halls. The qibla façades, due to their specific nature, generally sightly change to lateral ones, except Emin Pasha and Sinan Pasha mosques featured by a rectangular mihrab protrusion. The entrance façades vary in composition due to the differing design of the last prayer hall which is either in a form of colonnaded stone porch or wooden porch.

The stone decoration is mainly observed in the entrance gate, mihrab, minbar, and women mahfil's columns. The other common element was that most mosques in the mihrab area use colonnettes on the flanking sides.

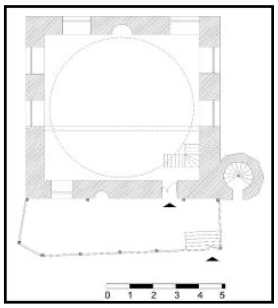
The original painting and calligraphic art decorations are well preserved in Sinan Pasha, Emin Pasha, and Gazi Mehmet Pasha mosques. The painting features between Sinan Pasha and Emin Pasha are the use the sun figure, Ottoman ideal mosques, and landscape paintings in the mihrab niche ceiling. The usage of similar painting decorations within these mosques suggests that these works' authorship should be the same painter masters. Thus, it also can be said that the Sinan Pasha mosque painting decorations should have been realized in the same period as the Emin Pasha mosque in the 19th century, as they reflect Ottoman Baroque features and partly Empire style features, which are dominant also in the imperial capital Istanbul.

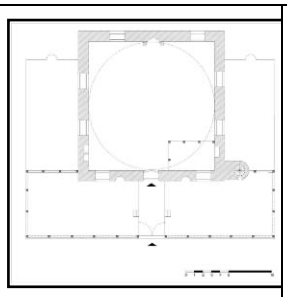
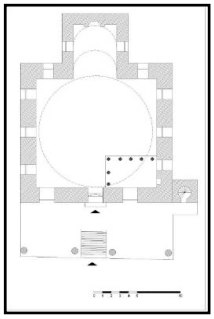
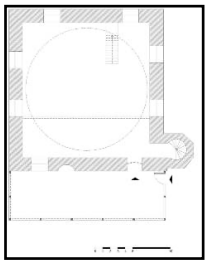
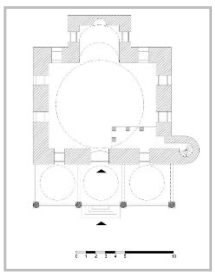
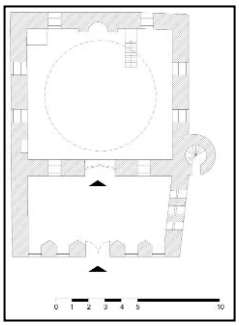
Although not in abundance, the stained-glass decorations are used in the mosques included in the study. Mainly these decorations were seen in upper row windows and were featured by geometrical and partly curvilinear motives.

The wooden decorations which deserve special attention are seen in the last prayer hall column capitals of the Gazi Mehmed Pasha Mosque.

At last, it can be said that the recent renovations work conducted by the Turkish Agency (TIKA) technically are well implemented. However, in certain rare cases, there are observed tendencies to use ornamental features typical to the Istanbul (centre), thus annihilating the local Islamic ornamental features. Further studies in the field can be focussed on analysing the ornamental features on an artistic level.

Table 1. Architectural, structural transition, and ornamental features of domed mosques built in the Ottoman period in Prizren.

Building Name Construction Date	Architectural Features		Structural Transition Features	Ornamental Features			
	Plan Scheme	Façade		Stone	Painting	Wooden	Glass
Kukli Beg Mosque Date: 1531 (16th century 1st half)		-2 rows of windows -Rubble Stone Exterior	Pendentive	-	-	Mahfil Minbar	-
Gazi Mehmet Pasha Mosque		-3 rows of windows	Squinch	Mihrab	Elliptical Medallions	Mahfil	Partly at 2nd and 3rd-row

Date: 1563-74 (16th century-2nd half)		-Neatly cut grey Stone Exterior -Laterally expanded last prayer hall		Minbar Entrance gate arch	Floral Motives Crown effects	Last Prayer Hall	windows as no colour is applied
Sinan Pasha Mosque Date: 1614 (17th century-1st half)		-4 rows of windows -Neatly cut limestone exterior -Protruded qibla façade	Squinch	Mihrab Minbar Mahfel	Imaginary Ottoman mosques Landscapes Floral Motives	mahfil	2nd, 3rd and 4th-row windows
Maksud Pasha Mosque Date: 1644 (mid-17th century)		-2 rows of windows -Plastered Exterior	Pendentive	Mihrab Mahfel's quasi-Corinthian capitals	Floral Motives	mahfil	2nd-row windows
Emin Pasha Mosque Date: 1831 (19th century-1st half)		-3 rows of windows -plastered exterior and entrance façade painted -protruded qibla façade	Squinch	Mihrab Minbar Mahfel	Imaginary Ottoman mosques Landscapes Floral Motives	mahfil	2nd row and drum windows
Katip Sinan Beg Mosque Date: 1893-94 (end of 19th century)		-3 rows of windows -Plastered Exterior	Squinch		Recently added Floral motives	mahfil	2nd and 3rd-row windows

REFERENCES

[1] Jones, H.L. (1924) Strabo: Books 1-7. 15-17 in English translation, at LacusCurtius

[2] Thayer, B. (1940) Procopius- 4th Book "On Buildings". available https://penelope.uchicago.edu/Thayer/E/Roman/Texts/Procopius/Buildings/4B*.html

[3] McGeer, E & Nesbitt J. (2019) Byzantium in the Time of Troubles: The Continuation of the Chronicle of John Skylitzes (1057-1079) Brill, Leiden. 149

[4] Fine, V. A. J. (1994) The Late Medieval Balkans: Critical Survey from the Late Twelfth Century to the Ottoman Conquest. University of Michigan Press.

[5] Osi, M. (2001) Prizreni qytet i lashtë muze me thesar të pasur kulturor, 27-29, Prizren

[6] Miftari, F. (2008) Xhamitë e Shumta të Prizrenit Dëshmi Konkrete të Qytetërimit Islam available at: http://drejtesia.blogspot.com/2008/02/xhamit-e-shumta-t-prizrenit-dshmi.html

[7] Suroy Recepoğlu, A. (2009) Prizren'de Türk Dönemi Kültür Mirasi, Prizren, Kosovo

[8] İbrahimgil, M. Z. & Konuk, N. (2006) Kosova'da Osmanlı Mimari Eserleri I-II, Türk Tarih Kurumu, Ankara

[9] Ayverdi, E. H. (2000) Avrupa'da Osmanlı mimârî eserleri. 2: Yugoslavya: (3. kitap), İstanbul Fetih Cemiyeti, İstanbul

[10] Vırmiça, R. (1996) Prizren Camileri, 19-31, Prizren, Kosovo

[11] Ibrahimi, N. (2000) Sofi Sinan Pasha dhe xhamia e tij në Prizren,

[12] Clayer N, (2013) Kosova: The Building Process of a Territory from the Nineteenth to the Twenty-First Century.

[13] Süreyya, M. (1996) Siccil-i Osmani II Book, Ed. Nuri Akbayar, Trans. by Seyit Ali Kahraman, Tarih Vakfı Yurt Yayınları, 547, Istanbul

[14] Manahasa, E. & Kolay Aktuğ, I. (2015) Observations on the Existing Ottoman Mosques in Albania. Al Z ITU Journal of the Faculty of Architecture, 12 (2), 69-81

[15] Manahasa, E. (2005) The Existing Mosques Built During Ottoman Empire Period in Albania, Master Thesis, Istanbul Technical University, Istanbul

[16] https://gazetainfokus.com/20-foto-te-rralla-me-ngjyra-te-prizrenit-dhe-prishtines/

[17] https://www.kultplus.com/tag/xhamia-sinan-pashes

[18] https://www.coe.int/t/dg4/expos/expoprizren/en/epic1029.htm_i0

[19] https://sharriregion.com/culture/

Spatial and Morphological Potentials of Urban Informality: "Shallvaret" Block

Odeta Manahasa[1], Bjorni Gjuzi[2], Olster Ukperaj[2]

[1] *Department of Architecture, EPOKA University, Albania*
[2] *Department of Architecture, Polytechnic University of Tirana, Albania*

ABSTRACT

To understand urban developments in a city or region, the informality has been and is always an issue of outlining. Albania has more than two decades that is dealing with informality. It is now part of the city, and the citizens cannot escape from this reality. Different stakeholders like real estate developers, urban planners or residents are engaged in exploring the meaning of this informality for the city's future. In this context, by pointing in one of the buildings that are considered a landmark for years in the city, this research aims to study the informality of "Shallvaret Block" by analyzing spatial and morphological interventions in these apartment blocks. The informality impacts on the visual layout the existing housing blocks and consequently on the urban morphology. This paper examines the potential of informality by using the methods of "zoning" and "overlapping" comparing the existing situation with the originally designed building. The findings reveal that interventions in the façade are proportional, and the users are aware of the architectural qualities. Further, the program interventions are unidimensional, often focusing on physical improvements. While these leads to improved housing conditions on one side, it opens discussion on the informality's spatial potentials.

Keywords: Urban informality, intervention, spatial quality, Tirana

INTRODUCTION

The central and Eastern European cities that were under the socialist rule, due to the étatist policies and practices of space production had a deep impact on the cities. The transition from communism to democracy in some of them was lived normally, but in some others, it happened very drastically. Even though there are some differences in the transition period from country to country, what can be said is that the "post-socialist transition may have a significant number of unique characteristics" depending on the country and "undoubtedly no one can support the fact of being the only transition of the moment" [1] and the time being.

These tremendous, spectacular, and chaotic changes that the post-socialist transition period draw researchers' interest, especially on the spatial change and urban reconstruction.

A more detailed observation to the post-socialist cities, would provide a better understanding of the changes that took place in the transition period. For example, Ludek Syroka witnessed post-socialist Prague for the "re-emergence of some pre-socialist pattern, transformation in some areas from socialist times and creation of new post-socialist landscapes." This city's characteristic post-socialist development is claimed to be "accelerated concentration of advanced functions through commercialization and densification of the city centre" [2]. A change in functions such as changing the residences' function to offices, developing multipurpose business centers, and facilities that serve to tourism like restaurants and hotels are subject characterizing the post-socialist cities. Residential spaces of post-socialist Sofia have been subject to some

consequences of the transition period, such as “the loss of compact urban form inherited from the socialism and the growth of a lower–density suburban periphery.” [3]. Sofia was experiencing the suburbanization process, which was a process that emerged in other countries too. Budapest, for example, experienced the same transformations as a consequence of commercialization [4]. The built environment of the newly formed capitalist cities (as in Sofia example) “organization of open spaces” is needed for the simple fact that the transformation period brought a “loss of public green spaces and their fragmentation into explicitly private enclosures” [3]. Tirana city is another example of this phenomenon. It is still suffering from the loss of public green areas. During the transition period, open spaces, boulevards, city parks, green spaces, and public plazas were occupied by kiosks of all sorts, losing their original character due to the lack of control and construction policy of the public sector [5].

For example, Aliaj, Lulo, and Myftiu [6] state generally the urban post-socialist Tirana transformations as follows:

What characterizes Tirana in the post-socialist time is an extreme degradation in the quality of urban environments and the occupation of lands by illegal developments, a process that is accompanied by serious harms to the environment.

Thus, this period is associated with the population’s indignation towards the public property and the “public” in general, manifested in various forms of occupation and intervention. This resulted in a conflict between the formal and informal.

This research focuses on the unexplored potentials of urban informality. It does not deal with the negative aspects that these huge interventions exhibit, but in a morphological and visual analysis between the originally designed housing block and informal interventions added in the post-socialist period.

By taking the case study of the “Shallvaret” block in Tirana, we aim to discuss the morphological changes and the informal additions' architectural potentials.

URBAN INFORMALITY

“Urban Informality” describes the intervention done to the existing buildings or erection of new objects in violation of urban government rules. It is mainly an action present in cases where the city cannot withstand the influx of people who chose to live in that city. The line between "formal" and "informal" is determined by the legislation of the country. It depends on the problems with which each country is faced. The United Nations has tried to set international standards, but their application in many cases has been ignored, making these standards not applicable in different contexts.

According to Dovey & King [7], these interventions are socially, spatially, and economically integrated with the urban context. Most developing cities are unsuitable without these informal interventions. In contrast, the general desire that exists in removing these interventions is related to the problems it causes in urban identity and image. Kucina [8] defines them as unpredicted changes of architectural and urban organisms. This situation makes the context spontaneous and continuously evolving, never being static and clearly defined. This always-evolving condition has a positive and negative aspect. The descriptions of informal urban interventions usually focus on the negative aspects because they change the urban relations unpredictably. On the other hand, it is important to study their spatial and morphological potentials to look for positive elements.

Huchzermeyer [9] insists that informal settlements should be studies in continuous practice since these structures are perpetually changing. Thus, understanding and learning from this process would give feedback on the need to understand urban informality.

According to Hakim [10], forms of urban informality appear and adapt to time through change-generating processes. These generative processes address the actions that need to be taken for changes depending on the needs rather than the results visualized in some drawings, detailed plans. Whereas for

Lapping [11], informal interventions can be considered "modern vernacular environments" as long as they are simultaneously spontaneous and continuously increasing.

Based on the context and needs, informal urban interventions are very flexible. The perplexing situation between formal and informal architecture forms in such city areas creates a sustainable interconnection process making the communities living in these buildings more sensitive to the problems they all have as a community.

FORMS OF INFORMALITY

Studied from morphological, spatial, and visual aspects, informality is categorized into different typologies.

Pojani [12] suggests several categories for informality based on a conceptual framework, including settlements, dwellings, inhabitants, and processes. Also, for each of the four primary categories, other specific divisions are proposed. Accordingly, settlements are split corresponding to location and size, distribution and density, land use, public spaces, image, and identity.

But dwellings are studied in relation to materials and technology, likewise, in relation to architecture and symbolism. The connection with architecture and symbolism is seen in these informal constructions' tendency to take traditional architecture or visible, influential buildings.

According to Dovey [7], there are three main processes of how these interventions take place:

The first is called "settling," construction in a not well-defined territory (unoccupied land). The other form is called "inserting," constructions in uninhabited or abandoned areas of the city. The third includes "attaching" informal constructions in the formal structures of the city.

In almost all countries, the forms of informality are similar. Though they are similar in categorizing interventions, they also show different characteristics from one country to another, making the issue more complex. Economy, social components, historical and legal conditions are among influential elements that affect the interventions.

INFORMALITY IN “SHALLVARET” BLOCK IN TIRANA

The division that UNECE [13] does upon the typologies of informality suits also for Albania. It differs from the socio-economic and historical context. In Albania, in addition to other specifics, based on the construction materials used, urban informality is better than in many countries on which the studies are based.

In the case of “Shallvaret,” the interventions are introduced in the "attachments" (attaching and adherence) as informal interventions on an existing formal structure and where the existing structure serves as an armature for the overlapping informal construction. Elements of the "behind the scenes" also appear with most informal interventions taking place behind the “Shallvaret” block's formal structures.

Based on the division made by UNECE [13], informal interventions in the “Shallvaret” Block belong to the first category where residents have had permits on the original property and have made unauthorized changes to the same property. The changes are structural, which includes the lateral extension of apartments or the addition of floors. These changes directly affect the morphology and spatial configuration of the block.

Regarding the division made by Pojani, [12] who includes the connection of the architecture of these interventions with the symbolic one, the urban informality of the “Shallvaret” is seen as a tendency to respect some of the existing ratios of the formal building on the visible side of the facade from the street. The symbolism of the inside of the block reflects the whole architecture in our country during these years, creating a "model" in itself in which elements of the vernacular architecture of the country can be found.

Table 1: Types of Informal Settlements in the Western Balkans [13]

Legal title to land and property – unauthorized adaptations	a) Minor adaptations to existing structures without building permission (e.g., closing balconies, the addition of one to two rooms in an existing attic). Turning existing premises into living areas (e.g., turning garages into living areas, turning basements into living areas); turning former common spaces (e.g., laundry rooms) into living areas, without a building permit. b) Structural changes to existing buildings, e.g., lateral extensions of apartments in multi-family buildings and floors on existing multi-family buildings.
Legal title to land - unauthorized construction	a) Construction on own land following the existing plans and regulations but without an actual permit (in cases where a detailed master plan exists). b) Construction without a permit on own land over existing plans. c) Construction with a permit on own land, but unauthorized changes to approved plans, building more than officially approved permit (e.g., building a multi-story building instead of the approved family home).
Legal land title – unauthorized subdivisions and unauthorized construction.	a) Legal title to land, but the illegal change of land use (e.g., agricultural land used for residential buildings) involving illegal subdivisions of land (and the selling thereof to a different owner). Housing was built without building permission. b) Public land or rural land subdivided and given (or sold at market price) by the local authority itself to im/migrants coming to the city, but without a change in the plans. c) Construction without a permit on land with unclear title to land (e.g., that resulted from an unclarified or unresolved process of land restitution).
No legal title to land – unauthorized construction	a) Illegal land occupation, housing without planning/building permission, not integrated into the broader urban system (relatively good living standards). b) Building in protected zones: national parks, natural reserves, coastal areas, protection areas (e.g., highways, industrial, flood barriers, etc.).
No legal title to land – squatter settlements	a) Unauthorized homes built by im/migrants settling in unserviced areas. b) Unauthorized shacks made in un-serviced areas by the low- or no-income population (e.g., Roma population).

SHALLVAREVE" BLOCK

The "Shallvaret" block is located near the city center at the intersection of "Ibrahim Rugova" street with "Gjergj Fishta" Boulevard (fig. 1). Built-in 1952, it is an example of apartment blocks built during the communist period. The regime itself put architecture and urban planning at the center of propaganda to restructure a socialist society.

Unlike other blocks identified by a rational architecture, in "Shallvaret," a neoclassical architecture was used in the facade's treatment. This was also influenced by the impact of bilateral relations with the Soviet Union. The block was designed with four floors, a constructive beam-column system, and constructive brick material. Further, it respects the urban network's outline defined by the existing roads (figure 1).

Through the morphological and spatial analysis of the building block in its initial designed condition with the changes that have taken place over the years, it can be better understood the occupants' needs and their input in the spatial organization of the dwellings. Through this temporal and layered arrangement, the spatial and morphological analysis of the block becomes valuable, making it possible to understand this urban informality's real potentials and the relations created with the existing formal building.



Figure 1. Location of the “Shallvaret” block [14]

Facade Analysis

Informality in the “Shllvaret” Block appears mainly as structure overlap over the existing building. It uses the latter as a base for developing the additions in the building (figure 4). To note the changes over the years and to find the quantity of these changes, we overlapped the current condition of the façade with the original, initial façade.

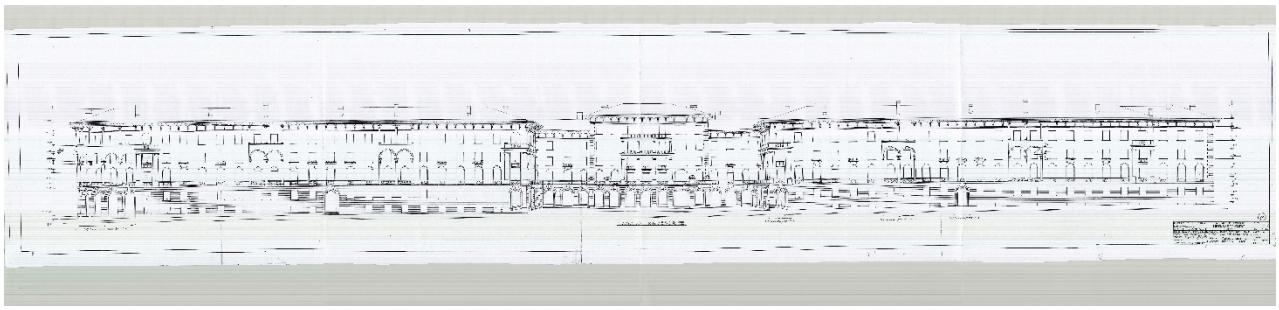


Figure 2. Main facade as designed initially [15]

Visually, the additions to the original building are in 1 to 3 ratios (Figure 3). Unlike similar interventions done in other countries, the informal portion has the general tendency to continue and preserve the openings and by treating so the façade compatible with the original design.



Figure 3. Interventions in the facade

Elements used in the original project disappeared with the years, but the materials are the same as initially constructed. By applying a simple solid-void analysis, it is possible to identify all the façade configurations. In the upper images, (Figure 3) the additions on the original building are marked with red color and voids (openings) with black.

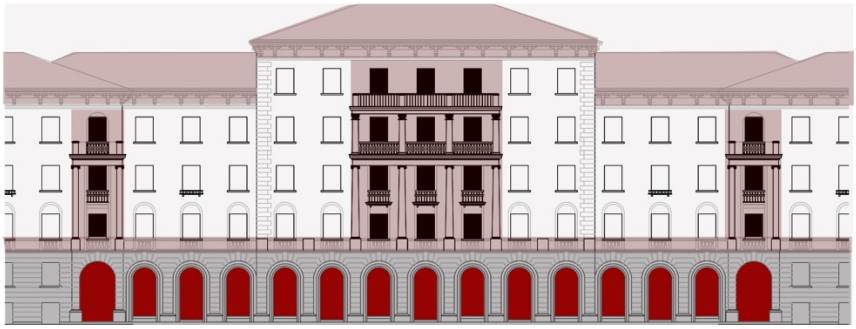


Figure 4. The depiction of the façade elements drawn on the images retrieved from AQN (courtesy of the authors)

The uppermost floor has undergone a noticeable change, together with the roof. This floor does not respect the existing morphology of the building façade, but it does more obey the utility.

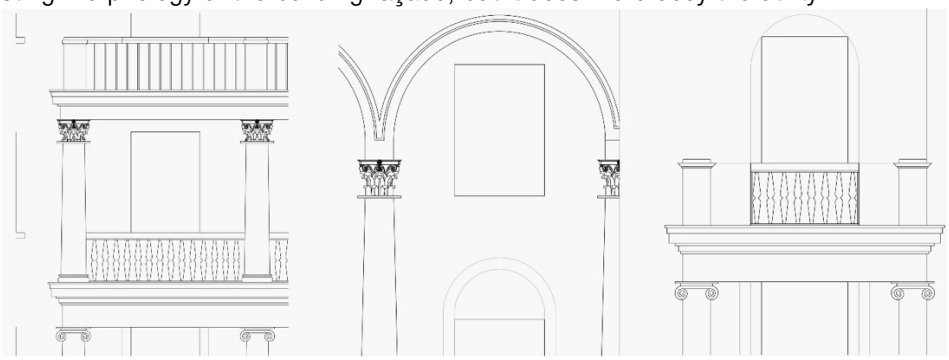


Figure 5. Ornamentation drawings, retrieved from AQN (courtesy of the authors)

The initial design was a 4-floor building with 3.3 m on each floor. Further, it also has one floor partially underground. The façade style is neo-classical with both Ionic and Corinthian elements. It also has a longitudinal ornamental badge that frames the cover (figure 4&5).

The roof of the building is made of a wooden structure. For the openings, a module with a width of 120 cm and a height of 170 cm was used. This module is repeated with a simple rhythm along the entire facade. The module of the openings changes only on the ground floor, where the height is 160 cm.

The entrance axis is central and at the same time serves as an axis of symmetry for the organization of the whole block. The entrance is evident as it is treated in the form of an arch. The central block, in contrast to the two side blocks, takes place on five floors.

The treatment of the façade on the ground floor also has a different composition. It is designed with successive arches that serve as passages to connect the blocks. The two floors in the façade are treated by rustication, provided by red brick usage [16].

The same cannot be said for the inner façade of the block. It is unrefined, and the decorating elements in the façade and the openings are missing. This kind of treatment of the façade only from the main streets is a typical approach of the communist regime to the residential architecture. The inner facade has remained the same in terms of refinement, even today (figure 6). However, it is the façade where the interventions

are more visible because they occur in the verticality and in the massive volumetric outputs that disrupt the facade's initial morphology.



Figure 6. Informal additions in the inner facade. (courtesy of the authors)

On the main façade, the informality is more controlled. The view from the two main roads tries to preserve the formal language which undergoes obvious changes only in verticality. While from the inside of the block, more significant interventions are out of context and do not respect the original design.



Figure 7. Program division and informal interventions. (courtesy of the authors)

Meanwhile, when we analyze the building's programmatic aspects, it is easily understood that the whole block is used for housing except the floors highlighted in blue that function as service areas. The service is concentrated on the lower floors. Still, the tendency is to continue to the other floors. There are already some interventions that the apartments have turned into businesses.

Figure 7 can be identified morphological changes and the ratio of intervention that is done through the years. The red color is the new addition, with the grey color missing from the initial design (the roof is missing now).

By fully defining the morphology of current informal interventions, it is possible to determine the tendency with which the shape of the block may change in the future. It helps to assist in a sustainable solution to similar problems.

Plan and Section Analysis

From the study of images obtained by the National Albanian archive, it is noticed that the plan of the block is organized according to a linear scheme, with a corridor in the center that serves to access the apartments on both sides. Thirteen sets of stairs access the block itself. A set of stairs serves four residential units. It moves from the quota - 1.65 to the quota ± 0.00 respectively with 11 step legs with dimensions 15x32 cm. In the main, centered object, the entrance is made through the existing colonnade.

The apartments are oriented only in one direction, depending on the block. They have a linear organization scheme with two rooms, one living room + kitchen, and one sanitary unit. The total area is 62 m2. The section shows the height of the floors, which is 3.3m, and the staircase. There is evidence of the ratio of the informal-formal construction (Image 9).

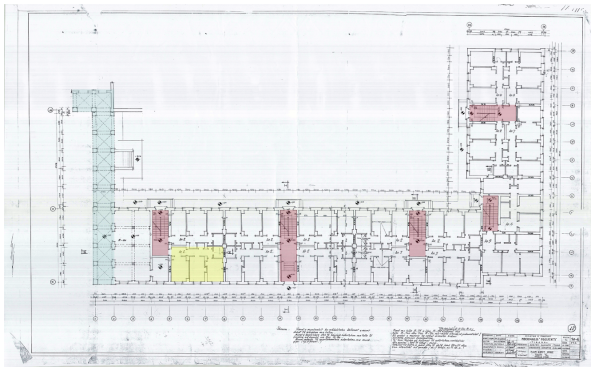


Figure 8. Plan from the Northern part, [15]

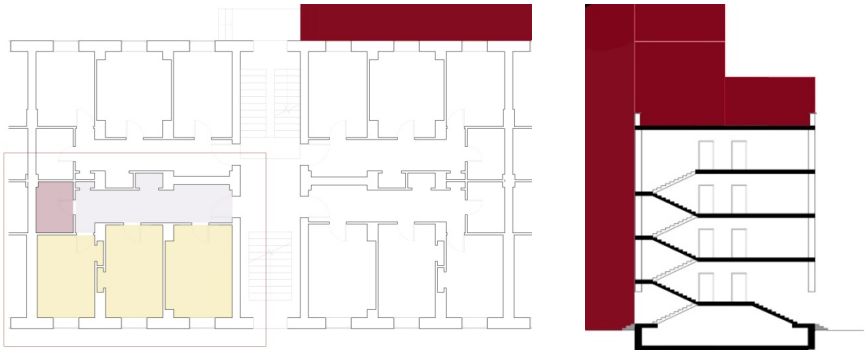


Figure 9. Plan of one apartment unit (on the left); Section (on the right). (Courtesy of the authors)

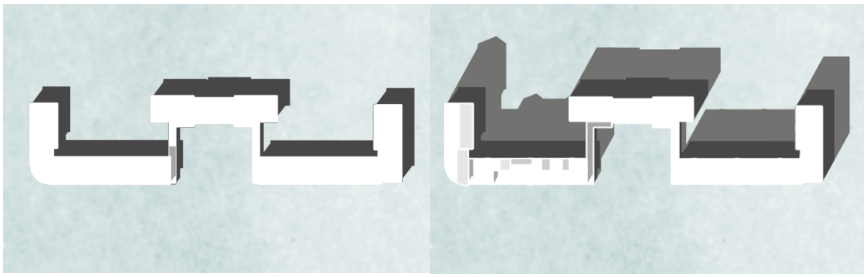


Figure 10. Shadow in the original block (on the left) and Shadow on the existing block (on the right)

Through the shade-shadow analysis made by the overlap of cast shadows, the impact has had additions concerning the existing building. The increase in the number of floors has also affected the urban scale's reconfiguration by changing the block's visual, morphological, and spatial perception—subsequent planning of the surrounding constructions (Image 10).

CONCLUSION

The study's purpose was to focus on the morphological and spatial analysis of urban informality in Albania and understand the characteristics of these interventions to be more predictable in future planning.

Compared with the other urban informalities, in the "Shallvaret" block, it is understood that urban informality appears in different forms and dimensions. Some informal processes and interventions shape not only the latest additions but also the initial design. The exiting line between formal and informal becomes more incomprehensible over time.

Further, through these spontaneous interventions, the whole block's spatial reconfiguration makes the urban situation never static, but always flexible and changing.

Informal interventions have caused a chain effect on the whole block because these informal additions have visually and spatially affected all the following constructions.

Based on the morphological and spatial analysis performed, it is identified that the interventions occur mostly from the inside of the block and show characteristics like the designed initially building.

Informal interventions that have taken place on the main façade, the one visible from the two main roads, are more reserved. The tendency is seen to preserve the existing form and spatial relations.

The changes that are part of the building's functional program are also reflected in the visual façade. This condition transforms the morphological ratios due to the need to adopt the spaces' new functions. In the future, the spaces' program may change again, so we advise that the façade configuration be done by thinking about the proportions and the other design elements of the existing building. Additionally, possible new interventions should be developed to collaborate with the dwellers to cope with such inclusive environments strategically. The "Shallvaret" example offers essential lessons about the capacity the buildings and the users have in terms of adaptability.

REFERENCES

[1] Enyedi, G. (1998). Social Change Transformation of Cities and Urban Reconstructing in Central Europe. Budapest: Akademiai Kiado.

[2] S´ykora, L. (1999). Changes in the internal spatial structure of post-communist Prague. GeoJournal, 78-89.

[3] Hirt, S., and Kovachev, A., in Sasha Tsenkova and Zorica Nedovic- Budic (eds.). (2006). The Urban Mosaic of Post-Socialist Europe, Germany: Physica- Verlag.

[4] Tosics, I., in Sasha Tsenkova and Zorica Nedovic- Budic (eds.). (2006). The Urban Mosaic of Post-Socialist, Germany: Physica- Verlag.

[5] Durmishi, O. (2008). Competing urban Visions for the capital of Albania: International projects for Tirana city centre. Ankara: METU. Master Thesis.

[6] Aliaj, B., Lulo, K., & Myftiu, G. (2003). Tirana the Challenge of Urban Development. Slovenia: Gorenjskitisk.

[7] Dovey, K. & King, R. (2011). Built Environment (1978-) Vol. 37, No. 1, Informal Urbanism

[8] Kucina, I. (2018). Architectures of Informality, DIASeries, Dessau.

[9] Huchzemeyer M. (2008) Settlement Informality. The Importance of Understanding Change, formality and land and the informal economy. Paper presented at the Groupement de Recherche sur Development International (GRDI) Workshop on Informality, Centre for Urban and Built Environment Studies (CUBES), 3-4 July 2008. University of the Witwatersrand, Witwatersrand.

[10] Hakim, B., (2008), Mediterranean urban and building codes: origins, content, impact, and lessons. Urban Des Int 13, 21–40. https://doi.org/10.1057/udi.2008.4

[11] Lapping, M. B.,(1973), Vernacular Environments: The Squatter Settlements. The Journal of Popular Culture 7, 2:446-450

[12] Pojani, D. (2019), "The self-built city: theorizing urban design of informal settlements", Archnet-IJAR, Vol. 13 No. 2, pp. 294- 313 https://doi.org/10.1108/ARCH-11-2018-0004
[13] UNECE (2012). Informal settlements in countries with economies in transition in the UNECE Region.(available online: https://unece.org/fileadmin/DAM/hlm/documents/Publications/Literature_Review_on_Informal_Settlements.pdf)
[14] https://geoportal.asig.gov.al/map/?auto=true
[15] Arkivi Qendror i Ndertimit (AQN)
[16] Manahasa, E. (2017). Place attachment as a tool in examining place identity: A multilayered evaluation through housing in Tirana. PhD dissertation, Istanbul Technical University.

Paper Folding Bio-Kinetic Façade: Application of Bat Wing Inspired Façade Design to the Building of Mediterranean University in Tirana, Albania

Anna Yunitsyna[1], Lorena Lika

[1]*Department of Architecture, EPOKA University, Albania*

ABSTRACT

Design of kinetic and adaptable building shells is one of the recent trends in sustainable construction. In this research the main topic is the application of the foldable and nature inspired kinetic facade onto the contemporary building in Tirana and evaluation of its advantages in terms of the light control and reduction of the cooling loads of the building. The paper starts from the overview of a history of kinetic architecture. Paper folding is selected as a technique and biomimicry is an approach which helps to design the repetitive units of the facade. The chosen form of nature and the source for the design inspiration is a bat wing. The anatomy of the wing has been adapted for the project and the mathematical calculation was done in order to get the facade module, which is flexible, foldable and which can be closed and opened using the movement which is similar to the bad wing. For the application it is selected the building which currently has the glass facade with very minor shading system. The adaptable kinetic facade is constructed using the series of modules. The calculation of solar radiation was done for the several models with different percentage of openness. The new building skin allows to have the better quality of light and regulates loss and gain of heat without wasting energy.

Keywords*: Biomimicry, kinetic facade, origami technique, responsive facade, sustainable design*

INTRODUCTION

One of the biggest problems today is the greenhouse effect. There have been a lot of discussions on about what is needed to do to minimize this effect and its damage. One of the responses of these challenge in architecture is the interactive skin of the building that allow to get the best light with the least amount of heat in building and changes immediately according to the climate conditions. Paper folding is often used as a kind of intermediate tool even to create foldable/changing houses. The paper folding art is with an eastern origin, and it has in its focus the mimicry of nature. The word kinetic, as a term, has not been used in architecture until 1961, and even than it didn't have a really deep understanding among architects on the possibilities it offered and kinetic architecture wasn't yet neither understood as such, nor named adequately. The meaning of the word kinetic is relating to or resulting from motion. At the beginning of the twentieth century kinetic architecture started to be explored and people became aware of the term as an architectural term while before the term "kinetic" was widely used in physics [1]. Firstly, movable structures and covers in buildings were used mostly for safety and privacy reasons. Kinetic architecture was seen as a mobility of a structure or part of the structure providing the adaptability with the surroundings. Kinetic architecture was present in the middle-ages in the form of drawbridges, which were used for connecting the castle to the ground for protection purposes [2]. Today besides the drawbridges it is known a large variety of kinetic bridges such as bascule and rolling bascule bridge, folding, curling, retractable, submersible, tilt, swing, transporter and vertical lift bridge. Until the eighteenth and nineteenth centuries,

there weren't many uses of kinetics in architecture besides doors, window or roofs. Nowadays kinetic architecture is getting more and more advanced, starting from kinetic doors, facades and roofs to whole moving houses. During the last decade there has been a growing interest in dynamic architecture, starting from louvers to the whole facades. The aim of a lot of this research is to present a changeable architecture that responds to the different needs throughout the day and time using the adaptable skins and materials. The variety of the kinetic facades can be classified according to the technique which is used to achieve the changeability.

USE OF BIOMIMICRY IN ORIGAMI DESIGN

The first term used was biomimetics, which was used to describe the transfer of ideas from biology to technology, then it became biomimicry. Another term used was bionics which than became associated more with robotics [3]. From ancient times people tried to imitate and learn from nature. Leonardo Da Vinci made the first drawings of a flying object (plane) imitating the wings of a bird. But, while they imitated nature and biology, it was still only the form finding. A new type of mimicking the nature started when people became to study how the natural processes work and why. Instead of mimicking the form, they started to study and mimic the process.

Origami is the ancient Japanese art of paper – folding. It comes from the word "ori" – folding and the word "kami" – paper. Today, origami comes in many shapes and forms, and also different techniques. Origami artist today use both ancient techniques, either with strategic cuts or just strategic paper creasing, and employ them in their own way. Many techniques exist today that have derived from the original ones [4]. Among all the origami techniques can be noted the Pureland origami, where there are used only the simple mountain/valley folds, and each of these folds must have a straightforward location. The second type of origami which is suitable for the kinetic architecture is origami tessellation which uses the repeated pattern of folds [5]. The most used pattern and origami technique in architecture is the Miura - Ori pattern (or the Miura fold). This fold has the ability to be folded in a very compact area, the thickness of which is only restricted by the thickness of the material. This pattern can be said to be rigid origami. It can be folded from a single sheet of paper and it is the same repeated form folding in itself. When closed it takes a rigid form, depending on the kind of pattern deployed, while when unfolded is a straight sheet of paper. The folds act as hinges. Usually the new folding patterns are designed based on the traditional ones, such as Miura-Ori or Waterbomb pattern. It is really complicated to create the new flat-foldable pattern. Each of the new designs should be manually folded in order to confirm the foldability [6].

The folding can also be found in living organisms, such as insects and birds wings, it is also typical for the leaves and petals. The folding patterns from nature can be transferred into the artificial structures. The main principles of the construction are its deployability, which means that the patterns should be constructed from a single flat sheet of paper, planarity of the faces and edges and transformation of joints and folds into hinges [7]. The pattern of folds can be organized in such a way that it provides the opening and closing of the material sheet only in one direction [8]. Folding method can be used in order to compose modular and responsive building skin (Figure 1). As an example, the modular conical plywood panels with the hygroscopically responsive elements were applied in ''HygroSkin - Meteosensitive Pavilion''. The panels are able to close or open depending on the weather conditions and the indoor microclimate, such as indoor and outdoor air temperature, humidity or solar radiation [9]. The idea of the self-regulating facade was applied also in the prototype pavilion, which was constructed using the ''Breazing Skins'' technology. What this skin essentially does is the adjustment of the flow of substances (heat, light, moisture) from inside and/to outside, regulating the amount of transfer of these substances to create a better quality of ambient. The skin is made up of a system of pneumatic muscles that regulate the amount of heat, light and visibility in the structure [10]. The skin of One Ocean pavilion is built by thin sheets of glass fibre reinforced polymers,

which allows for changing in different animated patterns. The skin is much like fish fins and make it possible for the structure to breathe through it by opening and closing in a kind of rippling effect [11]. Kinetic facade constructed by the honeycomb panels was applied in Al Bahar Towers in Aby-Dhabi. The hexagonal modules are constructed by six panels which can fold and unfold thus blocking or allowing the light and exchange of heat according to the needs of the indoor environment [12]. The foldable rectangular aluminium panels are applied in Kiefer Technic Showroom. Its façade is a curtain wall system that opens and closes in itself to regulate the amount of light that passes in accordance to the needs of the indoor environment. At the same time the facade can be controlled manually by the residents [13]. In the building of Syddansk University perforated triangular panels are applied as light control system. The panels are able to rotate using the vertical side as the rotation edge [14].

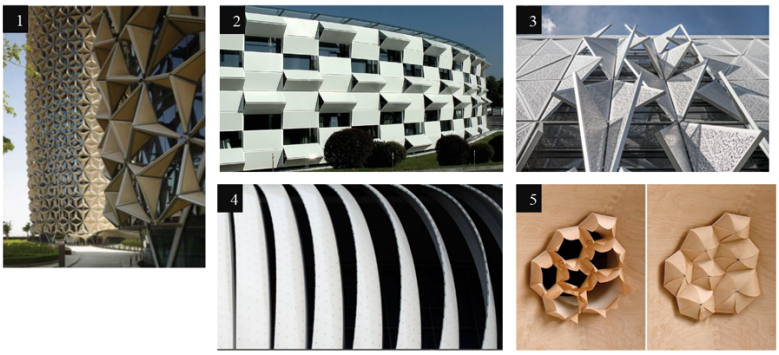


Figure 1. Kinetic facades of Al Bahar Towers (1), Kiefer Technic Showroom (2), Syddansk University (3), One Ocean Pavillion (4) and HygroSkin Pavilion (5).

ORIGAMI FAÇADE DEVELOPMENT

Case Study Selection

The selected site is the Mediterranean University building (Figure 2) which is located at Bulevard Gjergj Fishta in Tirana near the UET (European University of Tirana) and Tirana University. The reason for choosing this building as a study object is because of its façade made entirely of glass. Since it is a university, it is crucial that the light quality is good and there is no glare. Also, the heating and cooling loads are high, and it is necessary to use control the microclimate inside of the building in order to provide the comfortable environment. Currently there is a system of horizontal louvres covering the building facade, but it seems to be not efficient since there are used the curtains to control the light inside the classrooms. The building has a shape of narrow and tall cuboid. This increases the problem of the quality of the light, since there is lighter than needed for the shallow rooms. The building has six floors in total and it the highest object around. One site of the site is completely free of building and facing the street.

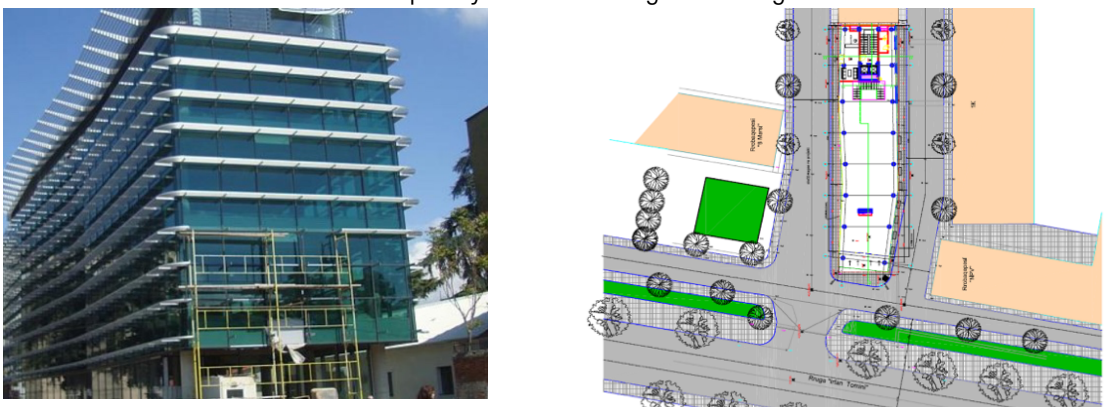


Figure 2. Glass facade of the Mediterranean University (left) and ground floor plan (right).

Development of the Origami-Folding Modular Façade Panel

The foldable module of the kinetic facade needs to satisfy three main conditions: to be open, semi-open, and closed, in order to allow different amounts of sunlight to enter the building. It also needs to be fluid and have a smooth movement which helps to pass easily through these three main fazes. One of the first things that comes to mind when thinking about fluid motions, are the wings of birds. Their wings also have these three main states; while the birds start to take flight (semi-open), while flying (open) and while resting (closed). While in flight the wing can bend and move in different angles, thus creating other intermediate phases. The bat wings have some specific details in anatomy and in movement that are much more useful in this study.

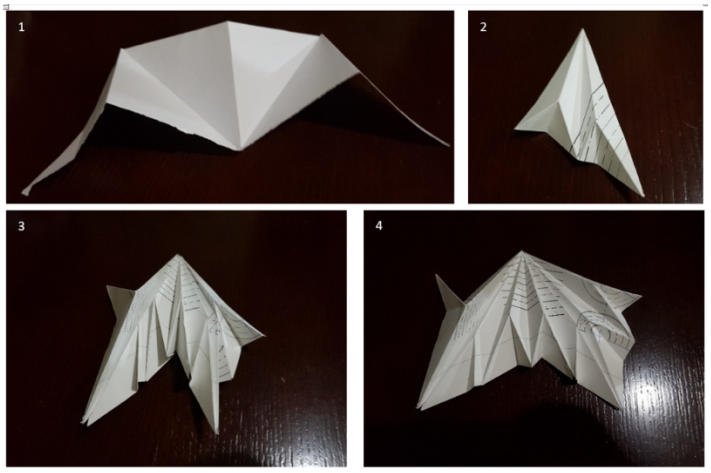


Figure 3. Partial paper models of the origami bat wing (1, 2) and full model in semi-opened (4) and semi-closed (3) positions.

The structure of the bat wing is a unique system which is combined by the bones which can be deformed during the flight. The bones are connected by over 20 flexible joints and covered by the anisotropic wing membrane [15]. Their unique anatomy makes the bat wings very flexible, and able to change position in different degrees in but a short moment of time. Despite the delicate look, the membrane is very strong. Different from bird that have stiff wing bone structure, in bats, the bone structure allows divided in three main bones, allows for a very swift and smooth movement. Another important thing is that their wings can flatten into a maximum opening, which none of the other winged beings can do, and provide the unique capacity of powered flight [16].

The origami/paper-folding art is used as a tool for translating the form of the bat wing to be used as a façade module. The study started from the origami tessellation of the part of the wing, while trying to understand the math and the rules behind the tessellation. To better understand the movements and the mechanics of it, models of the different techniques of the bat origami were needed. Below, there are pictures of the first conceptual models (Figure 3), while trying different styles, from the simplest moves to the more complicated bat wing.

Different from the majority of the origami shapes that start with a square page, the bat wing origami starts with a rectangle. Then, the folds are created according to the bat wing bone anatomy, but in a more conceptual and rigid form, turning the long three-part joint fingers in just a simple crease. The membrane of the bat wing is the paper between this simple folds. To give more flexibility to the membrane part (the paper) for closing and opening, there are needed other creases to make that part of the paper bendable and able to close. The most simplified action is to create a fold down the middle of this part of the paper (the membrane part) for giving the paper the ability to close, and three other creases between the membranes main crease and the creases related to the bone structure. This type of translation of form from nature to origami tessellation allows for a flexible and dynamic form and movement of the form. But this is

the understanding a in a conceptual and mechanical (working with hands) level, while it is needed a more mathematical approach to figure out the final form so the folds will fit with each other when closing and finding the right angle to make this type of closure correct.

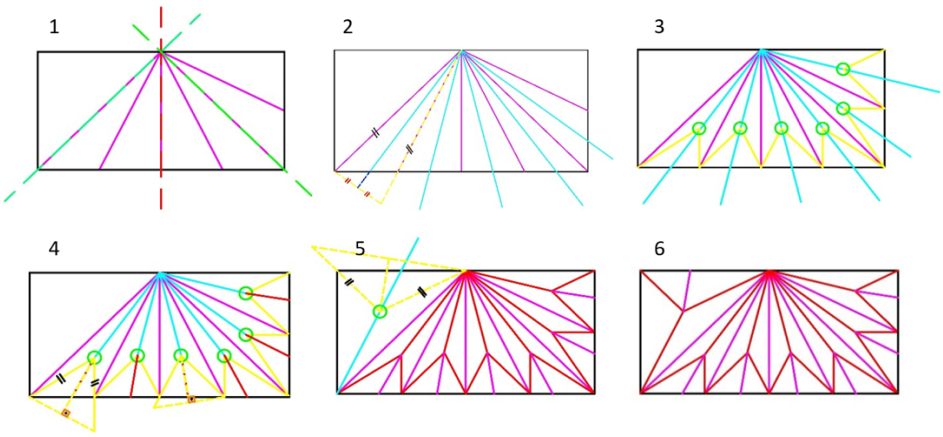


Figure 4. Stages of development of the geometry of facade module.

Origami is built on very precise mathematical calculations. One of the simplest and probably most used (most important) mathematical rules in origami are related to symmetry. Symmetrical rules make it possible for all the pieces of the paper to fit in with each other, and to fall in on itself creating a fluid movement of closing completely, and then opening to a flat surface. At the Figure 4 is explained step by step the logic behind finding the form of the façade module and the mathematics involved in it.

The first step is a rectangle piece of paper, with dimensions of the sides in ½ relation with each other. The rectangle is divided in the middle (red interrupted line), creating two equal squares. These squares get divided once more by a diagonal (green interrupted line) through each of them that pass through the upper middle point of the rectangle and intersect with the middle line. The point where they join mimics the elbow joint of the bat wing. There are four equal triangles and for the next step there will be used three of them (2), which are divided in the middle, with a line that starts from the angle where the other lines are intersecting, to the middle of the length facing that angle. The left triangle is left untouched for now because it serves as the part of the forelimb which allows for the opening and closing of the bat wing. The magenta lines make up the part of the bone structure of the bat wing. For the part of the membrane, it is needed another division in order to provide the flexibility of it. These lines (the cyan lines) are taken from the point where all the lines intersect, to the middle of the lengths in front of each angle, of the big isosceles triangle formed by extending the shortest line to make it the same as the longest line. To further deal with the flexibility of the membrane, there are needed these little triangles (3) which will fold on itself and give dynamic to the module. To build the triangles, first it is needed to find the middle point of the bigger triangles. This middle point is found by constructing a line from each angle, to the lengths in front of the angles. The intersecting point (marked with a green circle) is connected to the edges of the bigger triangles. So, find the valley (line of folding down-ward in origami), it is needed to find the right angle for the bigger triangles to fold in a symmetrical way (4). The symmetrical line of an isosceles triangle (a triangle with two equal lengths) is the line from the smallest angle of said triangle to the base, who form a right angle. So, to find the right angle the smallest length of the small triangle is elongated and made equal to the length in the front. Then it is created another triangle, which is an isosceles triangle (the yellow triangle), and the right angle which identifies the folding line. The bigger left triangle that was left untouched until now (5), mimics the forearm of the bat. It is needed to find the middle point and the folding line, following the same mathematical rules as above. The difference in this part is the direction of the fold, which allows and creates the fluid and dynamic movement, and also the ability to completely close the module. In the final image (6) it is shown the finished tessellation of the origami bat wing for the facade module. The red lines are the mountains –

the lines that are going up, while with magenta are the valleys- the lines that are going to go down during the folding process.

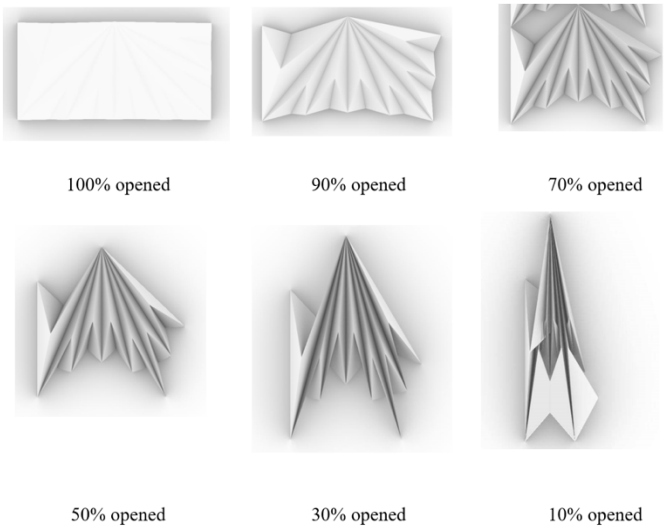


Figure 5. Simulation of opening and closing of the facade module.

The pattern of mountains and valleys was tested using the Grasshopper and Kangaroo live-physics engine. Kangaroo allows to model the objects and to simulate the behavior on them [17]. In this case it was tested the Grasshopper definition for origami folding. It is generated the set of 3d models with different level of openness/closeness, ranging from completely open to 10% closed (Figure 5).

Analysis of the Solar Radiation

The analysis of the solar radiation received by the building was performed for the variations of the origami facade with different level of openness and also for the initial glass facade of the building. The simulation was done using the Ladybug for Grasshopper, which is a tool for the wide range of environmental studies [18]. The advantage of this tool is that all the process of the design, development, model making and model evaluation is performed via Grasshopper, which means that there is no need to use any external software or to export the models of simulations (Figure 6). The solar radiation analysis was performed for Summer and Winter Solstices and Spring and Fall Equinoxes using the weather data from Albania.

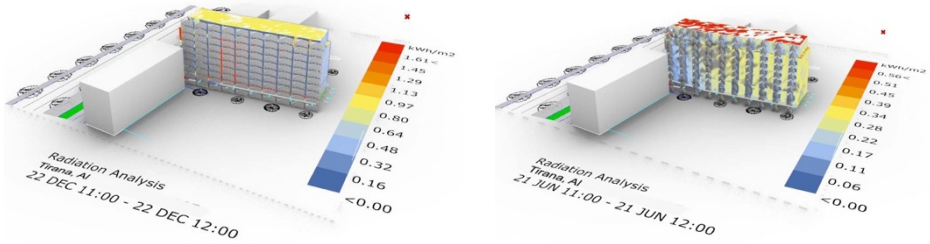
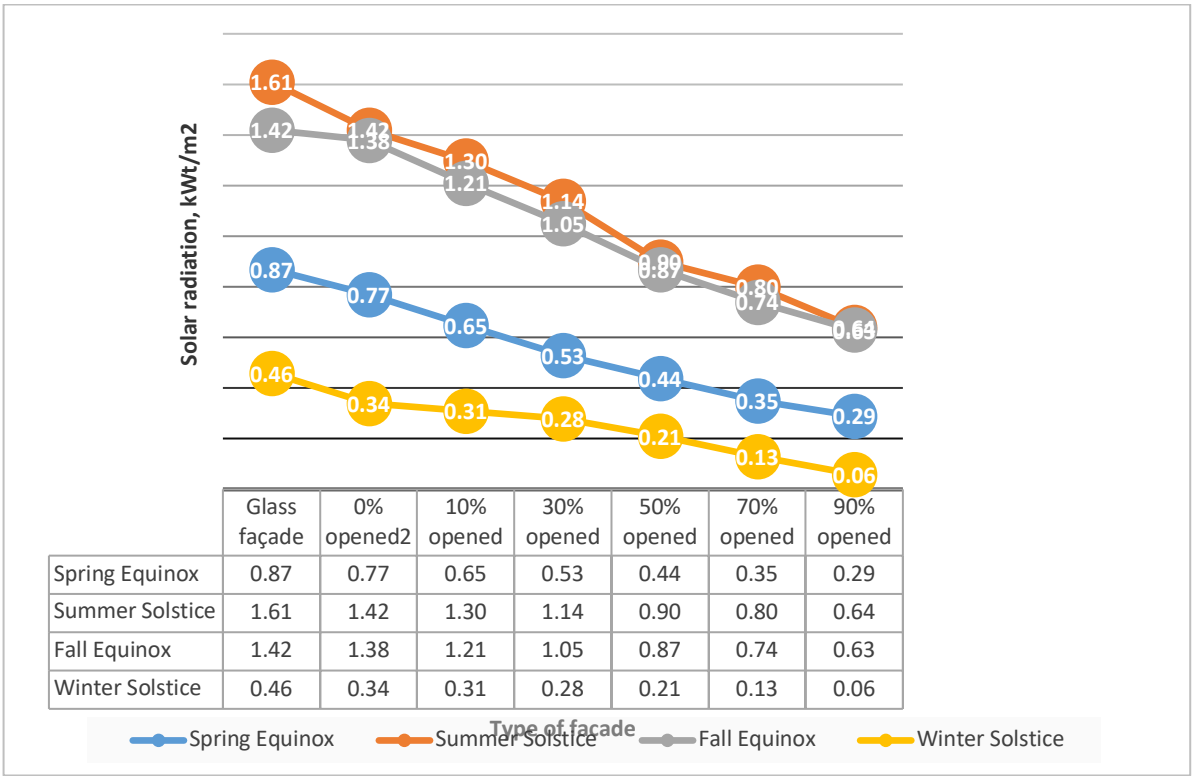


Figure 6. Solar radiation analysis of the building with different types of origami facades using Ladybug.

The results of the solar radiation analysis for the initial building and the origami folding facade in the six different stages of opening are shown in the Table 1.

From the simulation it can be noticed that the highest amount of solar radiation is received by the facade with no shading system and the amount of solar radiation is decreasing as far as the shading system is getting into the unfold position. During the Summer Solstice the building receives the highest amount of solar radiation, meanwhile the Fall Equinox has significantly higher numbers in comparison to the Spring Equinox.

Table 1. Solar radiation data



	Glass façade	0% opened2	10% opened	30% opened	50% opened	70% opened	90% opened
Spring Equinox	0.87	0.77	0.65	0.53	0.44	0.35	0.29
Summer Solstice	1.61	1.42	1.30	1.14	0.90	0.80	0.64
Fall Equinox	1.42	1.38	1.21	1.05	0.87	0.74	0.63
Winter Solstice	0.46	0.34	0.31	0.28	0.21	0.13	0.06

CONCLUSION

The research was developed in order to design a building façade that can respond to the environment, mainly the sun heat and sunlight, in a way that the building would have the best light possible and the lowest solar radiation, which would control the indoor temperature and reduce the cooling energy loads. Origami (or paper-folding art) and bio mimicry are used as methods to design the modular facade component. Origami helps to translate the chosen form from nature to module by discovering a specific tessellation that makes the project work. Biomimicry is the concept which makes possible the study of the chosen form in nature and finding of the way and the idea of the mechanics for the project. It defines how the module is going to move, what are its main positions and how much flexibility is the project going to have. The chosen form of nature to study was a bat wing, because of its flexibility in movement and the way it can take different positions during flight. The project module needed careful mathematical calculations to be built in a way that allows the parts of the module to be folded correctly, with no extra edges. The finished product has three main positions; open, semi-open, and closed; and other sub-positions (ways of opening) in different degrees.

The module is very flexible, and the opening is done by light and heat sensors attached to it to make the façade react to the environment. These sensors are what puts the façade in motion in different degrees of opening, according to the ideal light and heat that a building should have as by European standards. Application of the module can be done in different variations providing the various facade patterns (Figure 7).

The modules are connected to a metal mesh frame that envelopes the building. The modules are fixed in only one side and the other side is free to be able to move and have the needed flexibility. The selected membrane material is a carbon fiber sheets or fiber glass since it demonstrates the desired bendable ability, strength and flexibility.

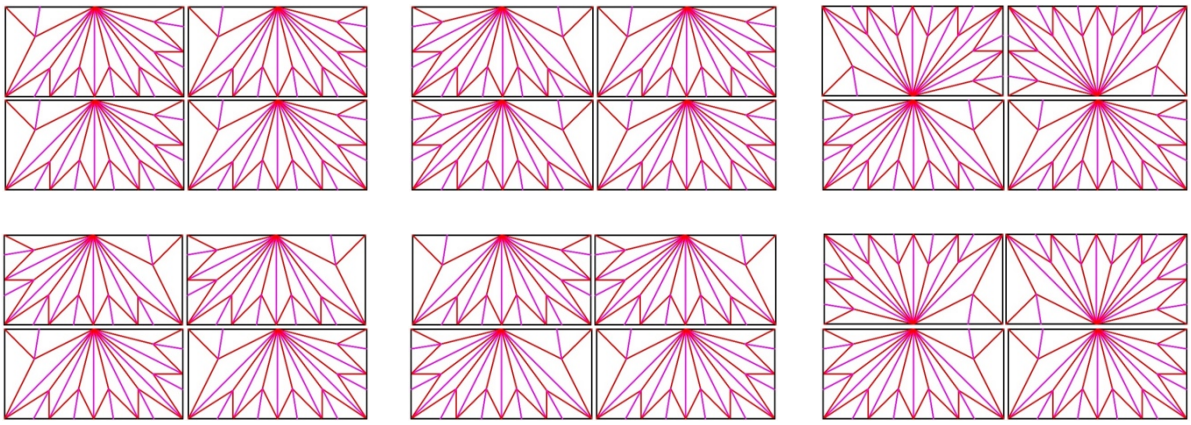


Figure 7. Façade pattern with different ccombinations of origami modules.

REFERENCES

[1] Fouad, S. M. A. E.-H. (2012) Design Methodology: Kinetic Architecture, Alexandria University, Alexandria, Egypt.

[2] Houston, K. (2015) Towards a Kinetic Architectural History: James Ackerman and the Moving Viewer, 1942-1961, SECAC Review, 622-632.

[3] Aziz, M. S. and El Sherif, A. Y. (2015) Biomimicry as an approach for bio-inspired structure with the aid of computation," AEJ - Alexandria Engineering Journal, 707-714.

[4] Richman-Abdou, K. (2017) Origami: How the Ancient Art of Paper Folding Evolved Over Time and Continues to Inspire," 20 November 2017. [Online]. Available: https://mymodernmet.com/history-of-origami-definition/.

[5] Robinson, N. (2004) The Origami Bible, Northlight, USA.

[6] Mitani, J. (2011) A Method for Designing Crease Patternsfor Flat-Foldable Origami withNumerical Optimization, Journal for Geometry and Graphics, 195-201.

[7] Baerlecken, D. Swarts, M. Gentry R. and Wonoto, N. (2012) Form finding and evaluation of origami structures, in 30th International Conference on Education and research in Computer Aided Architectural Design in Europe, Prague, Czech Republic.

[8] Filipov, E. T. Tachi T. and Paulino, G. H. (2015) Origami tubes assembled into stiff, yet reconfigurable structures and metamaterials," Proceedings of the National Academy of Sciences, 12321-12326.

[9] Reichert, S. Menges A.and Correa, D. (2015) Meteorosensitive architecture: Biomimetic building skins based on materially embedded and hygroscopically enabled responsiveness, Computer-Aided Design, 50-69.

[10] Becker T. and Huffer, S. (2015) Breazing Skins Technilogy, [Online]. Available: https://www.breathingskins.com/.

[11] Knippers, J. Scheible, F. Oppe M. and Jungjohann, H. (2012) Bio-inspired Kinetic GFRP-façade for the Thematic Pavilion of the EXPO 2012 in Yeosu, in IASS-APCS Symposium 2012: From Spatial Structures to Space Structures, Seoul, South Corea.

[12] Shadi, A. (2017) Evaluation of adaptive facades: The case study of Al Bahr Towers in the UAE, QScience Connect.

[13] Premier, A. and Dehò, A. (2012) Shading and darkening closures using mobile panels, Tenda International, 18-22.

[14] ElGhazi Y. S. and Mahmoud, A. H. (2016) Origami Explorations: A Generative Parametric Technique For kinetic cellular façade to optimize Daylight Performance, in SHAPE, FORM AND GEOMETRY | Application, Oulu, Finland.

[15] Schwartz, S. M. Iriarte-Diaz, J. Riskin, D. Tian, X. Song, A. and Breuer, K. (2012) Wing Structure and the Aerodynamic Basis of Flight in Bats, in 45th AAIA Aerospace Sciences Meeting and Exhibit, Reno, USA

[16] Schwartz, S. M. Iriarte-Diaz, J. Riskin, D. and Breuer, K. S. (2012) A bird? A plane? No, it's a bat: An introduction to the biomechanics of bat flight, in Evolutionary History of Bats: Fossils, Molecules and Morphology, Chapter 9, Cambridge University Press.

[17] Piker, D. (2013) Kangaroo: Form Finding with Computational Physics, Architectural Design.

[18] Roudsari M. S. and Pak, M. (2013) Ladybug: A parametric environmental plugin for grasshopper to help designers create an environmentally-conscious design, in 13th Conference of International Building Performance Simulation Association, Chambery, France.

Experiencing the Research-Based Learning: Case of the graduate course "Landscape Perspectives in Disaster Risk Management and Fire Safety"

Artan Hysa

Faculty of Architecture and Engineering, EPOKA University, Albania

ABSTRACT

This paper presents the research-based learning (RBL) experience in the graduate course "Arch451-Landscape Perspectives in Disaster Risk Management and Fire Safety". This experience relied on the principle "the student as researcher and the lecturer as moderator of the process". The research teams consisted of four students. The study areas were the metropolitan regions of Skopje, Novi Sad, Banja Luka, and Tirana. First, the students were introduced into the main theme of wildfire risk within wildland urban interface (WUI). The group discussions during class meetings were helpful in shortlisting the set of criteria implicated either with wildfire ignition or spreading regimes. Similarly, the weighted impact factor of each criteria was defined as average values of all participants via analytic hierarchy process (AHP) pairwise comparison method. Each group performed their GIS-based analysis for their specific study area following the same method that have been developed in the first part of the process. At the final stage, each team delivered a technical report and a poster presenting their research work and original findings about their specific study area. As a result, the RBL process enabled the students to experience a participatory research process that contributes to the enhancement of their teamwork and research skills.

***Keywords**: project-oriented research, wildfire, GIS, teamwork, EPOKA University*

INTRODUCTION

The quest for new methods in teaching that goes beyond knowledge gaining is not new. Many scholars have denounced the conventional instructions failure to prepare professionals that thinks critically [1]. The origin of the discussion is based on the student-engagement theory pioneered by [2-6]. Pike and Kuh (2005) [7] have performed an evaluation of the 30-year experience of student-centered university transformations in USA. They have defined six student-engagement types based on the profile of the higher education institution. For example, the collaborative one, promotes teamwork where peers depend on and support each other. Yet, they are continuously supervised by the faculty in a campus environment supported by technological means. This is the closest definition of the student-engagement type as experienced in Arch451 course.

This paper presents the research-based learning (RBL) experience in the graduate course "Arch451-Landscape Perspectives in Disaster Risk Management and Fire Safety". Arch451 is among the elective courses within the professional master (PM) program in Disaster Risk Management & Fire Safety (DRM&FS) in the department of Civil Engineering at EPOKA University. The PM program opened within the goals of K-Force Erasmus+ capacity building project. Twelve graduate students have been enrolled to the course and have actively participated in the RBL process during spring semester 2018-2019.

The landscape dimensions of fire safety theme expands towards the topic of wildfires. Despite the benefits that natural wildfires provides to regenerative cycles of many biomes on earth [8], if not controlled they can be severe threat to many endemic species and humans. The wildland urban interface (WUI) are

the hybrid territories where the natural lands and the human settlements meet, thus the forest fire risk is the highest.

The wildfire regimes are expected to change drastically in the upcoming decades affected by the consequences of global warming and climate change. The fire season in the southern Europe is projected to be stretched in time (within a year) and the wildfire events more frequent [9]. Thus, the assessment of wildfire risk within the WUI zones of western Balkans as Mediterranean regions is crucial. This was the main motivation of the RBL process design within Arch451 course.

DESIGNING THE RESEARCH-BASED LEARNING PROCESS

First, the students are presented the draft work-schedule of the semester and are invited to discuss on the draft for further improvement. Figure 1 presents the main work-packages to be performed during the semester and their time-lapse within the process. First, the students were introduced basics of wildfire phenomena in the landscape to have a general understanding on the main theme. Then, the group was organized into three groups of four members each. The students were free to select their peers. In principle they were free to make the task distribution within the group. The role of the lecturer was a mediator when needed.

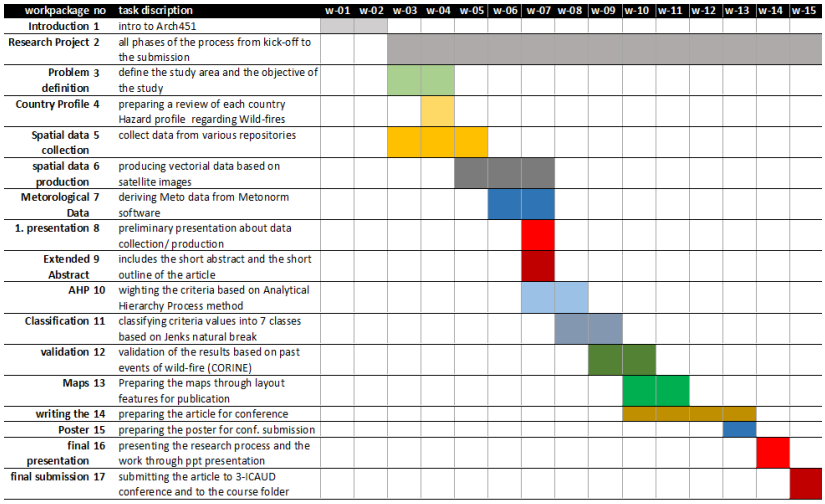


Figure 1. The work-schedule of the semester defining the main stages of the work.

First the participants have been presented a series of introductory short lectures on natural hazards and specifically the wildfires. A further focus of the presentations targeted the forest fire risk within the wildland urban interface (WUI). Apart from the general information on the problem definition, the students are introduced into the importance of GIS technology in dealing with the wildfire issue. There are a variety of forest fire risk assessment methodologies that are prepared using GIS technologies. This introduction aimed to provide a general understanding of the problem and the available tools for developing solving means.

The first task of the groups was the preparation of the national forest fire hazard profile of the specific study area. They have been delivered an assignment sheet as shown in Figure 2. The groups were asked to scan the available literature including published articles, reports or statistical data from reliable resources. These sources helped in collecting information about the fire regimes, major wildfire events, major causes and effects of fire events in the specific context. This task was meant to contribute to the contextual understanding of wildfire in the specific study area. At the same time, the results of this task could be very easily adapted as the “Study Area” part of the final report.

Epoka University	Department of Architecture
spring 2019	**Arch 451 _ Landscape Perspectives in DRM & FS**
instructor	Artan Hysa
Exercise 01	**National Forest fire Hazard Profile of your Study Area**
brief	The aim of this exercise is to become familiar with the available sources on inventory data and monitoring programs on DRM & FS with an emphasis on wildfire and forest fire hazard. You are expected to search on online national and international platforms dedicated to hazard monitoring and prevention. As a group, you are assigned to prepare the Disaster Risk profile of the Country of your study area, based on the Hazard type; wildfire and Forest Fires. This is the preliminary work of your group research project, specifically about the part explaining the study area. The report may include, the fire regimes, major events, major causes and effects of wildfire events in your case country as well as the focal study area.
Format	Report, about 5 pages (including the images), a title page including all info about the course and the task.
Evaluation	5 % of the term-grade
Due time	Monday [25.03.2019] @ 23:00 o'clock

Figure 2. The task of "Country profile" about wildfire phenomena.

Study Area

The metropolitan areas of Tirana, Skopje, Novi Sad, and Banja Luka are selected as the study area of process. All study areas are the urban centers where the K-force project partners are located, and their Urban Atlas data of 2012 were available. Tirana is selected as the demonstrative case and is handled by the instructor of the course during the explanatory tutorials. While other study areas are distributed one per group as shown in Table 1. The final selection of the specific study area was based on negotiations among groups.

Figure 3 shows the geographical location of all four metropolitan areas within the western Balkans region. Tirana and Skopje represent the capital metropolitan areas of Albania and Northern Macedonia. While Novi Sad and Banja Luka consist of secondary metropolitan areas of Serbia and Bosnia & Herzegovina. Yet, the available Urban Atlas (UA) data define similar in size metropolitan boundaries for the selected cities. The average total surface area of the selected study areas is about 2000km^2.

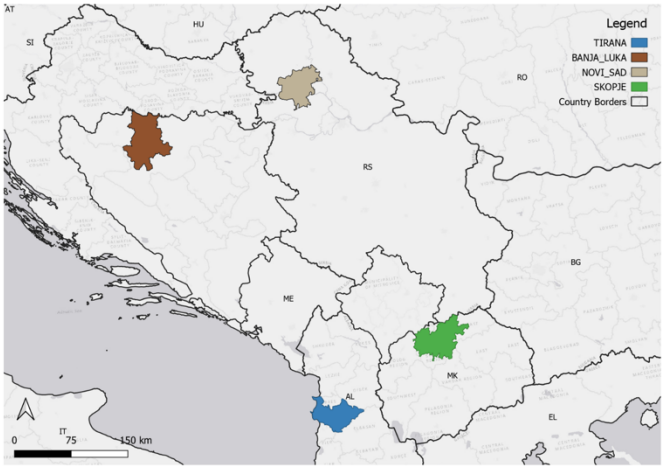


Figure 3. The study area including the metropolitan areas of Banja Luka, Novi Sad, Skopje, and Tirana.

The RBL process relied on a workflow consisting four stages and 7 steps as shown in Figure 4 following the model developed by [10]. The second stage is the inventory one, where all quantitative measurements are collected for each criterion. This stage followed the multi-criteria inventory method developed by [11].

		Goal	Method
Preliminary work	**1**	Identification of the Study Area within the protected Area	Identification of the vegetated natural surfaces from CORINE Land Cover data
	2	Data conversion	Shapefile to Raster (pixel size 250 m)
	3	Generate the point cloud of pixel centroids	Raster to Points operation
Inventory	**4**	Multi-criteria inventory	Calculating the values of all criteria for each point
Analyses	**5**	Data clustering	Clustering the values of each criteria into 7 classes according to Jenks natural breaks reclassification method via ArcGIS
Indexing	**6**	Calculating WIPI	Raster calculator (equation 1)
	7	Calculating WSCI	Raster calculator (equation 2)

Figure 4. The stages of the research.

Each stage is expanded into detailed procedures of GIS-based processes relevant to the goals of the specific stage. For example, Figure 5 presents detailed steps of the stage 1 of the workflow aiming data collection. Besides the demonstrative sessions explaining consecutive steps of the analysis, the students have been delivered detailed workflow steps as shown in Figure 5.

Epoka University | Department of Architecture
spring 2019 | Arch 451 _ Landscape Perspectives in DRM & FS
instructor | Artan Hysa

Checklist of Process Steps

		Task	Method	Time
1		**DATA GATHERING / PRODUCTION**		**>100 min**
	A	**Urban Atlas (UA)**	**Vector data**	**45 min**
	a	Download UA of study area	Copernicus website	~70mb
	b	Familiarize with/ visualize UA data	Free activity	10 min
	c	Extract Forest surfaces from UA	Attribute table/ Select by expression	5 min
	d	Create Reference Points (100m)	Vector/ research tools/ regular points	5 min
	e	Extract points within the forested areas	Vector/ research tools/ Select by location	5 min
	f	Extract Urban Centers (S1)	Attribute table/ Select by expression	5 min
	g	Extract Settlements (S2)	Attribute table/ Select by expression	5 min
	h	Extract Agricultural Land surfaces (S5)	Attribute table/ Select by expression	5 min
	i	Extract Water surfaces (P4)	Attribute table/ Select by expression	5 min
	B	**Digital Elevation Model (DEM)**	**Raster data**	**25 min**
	a	Download the DEM tile	Copernicus website	~5 gb
	b	Extract the DEM of study area	Raster/ Extraction/ mask layer by UA boundary	5 min
	c	Familiarize with/ visualize DEM	Free activity / generate Contour lines	5 min
	d	Generate SLOPE values from DEM (P1)	Raster/ Analysis/ Slope	5 min
	e	Generate ASPECT values from DEM (P2)	Raster/ Analysis/ Aspect	5 min
	f	Generate ALTITUDE values from DEM (P3)		5 min
	C	**Environmental Data**	**Raster data**	**20 min**
	a	Download data	Surfobs/ climate/ Copernicus	~5 gb each
	b	Maximum temperature tile	Surfobs/ climate/ Copernicus	5 min
	c	Precipitation tile	Surfobs/ climate/ Copernicus	5 min
	d	Pressure tile	Surfobs/ climate/ Copernicus	5 min
	e	Extract info by study area	Raster/ Extraction/ mask layer by UA boundary	5 min
	D	**Open Street Map (OSM)**	**Vector data**	**10 min**
	a	Download OSM data	OSM / Geofabric.de	~50 mb
	b	Extract Main Transportation (S3)	Attribute table/ Select by expression	5 min
	c	Extract Any Road (S4)	Attribute table/ Select by expression	5 min
	E	**Manually Generated**	**Vector data**	
	a	Power lines	Create shapefile	
	b	Fuel Stations	Create shapefile	
	c	Dump Areas	Create shapefile	

Figure 5. The detailed steps of the stage 1 of the workflow aiming data collection.

During the process, the students are asked certain pop-up assignments in order to fulfill important steps of the research. For example, Figure 6 presents the assignment that aimed the extended abstract. It was meant as an individual brainstorm in order to explore the personal potentials on drafting a research paper structure. Later these individual outputs were merged among the members of the group into a common paper draft. This assignment was organized as a take-home Mid-term exam.

The second half of the semester consisted of an intensive GIS-based work to perform the analytical steps according to the predefined plan. Within the steps of the workflow (see Figure 4.) there have been delivered some minor assignments. For example, the absolute values measured during the inventory phase needed to be reclassified into relative sub-classes. We decided to use the Jenks natural break normalizing method which targets the minimum diversity within a certain class and maximum difference among the classes.

Mid-term submission		**Research Proposal / Extended Abstract**	
task		*about*	*point*
Question	*1*	*Please, propose a tentative title for your term paper. It may indicate the main topic and focus, method, study area.*	*5*
Title of the Paper			
Question	*2*	*Write the draft abstract of your research. Try to shortly indicate the goal and objective, study area, methods and tools used, expected/ preliminary results, and the impact and contribution (up to 300 words). Conclude with 5-7 keywords.*	*15*
Abstract			
Question	*3*	*Please indicate the goals and objectives of your study. Indicating its relevancy and its contribution in the field of DRM&FS. (references are appreciated)*	*10*
Goals and objectives			
Question	*4*	*One paragraph summarizing the forest fire phenomena globally (refer to 3-4 sources).* *Another one summarizing the factors affecting the fire regimes in general and specifically in Mediterranean. (refer to 3-4 sources) try to differentiate between factors in terms of their relevancies to the ignition and spreading phases of a forest fire.*	*15*
Literature Review			
Question	*5*	*Please, explain shortly the methods, techniques, software, plugins you have used in different phases of your work. Graphics/ charts/ tables showing the workflow of the process and the methods used are more than welcome. The technique is free.*	*15*
Procedure & research steps			
Question	*6*	*Please, explain shortly the raw materials you have used. Indicate the way you collected. A table showing the materials and the way of acquisition (sources) is more than appreciated. (include sources in the references list as well)*	*10*
Materials			
Question	*7*	*AHP in this study is used to generate the impact factor each criteria would have in reference with their relevancy to either ignition or spreading of a forest fire. Please explain in one paragraph AHP method in principle and its specific use within this work. (2-3 references are expected)*	*5*
Analytical Hierarchy Process			
Question	*8*	Please explain in one paragraph natural break (Jenks) classification method. And, briefly explain its utility in this study. *(2-3 references are expected)*	*5*
Jenks natural break			
Question	*9*	*Please, explain the expected results from this study. What type of materials you are going to produce and deliver. Present preliminary results; tables, maps, statistics, etc.*	*10*
Expected/ Preliminary Results			
Question	10	Please list all references included in the previous answers. In total the list should consist of relevant 15-20 references from articles or books in the field.	10
References		1.	
Total GRADE			100

Figure 6. The structure of the take-home Mid-term exam.

Figure 7 presents the Jenks natural break reclassification task. After a common demonstrative session based on the case of Tirana, the students have been provided detailed instructions about the steps to follow. The procedure was expected to be performed to the absolute inventory records of all defined criteria. They have been asked to perform the analysis for their specific study area and discuss the results with their group members.

Reclassifying by
Jenks Natural Break

Step		**Explanation**
Import Reference points layer	**1**	The layer which includes all values of 13 criteria
Open attribute table	**2**	Toggle editing mode
Remove all "null" values	**3**	Select by expression: "field" is null / select & delete
Generate breaking values	**4**	Layer properties/ symbology/ Graduated/ Jenks natural break/ 10 classes
Remember breaking values	**5**	Snipping tool
Reclassify according to breaking values	**6**	Field calculator / create a new field / expression (example): *CASE* *WHEN "S1-urban c" > 24570.94 THEN '1'* *WHEN "S1-urban c" > 19989.89 THEN '2'* *WHEN "S1-urban c" > 16050.22 THEN '3'* *WHEN "S1-urban c" > 13081.63 THEN '4'* *WHEN "S1-urban c" > 10766.24 THEN '5'* *WHEN "S1-urban c" > 8371.39 THEN '6'* *WHEN "S1-urban c" > 6128.92 THEN '7'* *WHEN "S1-urban c" > 4169.67 THEN '8'* *WHEN "S1-urban c" > 2281.07 THEN '9'* *WHEN "S1-urban c" > 0 THEN '10'* *END*
Save changes	**7**	Finalize reclassification for all criteria
Close editing view	**8**	Finish the work

Figure 7. The task of clustering the inventory values into 7 classes via JNB.

RESULTS

At the final stage of the semester the groups were expected to organize the work distribution among group members to prepare the final submission. Table 1 presents the task distribution among group members for each cases study. Responsible members had to submit their term work in four main packages. The paper or the technical report was meant as the written material of the submission (following the academic writing standards).

Table 1. Responsibility distribution among group members.

	paper	maps	presentation	poster
Skopje	Iza or Eriola	Besmir or Iza	Eriola or Behar	Besmir or Behar
Novi Sad	Endrita or Fatma	Endrita or Fatma	Marjana or Terens	Marjana or Terens
Banja Luka	Izet	Dritan	Tanush or Klajdi	Tanush or Klajdi

Second, each group had to prepare a poster which had to be printed and graphically present all parts of the research. Furthermore, a presentation (PowerPoint) was required in order to structure the final group presentation during the final review meeting. The groups have been asked to submit a series of maps being prepared according to the professional standards of mapping techniques.

Table 2 presents the detailed explanation about the tasks and the required skills. The group members were asked to agree among each other on task distribution according to their personal skills and availability. For example, for the paper task the responsible person had to be experienced in academic writing standards, being proficient in written English as well as having written at least one conference paper before.

The group member that would deal with the maps must have relatively more experience in using GIS for mapping. Although all students was trained to produce qualitative maps within the objectives of the course, some of them has continuously used the GIS technologies in their professional works as well. While the tasks of PowerPoint presentation and the poster (see Figure 8 for a sample poster) required digital graphical experience. Some groups decided to share specific tasks among two group members as shown in Table 1.

Table 2. The detailed explanation and the required skills for the final work packages.

task	explanation	required skills
Paper/ Article	* The first step is to merge 4 extended abstracts into 1, by including the most relevant parts of each and avoiding repetition of information.	* good academic writing skills
	* prepare the paper in a conference paper format/ outline.	* proficiency in English
	* All other members are expected to contribute via the shared Google Docs file	* having been writing a conference paper before
GIS maps	* Prepare a set of maps of the study area from the layers you have worked and produced. (PDF or image)	* experience in GIS mapping
	* among them you may include; basic map of study area, raw layers classified by Jnb, WIPI-WSCI, etc.	* experience in digital graphics
	* These maps will be the main graphical material for the paper, presentation and poster. Thus the soonest they are produced the better.	
Presentation	* a ppt presentation explaining the process of the research, materials, results, etc.	* experience in PowerPoint presentations

	* Think this work as the presentation of the group work in a conference, where you are going to present to an audience that know nothing about your research.	* experience in digital graphics
Poster	* is the visual representation of the research process.	* moderate knowledge of any graphic software (Photoshop, Corel draw, illustrator, other)
	* you can consider as the poster presenting the group work in a conference in a poster format (no oral presentation), where you are going to show to an audience that know nothing about your research.	* experience in digital graphics

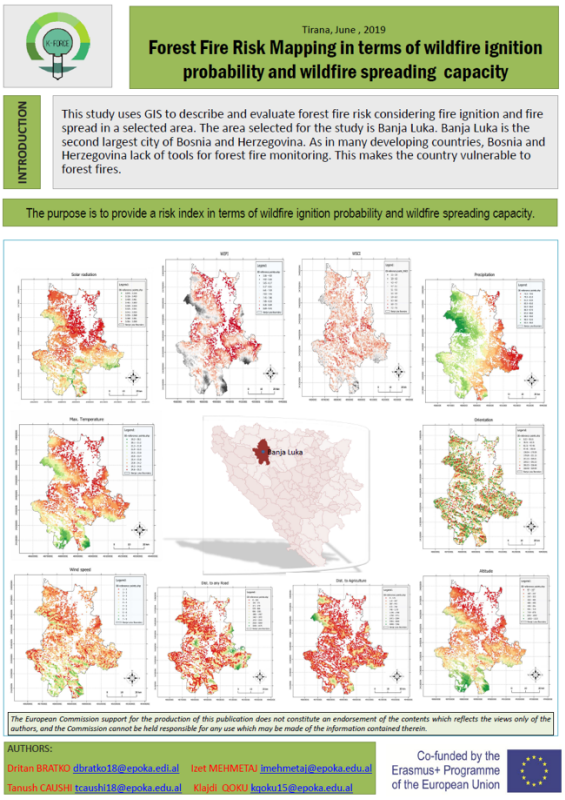


Figure 8. Poster submission of Novi Sad case, by Bratko, Mehmetaj, Caushi, and Qoku.

Fostering peer-review and peer-evaluation as a tool of transparency and responsibility in the grading system.

Figure 10 presents an image from the event of the final review presentations. The students participated as jury members as well by grading the presented works. Figure 9 presents the peer- review table delivered to each student during the final presentations. Each member was requested to evaluate each presentation following the delivered template. The questionnaire included evaluation of each task separately for paper (report), presentation, maps series, and poster. The evaluation was based on a Likert scale scoring instead of numerical grade. The peer-evaluation was transformed into numerical values by the instructor.

Epoka University | Department of Architecture
spring 2019 | Arch 451 _ Landscape Perspectives in DRM & FS
instructor | Artan Hysa

FINAL Peer-Review

Case	Work-package					
1 Skopje	Behar Besmir Erida Iza	Very Poor	Poor	Good enough	Very Good	Excellent
	Paper	☐	☐	☐	☐	☐
	Presentation	☐	☐	☐	☐	☐
	Maps	☐	☐	☐	☐	☐
	Poster	☐	☐	☐	☐	☐
2 Novi Sad	Endrita Fatma Marjana Terens	Very Poor	Poor	Good enough	Very Good	Excellent
Endrita	*Paper*	☐	☐	☐	☐	☐
Fatma	*Presentation*	☐	☐	☐	☐	☐
Marjana	*Maps*	☐	☐	☐	☐	☐
Terens	*Poster*	☐	☐	☐	☐	☐
3 Banja Luka	Dritan Izet Klajdi Tanush	Very Poor	Poor	Good enough	Very Good	Excellent
	Paper	☐	☐	☐	☐	☐
	Presentation	☐	☐	☐	☐	☐
	Maps	☐	☐	☐	☐	☐
	Poster	☐	☐	☐	☐	☐

Figure 9. Peer review form filled by each student during final presentation



Figure 10. Presentation of Novi Sad case, by Bratko, Mehmetaj, Caushi, and Qoku.

CONCLUSIONS

This paper presented the research-based learning (RBL) process as experienced in the graduate course “Arch451- Landscape Perspectives in Disaster Risk Management and Fire Safety”. Arch451 course opened within the curricula of Professional Master Program in Disaster Risk Management and Fire Safety in the department of Civil Engineering at EPOKA University.

Forest fires (wildfires) have been selected as a tangible problem to deal with during the theoretical and empirical sessions of the course. The wildfire phenomena is targeted as a phenomena emerging at landscape scale but with a clear interference with the human settlements. The research process was guided by a semi-structured workflow, which was revised through group discussions among participants.

Each class session was aimed as workshop more than a lecture. The students were invited as workshop participants into the process not as ‘classical’ listening students. Yet, it is very crucial to learn about and understand the professional background of each student in order to well define the goals and expectations of the research work. This is crucial for delivering relevant tasks during the research process.

Working in teams of 4 members resulted successful and a fair workload distribution. As well as, working on different but equivalent study areas enabled coordinated and comparative discussions during the evaluation sessions. QGIS software resulted a useful tool for a cost free and dynamic research process to enable not only geospatial analysis but also qualitative graphical results.

RBL resulted to be an effective teaching method which invites the student as a responsible professional into the learning process. Thus, it goes beyond knowledge gaining and enhances the skills of the student to perform a semi-independent research work. The applied method is appropriate for courses delivered in graduate level studies.

REFERENCES

[1] Van Heuvelen, A. (1991). Learning to think like a physicist: A review of research-based instructional strategies. American Journal of physics, 59(10), 891-897.
[2] Astin, A. W. (1984). Student involvement: A developmental theory for higher education. Journal of college student personnel, 25(4), 297-308.
[3] Kuh, G. D., Schuh, J. H., Whitt, E. J., and Associates (1991). Involving Colleges: Encouraging Student Learning and Personal Development through Out-of-Class Experiences, Jossey-Bass, San Francisco.
[4] Kuh, G. D., Whitt, E. J., and Strange, C. C. (1989, March). The contributions of institutional agents to high quality out-of-class experiences for college students, Paper presented at the annual meeting of the American Educational Research Association, San Francisco.
[5] Moriondo M, Good P, Durao R, Bindi M, Giannakopoulos C, Corte-Real J (2006). Potential impact of climate change on fire risk in the Mediterranean area. Climate Research 31(1):85-95.
[6] Pace, C. R. (1984). Measuring the Quality of College Student Experiences, Center for the Study of Evaluation University of California Los Angeles, Los Angeles
[7] Pike, G. R., & Kuh, G. D. (2005). A typology of student engagement for American colleges and universities. Research in higher education, 46(2), 185-209.
[8] Pausas J, Keeley J (2014) Abrupt climate independent fire regime changes. Ecosystems 17:1109–1120
[9] Hysa, A., Zeka, E., & Dervishi, S. (2017). Multi-criteria Inventory of Burned Areas in Landscape Scale; Case of Albania. K-FORCE first Symposium (pp. 86-100). Novi Sad: K-FORCE.
[10] Hysa, A., & Başkaya, F. A. T. (2019). A GIS based method for indexing the broad-leaved forest surfaces by their wildfire ignition probability and wildfire spreading capacity. Modeling Earth Systems and Environment, 5(1), 71-84.
[11] Hysa, A., Zhibaj, A., Lacl, A., Kuci, G., Logli, M., Hamzaj, M., . . . Dauti, K. (2020). Research Based Learning Report Series: Nature-driven Urban Planning and Design. Tirana. doi:10.13140/RG.2.2.24735.38563/1

The effect of Elbasan GGBFS addition on different properties of cement mortars

Erion Luga[1], Terens Lamaj[1], Erion Periku[1]

[1]*Department of Civil Engineering, EPOKA University, Tirana, Albania*

ABSTRACT

The purpose of this research is to study the effect of local ground granulated blast furnace slag as a partial replacing material in Portland cement mortars. The GGBFS used in this investigation is delivered as an industrial waste from the Steel Production Factory in Elbasan, Albania. For this reason, six different series of (0/100, 5/95, 10/90, 15/85, 20/80 and 25/75) GGBFS to cement ratios were produced. Normal consistency, initial and final setting time of the pastes as well as flexural strength and compressive strength of the hardened mortars were investigated. The test results showed that the use of the ground granulated blast furnace slag under investigation as a cement replacing material has different advantages and drawbacks.

Keywords*: GGBFS, cement mortar, flexural strength, compressive strength*

INTRODUCTION

Using mineral admixtures in the production of Portland cement concrete may improve several properties of concrete such as resistance to thermal cracking, ultimate strength, impermeability etc. [1]. If their quality is rigorously controlled, high amounts of different industrial by-products can be used in concrete production, in the form of blended Portland cement or as mineral admixtures. The use of pozzolanic materials as a partial replacement for Portland cement in concrete, reduces significantly the energy consumption and cost [2]. The pozzolanic reaction in Portland cement takes place due to the reaction of silica found in high amounts in the pozzolan combining with the free lime released during the hydration of Portland cement. This reaction can happen only in the presence of water, so the moisture level must be kept at a certain level for a long time for it to complete. During this reaction the finely ground glassy silica and hydrated lime react, resulting with the production of extra calcium silicate hydrate gel, similar to that produced from the hydration of Portland cement. The extra calcium silicate hydrate gel contributes in the impermeability, durability and increase of strength of concrete. The amount of pozzolan used as a replacement for cement, may vary between 10-30 % and it can be as low as 4-6% for natural pozzolans [3]. Slag is known as a non-metallic waste material disposed from the iron and steel production. When immediately cooled and ground to fine powder it has some good cementitious properties that can be used in many engineering fields. The first usage of slag starts back in the early 20th century, when the modern processes of iron and steel production began to be developed. The need to use all industrial by-products was strong and storage space was missing. Iron ores consist of compounds of iron, usually iron oxides such as hematite (Fe_2O_3), magnetite (Fe_2O_4), limonite ($Fe_3O_4.nH_2O$) and siderite ($FeCO_3$); these ores contain some silica, clay, etc., called gangue. For the removal of oxygen of iron oxides and the removal of the gangue, the ore is heated in a furnace with a high temperature under strongly reducing conditions in the presence of a flux. The flux combines with the gangue of the ore and ash of the fuel and produces a melt called slag.

"Blast-furnace slag it is known as the non-metallic product which consists of calcium silicates and other bases and is developed in a molten condition simultaneously with iron in a blast-furnace" [2]. The main composition of Blast-furnace slag is mainly silica (SiO_2), alumina (Al2O3) and lime (CaO). Slag also contains small percentages of iron (Fe_2O_3), magnesia (MgO), manganese oxide (MnO) and sulfur (S). The temperature of liquid slag taken out from blast furnace is approximately 1500 'C. The process of cooling of the liquid slag into a solid form is a crucial factor in forming the structure and characteristics of the solid slag [4]. The rate and cooling method of liquid BFS results in the production of three types of slag in solid form: air-cooled, expanded and granulated BFS. The granulated blast-furnace slag is the only product suitable for use as cementitious material when finely ground This is due to the high content of silica and alumina in non-crystalline form. GGBFS show pozzolanic properties similar to those of finely ground natural pozzolans and fly ash. The high content of CaO makes GGBFS somewhat self-cementitious besides the pozzolanic characteristics. The use of GGBFS may affect several properties of concrete such as: higher ultimate strength with lower early strength, improves sulfate and seawater resistance, improves resistance to alkali-silica reaction, decreases heat evolution, better finish and color, better durability to freezing and thawing, decreases porosity and chloride penetration [5]. During the communist period Albania developed as an intensive mining country consisting of a large number of mines and processing units of metals such as chrome, copper, coal, ferro-nickel, bitumen, tar sands etc. The foundations of steel production industry in Albania are settled since 1975. The slag, as a by-product of the process of production of steel, is in high amounts deposited in special fields in Elbasan where the production of steel is concentrated.



Figure 1 Slag deposits in Elbasan.

KURUM Holding produces an average of 600 tons of steel per year. Therefore, in Elbasan there are large amounts of slag dislocated in special areas. In Albania slag finds small usage by the construction companies, while worldwide slag is being used as a very useful and cheap building material. It is well good material for road construction because of its positive characteristics like durability and high skid resistance. It can be used in porous asphalts or as other construction materials. The only usage of GGBFS of Elbasan is in the road construction where it is proven to be a good stabilizing material. In its positive one year it is used 180 ton of slag in road construction. The usage of slag in this direction is growing while the companies are learning the benefits of slag as a stabilizing material. The exact amount of slag deposit it is not known but it has become a problem for the steel production companies. They are offering the material for free because of this. [6]. Since the slag is underused in Albanian construction projects and even though it is not a danger for the environment and is not harmful the large GGBFS stock is creating different problems to the region. The purpose of this research is to study the effect of local ground granulated blast furnace slag as a partial replacing material in Portland cement mortars.

MATERIALS AND EXPERIMENTAL PROGRAM

In this study different aspects of the use of GGBFS as a Portland cement replacing material were investigated through laboratory experiments, consisting in evaluating its effect on the normal consistency, initial and final setting time as well as flexural and compressive strength.

MATERIALS

The materials used in this experimental study are; sand (crushed limestone), water, cement CEM I 52.5 R, GGBFS.

Sand

The used sand is crushed limestone sand taken from Fushe-Kruja, Albania. This type of sand is very widely used in Albania in the production of concretes and mortars. It has a specific gravity of 2.56 and a maximum aggregate size of 4mm. Table 1 shows the grading of sand used in the production of the test mortars.

Table 1. Particle size distribution of limestone sand

Sieve Size	4	2	1	0.5	0.25	0.125	0.063	pan
Cumulative % retained	0	16.5	53.8	71.4	83.9	92.6	98.8	100

Table 2. Chemical characteristics of CEM I 52.2

Chemical Properties	As per Cement Declaration	Standard	Unit
SiO_2	20,09		%
Fe_2O_3	3,87		%
Al_2O_3	4,84		%
CaO	64,02		%
MgO	1,15	Max 5,0	%
SO_3	2,83	Max 4,0	%
Loss on Ignition	2,36	Max 5,0	%
Insoluble Residue	0,34	Max 5,0	%
Free Lime	0,80		%
Alkali Equivalent	0,65		%
Total Additive	3,85		%

Cement CEM I 52.5 R

The cement used in this experimental work is white Portland cement, CEM I 52.5 R produced by Heracles ™ Company in Greece. It complies with the requirements of EN 197-1 [7]. It can be used for plaster as well as for concrete applications. Table 2 shows the chemical composition of the cement used in this study.

Slag

The Ground Granulated Blast Furnace Slag (GGBFS) used in this study was provided form the Metallurgical factory in Elbasan, Albania. The results of the chemical analysis of the slag are given in the Table 3. The chemical analysis shows a high content of iron oxide. This brings a decrease in the amount of calcium oxide and silica, and therefore may affect the pozzolanic and cementitious properties of slag.

Table 3. Chemical composition of Elbasan GGBFS

Oxide type	CaO	SiO_2	Al_2O_3	Fe_2O_3	P	S	MgO
Amount in (%)	37.24	23.42	11.74	19.93	0.1	0.6	6.97

EXPERIMENTAL PROGRAM

Normal consistency, initial and final setting time

The Normal consistency is defined as the ratio of water to cement in order to obtain the required compaction. Normal consistency, initial and final setting time were assessed in accordance with EN 196-3 standard [8]. The same procedure was performed for all the six cement paste series.

Preparation of the specimen Mixtures

Six different series of mortars with 0.5 water to binder ratio and (0/100, 5/95,10/90,15/85.20/80 and 25/75) slag to cement ratios were prepared. The results were compared with those carried out with the control specimens produced with 0,5 w/c ratio and no other additives. All the materials used for the preparation of the specimens were weighed separately on a precision scale. The ingredient amounts used in the preparation of the mortar mixtures are given in Table 4. For all the mixtures, the sand weight is given in dry condition.

Table 4. Mortar mixture mix design

Specimen series	Cement replacement %	Sand (g)	Cement (g)	Water (g)	GGBFS (g)
C	0	1350	450.0	225	0.0
S1	5	1350	427.5	225	22.5
S2	10	1350	405.0	225	45.0
S3	15	1350	382.5	225	67.5
S4	20	1350	360.0	225	90.0
S5	25	1350	337.5	225	112.5

Casting of the mortar specimens

The mortars were mixed in the Hobart mixer according to EN 196-1 standard [9]. Firstly, the water and priorly prepared solid binder were mixed, then the sand is added slowly. After that the fresh mortar is mixed until obtaining a homogeneous mix. As the mixer stops, with an appropriate spoon the fresh mortar is casted into prismatic molds of 40 x 40 x 160 mm and covered with an impermeable cover. After 24 hours, the specimens are taken out of the molds and cured for 7 and 28 days in water at 21±1 ºC.

Flexural and compressive strength tests

The flexural test of the specimens was performed according to EN 1015–11 Standard [10] on mortars specimens of dimensions 40x40x160 mm were. The specimens were tested for 7 and 28-day strength under three-point loading with a 100 mm distance between the supports. Whereas the compressive strength test was carried out in accordance with relevant specification EN 196-1 [9]. The test is performed on a 40 x 40 mm area at a loading rate of 500 N/s. The average of value obtained from six test samples is reported as the compressive strength for each of the mortar series.

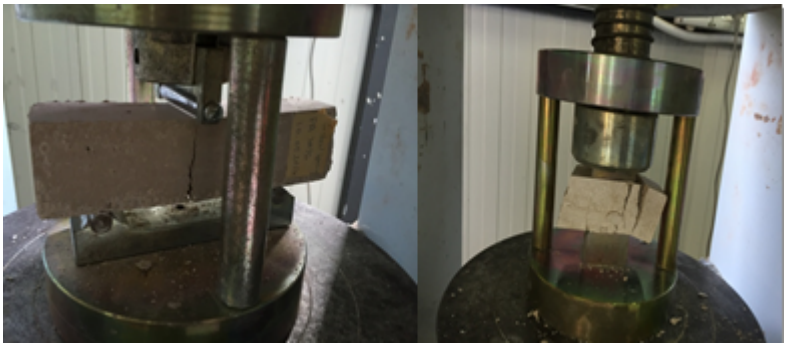


Figure 2 Flexural and compressive strength tests

RESULTS AND DISCUSSION

Normal consistency, initial and final setting time test results

Figure 3 shows the measurements of normal consistency, defined as water to binder ratio. From the results of the experiment shown in the graph, the water demand to reach normal consistency decreases as the percentage of slag increases. The comparison is made with the C sample which indicates the sample with Portland cement and no addition. As it is seen from the results the water demand decreases as the amount of slag increases.

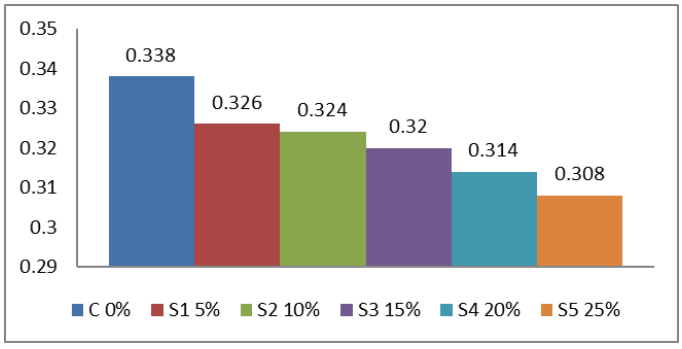


Figure 3. Normal consistency test results

On the other hand, Figure 4 shows the initial and final setting time test results. The results of the initial sett show that there is an increase in time up to 10% slag than as the slag ratio continues to increase the setting time decrease but it is still higher than that on Portland cement alone. Whereas final setting time results show an increase in time with the increase of slag percentage.

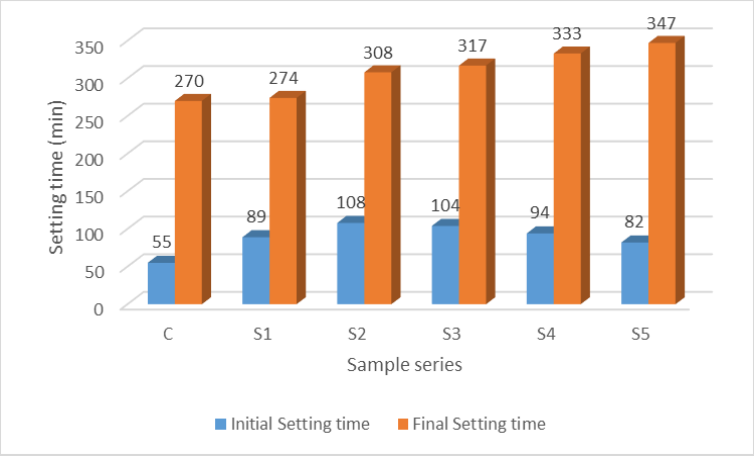


Figure 4. Initial and final setting time results

Flexural and compressive strength test results

In the Figure 5 are shown the flexural strength values of the samples after 7 and 28 days. It can be seen that the flexural strength values are very changeable and is difficult to define e certain trend.

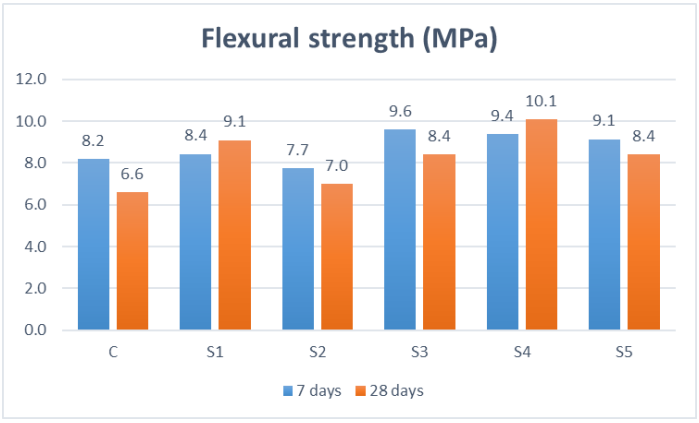


Figure 5. Flexural strength after 7 and 28 days

In the graph in Figure 6 are reflected the compressive strength test results of the mortar samples after 7 and 28 days.

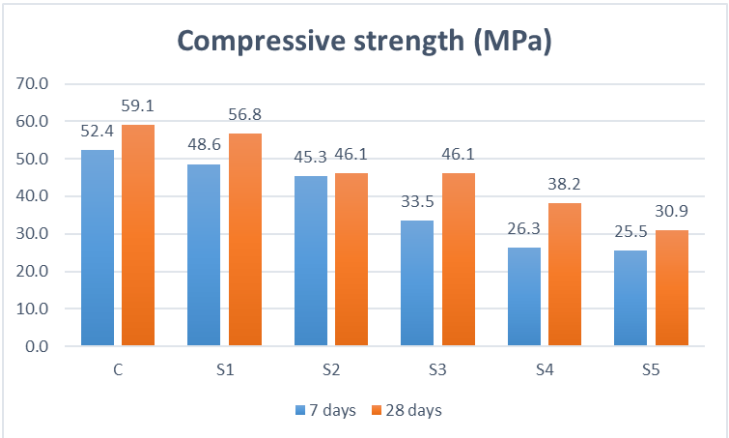


Figure 6. Compressive strength after 7 and 28 days

The results show a significant decrease in the compressive strength of the samples. The highest average value is obtained from the samples with 0% slag equal to 59 MPa and lowest from those with 25% slag equal to 30.9 MPa. In order to analyze the results, it must be taken in consideration the chemical composition of the Elbasan slag, which resulted with a high percentage of iron oxides. The high content of iron oxides decreases the percentage of CaO and SiO2 in the composition of the slag. This results in a decrease in the cementitious and pozzolanic properties of the slag.

CONCLUSION

In this study it is investigated the partial replacement of Elbasan slag in cement mortars and the results were compared with those carried out with the control specimens produced with 0,5 w/c ratio and no other additions. Based on the investigation is concluded that the GGBFS slag deposited in the Metallurgical factory of Elbasan, Albania is not very appropriate for its use as a mineral admixture because of its high amount of iron oxides in its composition. This also shows that a high amount of iron was lost during the production of steel, so by a better treatment of the raw materials higher amounts of pure iron or steel could be produced an at the same time the generated slag would have better properties and be more usable.

REFERENCES

[1] Hassan, K.E., Cabrera, J.G., & Maliehe, R.S. (2000) The effect of mineral admixtures on the properties of high-performance concrete, Cement and Concrete Composites, 22(4), 267-271
[2] P. K. Mehta and P. J. Monteiro, (2006) Concrete: Microstructure, Properties, and Materials, New York: McGraw-Hill Education, pp. 295-312.
[3] S. K. Duggal, (2008) Building Materials, 3rd ed., New Delhi: New Age International Publishers, pp. 234-242.
[4] J. Bijen, (1996) "Benefits of slag and fly ash," Construction and Building Materials, vol. 10, no. 5, pp. 309-314,
[5] J. R. Prusinski, (2006) "Slag as Cementitious Material," in Significance of Tests and Properties of Concrete and Concrete-Making Materials, J. F. &. P. J. H. Lamond, Ed., Massachusetts, ASTM International, pp. 512-528.
[6] H. Mueller, A. Vangjeli, R. Lurf and C. Redl, (2013) "Ferro Chrome Production in Albania," in INF ACON XIII: Efficient Technologies in Ferroalloy Industry, Almaty, Kazakhstan.
[7] EN 197-1, (2011) "Cement, Part 1: Composition, specifications and conformity criteria for common cements," European Committee for Standardization, Brussels.
[8] EN 196-3, (2008) "Methods of testing cement - Part 3: Determination of setting times and soundness," European Committee for Standardization, Brussels.
[9] EN 196-1, (2005) "Methods of testing cement - Part 1: Determination of strength," European Committee for Standardization, Brussels.
[10] EN 1015-11, (2006) "Methods of test for mortar for masonry - Part 11: Determination of flexural and compressive strength of hardened mortar," European Committee for Standardization, Brussels.

Towards a Disaster Risk Management Plan of Historical Centers: Case Study of The Historical Center of Gjirokastra

Julinda Keçi[1], Endrita Mulleti[2]

[1]*Department of Civil Engineering, EPOKA University, Albania*
[2] *Albanian Institute of Cultural Heritage, Albania*

ABSTRACT

Disasters, such as earthquakes, floods, wildfires, demonstrate that extreme events can have global impacts, threatening not only human lives and economy, but also cultural heritage. The UNESCO Venice Office, according to the priorities set by the government of Albania, have implemented the project "Natural Risk Preparedness and Mitigation - Building capacity in the field of risk mitigation for Cultural Heritage properties in Albania". The project aimed to streamline disaster risk management in the country, using its World Heritage properties as demonstration sites. The project was conceived to assist the country to enhance its capacity for Disasters Risk Management (DRM) and advancement in seismological and geological vulnerability of Cultural Heritage properties. This study identifies the key elements to take into consideration to draft an effective Disaster Risk Management Plan for the historic centres in Albania. In this framework, the World Heritage Property of the Historic Center of Gjirokastra is studied. The methodology used in this study and recommendations can be implemented also in the other historical sites.

***Keywords**: Disaster, Risk Management, Cultural Heritage, Gjirokastra*

INTRODUCTION

As confirmed by the 2009 Global Assessment Report on Disaster Risk Reduction [1], Risk and Poverty in a Changing Climate, the number of disasters around the world increases every year. This is due to growing exposure in terms of people and assets, in turn caused by rapid economic development and urban growth in cyclone coastal areas and earthquake-prone cities, combined with poor governance and the decline of ecosystems.

A disaster arises when an extreme natural event strikes a vulnerable society. Present day disaster risk management seeks to reduce a society's vulnerability to extreme natural events so that even such events occur they do not result in a disaster. Natural events can generally not be prevented, but their impact can be mitigated. It should be borne in mind that vulnerability arises from the susceptibility, coping capacity of individuals, households, communities, and states. Reducing vulnerability therefore involves reducing the factors that contribute to it at all levels [3].

It was the world-wide traumatic event of the Indian Ocean Tsunami in 2004 that determined the momentum necessary to set a framework of critical actions to be followed by the international community in the frame of a new International Strategy for Disaster Reduction (ISDR). UN member states recognized that they had to find new terms of commitment on Disaster Reduction. The Hyogo Declaration and Framework for Action (HFA) was therefore agreed upon. The HFA five core commitments recognize that besides the need to have national plans for Disaster Risk Reduction and Management on paper, the role of education and the role of local communities and authorities are equally crucial to achieving relevant results on building societies more resilient to risks. Resilience must be implemented on site, at the local level,

building capacities and empowering communities, including those at the grassroots level. This has recently been recalled and stressed also by the Synthesis report, "Consultations on a post 2015 framework on Disaster Risk Reduction" (HFA2- April 2013), where local action underpinning community leadership and engagement in DRR is considered a key element to mainstream International DRR principles and guidelines into national and local agendas for action [4].

Although heritage is usually not considered in global statistics regarding disaster risks, cultural and natural properties are continuously affected by events which are less and less 'natural' in their dynamics and causes. The progressive loss of these properties because of floods, mudslides, fire, earthquakes, civil unrest, and other hazards has become a major concern; partly because of the significant role that heritage plays in contributing to social cohesion and sustainable development, particularly at times of stress [2].

This study addresses three areas of concern: what to do before the hazard strikes, what to do immediately after, and what long-term actions remain to be taken. The main objective of this study is to introduce hints into formulating an integrated Disaster Management Plan in Historic Centers in Albania, focusing on a case study- the historical center of Gjirokastra.

HISTORIC CENTERS IN ALBANIA

Historic Centers, as a touchable Cultural-Historic Testimony, with urbanity-architectonic values are a very late occurrence which begins after the Second World War, if compared with other architectural monuments. These centers in Albania are mainly representatives of settlement which belong to the XVII-XIX centuries.

The Historic Center concept was known in Albania around the years 1960 as Museum City but in nowadays the concept is well-known internationally because of UNESCO merit. Today the Historic Center is considered a citizen or rural site which preserves historic-cultural values of its authenticity in different scales.

Decision No. 172, dated 02.06.1961 decided to proclaim the "Museum Cities of Gjirokastra and Berat; old part and subterranean of Durres city and Kruja Bazaar" under special state protection by the Council of Ministers of the Popular Republic of Albania. This decision indicated a very important result for the future of the Albanian monuments after the first list of cultural monuments issued in 1948. Immediately after the state protection of Berat Historic Center was compiled the Administrative regulation for this site and served as an essential principle and a reference point for protection of the different types of monuments. There are two types of monument categorization: first and second category cultural monuments. The first category monuments preserve: the compositional elements, architectural elements of exterior and interior, building technique and materials. The second category monuments preserve: their volumes and exterior façade; the interior compositional and architectural elements can be treated and changed accordingly.

THE HISTORICAL CENTER OF GJIROKASTRA

Gjirokastra is in Southern Albania, overlooking the Drino Valley. It is often named as "the Stone City" and its most distinctive feature is the silvery-colored roof with limestone tiles which gives the city its character. Two different types of limestones are quarried nearby and are used one in the construction of buildings and the other for roofs and streets paving.

Gjirokastra also with Berat are outstanding testimony to the diversity of urban societies in the Balkans. The town planning and housing of Gjirokastra are those of a citadel town built by notable landowners whose interests were directly linked to those of the central power. Berat bears the imprint of a more independent lifestyle, linked to its handicrafts and merchant functions.

In 2005 Gjirokastra was included in the UNESCO world heritage site and continues to be in the list of cities in danger.

The surrounding historical sites show evidence of the prehistoric period such as the Goranxi gorge. Evidence of other important sites in Antigoneia and Hadrianopolis testifies the importance of the region even during the greek and roman occupation. Both sites were abandoned because of more catastrophic earthquakes and consequent landslides [5].

The archaeology of Gjirokastra is relatively unknown. Because of the proximity of the Classical and Hellenistic settlement at Jermë (Antigoneia) and the Roman city of Hadrianopolis it has frequently been assumed that the medieval fortress represents the first occupation of the site. In fact, the town shows a 13th century founded Citadel, one of the biggest for-tress in the Balkans. With the decline of the Byzantine Empire, it became the residence of the powerful Zenebeshi feudal clan.

Latest excavations within the fortress have led to the discovery of ceramics from four different phases of occupation be-fore the Ottoman period: 5th -2nd centuries B.C., 5th -7th centuries A.D., 9th -10th centuries and 12th -13th centuries. The medieval fortress extension related to the second half of the 13th century, encompasses an area of 2.5 hectares.

The remains of five towers and three main entrances of the original fortress can still be seen, though the fortress was substantially rebuilt and extended to the south west in 1811-1812 by Ali Pasha of Tepelenë. Ali Pasha was also responsible for the construction of an aqueduct feeding the fortress from a water source on Mt. Sopot, some 10 km distant from Gjirokastra.

Complete sections of this aqueduct were still visible at the beginning of the 20th century but were destroyed in 1932. The fortress was used as a garrison in the 19th century. During the communism period the castle has also served as a prison for dissidents.

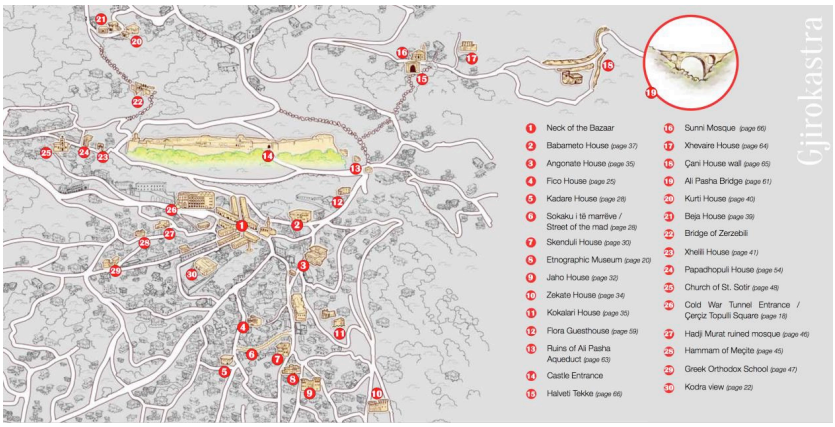


Figure 1. The Historic Center of Gjirokastra and key monuments

Hazard Identification and Risk Analysis in the Historical Center of Gjirokastra

The Historic Center of Gjirokastra site has recorded a set of natural threats affecting the property:

- Natural

• Seismic threat
• Wildland fires
• Erosion, landslides, rock falls

- Human

• Lack of financial support for the monuments
• Lack of a management plan
• Uncontrolled urban development of Gjirokastra

• Abandonment of the site by the inhabitants, which will contribute to the potential fire hazard and general degradation of the building over time

• Misuse of monument by the owner with the risk of damaging the authenticity and the integrity of the building.

Figure 2 represents some typical degradation of dwellings in Gjirokastra, Archive recordings of Institute of Cultural Monuments.

The Risk Analysis process consisted in:

- field survey for the collection of preliminary data on the state of conservation of the historic buildings;
- the methodology used was based on clear photographic data collection, technical schedules and identification of needs for interventions, leading to compilation of a preliminary list of interventions with cost list for each building (Figure 5);
- the results consisted of determining the nature of potential threats to the building:
    i. the ROOF, its condition is imperative to the state of conservation of the structure. If humidity infiltrates through and reaches the wooden structure, this is the starting point of degradation of the roof, leading to the wooden floors and the walls; the process is accelerated if the building is abandoned (Figure 3)
    ii. presence of HUMIDITY (capillary), LANDSLIDES, ELECTRICAL SYSTEM (Figure 4).

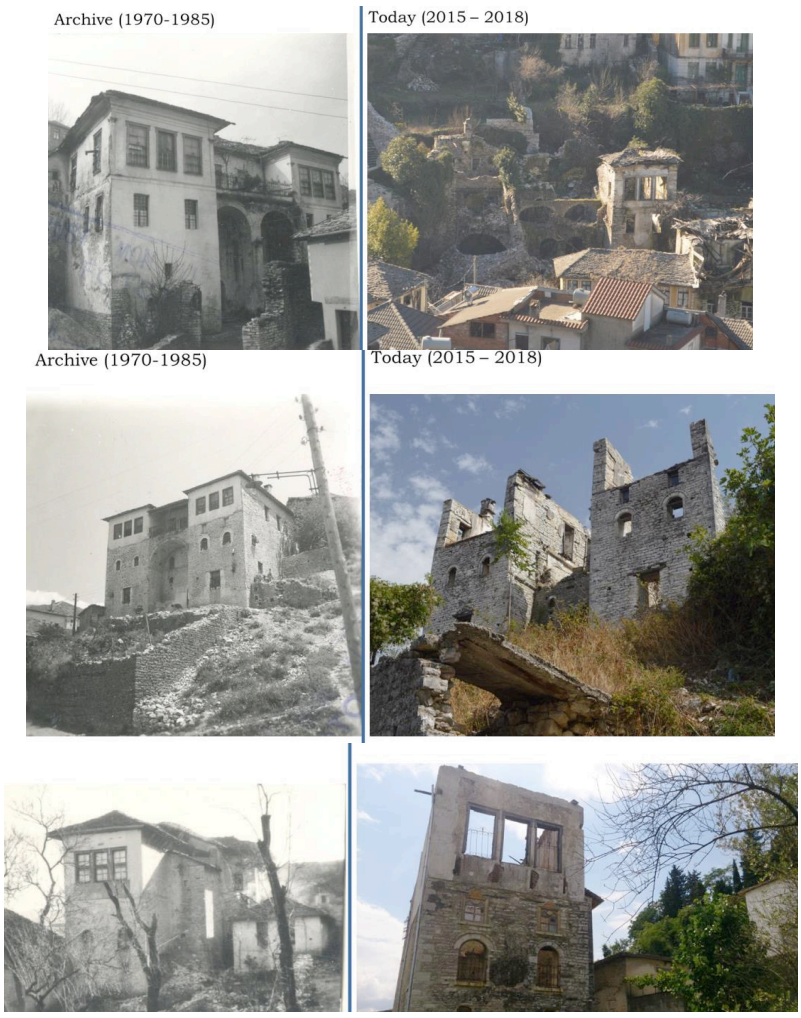


Figure 2. Degradation of dwellings in Gjirokastra [8]



Figure 3. Roof degradation



Figure 4. Presence of Humidity and degradation of wooden ceiling



14. BANESA " LOLOMANI " Kategori e II

VENDNDODHJA

Banesa ndodhet ne qender te lagjes " Pazari i Vjeter" . Eshte nje nga ndertesat me masive ne lagjen "Pazari i Vjeter" dhe me karakteristikja ne rrugen qe kalon permes ke saj lagje.

HISTORIKU/ PERSHKRIM ARKITEKTONIKO TIPOLOGJIK

Banesa ka te shenuar ne mure t e saj daten 1886. Perfaqeson nje faze me rendesi te banesave ne arkitekturen e qytetit kur kemi dhe daljet me erker dhe stilizimet e ndryshme. Ruhen disa elemente edhe ne brendi qe te lene te kuptosh per nje perpunim te larte artistik te tavaneve dhe elementeve te tjere te brendise.

GJENDJA AKTUALE

Gjendet ne kushte te rendura si ne eksterier edhe ne interier. Catia eshte e rrenuar dhe degradimi po perparon. Tavanet jane pothuajse te shkaterruara nderkohe qe eshte e braktisur nga pronaret dhe banohet nga familje te ndryshme. Nderkatet ne piesenme te madhe jane te dekompozuar dhe mbeturinate lena brenda baneses e rendojne situaten me peshen dhe lageshtine qe mbajne. Rrjeti i ujesjedhe sit dhe kanalizimeve qe perdoruesit kane vendosur ka probleme dhe rrjedhje> lageshtia nga keto rrjete deperton ne strukturen e monumentit duke e vene ate ne nje rezik te perhershem. Rreziku nga zjarri gjitha shtu eshte prezent. Banoret e tanishem e perdorin monumnetin pa kriter duke nderhyre me forma brutale.

NEVOJA PER NDERHYRJE

Nevojat te menjehershme ne pastrimin e monumetit, plotesimin e catise dhe muratures. Perforcime te nevojshme per sa i perket nderkateve etj.

RISKU KRYESOR :

Risku kryesor eshte zjarri. Nderhyrjet pa kriter jane nje rezik permanent. Gjithashtu kolapsi i catise dhe nderkateve hyn ne risqet e MEDHA qe ky monument po perballet.

PUNE PREGATITORE:

Skeda teknike dhe nje preventiv paraprak per rehabilitimin e baneses. Grumbullimi i materilit arkivor per kete banese.

KOSTO FINANCIARE PER NDERHYRJET SHPETUESE DHE RESTAURUESE:

2.500.000 - 4.000.000 AL

Figure 5. Example of the Risk Identification file [8]

List of buildings needing emergency interventions:

- The process realized in collaboration with RDNC Gjirokastra based on the survey on risk assessment carried out by CHwB
- Site survey of 82 historic buildings, gathering photos, notes on needed interventions, scale of degradation.
- The result is the identification of state of conservation, list of interventions, cost of interventions for rescuing the structure from the collapse state (Figure 6).
- An estimated cost = 2,440,000€, as detailed below:

- **1st category monument = 13 | cost of interventions 455.000 €**
  (1 does not exist, 4 are in ruins, 5 in collapse state, 3 state of advanced degradation)

- **2nd category monument = 66 | cost of interventions 1,935,000 €**
  (1 does not exist, 20 are in ruins, 22 in collapse state, 22 state of advanced degradation, 3 are inaccessible)

- **No status buildings = 3 | cost of interventions 55,000€**
  (1 does not exist, 1 in collapse state, 1 state of advanced degradation)

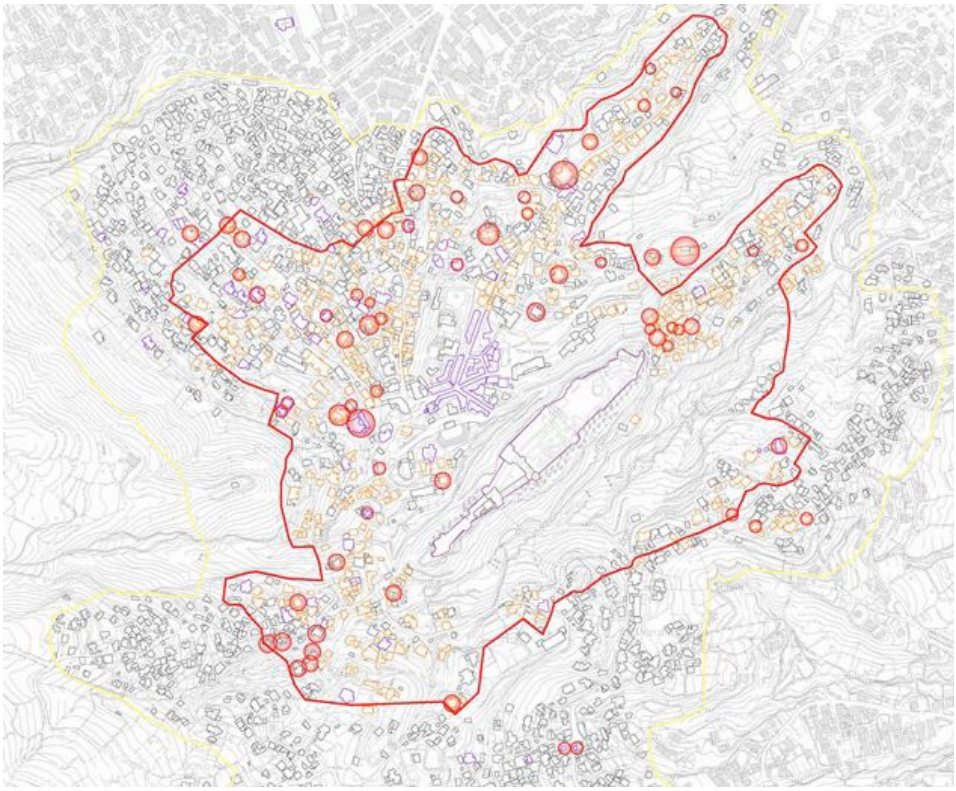


Figure 6. Map of the HC of Gjirokastra with the identified buildings at risk

Geological and Seismic Hazard of the Region

The region of Gjirokastra falls into the Ionian zone. This zone includes areas characterized by synclines and anticlines with NW-SE orientation, which from east to west are: Permeti syncline, anticline of Berat, the syncline of Memaliaj, anticline of Kurveleshi, syncline of Shushica and Cika anticline. These structures exhibit a westward asymmetry and are complicated by thrust faults located at their western flanks. The historic center of Gjirokastra is located, from a geological point of view, along the eastern flank of the Mali i Gere anticline, which is connected to the western flank of the Drino syncline. The deposits identified, mainly Mesozoic carbonates and Paleogene terrigenous units, constitute a homoclinic with a general NNW-SSE trend, gently dipping to ENE (ca. 20°). The terrigenous portion of the geological substrate, which houses the castle and much of the historic city center, lies in unconformity above the underlying carbonate units [6].

The seismicity of Albania is characterized by an intensive seismic micro activity ($1.0 < M \leq 3.0$), many small earthquakes ($3.0 < M \leq 5.0$), rare medium-sized earthquakes ($5.0 < M \leq 7$), and, very seldom, strong earthquakes ($M > 7.0$). As described by several authors, from the period of III-II centuries B.C. until

the present, Albania has been stricken by 55 strong earthquakes with intensities Io ≥ VIII degree (MSK-64), of which 15 have had the intensity Io ≥ IX degree (MSK-64). The number of disastrous earthquakes reported has obviously been underestimated or hidden in the depths of historical times. Reliable evidence show that Durres (Dyrrahum) has been stricken several times by strong earthquakes that have caused serious human and economic losses. From old records we can see that this town was almost destroyed in the years 177 B.C., 334 or 345 A.C., 506, 1273, 1279, 1869 and 1870 [7].

In the centuries III-II B.C., there is evidence that Apollonia, another ancient town, was struck by strong earthquakes which caused large casualties and damage. In the year 1153, the town of Butrint (old Buthrot) in the south of Albania, was destroyed by a strong earthquake. Also, Berat has been hit by strong earthquakes several times. One of the strongest, well evidenced ones is that of October 17, 1851, which caused a lot of destruction. The fortress of the town was damaged and under its ruins 400 soldiers were buried. Cracks on the ground were observed together with fountains of sand and water mixed, and a kind of a sulfur dust, which made respiration difficult, was discovered. There were big landslides as well. The highest intensity for this earthquake had to be 9.0 degrees (based mainly on the degree of destruction of the fortress of the town). Gjirokastra is located only 35km north of Butrint and around 72 km south of Berat [7].

Methodology used for Geological and Seismological Risk mapping in Gjirokstra

Quick Duty Builder

It was primarily decided to act in such a way as to enable a rapid screening of Seismic Risk in Historic Centers at relatively low cost, ensuring repeatability in other similar realities. This process has its strong point in the definition, co-ordinated among all study groups, of a rapidly compiled and continuously improved file, even at the next stage of expanded experimentation envisioned in an area of study. It is specifically aimed at collecting in a short time a large amount of data by not very expert personnel and trained in a short time and in processing as little of the data as possible influenced by interpretation factors subjective, leaving this stage for a later level that can be achieved through weighted processing of the collected values.

It was decided to further limit research on the exterior of buildings, avoiding access within them, increasingly difficult and not always possible in the case of uninhabited buildings or in a state of degradation. The impossibility of access to these buildings, feasible and realistic in the case of Historic Centers, would jeopardize the return of inhomogeneous data and therefore high risk of error.

The lack of data on the ceilings creates objectively problems in interpreting in terms of the Vulnerability of Buildings and above all in comparison to the GNDT file data used by us as the basis for the Quick Duty Builder. However, such a more correct methodology was considered in the context of the study program's goals, such as repeatability of the analysis and speed in data collection.

This system seems ideal to enable large-scale analysis to provide useful guidelines for reducing seismic risk, starting from such elements that, on a large scale, represent a minimum percentage of error. However, it should be said that the second stage for the risk and vulnerability-related analysis has been carried out deepening and field verifications, such as to enable a more accurate determination of the final values. It was done through general surveys, while for the values associated with the vulnerability of the buildings a more detailed survey was conducted on some frequent typologies, to verify the credibility of the rapid campaign of the surveys.

The program prepared using GIS, finalized in the data throwing in the form of analysis statements and mapping project, makes it possible in very short time to find exactly within the area taken in the examination interventions which are more priority compared to others, thus enabling them to address funding and incentive policies related to the reduction of the Seismic Resistance.

Clearly, the importance of setting in very concrete terms the priorities that will allow in a recent analysis a direct result in terms of realistic risk reduction for the population concerned, above all in a moment as the current one is characterized by the availability of scarcity of resources.

The data was aggregated to the maximum, starting from each building as it looked from cartography, but later verified and sometimes modified on the ground during compilation of the file. The initial hypothesis envisaged linking buildings, via the address, with the civil status data available to the Municipality, and, where possible, with the ISTAT registration data.

The ability to maintain a common core unit for all levels of analysis, from fast to later, with a greater level of deepening, guarantees the traceability of the cognitive process, its reversibility and integration with new elements of evaluation.

Elements that enable risk assessment in Historic Center

The elements that enable seismic risk assessment in a Historic Center are those normally used in new residential areas, integrated with a relevance of historical-architectural features that in the ancient part of the city have a special significance above all in the case of those products that have made ancient and recent history. It was started from the danger assessment of the part on which rises the area with ancient dwellings.

The initial idea was to reach a truly seismic microsite based on the extensive experience gathered by the region in this sector in the post-quake phase, such a hypothesis proved unfeasible due to the scarce economic resources available. Thus, a series of field analyzes were preferred to approach as many as needed for the micro session and enable simultaneous collection of data on lithology and on the seismic response of the terrain. Such data crossed with morphologic elements, even those collected through GIS, are reprocessed by the group of studios. The processing of inter-relationships between the data collected has facilitated to transfer the seismic risk of the area to each building for each level of risk.

For Vulnerability of Buildings, it was processed through the definition of the matrices to enable the determination of the sensitivity level of the building in a rapid way, to go on to a complete (and even internally) survey of some common typologies. Such action has been made possible through the realization of a higher-level file that represents the link at a later stage with a much more detailed survey and carried out by expert personnel.

Regarding the other elements involved in the risk level assessment, the structure of the Technical-Scientific Coordination has defined in the experimental way the following analysis processes:

- *Exposure of population to seismic risk*

Population exposure to risk represents graphically that part of the population directly affected by earthquake-related damage.

Even in this case, it has been done through not the maximum possible aggregation of data by keeping it always connected to each building to allow the linkage of this assessment element with others taken to the examination and to reach a final synthesis.

- *Elements for Determining Risk Exposure*

S = Surface (derived from cartography)

H = height of buildings (extracted from survey files - number of floors above ground multiplied by the average height of the floor, h=3m)

D = The predominant destination of use (extracted from the survey file)

V = Estimated volume

NA = Estimated Resident Ability (Number of Residents)

- *Criteria for setting risk exposure values*

Definition of the volume of the building:

$V = S \times H$

Destination Usage: the destination of the use of the building was examined by setting a m2 / p ratio, for residential, commercial, and tertiary use destinations, while public buildings are catalogued as Strategic Buildings by assigning the maximum risk category as the basic building for emergency organization.

- *Determination of estimated resident capacity*

In the case of Gjirokastra, the number of precious inhabitants is calculated by allocating to each inhabitant a volume equal to 200 m3 in consideration of low residential density, space for services and large deposits in historic buildings and of large thickness walls, using the following formula: NA = V / 200

In the case of constructions with tourist destination, this value has been modified by adding the number of tourists potentially present with a volume equal to 100 m3, this value is set in relation to the number of rooms present and the volume of each building, formulas that turns out to be: NA = V / 100 54

- *Criteria for Determination of Risk Exposure Levels*

For determining the level of risk exposure in the case of Gjirokastra, it has been determined by setting an increase in the function of the largest inhabitant of precious value with the following system:

N ° residents EXPOSURE LEVEL
From 0 to 2, Low
2 to 5, Medium
5 to 15, High
> 15, Very high

Results in the case of Gjirokastra (which for a building number taken on an examination equal to 922 represents an important sample) have identified a percentage of buildings equal to 34.92% that are part of the Exposure level High and Very high, while one third of the buildings (30.30%) are part of the Low exposure level.

- *The importance of historical-architectural characters*

The importance of historical-architectural characters represents the element of continuity with the Reconstruction Plan, from which, in fact, the intervention categories were derived using the basis for assigning values for each building.

The importance attached to the Historic-Architectural Value of the building makes it possible to evaluate in detail the importance of the building in the historical context, assigning a value in relation to its potential loss in relation to the historical memory and the urban structure just as it has been structured over the years.

- *Elements for determining exposure to risk:*

Are used Intervention Categories defined by Recovery Plan:
IP - Public Interest Building
CO - Contrast Building
TM - Small Structure
CU - Cultural Heritage Building
ST - Typical Building
TU - Protected Buildings

- *Criteria for setting risk exposure values*

It has considered the great or minor importance of the building in relation to what is stated in the Reconstruction Plan whose values are taken dogmatically. In the case of Gjirokastra, the review of the Reconstruction Plan was integrated with the studies carried out by the Office of the Plan for finding the buildings of Italian Rationalism in the 1930s and the 1940s.

- *The vulnerability of road infrastructure*

Such an analysis has led to the examination of the vulnerability of road infra-structures as a fundamental element in the event of an earthquake on the removal of residents and for the arrival of the aid.

The vulnerability is divided into two perspectives, one of which examines the vulnerability of the infrastructure based on the constituent elements and is defined as the direct vulnerability, the other that examines the elements that the road traffic is in direct connection because located in their vicinity (i.e., with their damage may aggravate the conditions of use in case of earthquake) that is defined as induced vulnerability.

- *Direct vulnerability*

Direct Vulnerability deals with constituent elements of road passage such as dimensions (width), slope, presence of stairs, roadbed, etc. Most of these elements were derived from aero-photogrammetric cartography and dogmatic deductions from the Recovery Plan in terms of road surface.

They are linked to each other by defining vulnerability classes in function of the number of parameters that affect a certain part of the road. Even in this case, the evaluation is of the fast type and each of the elements has been given the same weight, in order to avoid the same as for the rest of the interview of the expert staff intervention.

- *Induced Vulnerability*

Induced vulnerability deals with those elements that interact with road passage and that normally represent significant benefits but that in case of earthquake can turn into the weak link chain and stop access to important areas of the historic city.

Even in this case being treated for quick analysis, the information derived from normal aero-photogrammetric cartography was used to determine the walls on both sides of the road, those that serve the road itself, the bridges for the passage of streams or canals, underpasses.

The state of maintenance or the correct dimensioning of these elements has not been examined to avoid static analysis of certainly complex levels.

We have decided to add as additional elements the risk of the presence of Highly Vulnerable Structures (deduced from the Vulnerability Analysis) present on the sides of the route taken in the examination, because without preventive interventions can be considered as high-risk products that may interfere negatively with the use of road infrastructure in the event of a seismic event.

As a further factor the risk was to consider the collapse of the façades that make up the side of the road, giving them a hypothetical blocking capacity of the width equal to one-third of the height of the entire facade.

RESULTS

From the above parameters, a risk analysis table is created for buildings as well as for transport infrastructure facilities. Such a chart points to the immediate and, to a lesser extent, expert, the weakest points of the historic center system, points at which the greatest criticisms are centered, and thus allows the start of work, which at the stage of analysis, for the first determination of the elements necessary to reduce the risk.

Reclaiming the work done before actually faces the determination of interventions in order to significantly improve the situation with marked actions and calibrated on the available budget.

In fact, it may be very easy to think of the necessary investments to reach an acceptable level of security and whether it is necessary to control intervention based on available funds.

The Risk Reduction Table becomes the newest element that can be used as a supportive approach to planning of the Historic Centers.

In fact, by introducing the risk analysis table in the Traditional Reconstruction Plan, this important part of the city can be assessed from another perspective in such a way as to allow balanced choices not only of the state of degradation of buildings but also of people in the Historic Center who reside or want to reside, who should be aware of the level of risk they must face except that any construction interference made in this subtle part of the city interferes with the whole system.

CONCLUSION

The increase of awareness on disaster risk has induced an increased awareness of risks in cultural heritage as well. Damage and destruction of high-profile heritage sites has drawn attention to some measures to be taken before, during and after an earthquake:

- Create an inventory database of all cultural heritage sites/objects, encoded, and detailed with photos, plans and other important records, including geological studies of underground soil profile/structures.
- Perform risk analysis for critical infrastructure, such as roads, water/gas/electricity installations.
- Prepare evacuation plans and make them visible for public.
- Use insurance as a complementary plan for movable objects.
- Crate and train an emergency group, specialized on cultural properties, preferably with multidisciplinary team members.
- Prepare and update continuously disaster zonal maps, by performing disaster studies, developing vulnerability curves, etc.
- Continuously update and improve the building codes and publish guidelines for local builders.
- Increase the awareness, culture, and education on the importance of disaster risk management.

REFERENCES

[1] United Nations Office for Disaster Risk Reduction, "Risk and poverty in a changing climate," UNDRR, 2009.

[2] ICMS, Managing disaster risks for world heritage, UNESCO, 2010.

[3] Deutsche Gesellschaft für Internationale Zusammenarbeit , "giz.de," [Online].

[4] UNDRR, "The Risk Reduction Table becomes the newest element that can be used as a supportive approach to planning of the Historic CentersSynthesis report on consultations on the post-2015 framework on disaster risk reduction (HFA2)," UNDRR, 2013.

[5] UNESCO, MANAGING DISASTER RISKS for World Heritage, UNESCO, 2010.

[6] Fabrizio Torresi, Rischio Sismico nei Centri Storici, FAST Edit, 2008.

[7] National Research Council (Italy). Institute of Environmental Geology and Geoengineering, "Disaster risk management of cultural heritage sites in Albania," Rome, 2014.

[8] A. Institute of Cultural Monuments, "Archive Materials".

Behavior of RC frames under quasi-static diagonal loads

Erion Luga[1], Enea Mustafaraj[1], Ervis Lika[1]

[1]*Department of Civil Engineering, EPOKA University, Albania*

ABSTRACT

The aim of this investigation is to analyze the mechanical behavior of reinforced concrete frames under diagonal loads. The study provides a combination of analytical and experimental work related to the quasi-static diagonal loading of the reinforced concrete frames. The analytical modeling of the RC frames was performed in ETABS software on a real scale frame, whereas the experimental test was performed on a RC frame of a scale 1/3 of the analytical model. The load displacement curves were built from both the investigation methods and the maximum strength, yielding point, maximum displacement parallel and perpendicular to the loads, Modulus of Elasticity, and ductility factor (Rμ) of the RC frames were obtained and analyzed.

Keywords*: experimental testing, ductility, masonry, infill walls, RC frame, ETABS*

INTRODUCTION

Reinforced Concrete (RC) is a combination of concrete; a material with good compressive strength, but relatively low tensile strength and ductility, which are improved by using steel reinforcement bars that have good strength and ductility properties. RC structural members are generally designed to resist tensile stresses in special parts of the concrete that can cause unacceptable cracking or structural failure. Modern RC concrete can contain different RC materials made of steel, polymers or mixed composite material in conjunction with rebar or not [1].

Ductility may be defined as the ability of the structure to undergo big deformations without a substantial reduction in the flexural capacity of the structural members. This deformability is influenced by some factors such as the tensile reinforcement ratio, the amount of longitudinal compressive reinforcement, the number of lateral ties and the strength of concrete [2].

Ductile behavior in a structure can be achieved through the use of plastic hinges positioned at appropriate locations within the structural frames. These are designed to provide sufficient ductility to resist structural fall after the yield strength of the material has been achieved. The available ductility of plastic hinges in RC concrete is determined based on the shape of the moment-curvature connection [3].

The displacement ductility factor Rμ is defined by the ratio between failure displacements to yield displacement. The yield displacement (Δy) is the lateral displacements at 80% from ultimate load at arise part of curve while the failure displacement (Δf) is lateral displacement at 80% from ultimate load at subtracting part of the curve. The ductility factor and displacement ductility are computed using equation (1) below [4].

$$R\mu = \Delta f / \Delta y \quad (1)$$

where: Rμ is the ductility factor, Δf is the failure displacement and Δy is the yield displacement

Pushover analysis is an approach analysis method in which the structure is subjected to monotonically increasing lateral forces with an invariant height-wise distribution until a displacement is reached. Pushover analysis consists of a series of sequential elastic analysis, superimposed to approximate a force-displacement curve of the overall structure.

The lateral forces are increased up to some members will yield. The structure has been modified in push over analysis in order to decrease stiffness and then lateral forces will try to increase the yielding of members. The process of the putting lateral forces is continued in the structure until that the structure has reached a capacity and the deformation of the structure becomes unstable [5].

Assessment of the structural behavior of the RC frames has become an important topic especially in the earthquake prone countries. Tawfik, 2016, investigated the behavior and ductility of high strength frame concrete (HSFC). The experimental program was done on five specimens who have different dimensions. In the case of equal beam to column dimensions a plastic hinge was formed in the column, the plastic hinge was formed in the beam in case of stiffer column, the increase of inertia of beam for high strength RC frame increases the ultimate lateral load, energy distribution and stiffness by a small value while it decreases the ductility factor, increasing the inertia of column for H.S.R.C frame; the ultimate lateral load, energy distribution, and stiffness are increased by a significant value, while it decreases the ductility factor, increasing the stirrups at connections; the ultimate lateral load and displacement at ultimate lateral load are increased by a significant value [6].

Watson, 1989, carried out an experimental campaign to investigate the flexural strength and ductility of reinforced concrete columns under stimulated earthquake loading. Additionally, the behavior of columns with square and octagonal cross sections were also analyzed under simulated earthquake loading. For the columns, various amounts of shear reinforcement were applied [7].

Diagonal compression test as of ASTM E519-02 [8] is a widely used test to assess the shear resistance of masonry walls. Many researchers have used this method to assess the shear resistance of brick masonry panels [9,10] as well as stone masonry [11,12]. The obtained parameters provide good insights about the capacity of the wall to resist possible seismic forces.

The aim of this study is to investigate the mechanical behavior of reinforced concrete frames under quasi-static diagonal loading. And analyze the parameters such as maximum strength, yielding point, maximum displacement parallel and perpendicular to the loads, Modulus of Elasticity, and ductility factor (Rμ) of the RC frames.

METHODOLOGY

The methodology used in this study consists of modelling of a RC frame using ETABS software, as well as experimental testing of a reduced-size model of a scale 1/3 under diagonal compression. Prior to testing, all the materials mechanical characteristics were measured. The tests were conducted at the Civil Engineering Laboratory at EPOKA University.

Test set-up

The diagonal compression test is carried out by rotating the frame 45º, and application of the load exerted by a 50-tonne hydraulic jack, vertically. The frame edges sit on two loading shoes as seen in Figure 1a. The RC frame specimen was built by experienced worker and tested in the laboratory in order to avoid accidental stresses during transportation. In Figure 1 are presented the specimen ready to be tested and the CAD drawings for reinforcement. The frame has the following characteristics:

- frame dimensions:120 x 120 mm, reinforced with 4H12 and shear reinforcement of H6 @ 50 mm centers, 40 mm centers and 100 mm centers (depending upon the load distribution)
- concrete class C25/30
- steel grade B500C.

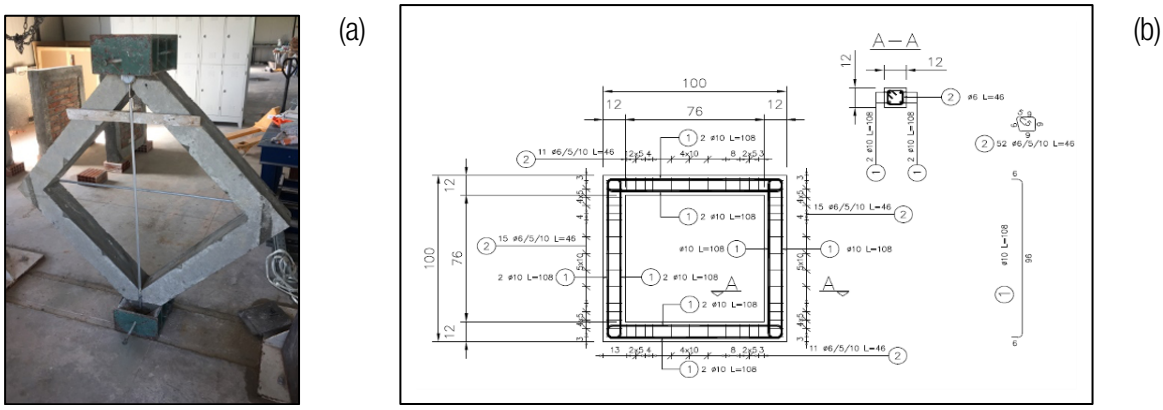


Figure 1. (a) RC frame ready for testing; (b) CAD drawing of the reinforcement detailing of the frame.

Finite Element Modelling

The finite element model of the RC frame specimen consists of linear frame elements modelled using ETABS software. A very important step in modelling is defining correctly the restrains as well as plastic hinges (Figure 2).

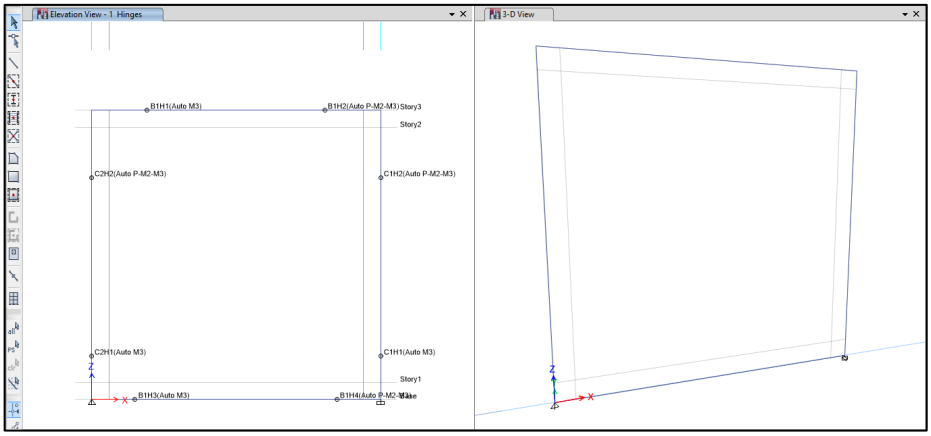


Figure 2. Frame model with hinges defined.

From the analysis output results, deformed shapes, joint displacements, base reactions, push over curves, etc. can be obtained.

RESULTS AND DISCUSSION

Experimental results

The exerted load was increased gradually. The first visible crack of the frame occurred at a load of 25 kN with a corresponding displacement in compression at 2.97 mm and a displacement in tension at 5.36 mm. The yielding stage of the RC frame occurred at a load of 45 kN. At this stage plastic behavior of the specimen is observed.

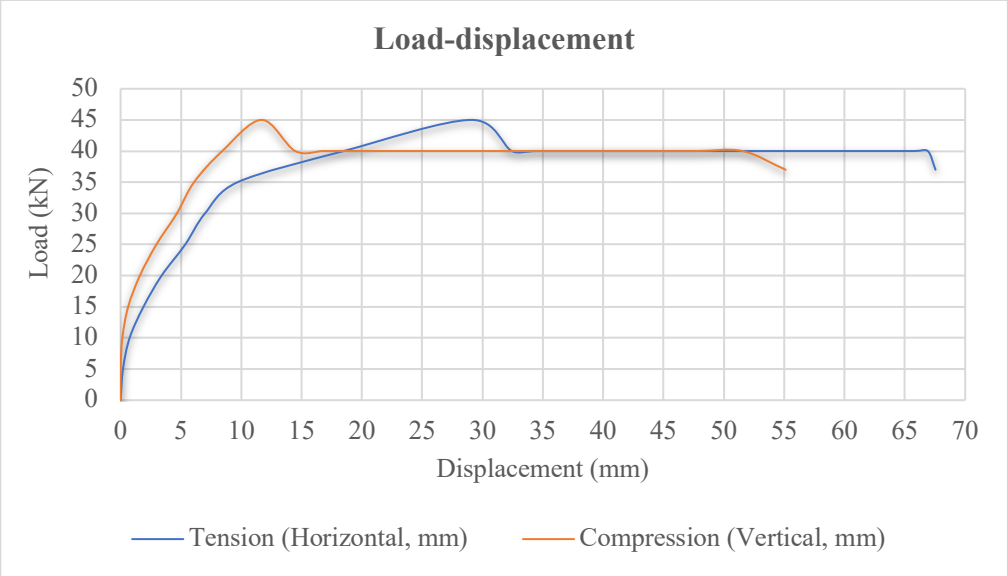


Figure 3. Load-displacement curve of RC frame

All the visible cracks in concrete occurred near the stirrups. The biggest crack width was observed near the top of the frame having a width of about 30 mm and had propagated along a length of 110 mm.



Figure 4. Deformed RC frame after the test and details of cracked joints.

Finite element analysis results

Finite element analysis results were obtained in terms of displacements, deformed shapes of the frames under dead load, P1 load, Combo load, P1 nonlinear load, G+P load; push over curve, FEMA 440 Displacements, effect of the hinges; etc.

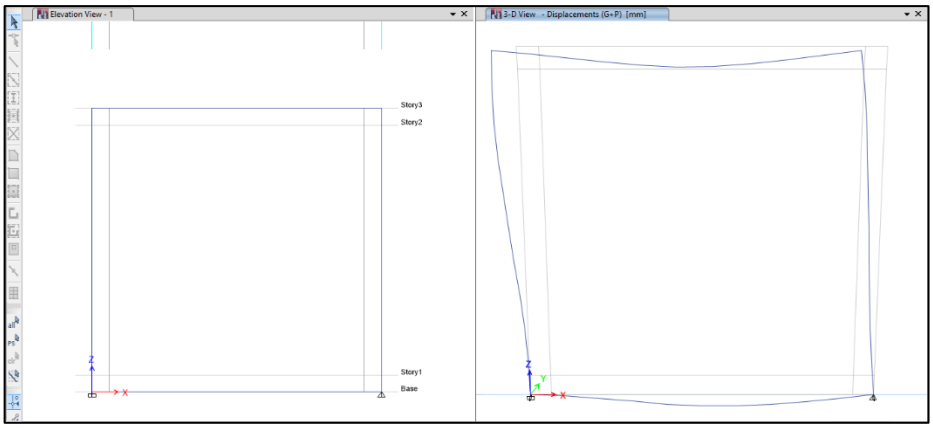


Figure 4. Deformed shaped under combination of applied load P and self-weight (P+G)

From the analysis results, three main cases were obtained from ETABS:

- Base shear vs. Monitored displacement - the intersection point of the base shear and the monitored displacement is at 47.00 kN and 120 mm.
- FEMA 440 Equivalent Linearization
- FEMA 440 Displacement Modification – the frame has base displacement of 2 mm and a base shear of 34.99 kN.

In Table 8 are presented the results of the base reactions of the frame under various load combinations of self-weight, G, the applied load P.

Table 8. Reaction of RC frame.

Load Case/Combo	F_x (kN)	F_z (kN)	My (kNm)
Dead (G)	0	38.8685	58.303
P1 Load	0.7	0.7	0
Combo Max	0	38.8685	58.303
Combo Min	0	38.8685	58.303
P1 Nonlinear Max	49.6242	49.6242	2.8505
P1 Nonlinear Min	0	0	0
G+P	0.7	39.5685	58.303

In Figure 5 is presented the monitored displacement and the base shear of the frame. In 2.8 mm displacement has a base force of 43.67 kN. The displacement and base shear continue to increase with the increase of the force on RC frame.

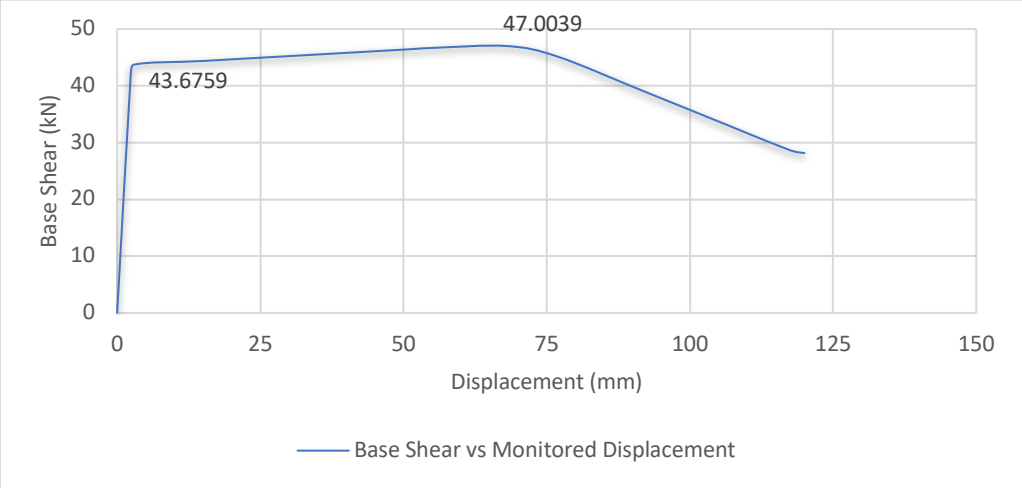


Figure 5. Base Shear versus Monitored displacement for RC frame.

Ductility of RC Frames

Calculation of the ductility factor for the frame was done using the equation 1. It was calculated taking into consideration horizontal and vertical directions.

- The ductility factor for RC frame in compression (y-direction):

$$R\mu = \frac{\Delta f}{\Delta y} = \frac{55.12\ mm}{11.7\ mm} = 4.71$$

- Ductility factor for RC frame in tension (x-direction).

$$R\mu = \frac{\Delta f}{\Delta y} = \frac{67.54\ mm}{5.36\ mm} = 12.60$$

- Ductility factor for RC frame from the numerical analysis.

$$R\mu = \frac{\Delta f}{\Delta y} = \frac{120\ mm}{2.8\ mm} = 42.85$$

CONCLUSION

In this study RC frame under diagonal quasi-static loading was investigated both experimentally and numerically. The numerical results obtained from ETABS software show that RC frame has a displacement of 2 mm and a base shear of 34.99 kN. On the other hand, from the laboratory results, it was seen that the RC frame has a displacement of 2.97 mm in compression and 5.36 mm in tension and a base shear of 25 kN.

The maximum displacement was recorded as 26.54 mm, whereas from the ETABS results, a maximum displacement of 120 mm was obtained.

The difference in the results is attributed the size difference between the specimen and the model. Nevertheless, the experimental results and the numerical results show a similar performance of the frames in both cases.

Yielding points on the frames that are tested in laboratory passes in five points beginning from the elastic zone, yielding point, strain hardening, ultimate strength, necking, and fracture stress

REFERENCES

[1] J.C.McCormac and R.H.Brown, Reinforced Concrete, NY: Clemsen University, 2014.

[2] P. &. Ruitong, Ductility, 1988.

[3] P. &. Park, Reinforced Concrete Structures, 1975.

[4] O.Monita, Curvature Ductility of RC Beam, 2016.

[5] H. Bhensdadia and S.Shah, Pushover Analysis of RC Frame Structure with Floating Column and Soft Story in Different Earthquake Zones, 2016.

[6] A. S. Tawfik, Behavior and ductility of H.S.R.C Frames, 2016.

[7] S.Watson, Design of RC frames of limited ductility, LA: University of Canterbury. Department of CE, 1989.

[8] ASTM E519-02, Standard Test Method for Diagonal Tension (Shear) in Masonry Assemblages, ASTM International, West Conshohocken, PA, 2002.

[9] E. Mustafaraj, and Y. Yardim. In-plane shear strengthening of unreinforced masonry walls using GFRP jacketing, Periodica Polytechnica Civil Engineering 62 (2), 330-336, 2018.

[10] E. Mustafaraj, and Y. Yardim. Retrofitting damaged unreinforced masonry using external shear strengthening techniques, Journal of Building Engineering, 26, 100913, 2019.

[11] M. Corradi, A. Borri, A. Vignoli. Experimental study on the determination of strength of masonry walls, Construction and building materials 17 (5), 325-337, 2003.

[12] A. Borri, G. Castori, M. Corradi, E. Speranzini. Shear behavior of unreinforced and reinforced masonry panels subjected to in situ diagonal compression tests, Construction and Building Materials 25 (12), 4403-4414, 2011.

Study of Microstructure of Waste Tyre Ash (WTA) Concrete Using the Scanning Electron Microscopy (SEM) and X – ray Diffraction (XRD) Techniques

Muhammad Magana Aliyu[1], Musa Adamu[1]

[1]*Department of Civil Engineering, Bayero University Kano, Nigeria*

ABSTRACT

This paper reports the findings of an investigation into the microstructure of WTA – Concrete. The WTA was obtained by open burning of waste tyre slices to a temperature of about 5000C for about five (5) hours at the local open burning sites in Kano. And after allowing to cool, it was sieved through 75 µm BS Sieve and characterized. The ash was subjected to chemical composition analysis using the X-Ray fluorescence (XRF) analytical method using the X –Ray spectrometer machine. The investigation was carried out on a concrete of 29 N/mm2 compressive strength, Water – cement ratio (w/c) of 0.65 and slump range of 10 – 50mm. The microstructure assessment was conducted on the concrete at WTA replacement levels of 0, 5, 10, 15, 20, 25, and 30% of cement weight, respectively to determine the influence of WTA on the microstructure of WTA – Concrete using SEM and XRD techniques. Both SEM analysis and XRD results of WTA – concrete indicated the occurrence of pozzolanic reaction between WTA and cement and that the WTA has more porous micro-structure than OPC concrete especially at higher WTA concrete.

Keywords*: Waste Tyre, Concrete, Microstructure, SEM, XRD*

INTRODUCTION

The study of concrete microstructure has benefited greatly from the use of microscopic examination and in particular, Scanning Electron Microscopy (SEM). SEM imaging and X-ray microanalysis techniques have been developed and used for imaging the complex microstructure of concrete providing images with sub-microstructure definition. By combining the information provided in the backscattered electron and X-ray images, an accurate segmentation of the images into their constituent phases may be achieved. According to Stutzman (2001) [1], the application of SEM can enhance the possibility of characterizing cement and concrete microstructure and subsequently aid in the influence of supplementary cementing materials, concrete durability problems and in the prediction of service life.

Microstructure imaging have been adopted as an essential tool in the study of materials related to the construction sector such as concrete, cement paste, soils and rocks [2] (Hassan, 2009). Scanning Electron Microscope (SEM) which is the modern generation concept of the microstructure imaging has been described as a versatile analytical work station capable of providing several different types of images, quantitative data relating to porosity and cement paste composition and information about the microstructure of the matrix. Also, according to Hassan (2014) [3], in the last two to three decades the microscope imaging has become established as an essential tool in the study of concrete and its related materials. Referred to as the scanning electron microscope (SEM), it is a versatile analytical work station, capable of providing several different types of images, quantitative data relating to porosity and cement paste composition and information about the microstructure of the matrix. The morphology of a solid phase can be defined as its shape, form or structure at the microscopic scale, that is, the scale of nanometers and microns. The morphology of a material often has a greater impact on its microscopic properties than

its chemical composition; this is certainly true of cement paste and concrete. The microstructure of cement paste revolves around the process of hydration.

The principal cementitious material in concrete and mortar is Portland cement, even though, nowadays, most concrete mixtures contain supplementary materials such as pozzolanas that make up a portion of the cementitious component in the concrete. These materials are generally by products from other processes or natural materials. They may or may not be further processed for use in concrete [4]. Pozzolanas by themselves do not have any cementitious properties, but when used with cement, react to form cementitious compound. But for these waste materials (used as Pozzolanas) to be utilized they need to meet requirements of established standards.

The performance of the Waste Tyre Ash as pozzolana for partial replacement of cement in concrete if positive and found to conform with the given standards would go a long way in providing a huge environmental benefit of disposing the ever-increasing scrap tyre nuisance in our environments and at the same time make our concrete more indigenous with less cost of production. According to Peter and John (2010) [5], well over 95% of cement used in concrete throughout the world is Portland cement in its various forms. So, any effort aimed at reducing the Portland cement content in our concretes will certainly be of interest.

A hydrous Portland cement cannot bind sand and stone; it acquires the adhesive property only when mixed with water. This is because the chemical reaction of cement with water referred to as the hydration of cement yields products that possess setting and hardening characteristics [6].

This paper attempts to show how the combination of SEM and XRD procedures can be as effective in explaining the microstructure of a pozzolana – cement - concrete during the hydration process, with Waste Tyre Ash (WTA) as the pozzolana. Conventionally the SEM with EDS provides an easier and more readily applied procedure.

MATERIALS AND METHODS

Materials

Ordinary Portland cement manufactured in Nigeria branded as Dangote 3X Grade 42.5 and having specific gravity of 3.15 was used. The oxide composition of the cement is shown in Table 1. Sharp sand from river Challawa, Kano, Nigeria, with specific gravity of 2.80 and classified as zone 1 was used. Crushed granite coarse aggregate of 20 mm nominal diameter and 2.85 specific gravity, bulk density of 1500 kg/m^3 and average impact value of 20.87% was used. The particle size distribution curve for the fine aggregate, coarse aggregate and WTA is shown in Figure 1 and the oxide composition of WTA as obtained and that of OPC is compared and presented in Table 1.

Table 1. Chemical composition of Ordinary Portland Cement (OPC) and Waste Tyre Ash (WTA)

Oxide (%)	Al_2O_3	SiO_2	CAO	Fe_2O_3	K_2O	MnO	MgO	SO_3	Na_2O	P_2O_5	TiO_2
OPC	2.10	18.69	65.23	3.96	0.48	0.09	1.96	2.33	2.32	-	0.31
WTA	3.41	37.40	2.13	6.39	0.54	0.05	1.20	14.71	9.32	1.64	0.37
Oxide (%)	V_2O_5	Cr_2O_3	BaO	CuO	ZnO_2	CL	LOI				
OPC	-	0.03	0.07	0.03	0.03	-	1.3				
WTA	0.03	0.01	-	-	22.39	0.38	14.6				

Methods

Concrete used for this study was obtained using the Absolute Volume Method based on a mixed ratio of 1:2:4. Using trial mixes initially concrete with compressive strength of 29N/mm2 at 28 days of curing

with w/c ratio of 0.65 and slump range of 50 mm was adopted. The slightly high w/c ratio of 0.65 was intentionally adopted because it is known that usually most mineral pozzolanic materials are known to be high water absorbers [7]. The formula for the Absolute Value Method used is given in equation 1 as;

$$\frac{w}{1000} + \frac{C}{1000\,Pc} + \frac{S}{1000\,Ps} + \frac{A}{1000\,PA} = 1m^3 \quad (1)$$

Where:
W = Weight of water/m^3 of concrete
C = Weight of cement/m^3 of concrete
S = Weight of fine aggregate/$m^3$of concrete
A = Weight coarse aggregate/m^3 of concrete
Pc = Specific gravity of cement
Ps = Specific gravity of fine aggregate
PA = Specific gravity of coarse aggregate

Using the above formula, seven mixes as shown in Table 2 for the batched quantities of the concrete materials and WTA were obtained. COMP 0-B is the control mix and COMP 5-B, COMP 10-B, COMP 15-B, COMP 20-B, COMP 25-B and COMP 30-B are mixes containing WTA at cement replacement levels of 5, 10, 15, 20, 25, and 30%, respectively.

Table 2. Quantity of Materials for WTA – Concrete Production

Mix No.	WTA %	Cement (kg/m³)	WTA (kg/m³)	Sand (kg/m³)	Crushed granite (kg/m³)	Water (kg/m³)	W/C
COMP 0 – B	0	324.12	0	648.24	1296.48	210.68	0.65
COMP 5 – B	5	307.91	16.21	648.24	1296.48	210.68	0.65
COMP 10 – B	10	291.71	32.41	648.24	1296.48	210.68	0.65
COMP 15 – B	15	275.5	48.62	648.24	1296.48	210.68	0.65
COMP 20 – B	20	259.3	64.82	648.24	1296.48	210.68	0.65
COMP 25 – B	25	243.09	81.03	648.24	1296.48	210.68	0.65
COMP 30 – B	30	226.88	97.24	648.24	1296.48	210.68	0.65

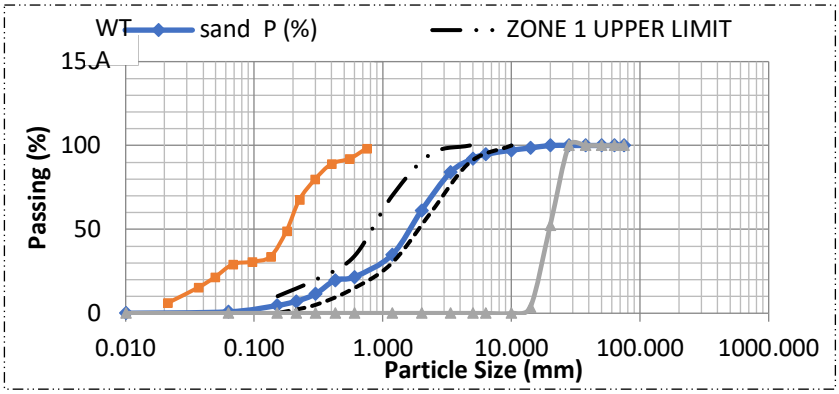


Figure 1. Particle Size Distribution of WTA, Fine Aggregates and Coarse Aggregates

The WTA was obtained by burning sliced pieces of waste tyres to ash through heating to a temperature of about 500°C in open burning for about five (5hrs) hours, at the local open burning site. The ash was allowed to cool and sieved through 75µm sieve. A chemical composition analysis of the waste tyre ash was conducted by use of X-Ray fluorescence (XRF) analytical method using X-Ray spectrometer.

The SEM works by aiming an electron beam at the surface of the Specimen. When the electron beam strikes a solid object, the electrons are either scattered or absorbed. The collection of these responses is what forms the SEM image. Crushed samples of WTA-Concrete cubes used for the compressive strength test were labeled and preserved (wrapped in foil paper and sealed in small polythene bags) for microstructure analysis of the concrete to study the effect of WTA on concrete.

X-ray Diffractometer is the equipment used to scan samples for XRD analysis. A small amount of powder sample is put into an aluminum sample holder and the surface is finished smoothly. The holder is then placed into the X-ray diffractometer. The samples are scanned by an X-ray diffractometer using CUK radiation at 40KV/20mA. CPS = 1k, width 2.5, speed 20/min and scanned with an angle of 2Θ from 3 – 70 0. The analysis is stepped at 0.04-degree increments and continued for a period of 3 seconds. In X-ray diffraction, X-rays are scattered by atoms in a pattern that indicates lattice spacing of elements present in the material analyzed. Once the X-ray analysis is completed, the scans are analyzed using Jade 7-Xray Diffraction (XRD) software. Using Jade, peak intensities at different angles are compared with a database of different minerals and compounds. Compounds with peak intensities matching those of the scans are identified and the compounds present in the samples are also determined.

RESULTS AND DISCUSSIONS

Microstructure of WTA Concrete

As already stated, SEM has become a useful tool in the study of concrete and its related materials. It has been described as a versatile analytical tool capable of providing several different types of images, qualitative data relating to porosity and cement paste composition and information about the microstructure of the concrete matrix [8]. For this study, the WTA – concrete matrix.

Accordingly, Figure 2 shows our SEM image of the control concrete (0% WTA) at seven days indicating large clusters of the light grey or brightest spots of anhydrous cement/ or calcium hydroxide crystals reflecting the early period of hydration of Ordinary Portland Cement (OPC).

OPC concrete sample at 28 days shown in Figure 3 on the other hand shows more areas of dark grey articles indicating sheet like habit of C-S-H, hexagonal habit of $Ca(OH)_2$, aggregate and the dark particles at the extreme points indicating voids. The SEM image also indicates some anhydrous cement particles through the brightest spots on the image. Overall the SEM photograph of the OPC concrete sample at 28 days (Figure 3) showed more C-S-H and $Ca(OH)_2$ than that at 7 days resulting from the hydration process. This is consistent with the Grey Image ranking analysis as presented by [2,9] respectively.

For concrete with 5 % WTA, the morphology at 28 days curing shown in the SEM picture in Figure 4 indicated observed WTA – Cement hydrated paste with large voids as evidenced by the dark patches of black areas indicating voids and the visible cracks seen consistent with the explanation of [3]. The voids here appear larger than the OPC concrete, residual cement grains appear brightest but with less hydration products of calcium hydroxide (CH) and C-S-H due to the dilution of OPC and low pozzolanic reaction of WTA at 28 days of hydration.

Figure 5 gives the SEM image of WTA concrete replacement at 10% for 28 days curing. The effect is similar to that of 5% at 28 days but with more formation of C-S-H and CH hydration products as evidenced by the presence of light gray irregular shape areas indicating calcium hydroxide crystals and dark grey areas representing calcium silicate hydrate. This observation is consistent with the explanation of [2] and [9] in their respective works on SEM image analysis.

Generally, the microstructure of WTA-concrete improved with curing age, but was more porous and exhibited more cracks with increase in WTA content.

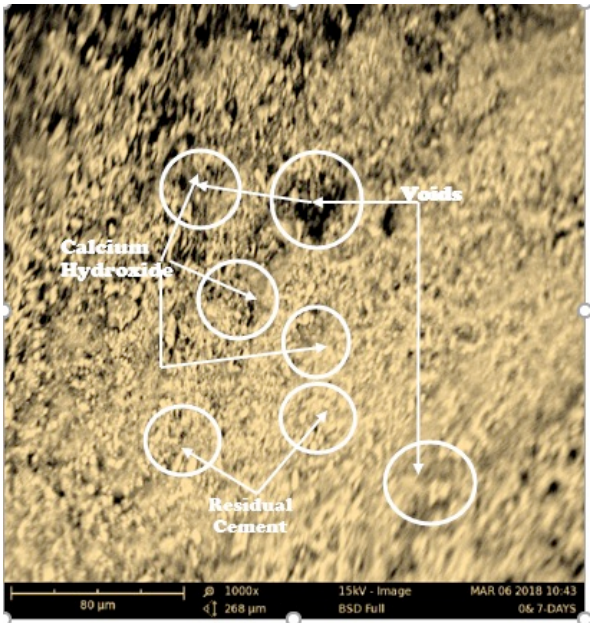


Figure 2: SEM of OPC Concrete at 7 Days

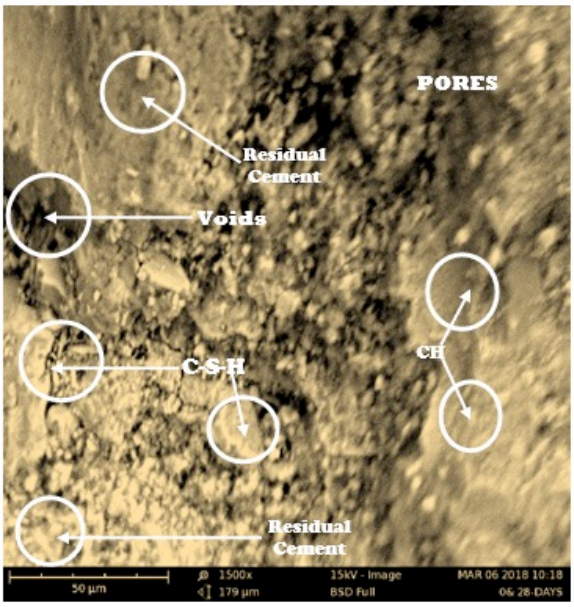


Figure 3: SEM of OPC Concrete at 28 Days

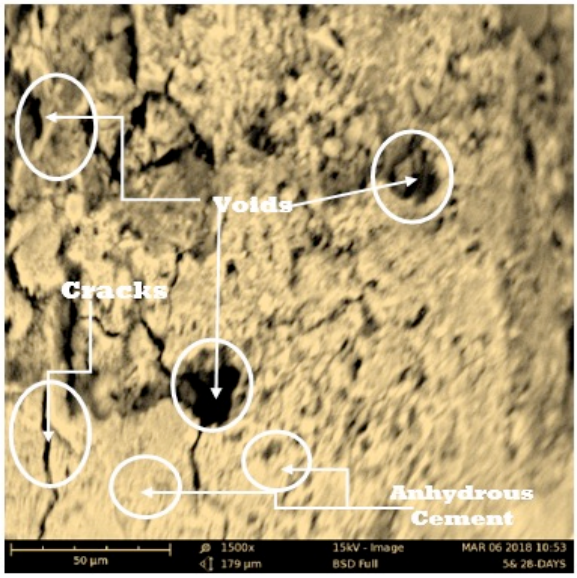


Figure 4: SEM of 5% WTA Concrete at 28 Days

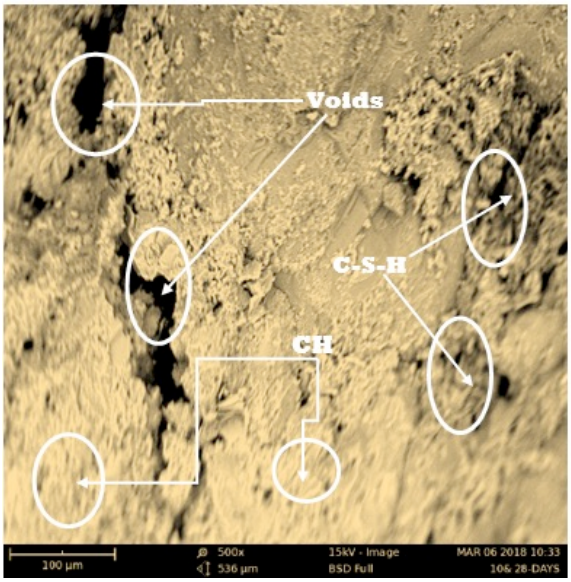


Figure 5: SEM of 10% WTA Concrete at 28 Days

XRD Result

Researchers have so far supported the combination of SEM and XRD techniques in explaining the microstructure of cement pastes and concrete materials [8, 10, 11].

In line with this approach, XRD analysis was carried out on the concrete used in this study to reveal the microstructure of WTA – concrete.

Figure 6 shows the XRD pattern indicating the development of reaction products in the control plain OPC concrete at day 7. At 7 days as shown in the Figure, the crystalline phases identified are Portlandite, Quartz and calcite. However, the focal point of interest here is the Portlandite content since it indicates the progress of cement hydration and pozzolanic reactions [10,11]. As expected, the concentration of Portlandite as observed in Figure 7 is seen to have considerably reduced for the OPC concrete curing age of 28 days. This may be attributed to the progressive hydration process expected. This further explains the increase in strength as the age of curing of the concrete increases.

At 5% WTA replacement as shown in Figure 8 for 28 days of curing respectively, the Portlandite content is either almost similar to or slightly lower than that of plain OPC indicating little or no contribution of WTA via pozzolanic reaction at early ages. The presence of calcite in all the mixes can be attributed to the secondary reaction of Portlandite with atmospheric carbon dioxide (CO2). This is consistent with the explanation of [10] in their work on Palm Oil Ash and metakaolin ternary blend cement mortar at elevated temperatures. At later age, 28 days and for higher WTA content, as shown in Figure 9, the amount of Portlandite and unreacted alite and belite progressively and significantly reduced, marking the progress of hydration and pozzolanic reaction. At 30% WTA replacement, however, as seen in Figure 10, the reduction in strength of WTA - Concrete may be due to dilution effect of cement at that level.

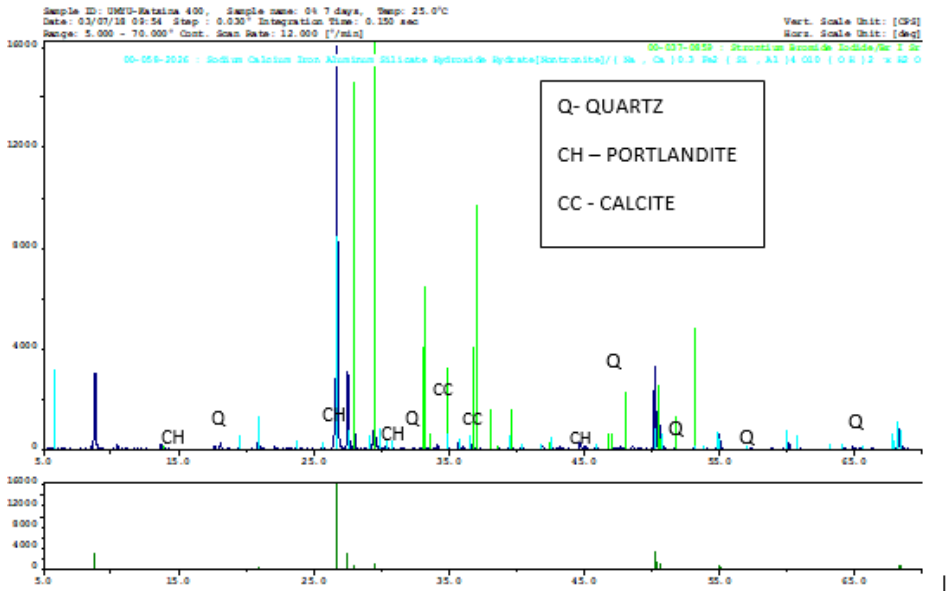


Figure 6. XRD Pattern of Control(OPC) Concrete Specimen for 0%WTA at 7 Days.

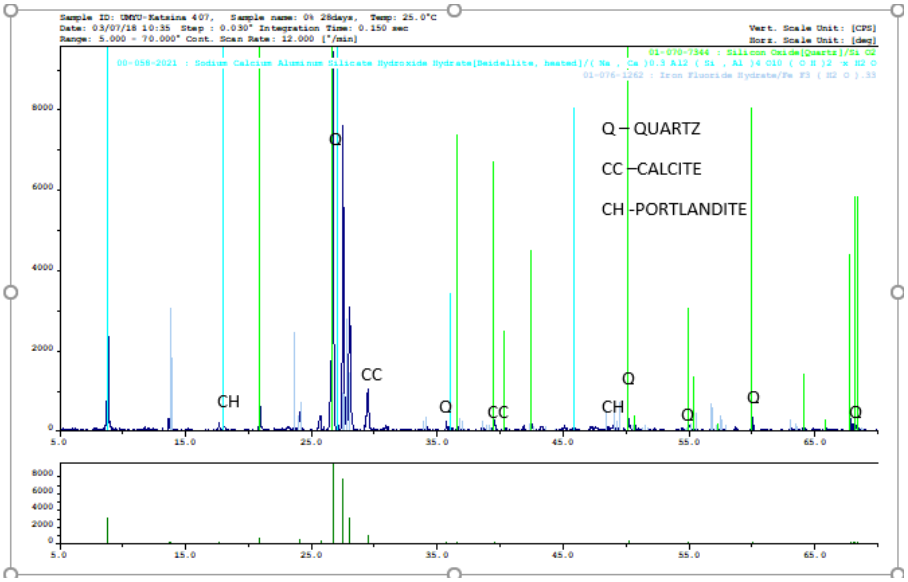


Figure 7. XRD Pattern of Control (OPC) Concrete Specimen at 28 days.

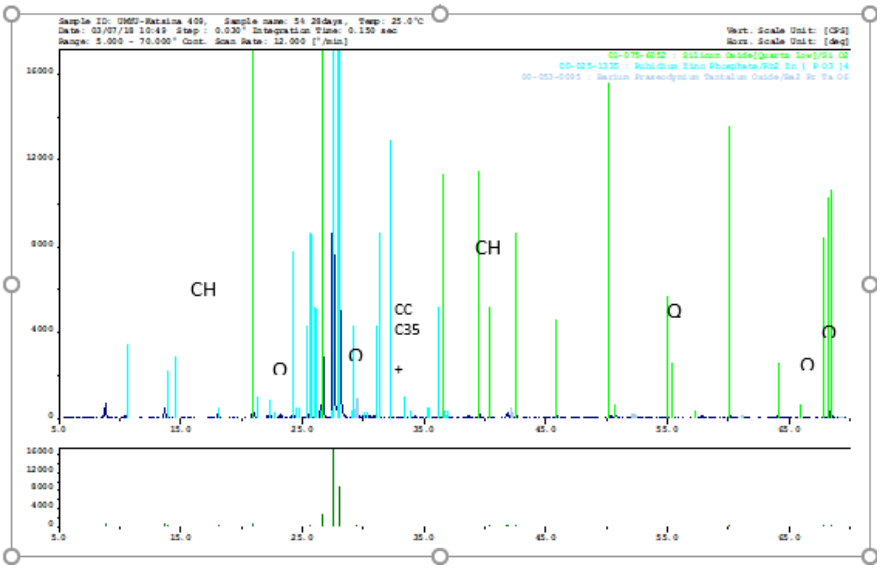


Figure 8. XRD Pattern of 5% WTA Replaced Concrete Specimen at 28 days.

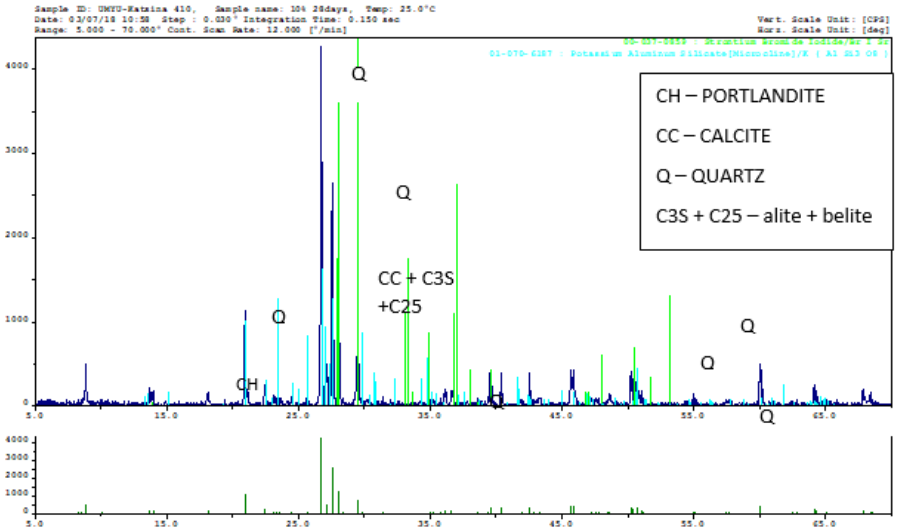


Figure 9. XRD Pattern of 10% WTA Replaced Concrete Specimen at 28 days.

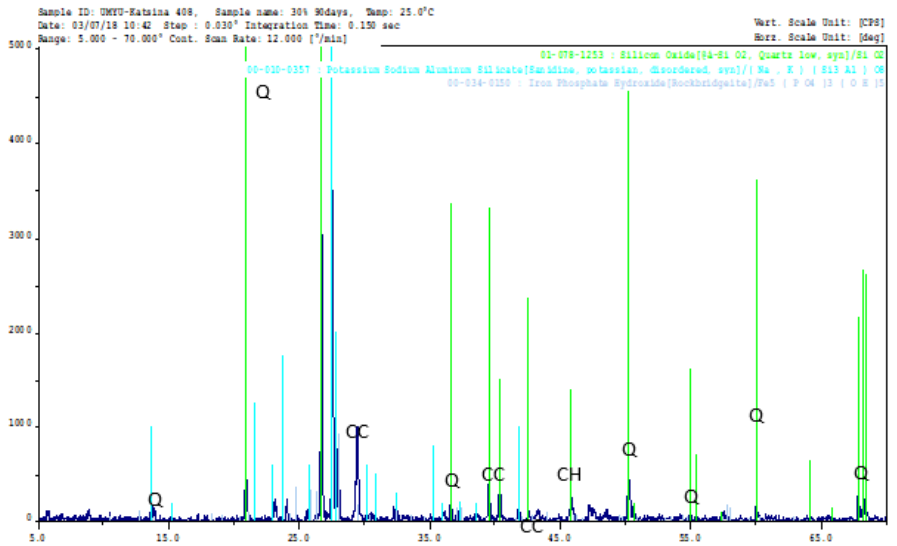


Figure 10. XRD Pattern of 30% WTA Replaced Concrete Specimen at 90 days

CONCLUSION

Both SEM analysis and XRD results of WTA – concrete indicated the occurrence of pozzolanic reaction between WTA and cement and that the WTA – concrete has more porous microstructure than the OPC concrete especially at higher WTA.

It also shows that the pores in the WTA concrete increase with increase in the waste tyre ash in the mix.

REFERENCES

[1] Stutzman P.E. (2001): Scanning Electron Microscopy in Concrete Petrography. Reprinted from Materials Science of Concrete Special Volume: Calcium Hydroxide in Concrete (Workshop on the Role of Calcium Hydroxide in Concrete). Proceedings. J.Skalny, J.Gebauer and I.Odler, eds. The American Ceramic Society. November 1-3, 2000. Anna Maria Island, Florida, 59-72, Pp. NIST.

[2] Hassan.M.S. (2009): "SEM – Back Scattered Electron Imaging Cement Paste in Concrete: Understanding and Visual Examination", Proceeding of the First Scientific Conference on Nanotechnology, Advance Materials and Their Application. Baghdad, Iraq.

[3] Hassan M.S (2014): SEM- Backscattered Imaging analyses of Cementitious Composite Matrix Incorporating Mineral Admixture. Eng. & Tech. Journal, Vol.32 Part(B), Nov.4 Pp 696-703.

[4] Meyer C (2009): The greening of the concrete industry. Cement & Concrete Composites 31, Elsevier Ltd. PP 601 – 605.

[5] Peter D. and John I (2010) Construction Materials: Their Nature and Behaviour. Fourth Edition. Spon Press.

[6] Mehta, P.K and Monteiro, PJ.M (2006): Concrete, Microstructure, Properties and Materials, 3rd Edition, McGraw-Hill, USA.

[7] Ogork, E.N, Uche, O.A., and Elinwa, A.U(2014): A Study on Groundnut Husk Ash (GHA- Concrete Under Acid Attack. International Journal of Modern Engineering Research (IJMER), Vol.4, Issue 7. ISSN:2249-6645. Pp 30-35.

[8] Stutzman, P.E., Feng P. and Bullard J.W. (2016): Phase Analysis of Portland Cement by Combined Quantitative X-Ray Powder Diffraction and Scanning Electron Microscopy. Journal of Research of the National Institute of Standards and Technology. Vol 121.

[9] Scrivener K.L. (2004): "Backscattered Electron Imaging of Cementitious Microstructure. Cement and Concrete Composites, Vol.26, Pp 935-945.

[10] Usman J; AbdulRahman M.S.; and Hussain M.W.(2017): Behaviour of Palm Oil Fuel Ash and Metakaolin Ternary Blend Cement Mortar at Elevated Temperatures. Journal of Materials in Civil Engineering 04016201. © ASCE, ISSN 0899-1561.

[11] Xiao-Lu G, Hui-Scheng S. and Hang-Yan L. (2009): Effects of a combined Admixture of Slag Powder and thermally treated flue gas desulphurization (FGD) gypsum on the Compressive Strength and Durability of Concrete. Materials and Structures (2009) 42-263-270. Dol 10. 1617/S 11527-008-9383-9 9(C) RILEM 2008.

Polypropylene reinforced mortar coating for improvement of unreinforced masonry (URM) shear resistance

Enea Mustafaraj[1], Yavuz Yardim[2], Marco Corradi[3,4]

[1] *Department of Civil Engineering, EPOKA University, Albania*
[2]*Department of Civil and Environmental Engineering, The University of Edinburgh, UK*
[3]*Department of Mechanical & Construction Engineering, Northumbria University, UK*
[4]*Department of Engineering, University of Perugia, Italy*

ABSTRACT

This paper describes an experimental program for improvement of the shear resistance of unreinforced masonry (URM) by plastering with two layers of short polypropylene fibers (fiber length = 12 mm) embedded into a cementitious matrix under in-plane loading. Six diagonal compression tests as of ASTM E519-02, were carried out on masonry panels of dimensions 1.2 x 1.2 x 0.25 m built and tested at the laboratory. The main mechanical parameters such as the shear strength, modulus of rigidity and ductility were assessed and compared before and after strengthening. Additionally, the panels were also modelled using discrete micro-modelling using DIANA 9.6 and a non-linear analysis was conducted.

The results showed that polypropylene reinforced mortar coating increased the in-plane capacity of the unreinforced masonry by 270%.

Keywords: polypropylene fibers, masonry retrofitting, URM, diagonal compression test

INTRODUCTION

Masonry is one of the most used construction types in the world. Traditional stone or brick masonry load bearing walls were designed to resist only gravitational loads, or even worse, have not been designed at all, but simply realized by the rules of common practice [1].

Unreinforced masonry (URM) structures have proven to be more susceptible to damage due to lateral forces, especially seismic loads. Recent earthquakes around the world have shown that these types of structures are the ones that suffer more damage. As the out-of-plane failure of URM walls can be restrained by improving connections and reinforcing the weakest structural elements, it is the in-plane capacity of the walls, especially the shear resistance that governs their behavior. For this reason, it is important that the strengthening strategies to be focused on improvement of shear strength and increasing ductility.

Over the years, several strengthening techniques such as i) filling cracks by grouting; ii) stitching of large cracks with metallic or brick elements; iii) external or internal post-tensioning with steel ties; iv) shotcrete jacketing; v) ferrocement and vi) center core, textile reinforced mortar (TRM) and Fiber reinforced polymers (FRP) etc. have been developed aiming at improving these parameters to comply with the modern design codes and extend their service life [2-16].

MATERIALS AND METHODS

This study is focused on testing of three unreinforced and three reinforced 1.2 m x 1.2 m x 0.25 m panels under diagonal compression to simulate shear failure as of ASTM E 519 [18]. The diagonal compression test has been used by many researchers [2-17]. All the panels were built of two leaf English bond of new clay bricks with 15 mm-thick bed mortar joints of a volumetric mix ratio of Portland cement: lime: sand 1:1:6. The specimens were built and tested in place at EPOKA University Civil Engineering laboratory.

The reinforcement method consists of plastering of both sides of the panels using polypropylene fiber reinforced mortar of a 25 mm-thick layer of cement: sand mortar of a volumetric mix ratio of 1:4 and water/ cement ratio of 0.4 plus 2% of fibers in volume (Figure 1). The walls were left to cure for 28 days. Before testing, a layer of white paint was applied to better visualize the cracks during the tests. Characteristics of the polypropylene fibers are given in Table 1.

The specimens letter designation is: URM for unreinforced panels and PP for panels plastered with polypropylene reinforced mortar coating.



Figure 1. Polypropylene reinforced mortar coating of the URM panels.

Table 1. Technical specifications of polypropylene fibers used for the reinforcement.

Property	Value/Rating
Specific gravity (g/cm³)	0.91
Fiber length (mm)	12
Fiber diameter (μm)	18
Melt point (°C)	160
Ignition point (°C)	365
Thermal conductivity	Low
Electrical conductivity	Low
Specific surface area of the fiber (m^2/kg)	250
Acid resistance	High
Alkali resistance (%)	100
Tensile strength (MPa)	300–400
Young's modulus (MPa)	4000

Test Set-up

The testing procedure is done according to ASTM E 519-02 standard [18]. It consists of application of a diagonal compression load exerted by a hydraulic jack which compresses the wall diagonally, providing the desired failure mode; diagonal cracking and/or bed joint sliding failure (Figure 2).

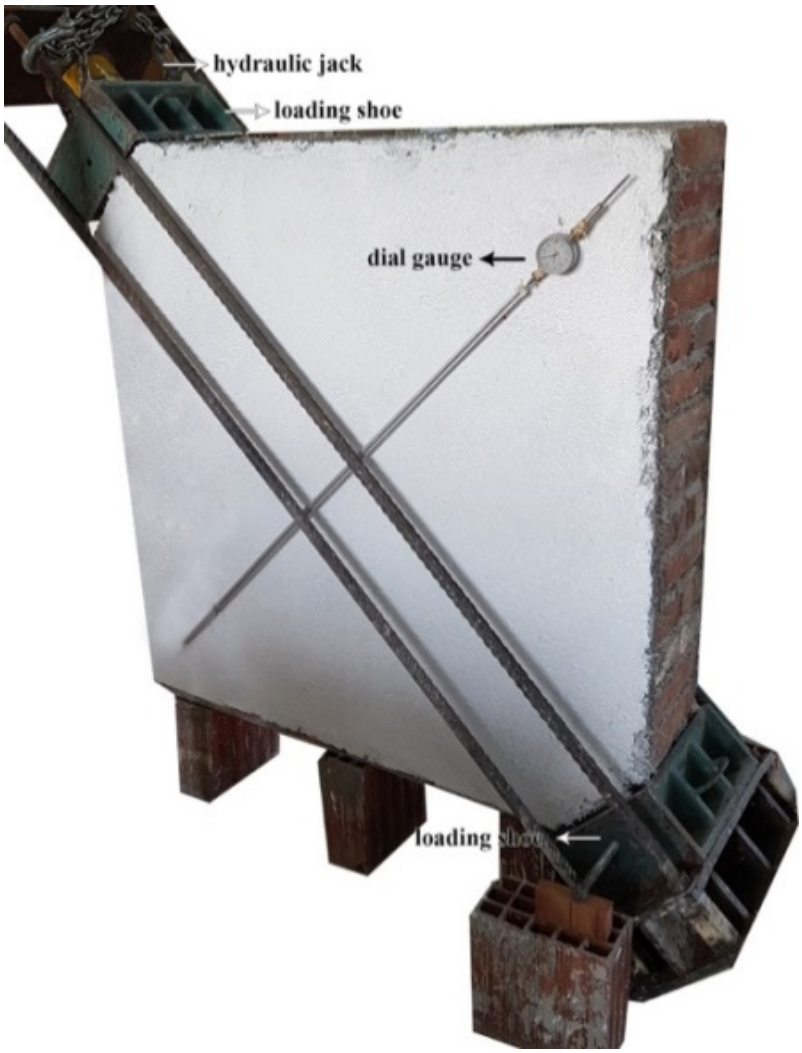


Figure 2. Diagonal compression test set-up.

The calculation procedure is as follows:

$$S_s = \frac{0.707P}{A_n} \quad \text{(Equation 1)}$$

where: S_s – shear stress (MPa); P – load exerted along the compression diagonal (N); A_n – net area of the specimen (mm^2);

$$A_n = \frac{w+h}{2} t \cdot n \quad \text{(Equation 2)}$$

where: w – width of specimen (mm); h – height of specimen (mm); t – total thickness of specimen (mm); n - percent of the gross area of the unit that is solid, expressed as a decimal.

$$\gamma = \frac{\Delta V + \Delta H}{g} \quad \text{(Equation 3)}$$

where: γ - shearing strain (mm/mm); ΔV– vertical shortening (mm); ΔH – horizontal extension; g – vertical gage length.

$$G = \frac{S_n}{\gamma} \quad \text{(Equation 4)}$$

where: G - modulus of rigidity, MPa

Finite Element Modelling

Apart from experimental test, the specimens were modelled adopting the simplified micro-modelling approach for modelling of masonry in midas FX+ for DIANA 9.6 suggested by Zijl et al. [19] (Figure 3). The "Simplified Modelling Method with Brick Crack Interface" consists of having the bricks and mortar are modelled separately as two different materials using the following elements: for bricks Q8MEM element [20]. The modelling procedure and the input parameters are carried out in-depth from another study of the authors [21].

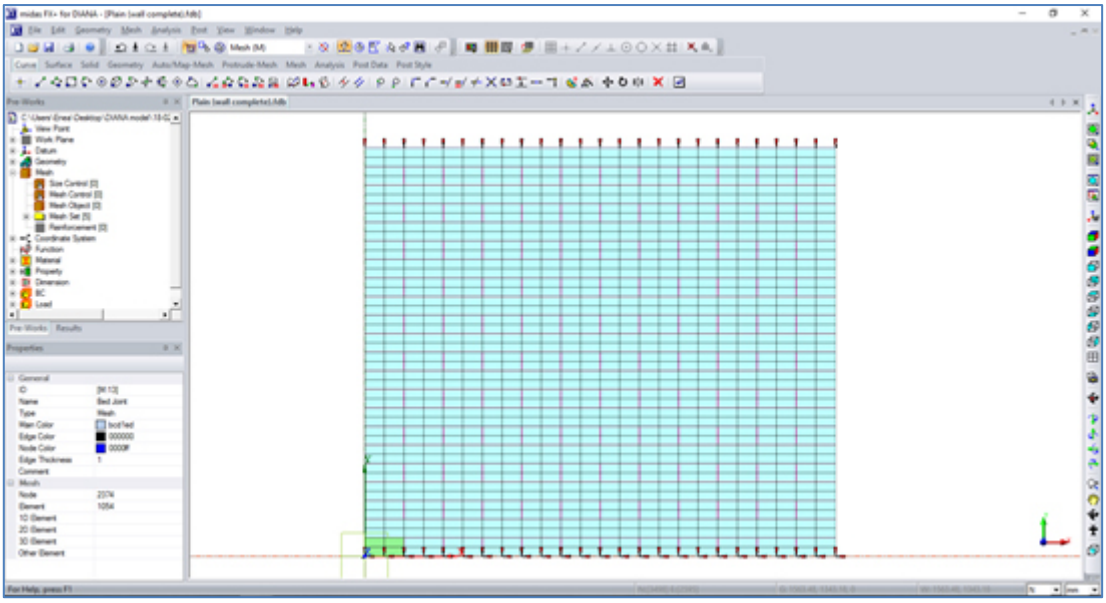


Figure 3. The finished model in midas FX+ for DIANA.

RESULTS AND DISCUSSION

The main results obtained from the experiments were the mode of failure mode for each panel, shear stress-strain diagrams, maximum shear resistance and the ultimate drift. Before testing, the individual characteristic strengths of mortar, brick and masonry assemblage was determined. For the bricks, the compressive strength was 24.03 MPa and the flexural strength 4.53 MPa. The mortar used for the construction of the walls had a compressive and flexural strength of 5.32 and 0.55 MPa, respectively. On the other hand, the reinforced plastering layer's compressive and flexural strengths were 17.64 and 2.12 MPa, respectively.

Failure mode

All the panels exhibited a similar failure. The overall failure mode of both types could be categorized as in-plane shear failure; a step-like crack developed along the loaded diagonal through the mortar joints (Figure 4 and Figure 5). The main crack started from the center of the wall panel and propagated along the mortar joints toward the panel's corners. The formation of the shear crack, i.e., the failure, was sudden, and all the panels exhibited a very brittle behavior. In the reinforced panels, the diagonal crack was deeper and wider, followed by smaller parallel cracks. The behavior of all the six panels was brittle.



Figure 4. Failure mode of the unreinforced panels.



Figure 5. Failure mode of the reinforced panels.

Shear stress-strain response

The shear stress versus shear strain response of all panels was determined by calculating the shear stress and the angular strain using Equations (1) and (3), respectively. For the URM panels, the relationship was approximately linear before the crack initiation, followed by a nonlinear response up to the maximum shear capacity. The panels exhibited little deformation before the sudden drop in their resistance, thus losing almost all of the load-carrying capacity. As it is seen in Figure 6, both shear resistance and deformation capacities are limited.

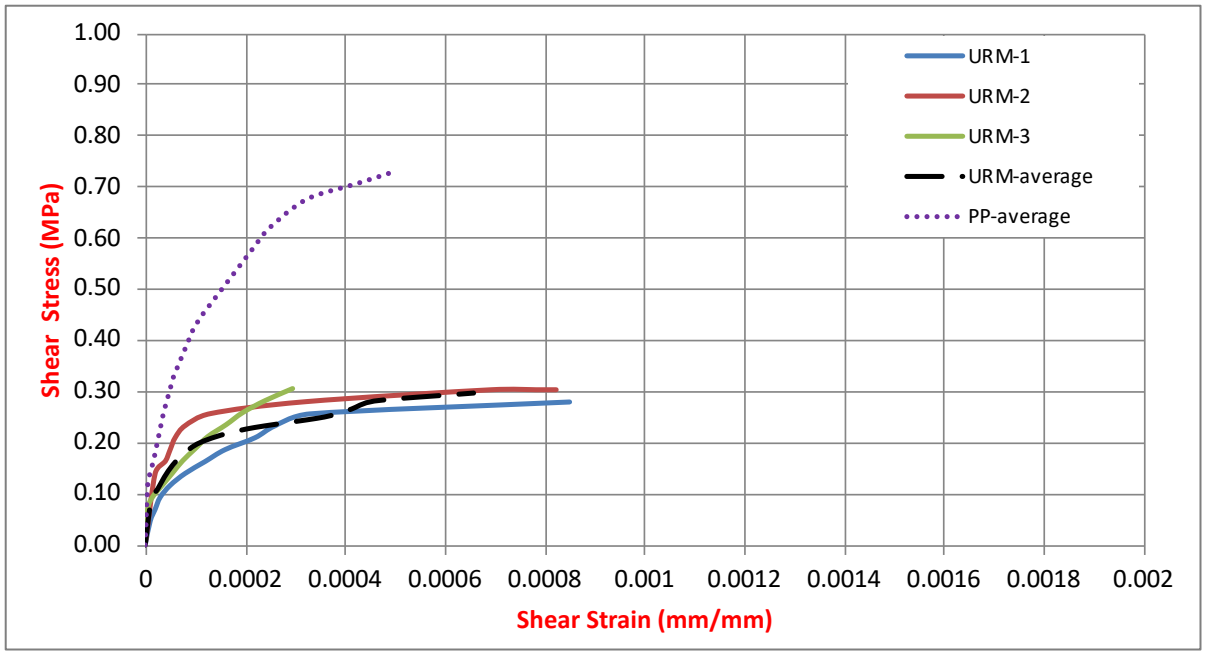


Figure 6. Shear stress-strain relationship of the URM panels.

For the PP reinforced panels, a similar behavior was observed. The stress-strain response of polypropylene strengthened panels is short (Figure 7), indicating a brittle behavior of the panels. Nevertheless, the shear strength is observed to be considerably higher when compared to the URM panels.

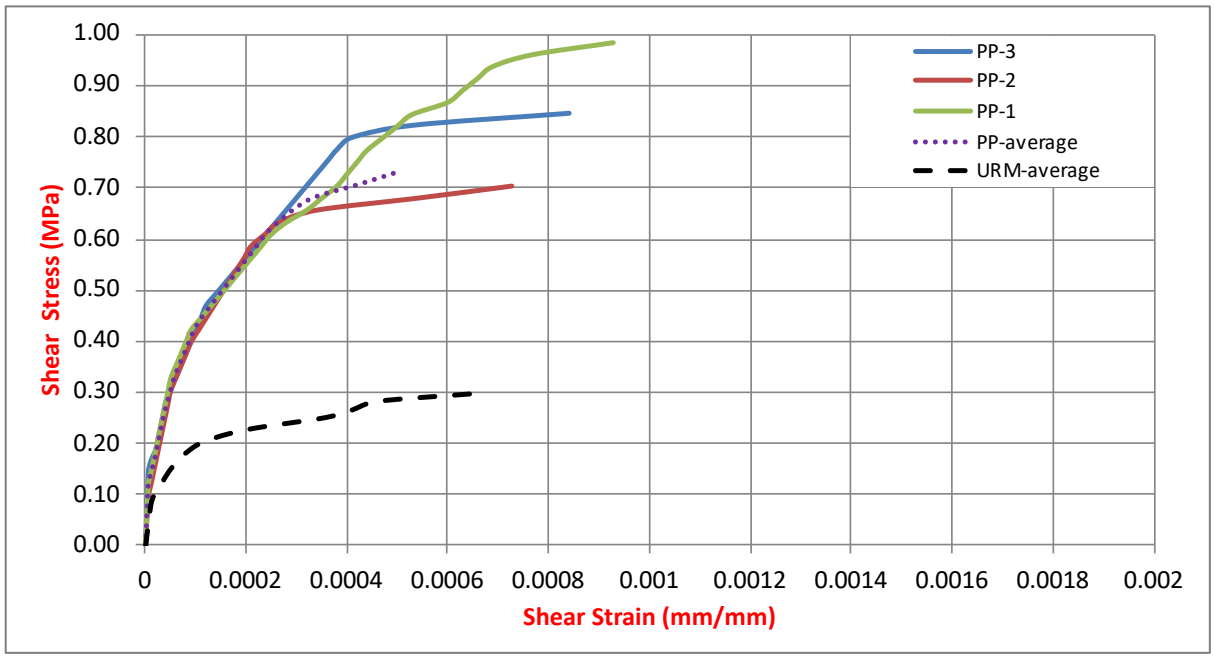


Figure 7. Shear stress-strain relationship of the PP panels.

Mechanical Parameters

A summary of all the mechanical parameters of the six tested specimens is presented in Table 2. The URM panels failed at an ultimate load ranging between 119 and149 kN. The average shear strength was 0.413 MPa, with a maximum value of 0.352 MPa occurring at URM-3 and a minimum value of 0.282

MPa occurring at URM-1. The average drift was calculated to be 0.104%, with a maximum value of 0.150% occurring at URM-1 and a minimum of 0.078% occurring at URM-2.

The PP reinforced panels failed at much higher loads but exhibited a brittle behavior. The ultimate load varies from 298 to418 kN. The average shear resistance was 0.845 MPa, with a maximum value of 0.986 MPa occurring at PP-1 and a minimum of 0.704 MPa, at PP-2. The average drift was recorded to be 0.084%.

Table 2. Summary of mechanical parameters of tested specimen.

Wall panel	P_{max} (kN)	ν_{max} (MPa)	δ_u (%)	G (MPa)	E (MPa)
URM-1	119.5	0.282	0.150	188	470
URM-2	129.5	0.305	0.078	392	978
URM-3	149.4	0.352	0.083	424	1060
URM-average	132.8	0.313	0.104	335	836
PP-1	418.4	0.986	0.096	1027	2568
PP-2	298.9	0.704	0.072	971	2429
PP-3	358.7	0.845	0.084	1006	2515
PP-average	358.7	0.845	0.084	1001	2504

P_{max}- ultimate load, ν_{max} – ultimate shear strength, δ_u – ultimate drift, G-shear modulus, E- Modulus of Elasticity

Comparison experimental vs. numerical

The main parameter that was used to assess the structural behavior of the panels is the comparison between stress-strain diagrams described in Figure 8.

The stress-strain diagram obtained after nonlinear analysis showed that the polypropylene reinforced panels exhibited similar behavior in both cases; high shear stress (0.845 MPa) but a very low shear strain value (0.0084), and in the numerical analysis a shear strength of 0.679 MPa and a maximum strain of 0.0013.

Plain panels, as expected showed a very brittle behavior and much lower values in both analyses; 0.228 MPa shear strength and a maximum strain of 0.0012.

Numerical analysis, even though based on several assumptions, provided good insights of the behavior of the panels during linear and nonlinear analysis. The aim of the analysis was to compare the experimental results with a previously done and well-established numerical procedures.

From the shear stress-strain curves, it is observed a good fit of the numerical model versus the experimental results.

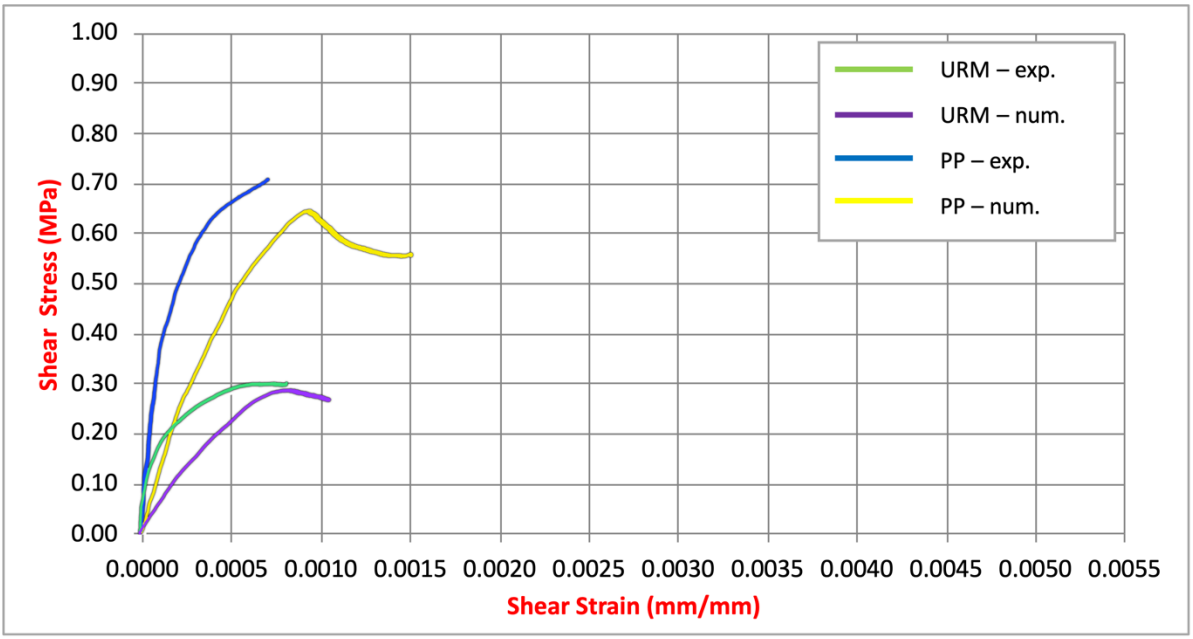


Figure 8. Comparison between experimental and numerical shear stress-strain relationship of URM and PP.

CONCLUSIONS

In this paper, the test results of an experimental investigation on brickwork shear walls that were strengthened with polypropylene fibers embedded into a cementitious matrix have been presented. The use of polypropylene to reinforce brickwork walls was ultimately effective.

The maximum increase in the in-plane load-capacity was achieved when two jacketing coatings were used as a retrofitting method: the shear capacity increment was 270% when compared to the unreinforced wall panels. Despite the improvement of the shear strength, the ductility of the reinforced panels remained limited.

Acknowledgements

The authors would like to thank Dr. Maziar Partovi from DIANA FEA for the help in acquiring and support for DIANA software.

REFERENCES

[1] C. Faella, E. Martinelli, E. Nigro, S. Paciello, Shear capacity of masonry walls externally strengthened by a cement-based composite material: an experimental campaign, Constr. Build. Mater. 24 (2010) 84–93.

[2] A. Kalali, M.Z. Kabir, Experimental response of double-wythe masonry panels strengthened with glass fiber reinforced polymers subjected to diagonal compression tests, Eng. Struct. 39 (2012) 24–37.

[3] D. Zhou, Z. Lei, J. Wang, In-plane behavior of seismically damaged masonry walls repaired with external BFRP, Compos. Struct. 102 (2013) 9–19.

[4] H. Santa-Maria, P. Alcaino, Repair of in-plane shear damaged masonry walls with external FRP, Constr. Build. Mater. 25 (3) (2011) 1172–1180.

[5] E. Mustafaraj, Y. Yardim. Retrofitting damaged unreinforced masonry using external shear strengthening techniques, J. Build. Eng. 26 (2019) 100913.

[6] N. Gattesco, I. Boem, Experimental and analytical study to evaluate the effectiveness of an in-plane reinforcement for masonry walls using GFRP meshes, Constr. Build. Mater. 88 (2015) 94–104.

[7] M. Corradi, C. Tedeschi, L. Binda, A. Borri, Experimental evaluation of shear and compression strength of masonry wall before and after reinforcement: deep repointing, Constr. Build. Mater. 22 (4) (2008) 463–472.

[8] A. Prota, G. Marcari, G. Fabbrocino, G. Manfredi, C. Aldea, Experimental in-plane behavior of tuff masonry strengthened with cementitious matrix–grid composites, J. Compos. Constr. 10 (3) (2006) 223–233.

[9] M.R. Valluzzi, D. Tinazzi, C. Modena, Shear behavior of masonry panels strengthened by FRP laminates, Constr. Build. Mater. 16 (2002) 409–416.

[10] E. Mustafaraj, Y. Yardim, External shear strengthening of unreinforced masonry panels using ferrocement jacketing, 16th International Scientific Conference VSU, 9–10. June 2016 Sofia, Bulgaria.

[11] E. Mustafaraj, Y. Yardim, In-plane shear strengthening of unreinforced masonry walls using GFRP jacketing, Period Polytech-Civ 62 (2) (2018) 330–336.

[12] S.B. Kadam, Y. Singh, B. Li. Strengthening of unreinforced masonry using welded wire mesh and micro-concrete – behaviour under in-plane action, Constr. Build. Mater. 54 (2014) 247–257.

[13] C. Calderini, S. Cattari, S. Lagomarsino. The use of the diagonal compression test to identify the shear mechanical parameters of masonry, Constr. Build. Mater. 24 (2010) 677–685.

[14] H. Mahmood, J.M. Ingham, Diagonal compression testing of FRP-retrofitted unreinforced clay brick masonry wallettes, J. Compos. Constr. 15 (2011) 810–820.

[15] [31] T.L. Bui, A.S. Larbi, N. Reboul, E. Ferrier, Shear behaviour of masonry walls strengthened by external bonded FRP and TRC, Compos. Struct. 132 (2015) 923–932.

[16] Mustafaraj E., Yardim Y., Corradi M., Borri A. Polypropylene as a Retrofitting Material for Shear Walls. Materials 13 (2020) 2503.

[17] M. Corradi, A. Borri, G. Castori, R. Sisti, Shear strengthening of wall panels through jacketing with cement mortar reinforced by GFRP grids, Compos. Part B 64 (2014) 33–42.

[18] ASTM E 519-07, Standard Test Method for Diagonal Tension (Shear) in Masonry Assemblages, ASTM International, USA, 2007.

[19] G. Van Zijl, P. De Vries and A. Vermeltfoort. Masonry wall damage by restraint to shrinkage. J. Struct. Eng. 130(7) (2004) 1075-1086.

[20] TNO DIANA, "DIANA – Finite Element Analysis-User's Manual release 9.6-Element Library," TNO DIANA, Delft, Netherlands, 2014.

[21] Mustafaraj, E. External shear strengthening of damaged unreinforced masonry walls, PhD Thesis, EPOKA University, 2016.

Public-Private Partnerships in Albania: From the Legislative Provisions to Risk Management

Julinda Keçi

Department of Civil Engineering, EPOKA University, Albania,

ABSTRACT

Public Private Partnerships (PPPs) are frequently used in Albania, mainly in the form of concession, as the main "engine" to make work the public sector in the field of investments. It is estimated that recently, there are more than 170 PPP-s only in the infrastructure sectors in Albania.

The focus in this policy was given by the European Union, and the application of this model initially was based on the EU directive 2004/18/EC of the European Parliament and that of Council of Europe on 31 March 2004 so far, as part the process of Acquis Communautaire. The renewed and increased interest on PPPs, where private sector finance public investments in return for realizing profits, is especially present in a fragile state like Albania.

The process is based in a legal framework, which in few years has been amended frequently, with the aim to make increase the investments fields, stakeholders, and benefits. It is to be emphasized that Albania has not only adopted new laws, but it has set up an ad hoc public institution, called the "Agency on the Treatment of Concessions". The examples of PPP-s contracted and implemented in Albania, are a lot, mainly considered as success story and pathfinders for strategical sectors of Albanian economy.

This paper will review the PPPs legal framework, performing a comparative study on legislative provisions in Western Balkans Countries.

***Keywords**: PPP-s, Legal framework, Risk management, Albania*

INTRODUCTION

In a time of economic uncertainty and increased demand for infrastructure, governments are seeking alternative ways of funding projects. This situation has led to researching for new approaches such as Public Private Partnerships (PPPs). "PPPs are arrangements where the public and private sectors both bring their complementary skills to a project, with varying levels of involvement and responsibility, for the purpose of providing public services or projects" [1]. These alternative delivery methods may employ three or more functions such as: Finance (F), Design (D), Build (B), Operate (O), Lease (L), Own (O), Maintain (M), and Transfer (T), mostly adopted in the form of BOT (Build- Operate- Transfer) or the so-called concession.

Researchers agreed that public financing in developing countries has become very unstable due to the lack of effectiveness in three main directions, such as time, cost, and quality. Most infrastructure and services are assessed to be in short supply when compared to the country's increasing demand. A McKinsey study in June 2016 [2], estimated a yearly investment need of US$3.3 trillion each year to 2030, to support current growth rates (equal to 3.8% of the global GDP). An analysis performed in Western Balkan Region [3], estimated a need of EUR110 billion in infrastructure investment for a ten-year period 2015-2024. Even the available infrastructure is not performing to the required standards due to low maintenance and public perceive as "no man's property".

In these conditions, the transition to the PPP approaches is recognized by many studies as a win-win solution due to the perceived benefits in government debt reduction, increase of private sector participation and prevention of tax escalation [4].

In analogy with world-wide experience, driven in part by the growing infrastructure investments with postponed payments, PPPs have proliferated in Western Balkan Region; Albania makes no exception. While governments seem eager to create such partnerships, not everyone is convinced of their value- criticizing the system's ability to deliver the promised benefits due to the inherent risks, long-term nature, their high value, and complex organizational structures.

Following the established legal framework in 2006, Albania has seen an increased number of PPP projects, mainly in the field of energy and transport. Studies have revealed a high mortality rate of PPPs in Western Balkans, especially during preparation phases [5]. Nevertheless, their applications remain still high, ranging from two projects in Serbia to eleven projects in Albania reaching financial closure. Most contracts are based on unsolicited proposals, hindering the planned public policy development, as private investors are choosing the projects they want to invest in.

It is though important to highlight that over the past years Albania has made efforts to learn best practices from its past and apply them to new procurements. Practice also showed that circumstance change in a country and what seemed to be good terms and conditions for PPP contracts in the 2000's was not that great for more recent projects. This study focuses on PPP legal framework, its compliance and effectiveness, as well as implementation and risk management, highlighting lessons learned from Albanian approach.

PPP DEVELOPMENT TRENDS IN WESTERN BALKANS (WB)

Infrastructure development is a crucial support to the regional economic recovery and growth, especially after the global crisis. The first development of PPPs in Western Balkans dates to 1998; Time by time the number of PPP projects is quickly increasing, influenced as well by recent trends and successful PPP deliveries and the ability to use the private sector know-how in building - operation- maintenance. It is important to highlight the high mortality rate of PPPs [5]. A study conducted for the Region [6], revealed that most successful projects were delivered in transportation sector (65%), followed by social and community services (20%), telecommunications (10%), and environmental (8%), mostly in Albania. Considering the frequent application mode, WB countries have developed their dedicated legal and institutional framework to support public authority in the PPP developments, conforms the EU directives 2004/18/EC1: transparency, equal treatment, fair and open competition, and solid procedures.

Large investments in WB delivered through PPP, instead of traditional public procurement, seem to match more with a national strategic attention rather than with a better Value for Money (VfM) delivery. Most of large projects in WB did not carry out a VfM analysis of the procurement method, as it was strategically very early decided not to adopt a traditional procurement. Considering the high need for large infrastructure investments in the Region, the developed projects are considered of strategic importance for the country. So, their development phases are generally supported by continuous studies and research of European Commission, international expertise and advisory, as well as financial support from USAID, IFC, EBRD.

Despite this, it was not uncommon for PPP project to go off-rail, mainly due to poor initial preparation of the project- with a predisposition for public authorities to launch the procurement before being sufficiently ready, and poor preparation and management of the procurement process. The first major PPP successful applications in WB countries are treated as 'pathfinder' projects, especially for the legal and institutional frameworks, to enable compliance with the respective procurement processes [5].

PPP as a mechanism for DEVELOPMEN IN ALBANIA

Although PPPs are only lately being extensively used, historical facts reveal their early history in Albania. According to Albanian National Archives documents, the public sector partnership with private sector dates to the early 1920, progressing through three main development phases: 1) 1920- 1944; 2) 1944-1992; 3)1992–ongoing.

Since 1922, the Albanian National Council used to discuss various requests from foreign companies to invest in various sectors in the form of concessions [7]. Due to the lack of a specific law on concessions, the government used to discuss and approve the contracts case by case.

The second development period (1944-1992) is considered as a dark phase of PPPs, as they were legally prohibited. Economic and political changes of 1992 in Albania increased the need for public private partnerships, requiring the realization of three basic conditions: Reconsidering the PPPs definition; Developing an adequate legal framework; Establishing an institutional framework.

Due to a large public funding gap, the potential of PPPs as a source of alternative finance was recognized quite early by the Albanian Government, making numerous efforts to create an enabling PPP environment. The legal reforms were introduced later on, with the PPP Law of 2013 (no. 125/2013), amended in 2015 (no. 77/2015). The current Albanian PPP law and its amendments establishes the legal framework for PPPs and describes institutional responsibilities. It is to be emphasized that Albania has not only adopted new laws, but it has set up an ad hoc public institution, called the "Agency on the Treatment of Concessions", serving as a PPP Unit in the Ministry of Finance.

Albania has a history of successful and less successful PPP procurements. In a recent World Bank analysis [16], Albania scores well in preparation and procurements of PPPs and with unsolicited proposals, medium score in preparation and lower score for PPP contract management.

The central budget authority's approval is needed before tendering and PPP's prioritization is consistent with public investment prioritization even though there is no detailed procedure regulated. It is missing a specific methodology for economic analysis, fiscal affordability, financial viability, risk assessment, and market assessment. During the preparation stage are used the standardized PPP model contracts and a draft contract is requested in the proposal. The Albanian government has created a system to manage the implementation of PPPs and a monitoring and evaluation system, with the private partner providing periodic information to the procuring public authority. The current regulation allows changes in the structure of public partner and modification or renegotiations of the PPP contract, limited on risk allocation only.

Currently a great focus is being placed on PPP market discussing the lack of specific comparative analyses in Value for Money with public procurement, Benefit Cost analyses, social assessment and high critical risks in "corruption" and lack of "respect of law". The changing economic circumstances have led to amendments being made in procurement laws, strategic approaches and specific PPP contract terms and conditions.

This section presents a review of two selected PPP projects developed and carried out in Albania. It analyses the practices and procedures used, as to be able to identify key issues as possible opportunities for improvement. Considering the limited data availability, the methodology used considered both documentation review and interviews.

Tirana International Airport "Mother Teresa"

In the framework of EU integration, Albanian government gave priority to improving infrastructure and services of Tirana International Airport (TIA) [8], [15]. 'Mother Teresa' Airport was built in 1957, 17 km North-West of Tirana, and had the latest upgrade of the runway on 2002. Considered as the first and last impressive image of Albania offered to air passengers as well as a connection point with the world, the government committed for the further development and improvement of its infrastructure through PPP [4]. The decision to deliver the intended investment through a PPP, instead of a traditional pubic procurement, results more a reflection of the national strategy than based on a VfM analysis.

The procurement process for the Tirana Airport pursued an international tender organized in two stages: pre-qualification stage followed by request for proposals. As reported on EPEC study [6], out of the 18 companies expressing their interest in the transaction, four entities were invited to tender. Following a competitive dialogue procedure, the contract was awarded to Tirana Airport Partners (TAP), a company established on September 20, 2004 specifically for the implementation of the concession contract. It was initially owned by Hochtief Airport GmbH 78.7% and Albanian-American Enterprise Fund 21.3%. In October 2004, Hochtief sold 31.7% of the shares of DEG - Deutsche Investments. The concession agreement provided for the investment of a share capital of 9,375,000 Euros. On October 6, 2016, the company was bought for 82.25 million euros by Real Fortress Private Limited, a company registered in Singapore, which owned 100 % of shares. On December 1st 2020, the concession was sold to Kastrati Group Sha. for 71

million euros [17]. The Concession Agreement was signed in October 2004, with the objective to construct, operate and maintain the International Airport "Mother Teresa" of Tirana, specifically including the designing, financing, installation, building, maintaining, operating, managing and developing the new terminal construction based on the old airport. BOT of "Mother Teresa" International Airport in Rinas, had exclusive rights to international flights to and from Albania for an initial period of 20 years starting from 2005. This contract was amended in 2016 and was extended with 2 years in exchange for the removal of the exclusivity clause on international flights.

The structure of the agreement allowed phased construction, with investments being made after reaching predetermined levels of passenger traffic. So, the project was delivered in three main phases, completed on schedule:

Phase 1: Construction works (2005-2007), during which were performed the following investments: New Passenger Terminal; New Car Parks (Area 1 and 2), covered and uncovered; New Air Cargo Centre; New Access Road; New Bridge on the Existing Road; New perimeter road; New circulatory road; Standardized in-house services; Additional operational facilities (waste water treatment plant).

Phase 2: New Passenger Terminal (2008-2009) and additional investments in airport facilities and operations, in the extension of apron; in improving the FFR Station.

Phase 3: Following investments in CCTV control system, Access Control system, Emergency Centre, Preparation of Standardized Operation, Maintenance, Security Manuals and others.

TIA was granted a one-off exemption from customs duties, import taxes and VAT on imports and materials supplied for construction and reconstruction work, although a part remains liable to corporate tax and VAT at the statutory rates [5]. The concessionaire fee is structured with an initial lump sum of 3million EUR and a variable fee per year representing 30% of private partner profits.

The risk allocation is mainly guided by the PPP principle “allocating the risks to the party that can best handle it”. So, the private partner retained the risks related to design, construction, operation, maintenance and market. The public part retained regulatory risks and responsibility related to specific operational aspects, such as delivery of secondary needed infrastructure (e.g. access roads), air traffic control. Other risks, such as financial and environmental are shared between parties). The environmental risk is shared, with the public part responsible for the existing site conditions, while the private partner responsible to fulfil with the legal environmental regulations. Financial risk as well is shared, with the public part responsible, in case of early termination, for any residual amount due to the lender, while the private part responsible for project finance availability [11]. It should be noted however that, studies reviewing current EU best practices ([9], [5]) highlight that public authorities are discouraged from accepting responsibility for full debt repayment in case of early termination of the concession as a result of private partner default.

The political risk, causing closure or disruption, is retained by the private authority, even though it was estimated with a low probability due to the high economic harmful impact. To ensure a fair return of the investment and to treat the potential risk of ‘over design’ (building today an infrastructure which will provide over capacity for the actual passenger traffic), the agreement allowed phased construction. To mitigate the risk of local currency devaluation aviation revenues are collected in foreign currency (EUR of Dollar) while unitary costs of non-aviation revenues- collected in Albanian Lek- are often indexed in a basket of international currency. Cost overruns, as a result of contract agreement using a preliminary non- detailed project, was addressed by an investment ceiling.

TIA is considered as a flagship project for Albania. Due to lack of experience, it was treated as a ‘pathfinder’, ratifying the concession contract by the national parliament. VfM is still under question mark. Having made an early strategic decision to adopt PPP, resulted in a lack of a formal quantitative value for money analysis, to compare PPP to the traditional procurement. A detailed comparative research on aviation charges was on performed, but a study investigating user satisfaction performed in 2017 [10], revealed the

user dissatisfaction with the high charges making TIA one of the most expensive in the Region. However, it is to be highlighted that high charges are not an indicator of poor value for money.

To conclude, the contract is considered as fair, with good partnership spirit. This was proved with the goodwill of both parts in managing the contract changes, such as the ownership change or the request for exclusivity, both not anticipated in the original contract. The contract is being currently managed by Civil Aviation Authority, under the Ministry of Transport and Infrastructure, and has an overall good operation.

ASHTA HPP

The new law on concessions affected directly the hydropower sector in Albania, which at the time had more than 80 proposals aiming at the design, construction and maintenance of hydropower plants through small concession agreements. The situation was further supported by several actions undertaken by the Albanian government, aiming to promote the participation of private sector in the provision of large infrastructure projects, such as offering guarantee for the energy market (for the first 15 years out of 35), including the right of financial institutions to 'step in' in case of possible failure, initiating the 'One Stop Shop' for licensing and permits, decreasing the taxes on infrastructure constructions into 0.1% of the investment value.

The history of PPP procurements in the hydroenergy sector has a mixed history. There was a proliferation of mini-hydroelectric concessions that were awarded by the government through unsolicited proposals, but unfortunately some of them seemed to have been opportunistic and have never met their project commitments to build operational hydroelectric plants [18].

The Ashta hydropower plant was Albania's first major hydro-power plant development in 30 years and the Government's first large public-private partnership (PPP) in the energy sector [12]. Located in Drini River, in northern Albania, it is the last of a chain of HPPs. The Ashta HPP was initially developed in the 70s-80s, with some structures of it constructed in 1973 (e.g. Spathara dam). As Summarized in IFC report [13], the project need identification dates back to 2001, with the Albania's power utility (KESH) contracting the China Water & Electricity Corporation (CWE) to build, on a turnkey basis, a hydropower plant on the lowest reach of the Drin River. Multiple socioeconomic and environmental questions forced Albanian government to suspend the contract in August 2001 for an independent feasibility assessment. Despite the study was completed in a few months, it took six years to the government to approve the new concept (Ashta) and to implement the pilot PPP under the new concession law.

The prequalification phase of the bidding process started in January 2008, including 12 possible bidders out of which only 10 were eligible and fulfilled the prequalification requirements. The IFC team and the possible bidders negotiated on the design of standard bidding and contract documents in a fair, transparent procedure. Even though the main conditions were discussed and negotiated, an important number of problematic issues were not included in the pre-negotiations, such as hydrological risks, geological risks, environmental risks, land appropriation risks, construction risks.

Furthermore, Ashta HPP, being the last HPP constructed in Drini river, is directly affected by

Vau i Dejes, Komani and Fierza HPP, which are property of KESH and as a result subject to public regulatory framework ("regulations on minimum ecological flows, water off-takes for irrigation, cascade operation rules, potential liabilities associated with existing structures" [13].

In June 2008, only two international companies Verbund and the joint venture Electrabel &Companie Nationale du Rhone, submitted their technical and financial proposals. In July 2008, Verbund was awarded as the winner and in a two months period the concessionaire agreement was signed adopting a Build Own Operate Transfer (Table 1). In 2010, EVN AG and Verbund negotiated a collaboration agreement, creating the joint venture Energji Ashta Shpk, to invest, design, construct, and operate Ashta HPP, which was later approved by the contracting authority.

Table 1. Ashta HPP project overview (UNFCCC, 2006)

ASHTA HPP, Albania	
Project Type:	BOOT
Contract duration:	35 Years
Investment amount	EUR 212.9M
Location	Shkoder, Albania
Schedule 2008 - 2043 PHASE 1 (planning/authorization phase): total duration: 18 months PHASE 2 (construction phase Ashta 1): - start of construction: March 2010 - commissioning: Autumn 2012 PHASE 3 (construction phase Ashta 2): - start of construction: April 2010 - commissioning: beginning of 2013 PHASE 4/5 (operational phase): 2012 - 2043	

The project consists of a two-stage diversion power plant which incorporates some pre-existing structures and some supporting infrastructure investments. The project construction lasted approximately 30 months, and the official inauguration was performed on September 2012. On March 2013, the project reached the final stage of testing and commissioning, competed successfully with 66 GWh produced electricity, sold to local companies GSA and CEZ. Officially, the Ashta HPP was considered as one of the worlds' largest hydro power plant using the matrix technology: 90 innovative hydro-matrix turbines, with a capacity of 52MWh, producing 278 million KWh per year electricity for Albania.

Being a pilot application under the new concession law, the project faced various problems and difficulties, directly affecting cost escalation. The financial risk, totally bared by the private partner, was treated by an additional contract clause giving the private partner the right to change the project without any additional obligation from the contractual authority (paragraph 7.2.3 of Concessionaire Agreement).

Being the last of a chain of HPPs, Ashta plant is fully reliant on water releases from the upstream state-owned plants. The risk that KESH may retain water for extended period and release it on certain peak times (e.g. peak power times), would impact negatively the project performance. Considering that Ashta has almost no storage, extreme water releases would overpass the dam with no electricity production. This risk was mitigated through an agreement assisted by IFC team between the concessionaire and KESH. The arrangement stipulates conditions for regular water releases under normal situations and directions crisis management in case of emergency events such as floods [13].

Other identified risks include (see Table 2):
- ***Hydrological risks***: temporary deficits, long-term deficits, flood damage (during construction phase), flood damage (during operation phase);
- ***Construction risks***: cost overruns, unforeseen geological conditions, time overruns;
- ***Performance risks***: equipment, project performance, transmission;
- ***Environmental risks***: permit, land ownership and occupancy; Market and credit risks;
- ***Political risks***: changes in permits, tax changes.

A formal quantitative VfM is missing. However, beside the main benefit directly related to the reduction of the countries' needs to import electricity, there are several other perceived benefits of the partnership project, such as: environmental benefits (e.g. reduced CO2 emission) [14]), an important economical impulse, job creation, benefiting from the international experience know-how, attraction of international investments, important social impacts

Table 2. Ashta HPP risk allocation overview [11]

Risks	PRIVATE	<= =>			PUBLIC
Hydrological		*	*		
Construction		*			
Financial		*			
Performance		*			
Environmental			*		
Political &Regulatory				*	
Force Major			*		

.

CONCLUSIONS

Weakness and threats:

- Sustainability assessment of PPP projects.

While reviewing the PPP developments in WBR, and especially in Albania, it was evident that decisions to use PPP deliveries was based more in a national strategy. There was no documentary evidence assessing the sustainability of a specific project delivered through PPP, neither a specific regulation.

- VfM is still under question mark.

No documentary evidence of quantitative VfM analysis or Benefit Cost analysis. A formal ex-ante VfM could have been a helpful tool, while comparing it with an ex-post analysis, to demonstrate the project deliveries.

- Unsolicited proposals are commonly used, causing some concern.

These practices allow the public part to avoid costs for project preparation. Furthermore, it hinders the centrally investment-oriented public policy, as there are private partners choosing the projects they want to invest in.

- Poor competition

Due to unsolicited proposals, encouraged by the bonus policy, the projects seem to have a readymade pathway, resulting in poor or no competition.

Strengths and Opportunities:

- Dedicated units for the PPP development.

Albania is appreciated from several EU studies for the lower PPP mortality rate in Western Balkans. Dedicated units for PPP development and clear definitions of roles and responsibilities, contributes to this success. The PPP unit should be empowered with technical and staff resources.

- Good practice in PPP procurement stage.

Case studies reviews have revealed following a good practice in procurement stage by following international tender procedures, being constantly supported by studies and research from European Commission, international expertise and advisory, and financial support. Anyway, it is to be highlighted that external support does not necessarily guarantee the project success.

- Phased construction allowed in the PPP agreement.

The phased construction agreement resulted a good practice to avoid 'over design', and as a result higher charges to end users.

REFERENCES

[1] Efficiency Unit, "An Introductory Guide to Public Private," 2008. [Online]. Available: http://www.changingroles09.nl/uploads/File/Final.Ke-Wang-Chan.pdf.

[2] PwC, "Global infrastructure investment," GIIA, PwC, 2017. [Online]. Available: https://www.pwc.com/gx/en/industries/assets/pwc-giia-global-infrastructure-investment-2017-web.pdf. [Accessed 05 January 2019].

[3] Ri, Berthomieu, Cingolani, "Priority Investments in the Western Balkans and Croatia: Analysis of medium-term needs, possible impacts and criteria for ranking in terms of efficiency and development potentia," STAREBEI Research Program, 2014.

[4] J. Keçi, "Public Private Partnership for Infrastructure Projects: Mapping the Key Risks," International Journal of Economics and Management Engineering, vol. 9, no. 9, pp. 3141- 3151, 2015.

[5] WBIF, EPEC, "PPP Projects in the Western Balkans: Good Practice, Challenges and Lessons Learnt," 2018.

[6] EPEC, EIB, "Overview of the PPP Legal and Institutional Frameworks in the Western Balkans," EPEC, Luxembourg, 2015.

[7] B. Berberi, Partneriteti Publik- Privat: Hallke e Rendesishme e Procesit Te Integrimit te Shqiperise ne Komunitetin Evropian, Dizertacion Doktoral, Tirane: UNIVERSITETI I TIRANËS, 2013.

[8] BENEFIT, "Case Studies: Tirana International Airport," 2016. [Online]. Available: http://daphne-new.aegean.gr/wiki/index.php/Case_Studies:_Tirana_International_Airport#Risk_Allocation. [Accessed 30 May 2015].

[9] Iossa E., Spagnolo G., Vellez M. , "Best Practices on Contract Design in Public-Private Partnerships," World Bank, 2007.

[10] Keci, J., MODEL PËR MENAXHIMIN E RISKUT NË PROJEKTET E MËDHA INFRASTRUKTURORE TË PARTNERITETIT PUBLIK PRIVAT, Tirana: Polytechnic University of Tirana, 2017.

[11] Keci, J, "Infrastructure Public Private Partnership Implementation and Risk," in IABSE Guimaraes 2019, Portugal, 2019.

[12] United Nations Economic Commission for Europe Team of Specialists on Public-Private Partnerships, "UNECE PPP STANDARDS FOR GRID-CONNECTED RENEWABLE ENERGY," United Nations Economic Commission for Europe, 2016.

[13] I. F. C. IFC, "Ashta Hydropower—Turning a Doubtful Concept into a Technological Trailblazer," IFC, 2009.

[14] UNFCCC, "CLEAN DEVELOPMENT MECHANISM -PROJECT DESIGN DOCUMENT FORM (CDM-PDD)," 2006.

[15] ". S. T. I. A. BENEFIT, "Case Studies: Tirana International Airport"., " 2016. [Online]. Available: http://daphne-new.aegean.gr/wiki/index.php?title=Case_Studies:_Tirana_International_Airport&oldid=844.

[16] W. Bank, "Benchmarking PPP Procurement 2017," World Bank Group, 2017-2018.

[17] ALBANIA'S PUBLIC PRIVATE PARTNERSHIPS, "http://ppp.reporter.al/," 30 January 2021. [Online].

[18] D. Baxter, "The Status Quo of PPPs in Albania," 2018.

4th International Balkans Conference Challenges of Civil Engineering

Tirana, 18-19 December 2020

Book of Proceedings / EPOKA University.

Editors:
Assist. Prof. Dr. Erion Luga
Dr. Enea Mustafaraj,
Dr. Julinda Keçi,

Tirana

EPOKA University Press, 2020

ISBN 978-9928-135-37-7

1. Inxhinieria civile 2. Konferenca 3. Gadishulli Ballkanik

CIP Katalogimi në botim BK Tiranë

Challenges of Civil Engineering : 4th International Balkans
Conference : Tirana, Albania, 18-19 December 2020 : book
of proceedings / ed. Erion Luga, Enea Mustafaraj, Julinda Keçi.
– Tiranë : EPOKA University, 2021
209 f. : me foto ; 21 cm.
ISBN 978-9928-135-37-7

1.Inxhinieria civile 2.Konferenca 3.Gadishulli Ballkanik

624(497) (062)



ISBN 978-9928-135-37-7